Investigation of CD27-CD70 co-stimulation in human regulatory T cells for enhanced cellular therapy in transplantation

Rebeca C. Arroyo Hornero

Balliol College

and Nuffield Department of Surgical Sciences,

University of Oxford

Supervisors: Dr Joanna Hester, Dr Fadi Issa and Prof Kathryn Wood

Thesis submitted for DPhil in Surgical Sciences in Hilary Term 2019

Abstract

Investigation of CD27-CD70 co-stimulation in human regulatory T cells
for enhanced cellular therapy in transplantation
Rebeca C. Arroyo Hornero, Balliol College. University of Oxford. DPhil in Surgical Sciences.

$CD4^+FOXP3^+$ regulatory T cells (Tregs) are essential for maintaining immune homeostasis and are a focus of investigation in the treatment of transplant rejection and autoimmune diseases. Current clinical protocols for Treg cellular therapy production are heavily reliant on *in vitro* expansion techniques. However, post-expansion Tregs demonstrate heterogeneity with some subpopulations displaying unstable regulatory phenotype and function. The aim of this study was to investigate this phenomenon in depth, in order to improve the efficacy and safety of Treg cellular therapy.

Cell surface CD27 is a useful marker for the identification of Tregs with potent suppressive capacity after expansion. Signalling via the CD27-CD70 co-stimulatory receptor-ligand interaction is important for T cell function but its role in Tregs is not known. In this study, the $CD27^+$ Treg population is characterised in depth. The differential expression of CD27 and CD70 is shown to identify distinct human Treg populations. Stable and potent suppressive function after *in vitro* expansion is confined principally to cells with a $CD27^+CD70^-$ phenotype. However, this suppressive function is not reliant on CD27 expression. Prolonged *in vitro* expansion of Tregs results in stable CD70 expression with concomitant CD27 downregulation in a subset of Tregs, and these $CD27^-CD70^+$ Tregs provide pro-inflammatory co-stimulation to conventional T cells via CD70. Genetic deletion (using CRISPR/Cas9) or monoclonal antibody-based blockade of CD70 rescues Tregs from hypofunctionality, highlighting a potential therapeutic intervention.

Taken together, our data identify CD70 as a molecular target via which *in vitro*-expanded human Tregs exert detrimental pro-inflammatory effects. For clinical application, the availability and ongoing development of antibodies that target the CD27/CD70 pathway provides an opportunity for the therapeutic manipulation of Tregs. Furthermore, relatively straightforward genetic engineering techniques could be exploited to disrupt CD70 expression and improve the efficacy of Treg cellular therapy.

Acknowledgments

During my DPhil studies I have been incredibly fortunate to have been supported by many individuals. I would particularly like to thank my supervisors Dr Joanna Hester, Dr Fadi Issa and Professor Kathryn Wood. Joanna, with wealth of laboratory advice, for answering any question with patience and good humour. Fadi Issa, for his advice and support during multiple congresses and conferences worldwide. Kathryn Wood, firstly for employing me as a completely inexperienced immunologist into her lab, and then encouraging me to take on new challenges and to embark into the DPhil life. They all have contributed guiding the direction of the project.

I would also like to thank Restore and the Nuffield Department of Surgical Sciences, for funding my studies and for always keeping track of my research.

Other members of TRIG have all played a part in this project. Gareth Betts taught me about research and laboratory practice and did so with inexhaustible patience and kindness. Kate Mildward, for all her suggestions and help during endless days. Monica Dolton, who can solve any administrative, organisational or grant related question in the most efficient manner. The departmental facilities have been managed brilliantly by Jakub Kupinski. My colleagues in level 5, for helpful discussion and, more importantly, for those long chats that helped to recharge my batteries.

Aside from TIRG lab, I would like to thank Dr Paul Harden, Professor Chris Pugh and Professor Richard Cornall, my examiners for Transfer of Status and Confirmation of Status; Li-Zhen He and Tibor Keller, from Celldex Therapeutics, for suppling crucial reagents for our experiments; and Dr Peng Hua for performing RNA-seq analysis. I am also grateful to Professor Waseem Qasim for kindly allowing me to use his laboratory facilities and Dr Christos Georgiadis, who provided invaluable training for the genetic editing experiments.

Finally, I owe a huge debt of gratitude to my family and friends, for being a perpetual source of moral support, for their kind understating and for forcing me to carry on when it all got too much.

Abbreviations

#	number of cells
7-AAD	7-aminoactinomycin D
Ab	Antibody
ADCC	Antibody-mediated cellular cytotoxicity
AIRE	Autoimmune regulator
Allo moDCs	Allogenic monocyte-derived dendritic cells
AMP	Adenosine monophosphate
AP-1	Activator protein-1
APC	Antigen presenting cell or Allophycocyanin
ATP	Adenosine triphosphate
B_2M	β2-microglobulin
BCL-XL	BCL-like 1 isoform 1
BCR	B cell receptor
Breg	Regulatory B cell
cAMP	Cyclic adenosine monophosphate
CAR	Chimeric antigen receptor
Cas9	CRISPR-associated protein 9
CCL	Chemokine ligand
CCR	Chemokine receptor
CD	Cluster of differentiation
CD127	IL-7 receptor
CD25	High affinity IL-2 receptor α-chain
CFSE	Carboxyfluorescein succinimidyl ester
CMV	Cytomegalovirus
CNS	Conserved non-coding sequence
CRISPR	Clustered regularly interspaced short palindromic repeats
CTL	Cytotoxic T lymphocyte
CTLA-4 (CD152)	Cytotoxic T lymphocyte-associated antigen 4
CXCR	Chemokine receptor
Cy7	Cyanine 7
DAMP	Damage-associated molecular pattern
DC	Dendritic cell

Div index	Division index
dLN	Draining lymph node
DMEM	Dulbecco's Modified Eagle's Medium
DNA	Deoxyribonucleic Acid
DSA	*De novo* donor-specific antibodies
EAE	Experimental autoimmune encephalomyelitis
EBV	Epstein-Barr virus
EDTA	Ethylenediaminetetraacetic acid
ELISA	Enzyme-linked immunosorbent assay
ENTPD1 (CD39)	Ectonucleoside triphosphate diphosphohydrolase-1
FACS	Fluorescence-activated cell sorting
FCS	Foetal calf serum
FITC	Fluorescein isothiocyanate
FMO	Fluorescence minus 1
FOXP3	Forkhead box P3
GATA-3	GATA-binding protein 3
GFP	Green fluorescent protein
GITR	Glucocorticoid-induced tumor necrosis factor receptor
GM-CSF	Granulocyte-monocyte colony-stimulating factor
GMP	Good manufacturing practice
GvHD	Graft versus host disease
HLA	Human leukocyte antigen
IBD	Inflammatory bowel disease
ICOS	Inducible co-stimulatory molecule
IDO	Indoleamine 2,3-dioxygenase
IFN	Interferon
IKZF	Ikaros family zing finger
IL	Interleukin
IRF4	Interferon regulatory factor 4
iTreg	*In vitro*-induced Treg
IU	Infection units
KO	Knock out
LN	Lymph node
mAb	Monoclonal antibody
MACS	Magnetic activated cell sorting

MFI	Median fluorescence intensity
MHC	Major histocompatibility complex
miH	Minor histocompatibility antigen
MLR	Mixed lymphocyte reaction
MOI	Multiplicity of infection
mTOR	Mammalian target of rapamycin
NFAT	Nuclear factor of activated T cells
NF-κB	Nuclear factor-κB
NK cells	Natural killer cell
PAMP	Pathogen-associated molecular pattern
PBMC	Peripheral blood mononuclear cell
PBS	Phosphate-buffer saline
PCR	Polymerase chain reaction
PD-1	Programmed cell death protein 1
PE	Phycerythrin
PerCP	Peridin chlorophyll protein
PFA	Paraformaldehyde
PI3K	Phosphatidylinositol 3-kinase
PMA	Phorbol 12-myristate 13-acetate
PRR	Pattern recognition receptor
pTreg	Peripherally-derived Treg
rhIL-2	Recombinant human IL-2
RNA	Ribonucleic acid
RNA-seq	RNA sequencing
RNP	Ribonucleoprotein
ROR	RAR-related orphan receptor
RPMI	Roswell Park Memorial Institute
SD	Standard deviation
SEM	Standard error mean
sgRNA	Single guide RNA
STAT	Signal transduced and activator of transcription protein
T-bet	T box expressed in T cells
Tconv	Conventional T cell
TCR	T cell receptor
Teff	Effector T cell

Tfh	Follicular T helper cell
TGF-β	Transforming growth factor-beta
Th	Helper T cell
TIGIT	T cell immunoreceptor with Ig and ITIM domains
TLR	Toll-like receptor
TNF	Tumour necrosis factor
TNFRSF	Tumor necrosis factor receptor superfamily
Treg	Regulatory T cell
Tresp	Responder T cell
TSDR	Treg cell-specific demethylated region
tTreg	Thymic-derived Treg
VPD	Violet proliferation dye 450
WT	Wild type

Table of contents

Chapter 1: General Introduction

1.1. Transplantation immunology

Over the past 50 years organ transplantation has become an effective treatment worldwide for end-stage organ failure, benefiting hundreds of thousands of patients with terminal organ dysfunction. In total, 5090 patients received a transplant in the UK in the last year (2017/2018) (*1*). Kidney transplantation has proven to offer a better quality of life, lower mortality and reduced costs to healthcare systems than dialysis (*2*). Kidney, followed by liver and pancreas, is the most commonly transplanted organ (*1*), and, in patients with heart and lung failure, transplantation often represents the only life-saving treatment.

The first human transplant with positive long-term result was a cornea in 1906 (*3*). Alexis Carrel, the first scientist to receive a Nobel Prize for work related to transplantation, developed newly refined sutures to anastomose blood vessels that allowed for technically successful kidney transplantation. In 1954, after multiple ineffective attempts in dogs and in humans transplanting animal organs or organs from one person to another, the first kidney was transplanted successfully in a human patient (*4*). Interestingly, in both successful cases the immune response against the allograft (graft from one individual transplanted to another of the same species) was attenuated: (I) the eyes are considered to be the prototypic immune privileged tissue (*3*), and (II) kidney transplantation was performed between identical twins, with minimal genetic disparity (*4*).

Extensive research in transplant immunology needed to be conducted until Murray's team successfully broke for first time the genetic barrier for human kidney transplantation in 1958, transplanting a kidney between non-identical twins that maintained adequate function for 20 years (*5*). George Schone, Leo Loeb and James B. Murphy were pioneer in identifying transplant rejection as an immunological phenomenon (*6*) and, in the early

1940s, Peter Medawar and colleagues described experimental methods of inducing tolerance. Medawar observed that allogenic skin grafts were lost whereas autologous skin grafts were maintained, and subsequent allogenic grafts from the same donor failed more rapidly than the first one (*7-9*). In following studies, Billingham, Brent and Medawar demonstrated the phenomenon termed “actively acquired tolerance” (1953), whereby immunological tolerance could be induced by exposing the recipient to donor cells during foetal life (*10*). This hypothesis was previously proposed by Frank Macfarlane Burnet, based on Ray Owen’s chimerism studies showing the inability of dizygotic twin calves with shared circulations to reject one-another's different blood groups. Burnet indicated that exposure of genetically different cells during embryonic life would not lead to antibody formation (*11*).

The work of John Main and Richmond Prehn in animal models reported successful outcomes in allotransplantation when chimerism was induced in adult donors by total-body irradiation and inoculation of donor-derived bone marrow (*12*). Later, human data showed that irradiation, but not total chimerism, was necessary for inducing tolerance to an allograft (*13*). However, side effects of total-body irradiation lead to high rate of infections and mortality. It was the introduction of immunosuppressive agents in the 1970s that overcame acute rejection and made transplantation a feasible treatment.

The existence of alloantigens was proved in 1938 by Peter Gorer, who showed production of antibodies against “Antigen II” (today named as H-2) when transplanting tumours from an Antigen II-expressing mouse strain into an Antigen II-negative strain. In 1950, George Snell and George Higgins characterised the Major Histocompatibility Complex (MHC) as a critical antigenic determinant to cause rejection (*14*).

Genetic matching of donor and recipient and immunosuppressive treatments have made possible over 90% one-year graft-survival for most types of organs (*15*). However, the majority of transplanted organs fail within the first 20 years following transplantation (*1,*

16-19) due to rejection and toxicity of immunosuppressive drugs (*2*). The number of transplantation procedures has been growing over the last two decades but, due to the scarce availability of human organs and the higher risk of rejection in second transplants, there is an urgent need for extending the half-life of transplanted organs. There were 6,044 patients registered for organ transplantation in the UK as of March 2018. Unfortunately, 411 of these patients died while on the waiting list for a transplant (*1*).

Allografts are subjected to a complex immune response and the balance between inflammatory and suppressive mechanisms would eventually determine the long-term outcome of the transplanted organ. Manipulation of the immune system can extend long-term survival of the graft ensuring that every transplanted organ is as successful as possible. In 1971, Gershon and Kondo made the seminal finding that some T cells, different from helper T cells, can inhibit allogenic immune responses (*20*). Subsequent work by Bruce Hall and Shimon Sakaguchi identified these suppressor cells as $CD4^+CD25^+$ T cells (*21, 22*), today named as regulatory T cells (Tregs) and described in detail in section 1.2. With the discovery of FOXP3 as the "master transcription factor" for Tregs (*23-25*), Tregs have become a cell population of interest to induce transplant tolerance in the clinic.

1.1.1. Mechanisms of rejection

The immune system is designed to defend the host against pathogens and mutated cells. In higher organisms, the immune response includes an innate and an adaptive system which are interconnected. While the innate immune response is generally considered the first line of immunological defence, providing a fast and non-specific response, the adaptive immune system is characterised by a specific and potent response against allogenic antigens. Although the innate immune response is rarely able to reject an allograft in the absence of adaptive immunity, it elicits some graft damage that can be augmented if the adaptive immune response is active. Moreover, pro-inflammatory

signals from innate immune cells initiate and amplify the adaptive immune response. Besides, an emerging paradigm has arisen that there are innate immune cells that can recognise non-self antigens. Monocytes, macrophages and natural killer (NK) cells are capable of mediating innate allorecognition and, even in mice that lack lymphocytes, inflammatory reactions are induced at a greater magnitude by allogeneic transplants than by syngeneic transplants (*26-28*). Hence, the innate and the adaptive immune response convey together and lead to the destruction of the graft.

The adaptive immune response to an allograft involves the activation of both T and B lymphocytes from the transplant recipient patient that recognise genetic disparity between donor and recipient. The specificity of the adaptive immune response is provided by antigen-specific receptors in B cells (BCR) and T cells (TCR). Since the *mhc* locus (also named as Human Leukocyte Antigen (*hla*) in humans) is the most polymorphic gene complex in the genome and given its high density and broad expression, MHC antigens are potently immunogenic and represent the main drivers of rejection. Immune responses against MHC are comprised of both cellular and humoral immune mechanisms. MHC expressed on the cell surface can be bound by antibodies and by B cell receptors, and antigen presenting cells (APCs) can present antigenic peptides from donor MHC to activate T cells (Figure 1.1). Therefore, matching recipients to donors with the closest genetic background at the *mhc* locus greatly reduces the risk of rejection (*29*).

Still, transplants between individuals with identical MHC haplotypes can be rejected. This is a result of other polymorphic non-MHC molecules, named as minor histocompatibility antigens (miHs), such as HA-1, HA-2, HA-3, HA-8, ACC-6 or peptides encoded by Y chromosome in female transplant recipients of male organs (*30*). Consequently, an allograft will inevitably stimulate an immune response against it, which, if allowed to act without restraint, will lead to rejection. The destruction of the allograft is ultimately conducted by antibodies produced by plasma cells, cytotoxic $CD8^+$ T cells and NK cells (*31*).

T cells are the main protagonists of cell-mediated alloreactivity. T cells, once activated by APCs bearing donor-derived peptides, differentiate into effector T cells (Teff) which migrate out of the lymphoid organs to perform their functions in peripheral tissues and/or interact with B cells in germinal centers. Most of Teff are short-lived, but some cells remain as long-lived memory cells, able to remember foreign antigens for most of the life of the individual, and to act rapidly initiating an immune response if the same alloantigen is reencountered. $CD4^+$ T cells (or helper T cells (Th)) interact with peptide-MHC class II complexes expressed on APCs and propagate the allogenic immune response by secreting cytokines and chemokines, and by expressing surface ligands that potentiate the activity of other immune cells (Figure 1.1A). $CD8^+$ T cells recognise peptides presented by MHC class I molecules expressed on all body cells. $CD4^+$ Th cells help $CD8^+$ T cells for their differentiation into cytotoxic T lymphocytes (CTLs). CTLs migrate into the graft and induce apoptosis of target cells by release of soluble factors (such as perforin, granzyme B and tumor necrosis factor alpha (TNF-α)) and by upregulation of death ligands (e.g. Fas ligand) on the cell surface (Figure 1.1B) (*31, 32*).

Th cells also provide help signals to B cells, initiating the humoral immune response (discussed in section 1.1.1.4) (Figure 1.1C).

Transplantation will also elicit the activation and induction of Tregs, whose function will be to counteract the inflammatory response by a wide range of molecular mechanisms (described in section 1.2.3). Ultimately, the proportion of stimulatory and inhibitory signals will determine the strength of the immune response against the allograft.

Figure 1.1

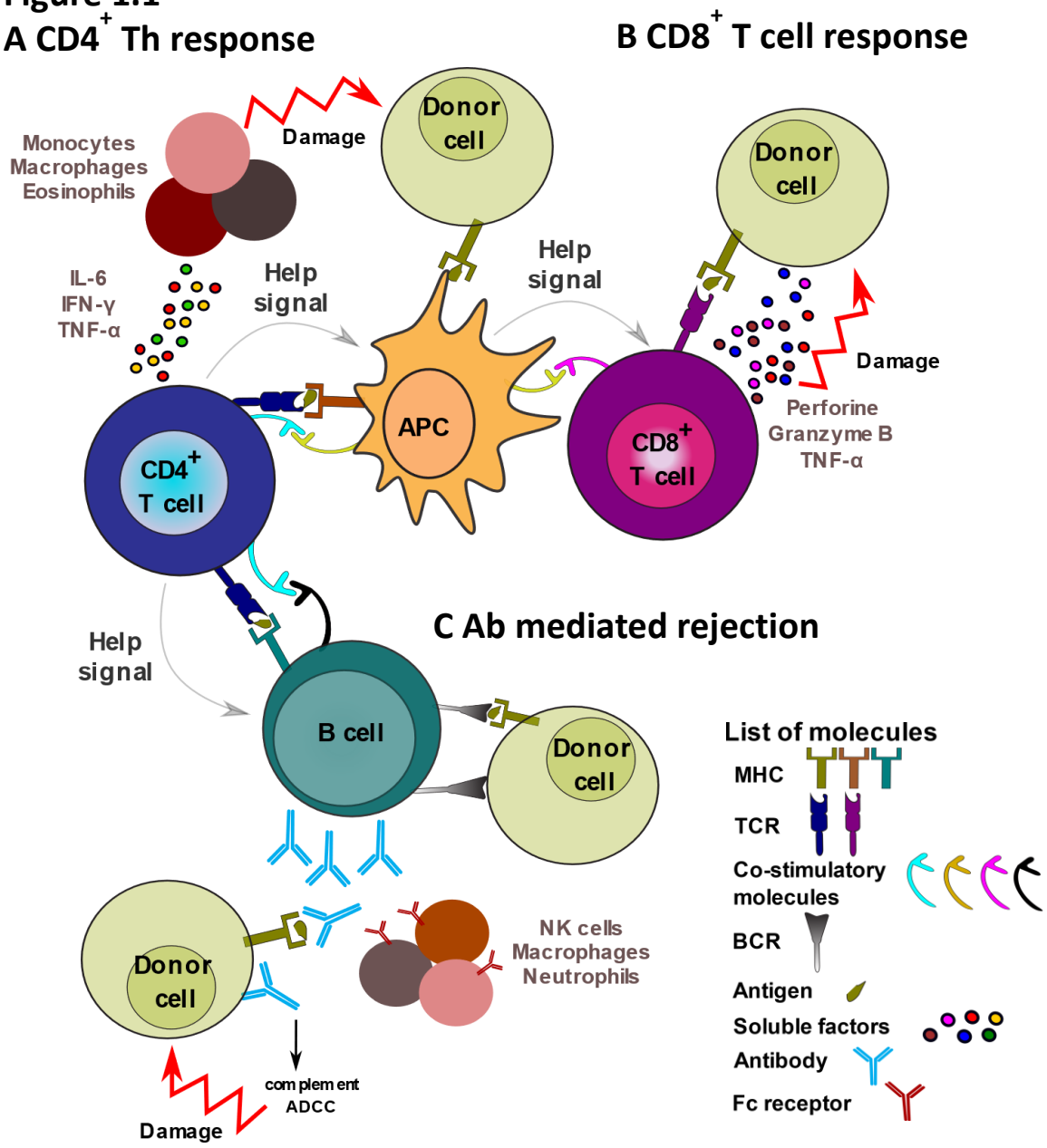

Figure. 1.1. Immune mechanisms of rejection.

(A) Antigen presenting cells (APC) process donor-derived antigens and present them to $CD4^+$ helper T (Th) cells. Additional pro-stimulatory signals for T cell activation, through co-stimulation and cytokines, are also provided by activated DCs. Activated $CD4^+$ T cells secrete pro-inflammatory factors such as IL-6, IFN-γ and TNF-α, which attract monocytes, macrophages and eosinophils that will cause damage to the graft.

(B) $CD8^+$ cytotoxic T cells recognise donor antigens presented by MHC class I. Further help signals from $CD4^+$ Th cells contribute to activation of $CD8^+$ T cells. $CD8^+$ T cells then migrate to the graft and kill target cells by induction of apoptosis through the release of perforin, granzyme B and other soluble factors such as TNF-α.

(C) B cells are responsible for antibody-mediated rejection. B cells can recognise alloantigens presented on MHC class I molecules of donor cells or bind to unprocessed alloantigens in a MHC independent manner. With $CD4^+$ T cell help, B cells then produce antibodies (Ab) that are specific to these alloantigens. The binding of alloantibodies to the graft induces antibody-dependent cellular toxicity (ADCC) and complement fixation, leading to graft damage.

1.1.1.1. Innate mechanisms of graft rejection

The innate immune system from both the donor and the recipient can affect the condition of the graft. Brain or cardiac death, the surgical procedure to retrieve and re-implant the tissue, and reperfusion of the tissue, can all stimulate the innate immune system in response to tissue damage and lead to inflammation (*33-36*). Cells of the innate immune system express pattern recognition receptors (PRRs) specialised in the recognition of repeating structural units in molecules expressed by pathogens (pathogen-associated molecular patterns; PAMPs) or by cells undergoing physiological stress (Damage-Associated Molecular Patterns; DAMPs). Potential infections under non-sterile conditions (e.g. during skin transplantation), local tissue damage and ischemia reperfusion injury will generate many ligands for PRRs. The sensing of PAMPs and DAMPs allows the immune system to clear potentially infected cells and damaged tissue, but also promotes graft rejection. DAMPs can activate the complement system, a proteolytic cascade that plays a significant role in organ damage and activates the adaptive immune response (*37, 38*). Moreover, upon PRR binding, activated leukocytes release pro-inflammatory molecules (including pro-inflammatory cytokines (e.g. interleukin (IL)-1, IL-6 and tumor necrosis factors (TNF)) and chemoattractant cytokines and chemokines which identify the transplant as a site of injury, triggering migration and activation of immune cells into the graft (*39*). Macrophages, neutrophils and other innate immune cells, activated by ligation to DAMPs and in response to cytokines and chemokines, contribute to the local inflammatory environment and can elicit physical damage to the graft (*40, 41*). NK cells are part of the innate immune system but possess a unique recognition system to target and kill cells that lack self-MHC class I, making them relevant during the allogenic response to an allograft (*42*).

New strategies for organ preservation and preconditioning treatments are aiming at the reduction of DAMPs. However, it is still not possible to prevent all tissue damage created by the surgical procedure and ischemia reperfusion injury. The consequent pro-

inflammatory environment within the surrounding of the transplanted organ will activate the innate immune system, which will initiate and amplify the adaptive immune response.

1.1.1.2. The adaptive immune response: T cells

PRR-mediated danger signals results in activation and maturation of APCs, especially dendritic cells (DCs), which upregulate expression of co-stimulatory molecules and pro-inflammatory cytokines and migrate from the transplant to recipient secondary lymphoid tissues (*43, 44*). DCs initiate the adaptive immune response by presentation of alloantigens from the graft to recipient T cells (Figure 1.1). Three main pathways for alloantigen recognition have been described: direct, indirect and semi-direct pathways (*31, 44*). In the direct pathway recipient T cells interact via TCR with donor-derived DCs presenting donor MHC-peptide complexes (*45*). During thymic selection (see section 1.1.2.1), T cells that do not interact with self-MHC are eliminated and, therefore, are not present in the periphery. However, some mature T cells in peripheral tissues can also interact with allogenic MHC-peptide complexes due to TCR cross-reactivity (between self and allogenic MHC), as a consequence of heterologous immunity (a phenomenon in which memory T cells generated against one antigen (such as a pathogen-derived antigen) become activated by an unrelated antigen (such as an allo-antigen) (*46, 47*). In the indirect pathway, recipient APCs capture donor-derived peptides, degrade them intracellularly by the exogenous antigen processing pathway and present alloantigens via their own MHC to T cells. Semi-direct presentation occurs when host T cells interact with donor MHC-antigen complexes expressed on recipient DCs. Recipient DCs can uptake intact donor MHC-peptide complexes by exchange of fragments of plasma membrane with allogenic cells via exosomes or trogocytosis (*48*). While direct recognition dominates early after transplantation, the limited lifetime of donor APCs results in a relatively short time frame for this allo-recognition pathway to occur. Indirect presentation can persist for the life of the graft and predominates in the long term (*49*).

Recognition of alloantigens presented via MHC by APCs activates intracellular signalling in T cells through the TCR-CD3 complex, which is indispensable for T cell activation. Intracellular signals downstream of TCR are complex and ultimately activate the transcription factors nuclear factor-κB (NF-κB), activator protein 1 (AP-1) and nuclear factor of activated T-cells (NFAT), responsible for upregulation of IL-2 (T cell growth factor) and high affinity IL-2 receptor α-chain (CD25) among other targets.

Although being crucial for activation of antigen-specific T cells, TCR stimulation alone is not sufficient to fully activate naive T cells and, in the absence of further signals, T cells become anergic (*50-52*). A “three-signal model” for T cell activation has been postulated: naive T cells (I) need to recognise antigenic peptides by interaction of TCRs with antigen-MHC complexes, additional (II) co-stimulatory signals and (III) cytokines, typically provided by activated APCs, further promote T cell activation and differentiation. Finally, subsequent recruitment of signalling and adhesion molecules into an immunological synapse allows full T cell activation.

Even though signals delivered by co-stimulatory molecules and cytokines are not antigen-specific, these signals are essential for the development of an anti-graft response. Co-stimulation and cytokines regulate T cell function, proliferation and polarisation towards different T cell subsets. For example, secretion of IL-2, which is upregulated in $CD4^+$ and $CD8^+$ T cells upon TCR activation, acts as a growth factor in autocrine and paracrine manner. Depending on the cytokine milieu, $CD4^+$ T cells can differentiate into different Th subsets referred to as Th1, Th2, Th9, Th17, Th22, Tfh (T follicular helper) or Treg cells, with distinct migratory and effector functions that allow for a specialised immune response against different pathologies (*53-55*). Co-stimulation, co-inhibition and cytokines play also an important role in modulating effector function and exhaustion in both $CD4^+$ and $CD8^+$ T cell subsets (*56*).

Co-stimulatory and co-inhibitory receptors (named collectively as co-signalling molecules) can be divided into two superfamilies: the immunoglobulin superfamily (IgSF) (e.g. CD28, ICOS, CTLA-4 and PD-1) and the tumor necrosis factor receptor superfamily (TNFRSF) (e.g. CD27, 4-1BB, OX-40 and CD40). Members of both families can act as co-stimulatory or co-inhibitory receptors, promoting or limiting the T cell response respectively. Co-signalling pathways act on particular aspects of the T cell response, such as cell cycle progression, acquisition of effector or memory function, differentiation into specific T cell subsets or progression towards exhaustion. Therefore, they are critical in directing T cell activity and fate. The function of each co-signalling molecule is regulated by the expression pattern of receptor-ligand molecules according to the type and activation status of the cell. It is noteworthy that different co-signalling molecules are expressed in an overlapping spatiotemporal fashion and can activate similar intracellular pathways. Hence, it is important to study the function of individual co-signalling pathways during the T cell response as well as to know how these signals integrate. An overview of main co-stimulatory and co-inhibitory receptor-ligand pairs in T cell function is shown in Table 1.1.

Table 1.1. Major co-stimulatory and co-inhibitory molecules in T cell function

Receptor	Receptor expression	Major effect in T cell activity	Ligand	Ligand expression	Refs
Co-stimulatory molecules					
CD28	Constitutive in most T cells, including Tregs	- Lowers TCR signalling threshold and promotes T cell proliferation and activation. Important for initiation and amplification of the T cell response. - Crucial co-stimulatory molecule for Treg development and function	B7-1 (CD80) B7-2 (CD86)	Activated APCs	(*57-62*)
CD40L (CD154)	Induced upon activation on T cells, NK cells, macrophages, monocytes	- Induces DC maturation and T cell activation and proliferation	CD40 (TNFRSF5)	APCs, B cells, monocytes, fibroblasts, endothelial cells	(*63*)
ICOS	Activated T cells and B cells	- Induces T cell activation and proliferation - Contributes to survival and proliferation of Teff	ICOSL (B7-H2)	DCs, B cells, monocytes and non-	(*61, 64, 65*)

		- Promotes Treg maintenance - Induces Tfh differentiation		lymphoid tissues	
4-1BB (CD137) (TNFRSF9)	Induced on activated cells: T cells, Tregs, DCs, B cells, NK cells, NKT cells, monocytes, neutrophils, endothelial cells	- Promotes T cell activation and proliferation - Enhances Treg proliferation	4-1BBL	Induced upon activation by APCs, T cells, NK cells	(*66, 67*)
CD27 (TNFRSF7)	Constitutive on T cells, Tregs, NK cells, NKT cells, γδT cells and memory B cells	- Promotes survival of activated T cells, favouring memory cell responses	CD70	Constitutive on thymic epithelium and induced upon activation on: T cells, APCs, NK cells	(*68-74*)
OX40 (TNFRSF4)	Activated T cells, Tregs, NK cells, NKT cells, neutrophils	- Exerts co-stimulatory signalling to T cells - Prevents induction of Tregs in the periphery	OX40L	Activated APCs, T cells, NK cells, endothelial cells	(*75-77*)
GITR (CD357) (TNFRSF18)	Resting and activated T cells, Tregs, DCs, B cells, NK cells, NKT cells, macrophages	- Exerts co-stimulatory signalling to T cells - Reduces Treg suppressive activity but promotes Treg differentiation and proliferation	GITRL (TNFSF 18)	Constitutive on DCs and endothelial cells and upregulated by activated T cells	(*78*)
HVEM (CD270) (TNFRSF14)	T cells, Tregs, APCs, NK cells, monocytes, neutrophils and endothelial cells	- Exerts co-stimulatory signalling to T cells	LIGHT (CD258) (TNFSF 14)	Activated T cells and immature DCs, NK cells, B cells	(*75, 79*)
DR3 (TNFRSF25)	T cells, Tregs, NK cells, NKT cells	- Exerts co-stimulatory signalling to T cells	TL1A (TNFSF 15)	Activated APCs, T cells, endothelial cells	(*75*)
CD30 (TNFRSF8)	Activated T cells, B cells, NK cells, macrophages	- Exerts co-stimulatory signalling to T cells - Promotes Treg function	CD30L (CD153) (TNFSF 8)	Activated T cells, B cells, monocytes, neutrophils	(*75, 80*)
Co-inhibitory molecules					
CTLA-4 (CD152)	Transient expression on activated T cells. Constitutive expression on Tregs	- Competes with CD28 for its ligands impairing T cell activation and proliferation - Supports Treg suppressive function - Induces IDO expression by DCs	B7-1 (CD80) B7-2 (CD86)	Activated APCs	(*58, 60, 81, 82*)

PD-1	Activated T and B cells, Tregs	- Blocks T cell activation and proliferation - Promotes exhaustion in T cells	PD-L1 (B7-H1) PD-L2 (B7-DC)	T cells, B cells, DCs, macrophages and non-lymphoid tissues	(*61, 75*)
TIGIT	Activated T cells, Tregs, NK cells	- Represses TCR-driven activating signals - Induction of tolerogenic DCs	CD155 CD112 CD113	APCs	(*83*) (*84*)
LAG3	Activated T cells, Treg	- Suppresses Teff cell functions - Promotes T cell exhaustion	MHC II	APCs	(*75*)
TIM-3	Activated T cells	- Represses Teff cell responses - Induces exhaustion in T cells	Gal-9 PtdSer HMGB1 CEACAM1	Activated T cells, Tregs, apoptotic cells, endothelial cells	(*75, 85*)
BTLA (CD272)	Naive and activated T cells, naive B cells, DCs, NK cells, NKT cells	- Suppresses T cell proliferation and induces Treg activity - Identifies exhausted T cells	HVEM	Mature DCs	(*79, 86*)
CD160	T cells, NK cells, NKT cells, γδTcells	- Imparts co-inhibitory signals to T cells - Identifies exhausted T cells	HVEM	Mature DCs	(*79*)

ICOS: inducible T cell co-stimulator; GITR: glucocorticoid-induced TNFR-related protein; HVEM: herpes virus entry mediator; DR3: death receptor 3; CTLA-4: cytotoxic T lymphocyte antigen 4; PD-1: programmed cell death 1; TIGIT: T cell immunoreceptor with immunoglobulin and ITIM domains; LAG3: lymphocyte activation gene 3 protein; TIM: type I transmembrane (or T cell) immunoglobulin and mucin; Gal-9: galectin-9; PtdSer: phosphatidylserine; HMGB1: high mobility group box 1; CEACAM1: carcinoembryonic antigen cell adhesion molecule 1; BTLA: B and T lymphocyte attenuator; Tfh: T follicular helper cell.

CD28, the best characterised co-stimulatory receptor, is constitutively expressed by T cells and, upon ligation to members of the B7 family CD80 and CD86 on APCs, transduces intracellular signalling that synergises with the TCR-CD3 intracellular pathway and triggers T cell activation. Co-stimulation via CD28 lowers the threshold for T cell activation, increases IL-2 production and prevents apoptosis (*87*). Activated T cells upregulate CTLA-4, a co-inhibitory receptor that prevents CD28 signalling by binding to CD80 and CD86 with an affinity 10 to 20 times higher than CD28 (*82, 88-90*), and provides a negative feedback of T cell activation. Although CD28 is the most well-described co-

stimulatory receptor, a wide range of co-stimulatory molecules control T cell responses (*75, 91*).

Immunotherapy targeting T cell co-signalling has proven successful for the treatment of several autoimmune diseases, cancer and allograft rejection (*92-97*). Importantly, Tregs express co-stimulatory and co-inhibitory molecules and are, therefore, targeted by agents regulating co-stimulation. For instance, CD28 is crucial for the development and survival of Tregs (*62*), ICOS provides survival signals to Tregs in the periphery, promoting their proliferation and maintenance (*64*), and Treg suppressive activity can be enhanced or impaired by signals through HVEM, GITR and CD30 or 4-1BB, OX40 and DR3 respectively (*66, 75, 77-80*). Moreover, co-signalling molecules expressed on Tregs can exert extrinsic roles engaging receptors on conventional T cells (Tconv) or DCs, an example being interaction of CTLA-4 on Tregs with CD80/CD86 on DCs (*82, 88-90*). Therefore, manipulation of co-signalling pathways may lead to unanticipated outcomes due to their effects in specific T cell subsets. Understating the precise role of co-signalling molecules in different cell populations may further improve and expand clinical therapies based on modulation of co-signalling pathways. In fact, the success of current widely applied therapies targeting CTLA-4 or PD-1 might rely on their effect on multiple cell populations such as $CD8^+$ T cells, $CD4^+$ T cells and Tregs (*98*).

1.1.1.3. The CD27/CD70 co-stimulatory pathway

T cells receive co-stimulatory signals at each stage of differentiation from naive to effector and memory stages. Co-stimulatory molecules from the tumor necrosis factor receptor superfamily (TNFRSF) are important regulators of the T cell response subsequent to the initial CD28 signalling (*99*).

CD27, firstly described by van Lier and colleagues in the 1980s, was found to be expressed by more than 70% of human resting $CD4^+$ and $CD8^+$ T cells in peripheral blood (with some interdonor variability) (*100*). Following studies showed that CD27 is expressed

by NK cells, activated B cells and $CD4^+FOXP3^+$ Tregs (*68-70*), displaying a broad expression pattern. CD27 is transiently increased upon TCR activation but downregulated after prolonged stimulation (*100, 101*).

Soon after the characterisation of CD27, Goodwin and co-workers identified CD70, the unique ligand known for CD27, being expressed by activated T cells and B cells and able to enhance T cell proliferation and effector function upon ligation to CD27 (*102*). More recently, the expression pattern of CD70 has been studied further and found to be tightly controlled and upregulated exclusively upon activation on T cells, B cells, NK cells and certain subsets of DCs (*73, 74*). Therefore, despite its broad expression, CD27 is only stimulated by activated cells in the presence of inflammation, when CD70 expression is upregulated. CD70 expression is very limited in the steady state, although increased levels of CD70 have been associated with inflammatory conditions such as chronic viral infection, cancer or autoimmune disease (*103-112*). Highlighting the importance of this interaction, genetic mutations in CD27 or CD70 in humans can result in persistent symptomatic Epstein-Barr Virus (EBV) infection and EBV-associated lymphoproliferative disorders (*113-117*).

Studies in CD27-deficient mice have shown that CD27 is not essential for T cell development, but provides survival signals to activated T cells through successive rounds of division and, therefore, promotes an antigen-specific memory T cell response (*71, 72*). $CD27^{-/-}$ mice have normal T cell development and number of naive T cells in secondary lymphoid organs, but reduced numbers of effector $CD4^+$ and $CD8^+$ T cells and a defective memory T cell response to a secondary challenge with influenza virus compared to wild type mice (*71*). Similarly, in a mouse model of allotransplantation using $CD27^{-/-}$ mice, accumulation of $CD8^+$ Teff and graft rejection in response to a second allograft appeared to be potentiated by CD27 signals (*118*).

According to their expression patterns, $CD27^+$ T cells can bind CD70 expressed on DCs during priming and CD70 expressed on T cells, DCs and B cells during expansion phase. Mouse strains with constitutive CD70 expression on B cells or DCs develop increased numbers of effector $CD4^+$ and $CD8^+$ T cells, with higher proliferative capacity than wild type mice upon virus infection (*119, 120*). Furthermore, even in the absence of immunization, naive T cells of CD70 transgenic mice (CD70 expressed by DCs or B cells) progressively convert into Teff if stimulated via TCR upon recognition of environmental or autologous antigens (*74, 120, 121*). These results suggest that CD27 signalling promotes activation of T cells with low TCR reactivity and the recruitment of new TCR repertoire into the responding population, identifying a risk for CD27 stimulation in enhancing autoimmune pathologies and rejection to allografts.

Interestingly, discrepancies in $CD27^+$ T cell responses have been observed when CD70 co-stimulation is provided by $CD70^+$ T cells under transient or chronic antigen exposure. Constitutive expression of CD70 on T cells results in accumulation of $CD8^+$ Teff and enhanced primary T cell response against influenza virus infection. However, upon secondary viral challenge, $CD8^+$ T cells become exhausted and memory immune response is impaired (*122*). In agreement with these data, O'Neill *et al*. have proposed that CD70 expressed on T cells delivers apoptotic signals to CD27-expressing T cells. In mouse models of inflammatory bowel disease (IBD) and allogenic graft-versus host disease (GvHD), $CD70^{-/-}$ mice have a more severe phenotype than wild type due to increased survival of activated T cells (*123*).

Additional differences between constitutive CD70 expression on APCs or T cells have been observed *in vivo*. Chronic CD27 stimulation, when binding to CD70 expressed on DCs or B cells, leads to conversion of naive T cells into effector and memory T cells and, eventually, exhaustion of the naive T cell pool. Moreover, increased interferon gamma (IFN-γ) expression from activated T cells results in B cell depletion and profound immunodeficiency symptoms, a phenotype similar to patients with chronic infections like

Human Immunodeficiency Virus (HIV) (*74, 119, 120, 124*). When CD70 is constitutively expressed on T cells, the naive T cell pool is not lost, and B cell depletion is not as severe as in mice with CD70 transgenic-APCs (*122, 125*). Overall, these data indicate that the effect of CD27 signalling might vary depending on the timing and the intensity of the signal. A summary with the major findings in the CD27/CD70 co-stimulatory pathway is listed in Table 1.2.

Table 1.2. Major findings in the CD27/CD70 pathway

Finding/ Model	**Condition**	**Major effects**	**Refs**
CD27 discovery in human	*In vitro*	- CD27 is expressed in resting $CD4^+$ and $CD8^+$ T cells - CD27 increases upon TCR stimulation - CD27 ligation promotes T cell proliferation	(*100*)
CD70 discovery in human	*In vitro*	- CD70 provides co-stimulation for T cell proliferation - CD70 co-stimulation enhances $CD8^+$ Teff cytolytic functions	(*102*)
$CD27^{-/-}$ mice	Steady state	- Normal T cell development and homeostasis: CD27 is not required for generation or antigen-independent expansion/differentiation of T and B cells	(*71*)
	Influenza virus infection	- Reduced numbers of virus-specific T cells during primary response at the site of infection: CD27 is required for survival of Teff - Reduced numbers of virus-specific T cells after secondary infection: CD27 is essential for generation and long-term maintenance of antigen-specific $CD4^+$ and $CD8^+$ T cell immunity	(*71, 72*)
	Allotransplantation	- Allografts are rejected at similar tempo: CD27 signalling is not essential during primary T cell alloimmune responses - Improved allograft survival in sensitised recipients due to deficiency in $CD8^+$ T cell memory formation	(*118*)
Anti-CD70 blocking mAb	Allotransplantation	- Induces long-term survival of allografts in CD28-deficient recipients by inhibiting the activation of effector and memory $CD8^+$ T cells	(*126*)
Treatment with soluble CD70 (agonist for CD27)	OVA-peptide immunisation	- Elicits adjuvant effects for $CD8^+$ T cell responses enhancing proliferation and survival of primed Ag-specific T cells	(*127*)
CD19-CD70tg	Steady state	- Lower activation threshold for priming of naive T cells and favoured conversion into Teff	(*119, 124*)

(constitutive expression of CD70 on B cells)		- Increased numbers of $CD4^+$ and $CD8^+$ Teff - Depletion of the naive T cell pool - Depletion of B cells by IFN-γ-secreting T cells	
	- Influenza virus infection - Tumor challenge	- Augmented expansion of antigen-specific $CD8^+$ T cells and maintenance in memory stage by avoiding the contraction phase - Increased $CD8^+$ Teff functions	(*121*)
CD11c-CD70tg (constitutive expression of CD70 on DCs)	Steady state	- Lower activation threshold of naive T cells and favoured conversion into Teff - Depletion of the naive T cell pool and B cells	(*120*)
	Peptide immunisation prior to OVA or tumor challenge	- Breaks T cell tolerance: conversion of $CD8^+$ T cell tolerance into potent antitumor and antiviral memory immunity	(*120*)
CD2-CD70tg (constitutive expression of CD70 on T cells)	Steady state	- Increased $CD8^+$ Teff cell numbers - $CD8^+$ and $CD4^+$ Teff cells with exhausted phenotype	(*122*)
	Influenza virus infection	- Enhanced primary $CD8^+$ T cell response - Impaired memory $CD8^+$ and $CD4^+$ T cell response upon chronic infection	(*122*)
$CD70^{-/-}$ mice	IBD and GvHD	- More severe IBD and GvHD: CD70 co-stimulation induces caspase-dependent T cell apoptosis and upregulation of inhibitory immune checkpoint molecules	(*123*)
Treatment with anti-CD27 mAbs	Diverse tumor models	- Different outcomes depending on the backbone of the mAb due to Fc crosslinking with different type of cells	(*128*)

Teff: effector T cells; mAb: monoclonal antibody; OVA: ovalbumin; EAE: experimental autoimmune encephalomyelitis; IBD: inflammatory bowel disease; GvHD: graft versus host disease

1.1.1.4. The adaptive immune response: B cells

B cell receptors (BCRs) bind to donor MHC class I molecules or to unprocessed alloantigens, either soluble or on the cell surface, in a MHC-independent manner (Figure 1.1C). B cells take up or engulf antigens, process them and present antigenic peptides via MHC class II to $CD4^+$ T cells. $CD4^+$ T cells will then provide additional signals required for B cell activation, often as CD40-CD40L interaction and cytokine signalling. In most of cases, B cells require help from $CD4^+$ T cells that are reactive to the same antigen, becoming anergic otherwise (*129*). B cells are an important part of the humoral immune response as they can differentiate into plasma cells and produce high-affinity antibodies

against donor MHC and miHs. Antibodies bind to alloantigens on the cell surface of donor cells, identifying them as targets for phagocytosis, antibody-dependent cellular cytotoxicity (ADCC) or for complement-mediated cytolysis (*31, 130, 131*). Antibody binding to endothelial cells guides complement activation that causes pores in the cell membrane and leads to destruction of the vascular integrity (*37, 38, 131*). During ADCC, NK cells, neutrophils and macrophages bind to antibody-coated target cells via low affinity Fc receptors and exert cytotoxic mechanisms, such as secretion of perforin, granzymes and cytokines, that result in apoptosis of target cells (Figure 1.1C) (*31, 131*).

Patients that have donor-reactive antibodies at the time of transplantation often suffer from hyperacute rejection due to antibodies activating the coagulation and complement cascades just after reperfusion of the organ (*132*). This type of rejection is avoided by checking for ABO compatibility and for the presence of anti-donor HLA antibodies. Moreover, increasing evidence is implicating the generation of *de novo* donor-specific antibodies (DSA) as an essential mechanism for acute and chronic allograft damage (*130, 133, 134*). B cells can also differentiate into antigen specific memory B cells and sustain long-term humoral memory against the graft.

The role of B cells in the response towards and allograft goes beyond production of antibodies. B cells act as APCs, presenting antigens and providing co-stimulation to $CD4^+$ T cells, secrete cytokines that modulate the T cell response and form tertiary lymphoid organs within the allograft that may propagate local humoral and cellular alloimmune responses (*135-137*). Moreover, B cells with immunosuppressive properties have also been described and may help in inducing tolerance (*138*).

1.1.2. Mechanisms of immune tolerance

1.1.2.1. Central tolerance

During lymphocyte development, somatic recombination generates a huge variety of T cell and B cell receptors and forms the basis of the highly specific response of the adaptive immune system. The TCR in T cells needs to bind residues in both the peptide presented by MHC and the MHC molecule itself. In the thymus, T cell precursors that possess TCRs able to bind to self-MHC on thymic epithelial cells are positively selected, while T cells with TCRs with low or non affinity for self-MHC undergoes programmed cell death (*139*). In order to avoid autoimmunity, it is crucial to eliminate cells that contain receptors that interact with autoantigens. Clonal deletion in the thymus is the first line of defence against pathogenic auto-reactive T cells. Thymic medullary cells, under the control of the autoimmune regulator (AIRE) transcription factor, express a wide range of antigens from all parts of the body and guide the elimination of self-reactive T cells (*140*).

In a similar process to T cells, immature B cells expressing BCR reactive for self-antigens are subjected to clonal deletion (apoptosis-mediated), anergy (unresponsiveness) or receptor editing (BCR re-arrangement) in the bone marrow (*130, 141*).

1.1.2.2. Peripheral tolerance

Negative selection is not a perfect process and some cells with some degree of autoreactivity escape into the periphery. Moreover, the immune system must be able to tolerate harmless foreign antigens, for example those generated from microbiota. Tolerance mechanisms in the periphery offer a second layer of protection to avoid damage to self-tissue.

Certain autoantigens are being ignored because their low immunogenicity or their anatomical location in immune-privileged sites such as the eye, the brain, the placenta,

the reproductive tract or the testis (*142*). If autoantigens are encountered by T cells in the absence of inflammation, the absence of co-stimulation by APCs induces anergy rather than T cell activation (*50-52, 143*). Co-inhibitory signals, provided by co-inhibitory receptors such as PD-1 and CTLA-4, also inhibit T cell proliferation and can control self-reactive T cell responses (*139*). Moreover, T cells that have been stimulated repetitively overexpress death receptors (e.g. Fas (CD95)) and their ligands, leading to apoptosis (*139*).

Autoreactive B cells that have not be eliminated in the bone marrow are also subjected to apoptosis, anergy or receptor editing in the spleen (*130, 141*).

Additionally, regulatory cell populations, including $CD4^+FOXP3^+$ Tregs (discussed in section 1.2), offer active and dominant regulatory mechanisms suppressing T cells reactive to self or innocuous antigens, which control excessive immune responses and maintain immune homeostasis (*144*).

1.2. Overview of regulatory T cells

1.2.1. Development of Tregs

$CD4^+FOXP3^+$ Tregs are generated both in the thymus (tTregs), as a separate lineage from Tconv cells, and in the periphery (pTregs) by induction of FOXP3 expression in naive $CD4^+CD25^-FOXP3^-$ T cells.

In the thymus, $CD4^+$ T cells are positively selected for self-MHC interaction and negatively selected for recognition of self-peptide-MHC complexes (see section 1.1.2.1). In contrast to $CD4^+$ Tconv cells, Tregs have an autoreactive TCR repertoire implying that Tregs can escape negative selection in the thymus. During thymic development, a Treg progenitor within single positive $CD4^+$ cells emerges expressing CD25. FOXP3 expression is then

induced upon TCR signalling, CD28 co-stimulation, and IL-2 stimulation in $CD4^+CD25^+$ Treg precursor cells (Figure 1.2A) (*145-147*).

Several hypotheses have been suggested to explain the resistance of Tregs to clonal deletion. The strength and duration of TCR signalling during thymic differentiation may control whether autoreactive T cells are eliminated or converted into Tregs (*148*). A role for AIRE-expressing medullary thymic epithelial cells (mTECs) in inducing FOXP3 expression has also been proposed. Studies using mice with a fluorescent protein expressed broadly or tissue-specific show that T cells reactive to ubiquitously expressed antigens are mostly eliminated, whereas T cells reactive to tissue-restricted peptides are likely to develop into Tregs. Hence, mice lacking AIRE have twofold reduction in Treg numbers in the thymus (*149*).

Moreover, Coquet *el al*. have proposed that CD70 co-stimulation can rescue Tregs from apoptosis during clonal deletion without acting on Tconv cells (*150*). CD70 is expressed on DCs and epithelial cells in the thymic medulla, including AIRE-expressing cells. The authors suggest that both CD28 and CD27 co-stimulatory signals contribute, in a non-redundant manner, to Treg development. While CD28 signals support FOXP3 induction (*146*), CD27 provides survival signals to developing Tregs by counteracting the mitochondrial apoptosis pathway. Hence, $CD27^{-/-}$ mice have reduced Treg but similar Tconv cell numbers as wild type mice (*150*).

Peripheral Tregs (pTregs) develop from $CD4^+$ Tconv cells in the periphery (Figure 1.2A) and are believed to confer tolerance against foreign antigens, although it is difficult to discern the effect of pTregs from tTregs. pTregs are generated upon TCR stimulation under tolerogenic conditions, such as the presence of tumor growth factor-beta (TGF-β) or activation by tolerogenic APCs. The gut is considered a major site for pTreg induction, which confers tolerance to non-pathogenic antigens derived from commensal microbiota and food allergens. Metabolites of the microbiota, such as butyrate or

propionate, and certain bacterial short chain fatty acids stimulate Treg differentiation in the colon (*151*). Tolerogenic DCs, by expression of co-inhibitory molecules and secretion of soluble factors like indoleamine 2,3-dioxygenase (IDO), TGF-β or retinoic acid can also contribute to pTreg induction (*152*).

In vitro, FOXP3$^+$ suppressive Tregs can be generated from naive CD4$^+$FOXP3$^-$ T cells by culturing in the presence of TGF-β, IL-2 and anti-CD3 stimulation (Figure 1.2B) (*54*). Importantly, these *in vitro*-induced Tregs (iTregs) do not completely recapitulate all characteristics of *in vivo* generated pTregs. iTregs have reduced suppressive potency and different epigenetic and transcriptional profiles compared to pTregs (*153, 154*), which needs to be considered for the potential clinical application of iTregs.

Figure 1.2

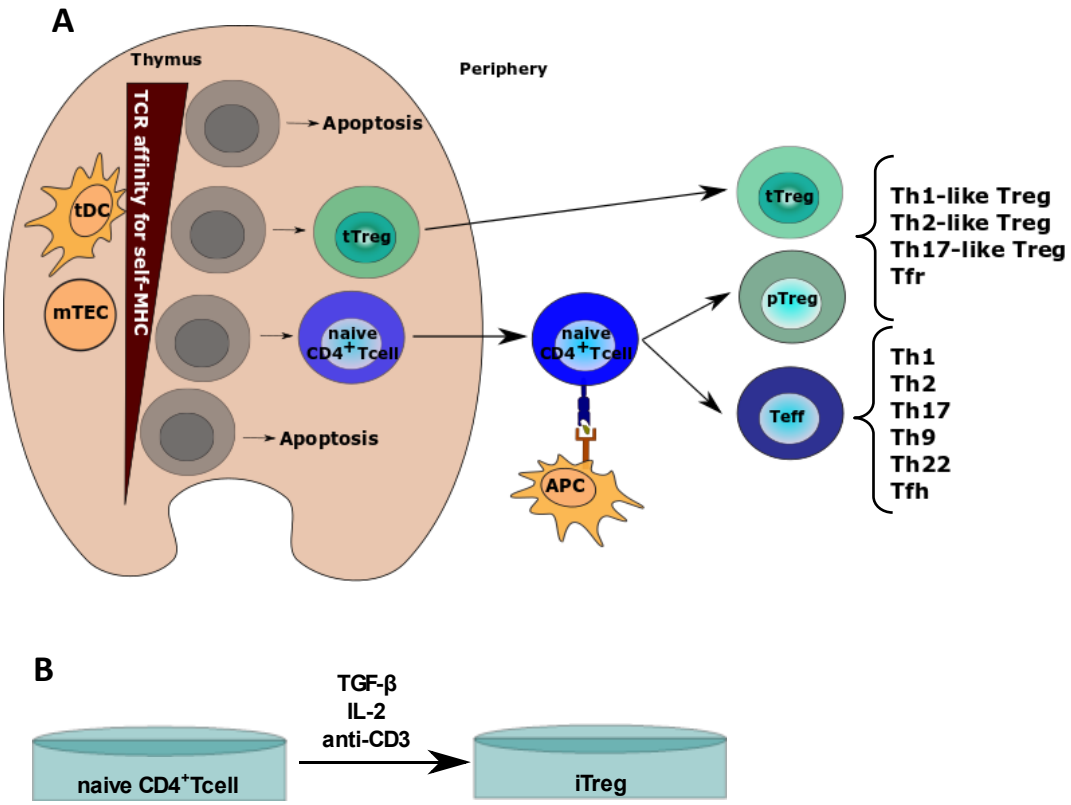

Figure 1.2. Development of Treg subsets.

(A) T cell precursors migrate from the bone marrow to the thymus where they undergo TCR gene rearrangement and, upon interaction with thymic dendritic cells (tDC) and medullary thymic epithelial cells (mTEC), are subjected to positive selection for self-MHC and negative selection for self-antigens. Naive T cells with low-affinity for self-antigen-MHC complexes are selected for maturation and occupancy of peripheral tissues. Treg cell fate in the thymus appears to be regulated by the strength of TCR signalling and additional co-stimulatory signals. Naive T cells and thymic Tregs (tTregs) migrate to peripheral tissues. Naive T cells, upon interaction with activated antigen presenting cells (APC) will maturate to effector T cells (Teff). Alternatively, a regulatory phenotype can be induced in Teff within secondary lymphoid organs, resulting in development of peripheral Tregs (pTreg). Differential expression of transcription factors, chemokine receptors and other functional properties distinguish different T cell subsets within tTreg, pTreg and Teff cell populations. Some of these cell subpopulations are Th1, Th2, Th9, Th17, Th22, T follicular helper (Tfh) and T follicular regulatory (Tfr) cells.

(B) *In vitro*-induced Tregs (iTreg) can be generated from naive $CD4^+FOXP3^-$ T cells when cultured in the presence of TGF-β, IL-2 and anti-CD3 stimulation.

tTregs and pTregs have distinct methylation patterns at the *foxp3* locus, which are responsible of differential regulation of FOXP3 expression between both cell populations (*155*). The *foxp3* gene contains three highly conserved non-coding sequences (CNS) and a promoter region with binding sites for transcription factors such as NFAT, AP-1, c-Rel,

FOXO1, FOXO3, SMAD3 or STAT5 (*156*). Demethylation at each CNS region allows binding of transcription factors that control FOXP3 expression at different stages of Treg development. CNS3, also named as pioneer element, is required for opening the *foxp3* locus in first instance. A demethylated CNS1 is crucial for FOXP3 expression in pTregs, although is dispensable during tTreg development. Demethylation at CNS2 (also named as Treg cell-specific demethylated region (TSDR)) is not essential for induction of FOXP3 expression but is required for sustained FOXP3 expression in dividing Tregs. Hence, a demethylated TSDR ensures stability of FOXP3 expression during proliferation and distinguishes tTregs from pTregs (*155*).

HELIOS and neuropilin-1 have also been proposed to distinguish tTregs from pTregs in mice (*157-159*). Upon transfer to lymphopenic mice, FOXP3 is downregulated preferentially in HELIOS$^-$ Tregs than in HELIOS$^+$ Tregs. However, HELIOS expression does not affect the ability of Tregs to suppress IBD *in vivo* (*160*). In human, HELIOS has been found to be expressed by pTregs and activated T cells, and not expressed in some tTregs (*161-163*). Similarly, neuropilin-1 does not seem to be regulated in the same way in human Tregs, since levels of expression in human is much lower than in mice (*164*). Therefore, the applicability of HELIOS and neuropilin-1 to identify human tTregs and pTregs is limited. Still, they may act as markers for the identification of Treg subsets with potent suppressive activity and prolonged stability (*165*).

1.2.2. Treg phenotype

In spite of the discovery of suppressor T cells in the 1970s (*20*), the inability to phenotypically identify the specific cell subset with suppressive capacity limited their understanding and usage. Bruce Hall studied how rats treated with cyclosporine developed operational tolerance towards a cardiac allograft. He showed that, when transferred into a naive irradiated recipient, T cells from these rats were capable of conferring tolerance to an allograft from the same donor strain as the primary graft (but

not to a third-party graft) (*166*). Moreover, he already identified these immune suppressive cells as $CD4^+CD25^+$ T cells (*21*). In subsequent investigations, Sakaguchi and co-workers discovered that $CD4^+CD25^+$ Tregs were present within the normal T cell repertoire in healthy tissue and had the ability to inhibit activation of $CD25^-$ T cells and to maintain and induce tolerance to self and non-self antigens (*22*). While depletion of $CD4^+CD25^+$ T cells in mice led to autoimmunity and enhanced immune response towards allogenic transplants, reconstitution with $CD4^+CD25^+$ T cells inhibited exacerbated inflammatory responses (*22*). In humans, high CD25 (IL-2 receptor α-chain) in combination with low or absent CD127 (IL-7 receptor) cell surface expression allows a better distinction of Tregs from $CD4^+$ Teff cells (*167, 168*).

In 2001, the role of the transcription factor FOXP3 (Forkhead-Box-Protein P3) in maintaining immune homeostasis in mice and humans was discovered. In scurfy mice, loss-of-function mutations in *foxp3* result in the development of a fatal autoimmune disorder (*169*), while in humans, inactivating *foxp3* mutations have been found to be associated with an X-linked disorder, IPEX (immunodysregulation polyendocrinopathy enteropathy X-linked) (*170, 171*). More detailed analysis of scurfy mice by Khattri and colleagues linked FOXP3 expression with $CD4^+CD25^+$ Tregs (*172*). Subsequent studies demonstrated the essential role of FOXP3 as key transcription factor for Treg development and function showing that ectopic expression of FOXP3 into $CD4^+CD25^-$ Tconv cells confers suppressive capacity, and adoptive transfer of $FOXP3^+$ cells into $FOXP3^{-/-}$ scurfy mice rescues mice from their lymphoproliferative disorder (*23-25*).

A specific phenotypic identification of Tregs would improve our understanding of the role of Tregs during the course of a disease (such as transplant rejection, autoimmunity, infections and cancer) or in response to therapeutic interventions. However, both CD25 and FOXP3 are upregulated upon TCR stimulation and the $CD4^+CD25^+FOXP3^+$ phenotype does not uniquely differentiate human Tregs from other activated T cells (*173*). Currently, differential methylation levels at the *foxp3* locus, particularly a demethylated

TSDR, constitutes the most accurate marker to distinguish Tregs from $CD4^+$ Tconv cells and iTregs (*154, 173*).

Intracellular markers are not compatible with isolation of viable cells and limit their applicability for research and therapeutic applications. Although transcriptomic studies have defined a "Treg-gene signature" that further helps in the discrimination between Tregs and Tconv cells (*174, 175*), a definitive cell surface marker for $FOXP3^+$ Tregs has not yet been identified. Still, a wide range of cell surface molecules have been found to be preferentially expressed by Tregs or involved in Treg function. Some of these include CD25 (*22*), Glucocorticoid-Induced Tumour Necrosis Factor Receptor (GITR) (*78*), CD39 (*176*), CD62L (*177*), CD45RA (*178*), CD27 (*179, 180*), ICOS (*181*), HLA-DR (*182*), CTLA-4 (*82, 88-90*), Lymphocyte Activation Gene 3 (LAG-3) (*183*) and CD15s (*184*) among others. Increasing evidence shows heterogeneity in the $FOXP3^+$ Treg population, in which additional makers identify Treg subsets at different stages of differentiation and with distinct stability, migration and functional capacities (*185, 186*).

1.2.3. Regulatory activity of Tregs

Tregs can suppress immune responses by acting on cells of the innate immune system (DCs and NK cells) as well as adaptive T or B lymphocytes. Tregs use a broad array of molecular mechanisms which involve cell-contact dependent mechanisms (*88, 90, 187, 188*), the release of immunosuppressive soluble factors (TGF-β, IL-10, IL-35) (*189, 190*), or chemokines (*191*), deprivation of growth factors (in particular IL-2 by expression of CD25) (*192*), induction of apoptosis of target cells by secretion of granzyme A, granzyme B and perforin (*193*), or ATP consumption and adenosine production by the action of CD39 and CD73 (*176, 194*).

Tregs inhibit activation and proliferation of Tconv cells directly or by hindering the function of APCs suppressing their maturation, inducing secretion of anti-inflammatory molecules

and stripping co-stimulatory ligands from APCs (*183, 195*). In this regard, secretion of IL-10 and CTLA-4 expression are the best studied regulatory mechanisms in Tregs. In mice, Treg-secreted IL-10 is required for suppression of skin rejection (*196*), protection against experimental colitis (*189*), and tolerance to leishmania (*197*). CTLA-4 expressed by Tregs binds to CD80 and CD86 co-stimulatory molecules expressed on DCs. This interaction inhibits DC maturation and induces the release of IDO by DCs (*187*). CTLA-4 intracellular signaling is also important for Treg function promoting FOXP3 expression (*88, 198*). Moreover, CTLA-4 antagonises the binding of CD80/CD86 to CD28 on Tconv cells, impairing DC-driven co-stimulation (*82, 88-90*). Dhainaut *et al.* have reported a similar role for CD27 expressed on Tregs, whereby $CD27^+$ Tregs bind to CD70 on DCs and prevent DCs to provide co-stimulation via the CD27/CD70 pathway to Tconv cells (*188*).

Although activation of Tregs is antigen specific, since it requires TCR stimulation via interaction with antigen-MHC complexes, their suppressive function is non-antigen specific; Tregs activated in response to a specific antigen are capable to suppress T cells with different antigen-specificity. This phenomenon has been termed “bystander suppression”. Moreover, the suppressed T cell can acquire a Treg phenotype and induce other naive T cells to become Tregs. This propagating regulatory mechanism is named infectious tolerance (*199*) and has great importance for achieving tolerance by Treg cell therapy.

Of note, other cell subsets with regulatory activity have been described (summarised in Table 1.3), such as IL-10 producing T cells (Tr1 cells) (*200-203*), TGF-β-secreting T cells (Th3 cells) (*204*), IL-35-secreting $FOXP3^-$ iT(R)35 cells (*205*), $CD8^+$ Tregs (*206, 207*), γδ T cells (*208, 209*), NKT cells (*210-213*), $CD4^-CD8^-$ double negative (DN) Tregs (*214*), regulatory B cells (Bregs) (*138, 215*), mesenchymal stromal cells (MSCs) (*215*), myeloid-derived suppressor cells (MDSCs) (*215*) and tolerogenic DCs (*216*).

Table 1.3. Regulatory cell populations

Cell population	Phenotype (human)	Main regulatory mechanism	Published clinical trials
CD4$^+$ regulatory T cells (Tregs)	CD4$^+$ CD25$^+$ CD127$^{-/low}$ FOXP3$^+$	See section 1.2.3.	https://clinicaltrials.gov/ GvHD (*217-223*), solid organ transplantation (*224*), and autoimmunity (*225-228*)
Tr1 cells (*200-203*)	CD4$^+$ CD45RO$^+$ FOXP3$^-$ CD49b$^+$ LAG3$^+$	IL-10 secretion	GvHD (*221*)
CD8$^+$ Tregs (*206, 207*)	• CD8$^+$ CD25$^-$ CD28$^-$ • CD8$^+$ CD25$^+$	• Inhibition of APC-mediated T cell activation and secretion of IL-10 • Inhibition of T cell proliferation by expression of CTLA-4 and TGF-β	
Regulatory B cells (Bregs) (*138, 215*)	CD19$^+$ CD20$^+$ CD24^{hi} CD27$^-$ CD38^{hi}	• Secretion of inhibitory cytokines (IL-10, TGF-β and IL-35) • Treg induction	
Tolerogenic DCs (*216*)	MHCII^{lo} CD86^{lo} CD80^{lo} CD40^{lo}	• Cell surface expression or secretion of inhibitory molecules (i.e. PD-L1, FasL, IL-10, IDO) • Treg induction • Induction of anergy in T cells	Phase I healthy volunteers (*229*), diabetes (*230*), rheumatoid arthritis (*231, 232*), Crohn disease (*233*) and solid organ transplantation (prospective) (*234*)
Regulatory macrophages (*235*)		• IL-10 secretion • Inhibition of T cell proliferation	Kidney transplantation (*236*)
Mesenchymal stromal cells (MSCs) (*215*)	CD34$^-$ CD45$^-$ CD73$^+$ CD90$^+$ CD105$^+$ HLA$^-$DR$^-$	• Treg induction	Rheumatoid arthritis (*237*) and kidney transplantation (*238, 239*)
Myeloid-derived suppressor cells (MDSCs) (*215*)	CD11b$^+$ CD33$^+$ CD34$^+$ HLA-DR^{low}	• iNOS and Arg-1-dependent inhibition of T cells, B cells and NK cells • Treg induction • IL-10 secretion • Inhibition of DC maturation by HO-1	
γδ T cells (*208, 209*)		• TGF-β and IL-10 secretion • CTLA-4 and PD-L1 - mediated suppression	

NKT cells (*210-213*)	Vα24Jα18^{+} Vβ11^{+}	• IL-10 production • Cytokine mediated-promotion of Tregs and regulatory DCs	
Double negative (DN) Tregs (*214*)	CD25^{lo} CD28^{lo} CTLA4^{-} CD38^{lo}	• Inhibition of T cell proliferation • Inhibition of APC-mediated T cell activation	
Facilitating cells (*240*)	Several populations	• Enhance stem cell engraftment for mixed chimerism therapy • Induction of Treg function	Kidney transplantation (*241, 242*)

GvHD: graft versus host disease; FasL: Fas ligand; PD-L1: programmed death ligand-1; IDO: indoleamine dioxygenase; iNOS: inducible nitric oxide synthase; Arg-1: arginase 1; HO-1: heme oxygenase 1

1.2.4. Functional plasticity of Tregs

Originally, tTreg were thought to be a phenotypically and functionally stable population while iTregs and pTregs displayed unstable regulatory activity. However, a number of studies have now shown that some tTreg might become unstable under certain inflammatory conditions and adopt a phenotype more characteristic of effector CD4^{+} T cells, losing their suppressive function and secreting pro-inflammatory cytokines (*243-248*). Zhou *et al.* examined Treg plasticity using tracer mice containing FOXP3-GFP-Cre crossed with Rosa26-YFP, which allows to study FOXP3 induction and down-regulation simultaneously. Downregulation or loss of FOXP3 expression was demonstrated in a substantial percentage of cells under homeostatic and autoimmune conditions (*245*). However, Rubtsov *et al*., using similar approach (GFP-FOXP3-Cre-ER x Rosa26-YFP mice), showed stable FOXP3 expression in healthy mice (*249*). Tsuji *et al.* proved that some FOXP3^{+} T cells from FOXP3-GFP mice transferred to T cell-deficient mice can convert into FOXP3^{-} cells and differentiate into Tfh cells (*244*). Oldenhove *et al.* suggested that pro-inflammatory cytokines in mice infected with *Toxoplasma gondii* cause Tregs to downregulate FOXP3 and acquire T-bet and IFN-γ expression (*243*). Supporting the

destabilising role of pro-inflammatory cytokines, Yang *et al.* showed that *in vitro* treatment with IL-6 and IL-1 or IL-23 leads to a Treg population that express IL-17 and has impaired suppressive capacity (*248*). All suggest that the stability of the Treg lineage may be regulated by environmental cues.

Importantly, Treg suppressive function is not attributed to a single regulatory pathway. Instead, Tregs use numerous suppressive mechanisms, which allow for a specialised response according to the environment, the anatomical location, and the type of the cell to suppress (*250, 251*). Thus, there is versatility and adaptability in the Treg response and it is likely that individual regulatory pathways are differentially redundant depending on the immune setting. Likewise, it is possible that particular subpopulations of Tregs may use distinct mechanisms of suppression or preferentially mediate inhibition of different immune cell populations.

Interestingly, phenotypically distinct Treg subsets have been described that mirror $CD4^+$ Th cell populations by specific co-expression of chemokine receptors, cytokines, and lineage specifying-transcription factors classically associated with Th effector cells (*186*). For instance, Tregs can upregulate T-bet and CXCR3, IRF4 and CCR4, RORγt, STAT3 and CCR6 or Bcl6 and CXCR5 mirroring Th1, Th2, Th17 and Tfh cells respectively. Acquisition of Th-lineage specific transcription factors in Tregs may induce the expression of particular genes involved in selectively suppressing their Teff cell counterpart. It has been suggested that inflammatory cues from the immune environment drive Th and Treg subsets to differentiate in parallel, resulting in the development of Treg subsets capable to co-localise with particular Th cell subsets *in vivo* and to exert specific immune regulatory activity towards different types of inflammatory responses (*186*).

However, the expression of Th-associated molecular signatures by Tregs might also be an indication of loss of suppressive activity. An increase in IFN-γ-producing Tregs has been associated with type-1 diabetes and multiple sclerosis (*252, 253*). Also, the

frequency of Tregs expressing IL-17 is increased in human patients affected by psoriasis, IBD and rheumatoid arthritis, compared to healthy individuals (*254-256*). These data suggest that some Th-like Tregs may lose their ability to suppress immune responses and, instead, may contribute to autoimmune pathogenesis.

1.3. Clinical strategies to prevent allograft rejection

1.3.1. Pharmacological immunosuppression

The current strategy to avoid rejection in solid organ transplantation is pharmacological immunosuppression, which usually includes induction of strong immunosuppression for short-term followed by life-long treatment with a combination of immunosuppressive drugs. Immediately after transplantation, significant group of patients is being treated with monoclonal or polyclonal antibodies (e.g. alemtuzumab (anti-CD52 mAb) or anti-thymocyte globulin) that deplete recipient's leukocytes. After leukocyte depletion, Tregs and Bregs have been found within the repopulating leukocytes, suggesting that leukocyte depletion may favor regulatory cells to outnumber pro-inflammatory cells (*215*).

For maintenance of immunosuppression, kidney transplant patients are usually treated with anti-proliferative drugs (e.g. mycophenolate mofetil (MMF)) in combination with drugs that inhibit T cell activation, such as calcineurin inhibitors (tacrolimus or cyclosporine A) or rapamycin (inhibitor of the mammalian target of rapamycin (mTOR) pathway). Depending on the type of transplant and the protocol of the hospital, the combination of drugs selected may vary. For example, anti-CD25 monoclonal antibody therapy is also used as an induction therapy to inhibit T cell proliferation and survival. Other agents directed to prevent T cell or B cell activation are monoclonal antibodies against TCR or BCR, or drugs that block co-stimulation (*215*).

Whilst immunosuppressive treatments have greatly reduced episodes of acute graft rejection leading to a considerable success in short term allograft outcomes, improvement is still needed to extend long-term survival and avoid chronic allograft dysfunction. This is due to direct organ toxicity of the drugs and severe side-effects associated with nonspecific and systemic immune suppression, which results in increased risk of infection, malignancy and cardiovascular disease (*2*). The major goal in clinical organ transplantation is to generate a state of specific unresponsiveness towards the donor; a state of immunologic tolerance whereby the recipient's immune system accepts the graft in the absence of maintenance immunosuppression. A first step in this endeavour is to define the therapeutic strategies that promote donor-specific hyporesponsiveness and determine the mechanisms of tolerance in humans.

1.3.2. Methods to induce tolerance in allogenic transplantation

Data from animal models and operationally tolerant kidney and liver transplant patients (transplant recipients who have been successfully weaned from immunosuppression and have maintained stable graft function for at least one year) provide the proof-of-principle that achieving tolerance in organ transplantation is possible (*257-259*). Experimental methods to induce transplantation tolerance have harnessed (I) central tolerance by induction of chimerism or administration of antigen in the thymus and (II) peripheral tolerance by modulating T cell proliferation and activation using monoclonal antibodies, pharmacological agents or cellular therapies (*259*).

Multiple studies in animal models have confirmed that intrathymic injection of donor antigens coupled to peripheral leukocyte depletion lead to induction of operational tolerance. However, the feasibility of this approach and its efficacy in humans is not optimal (*260*). Another strategy to induce central tolerance to donor antigens is the establishment of hematopoietic chimerism (*261*). In recipients with an established immune system, transplantation of donor bone marrow or haematopoietic stem cells

along with irradiation allows donor cells to engraft in recipient's bone marrow, leading to a state in which donor and recipient cells coexist (state named as mixed chimerism) (*261, 262*). The presence of thymic DCs of recipient and donor origin leads to the development of T cells being educated to become tolerant to recipient and donor antigens. Although, toxicity of the conditioning treatment and development of GvHD have limited its clinical application, promising results in patients of kidney transplantation have been recently reported (*241, 242, 263, 264*). Of note, the work of Megan Sykes and colleagues deserves especial attention. They developed an approach for establishing mixed chimerism using non-myeloablative induction therapy in human patients, which allowed for withdrawal of chronic immunosuppressive therapy after kidney transplantation in HLA-matched and HLA-mismatched settings (*265, 266*).

With the discovery that blocking mAbs against the T cell co-receptors CD4 and CD8 can induce allogenic tolerance in adult mice in a thymus-independent manner, without the need of T cell depletion or stable chimerism (*267*), the concept of reprogramming the peripheral immune system towards a state of transplant tolerance became achievable. In this regard, blockade of co-stimulatory signals leads to anergy of TCR-stimulated T cells (see section 1.1.2.2) and many strategies have focused on blocking CD28 co-stimulatory signalling to induce transplant tolerance. Treatment with the immunoglobulin (Ig) fusion protein CTLA-4Ig (abatacept or belatacept), which binds to CD80/86 and prevents CD28 co-stimulation to T cells, has been studied clinically in renal transplant patients (*97*). Blocking the CD40/CD40L co-stimulatory pathway has also shown promising results in murine and non-human primate models when used as monotherapy or in combination with CD28 blockade (*268-270*). Despite unfortunate side effects related to thrombosis using anti-CD40L mAbs in humans, new strategies targeting CD40 are in development (*271, 272*).

Although naive $CD4^+$ T cells are generally highly dependent on co-stimulation, $CD8^+$ T cells and memory T cells are less susceptible to CD28 or CD40L co-stimulation blockade

(*273-275*). In transplantation, the presence of memory cells is a critical determinant of graft rejection (*47*). Memory T cells can be activated within the graft at lower activation threshold, and their capacity to proliferate, secrete cytokines and exert effector functions is enhanced compared to naive T cells (*47*). Memory T cells reactive for donor-derived antigens can be generated after exposure to blood transfusions, pregnancy, rejection of a previous transplant, homeostatic proliferation, and heterologous immunity (*46*). Memory T cells, therefore, appear as one of the next barriers to overcome in the quest to induce transplantation tolerance.

Other co-stimulatory pathways may have a major role in the regulation of these resistant cell populations. ICOS signalling is important for activation and function of Teff cells and treatment with anti-ICOS blocking mAb prolongs allograft survival (*276-279*). Although CD27 is constitutively expressed on T cells, the inducible expression of CD70 on activated cells suggests a role for CD27-CD70 interaction during the clonal-expansion phase of the T-cell response. In fact, a crucial role for CD27/CD70 pathway in the generation and maintenance of antigen-specific T cell response is well described (see section 1.1.1.3) (*71, 72, 118, 126*). In a fully MHC-mismatched murine model of cardiac transplantation, Yamada *et al*. showed that blockade of CD27/CD70 interaction prevents $CD8^+$ T cell-mediated rejection in CD28-deficient mice (*126*). Yamaura *et al*. demonstrated that while CD27 signalling is not essential for activation of naive alloreactive T cells, memory $CD8^+$ T cell formation is impaired in $CD27^{-/-}$ mice compared to wild type control (*118*). These data confirm the importance of CD27 as a co-stimulatory receptor for alloreactive $CD8^+$ memory T cells in allograft rejection and identifies a potential target to improve co-stimulatory blockade treatments.

An additional natural mechanism by which the immune system suppresses autoreactive T cells that escape deletion in the thymus is by the action of regulatory cell populations in the periphery. Importantly, regulatory immune cells can also prevent immune activation towards alloantigens, being able to induce tolerance and long-term survival of

transplanted grafts (*215, 280*). The concept of clinical therapies aimed at increasing the number or the function of immune regulatory cells over pro-inflammatory cells is appealing since it may allow a reduction in immunosuppressive drugs and toxic side effects.

A broad range of cell subsets with regulatory activity has been described and some of them are being explored as putative cell therapies for immune-mediated pathologies, including transplantation (*215*) (Table 1.3). The ONE Study, a multicenter Phase I/II study, is investigating the safety of infusing immune regulatory cells including Tregs, Tr1 cells, tolerogenic DCs and regulatory macrophages in transplant patients. Tregs have probably the strongest body of evidence supporting transplant tolerance and its applicability as a cellular therapy is discussed in more detail below. One of the concerns about the use of Tregs as clinical therapy is whether global immunosuppression will occur, due to their ability to suppress immune cells with different antigen specificities (see section 1.2.3). If so, it could be argued that Treg therapy may result in increased risk of infections and cancer and offer limited advantage over current immunosuppressive regimens. However, studies in murine models of solid organ transplantation show that mice transferred with Tregs are able to control cytomegalovirus (CMV) infection (*281, 282*), and clinical trials using Treg therapy in humans show no evidence for an increase in susceptibility to infections (*220*). Tregs are activated highly specifically towards donor antigens and locally at the site of antigen deposition (*283*), so they likely act on surrounded donor-reactive T cells. Thus, Treg therapy may well improve current treatments for transplantation.

1.3.3. Treg cellular therapy and strategies to enhance Treg *in vivo* activity

The therapeutic potential of manipulating Tregs as a mean to modulate the immune system is well known. Some immunosuppressive agents can promote or inhibit the generation or function of Tregs; selection of those agents that suppress effector cells while maintaining the function of regulatory cells may help in promoting tolerance. For

example, FR104 (an antagonist anti-CD28 antibody) blocks CD28 co-stimulation in T cells but allows CTLA-4 signalling into Tregs, which makes it more permissive for Treg activity than CTLA-4Ig (*284*). Using rapamycin instead of calcineurin inhibitors favours induction of Tregs and proliferation of Tregs over Teff cells (*285, 286*). Joanna Hester *et al*. demonstrated the adjuvant effect of low-dose rapamycin treatment in Treg activity inhibiting transplant arteriosclerosis *in vivo* (*286*). Clinical studies have shown that low-dose IL-2 therapy preferentially expands Tregs up to 2 to 8 fold without significant changes in the number of Teff and is safe and efficacious in patients with autoimmunity or GvHD (*287*). Phase II clinical trials using low dose IL-2 therapy in liver transplant patients are now ongoing aiming at gradually discontinuing immunosuppressive drugs (the LITE Trial (NCT02949492)). Furthermore, improved IL-2 based therapies are possible using IL-2 antibody complexes with higher selectivity for Tregs than Teff (*288, 289*), or by engineering IL-2 and IL-2 receptors in Tregs, so modified IL-2 can exclusively signal to Tregs (*290*).

Adoptive transfer of Tregs has several advantages over *in vivo* cell manipulation. Tregs are closely related to Teff cells, meaning that specifically targeting one subset and not the other can be challenging. Furthermore, infusion of *ex vivo* cultured cells provides an opportunity to manipulate them by selection of more efficient cell subsets or by enhancing their regulatory properties using exogenous treatments or genetic engineering tools. However, their paucity in peripheral blood requires extensive expansion of Tregs *in vitro* in order to obtain enough yield for clinical application, which can affect cell function and greatly increases the cost of the therapy. Protocols for Treg expansion following good manufacturing practice (GMP) techniques have been described that result in successful yield (*217, 291-294*) (Figure 1.3). However, the impurity of the Treg expanded product, due to contamination of effector cells during Treg isolation or conversion of Tregs into effector cells during culture, might confer a risk of infusing long-term *in vitro* expanded

Tregs into patients. Therefore, new strategies are needed to improve the purity and the efficacy of the expanded Treg product.

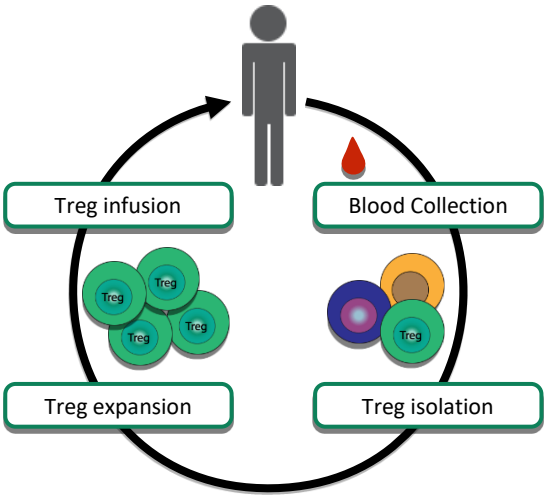

Figure 1.3. Schematic diagram for adoptive Treg cellular therapy. Tregs are isolated from peripheral blood of transplant recipient patients, expanded *in vitro* and re-infused back into the patient in greater numbers.

Key elements to expand human Tregs *in vitro* involve anti-CD3 and anti-CD28 mAbs along with the addition of IL-2, with the concentration of each of these elements affecting the overall expansion, phenotype and function of the resulting Treg product (*294, 295*). Moreovoer, different sera batches and medium components may further alter the state of Tregs during expansion (*296*). Protocols using anti-CD3/anti-CD28 coated beads show that a high bead:Treg ratio is required for initiation of expansion (usually 3:1 or 4:1), while 1 bead per cell can maintain long-term proliferation in the presence of high levels of IL-2 (ranging from 300 to 1000 U/ml) (*294, 297*). Previous results from our laboratory have shown that weaker stimulation (e.g. 5 Treg per 1 bead in 250U/ml IL-2) can also induce Treg activation, resulting in phenotypic changes such as upregulation of co-stimulatory molecules, although this stimulation is suboptimal for substantial Treg expansion.

As discussed in section 1.2, multiple Treg subsets, potentially with specialised mechanisms to target different immune cell populations, have been described according to their phenotype. Therefore, it would be possible to select those cells with the best

properties before infusion, but, firstly, it is essential to gain a full understanding of the constituent subcellular phenotypes present in the Treg population.

Modification of *ex vivo* culture conditions can also affect the resulting cell product. Addition of supplements, such as rapamycin, all-trans retinoic acid (ATRA) or vitamin D during *ex vivo* culture promotes proliferation of Tregs over Teff, induces the generation of iTregs from $CD4^+$ Tconv cells and enhances the stability of the regulatory phenotype (*298*). However, whether these modifications in Treg function are maintained after discontinuing the treatment, once cells are transferred into the patient, is not well known.

Another strategy to expand Tregs with enhanced tolerogenic properties is the generation of donor-reactive Tregs by stimulating recipient's Tregs with donor-derived APCs or APCs pulsed with donor peptides (*298*). It has been widely shown that donor antigen-reactive Tregs are more potent inducing long-term allograft acceptance than polyclonally expanded Tregs (*283, 299, 300*). Although fewer cells would need to be infused, the increased difficulty of generating donor-reactive Tregs compared to polyclonal Tregs makes this approach more challenging.

Recent advances in genetic engineering tools provide the opportunity to safely genetically edit mechanisms that control Treg specificity, stability and function. For example, gene transfer has been used to induce expression of antigen-specific TCRs or chimeric antigen receptors for the development of antigen-specific CAR-Tregs (*298, 301, 302*). Also, $CD4^+$ Teff cells have been engineered to overexpress FOXP3 and show reduced pro-inflammatory activity while gaining suppressive activity. However, FOXP3 expression itself is not enough to recapitulate the canonical Treg signature (*153, 154*) and their long-term stability is not known. Progress in understanding Treg phenotype, function and stability may well help in identifying further functional targets to improve Treg therapy.

1.4. Hypothesis and aims of the project

The holy grail of allogenic transplantation is to achieve life-long tolerance to the graft without the use of immunosuppressive drugs. Despite excellent short-term results, toxicity of immunosuppressive drugs and chronic allograft rejection hamper long-term graft survival. It is believed that induction of immunological tolerance towards donor antigens in transplant recipients would allow one transplant for life in the absence of immunosuppressive drugs.

The physiological role of Tregs is to dampen unnecessary immune responses, especially important to suppress auto-reactive T cells that might otherwise cause autoimmunity. Importantly, Tregs, acting on different types of immune and non-immune cells, can also suppress allogenic immune responses (*215, 280*). Besides, donor-reactive Tregs have the ability to propagate their suppressive phenotype to other immune cells (infectious tolerance) and are able to generate a state of immune unresponsiveness towards donor antigens (*199*). Experiments in animal models suggest a significant role for Treg activity in the initial and in the maintenance phase of graft tolerance (*303-306*) and highlight a promising population to target and employ in order to achieve long-term allograft tolerance.

Treg function can be induced *in vivo* or Tregs can be isolated, cultured *ex vivo* and then re-infused into patients. Protocols for manufacturing clinical Treg products based on *in vitro* expanded polyclonal Tregs are already available and are being used in clinical trials for kidney transplantation (ONE Study) (*294*).

While progress has been made in obtaining relevant numbers for clinical application, we do not fully know the physiology of *in vitro* expanded Tregs. Treg subsets that produce pro-inflammatory cytokines (mainly IL-17A and IFN-y), with defective suppressive function and increased TSDR methylation are found within the *in vitro* expanded Treg product

(*178, 307-310*). Research on Treg cellular therapy is now focused on optimising Treg expansion protocols, aiming at identifying specific phenotypic features that convey the suppressive functionality and stability, and at minimising contamination by other non-suppressive cells. Separation into different cell subsets based on cell surface markers, treatment with pharmacological agents and genetic editing procedures are some of the approaches that are being explored to increase the efficacy of the expanded Treg cell product.

1.4.1. Overall hypothesis

Given previous studies showing a strong correlation between CD27 expression and suppressive function in *in vitro* expanded $CD4^+CD25^+$ Tregs (*179, 180, 311*), we hypothesised that **interaction of CD27 with its ligand CD70 may account for Treg stability and regulatory function.** However, little is known about the role of CD27 on Tregs. It has been shown that CD27 expressed on Tregs could impair co-stimulatory signals from CD70-expressing DCs to CD27-expressing Tconv cells (*188*). Moreover, CD27 intracellular signalling limits Th17 differentiation in murine Teff cells (*312*), suggesting that the CD27/CD70 pathway may play a role in maintaining stable Treg function by regulating the Th17 programme in Tregs. We, therefore, hypothesised that **modulation of the CD27-CD70 co-stimulatory pathway during *in vitro* cell expansion may allow for the generation of a more potent Treg cell product**.

CD70 is the unique ligand for CD27 and its expression is tightly controlled (*73, 74*). Since CD70 expression has been reported on activated T cells (*73, 74, 102*), we hypothesised that **CD70 expressed on expanded Tregs might play a role for their regulatory function by interacting with other immune cells expressing CD27**.

1.4.2. Aims

- To determine CD27 and CD70 expression patterns in human Tregs and its changes upon *in vitro* stimulation (Chapter 3).

- To optimise a protocol based on CD27/CD70 expression for the generation of a Treg cellular product with potent suppressive activity upon prolonged *in vitro* expansion (Chapter 3).

- To phenotypically characterise Treg subsets with differential suppressive potency based on CD27/CD70 expression (Chapter 3).

- To determine molecular mechanisms by which the CD27/CD70 co-stimulatory pathway influences Treg activity (Chapter 4).

- To explore the feasibility of enhancing regulatory T cell therapy efficacy by targeting the CD27/CD70 co-stimulatory pathway (Chapter 5).

Chapter 2: Materials and methods

2.1. *In vitro* cell isolation and cell culture

2.1.1. Treg flow-sorting strategies

Peripheral blood mononuclear cells (PBMCs) were isolated from blood cones obtained from healthy donors (NHS Blood and Transplant [NHSBT] UK) by density gradient centrifugation using lymphocyte separation medium (25-072-CV, Corning). PBMCs were then incubated with $CD25^+$ Microbeads (130-092-983, Miltenyi Biotec, Bergisch Gladbach, Germany) to isolate $CD25^+$ enriched cells using LS columns (130-042-401, Miltenty Biotec) according to the manufacturer's protocol. $CD4^+CD25^+CD127^{-/low}$ Tregs (total Tregs) were isolated from $CD25^+$ enriched PBMCs by flow cytometry sorting using a BD FACSAria II cell sorter, after staining with 7-aminoactinomycin D (7-AAD) viability dye (00-6993, eBioscience), anti-CD4 PE-eFluor 610 (eBioscience; details for all antibodies used in the thesis are given in Table 2.1), anti-CD25 PE-Cy7 (BD Biosciences) and anti-CD127 PE (BD Biosciences) monoclonal antibodies (mAb). Meanwhile, from the $CD25^-$ fraction of cells, $CD4^+$ Tconv cells were FACS-sorted after staining with 7-AAD viability dye (eBioscience) and anti-CD4 PE-eFluor 610 (eBioscience).

Expanded total Tregs were stained with anti-CD27 eFluor 450 (eBiosciences) or anti-CD27 PE-Cy7 (Biolegend) and anti-CD70 APC (BioLegend) mAbs in order to separate $CD27^+CD70^-$ and $CD27^-CD70^+$ Tregs (Figure 3.8A). Cell isolations were performed by FACS using a BD FACSAria II cell sorter.

2.1.2. *In vitro* expansion of human Tregs and CD4$^+$ Tconv cells

Cells were cultured in complete media for 16-32 days, composed of RPMI 1640 media (R0883, Sigma-Aldrich Co Ltd) supplemented with L-glutamine (G7513, Sigma-Aldrich, St. Louis, MO, USA), sodium pyruvate (11360-070, Sigma Aldrich), 100U/ml penicillin and 10mg/ml streptomycin (P4333, Sigma-Aldrich). For cell expansion, 10% of human antibody pooled serum (S-101, Life Science Production) (heat-inactivated for 20 min at 56^{o}C) was added to the media. Sorted Tregs and Tconv cells were stimulated with Dynabead Human T-activator anti-CD3/anti-CD28 beads (11132D, Thermo Fisher Scientific, MA, USA) in a 1:1 cell:bead ratio in complete media. Recombinant human IL-2 (rhIL-2) (Proleukin, Novartis, Frimley, UK) was added to the media at a concentration of 1000U/ml for Treg expansion or 100U/ml for Tconv expansion. Tregs and Tconv cells were stimulated on days 0, 7, 14, 16 and 23 of culture. Cultures were split, and medium replaced as required. Tregs and Tconv cells were rested, without stimulating beads, in the presence of 250U/ml or 25U/ml rhUL-2, respectively, for 2 days on day 14 and 30 of culture.

2.1.3. Generation of human monocyte-derived dendritic cells (moDCs)

CD14$^+$ monocytes were isolated from PBMCs using MACS CD14$^+$ microbeads (130-050-201, Miltenyi Biotec) and LS columns (130-042-401, Miltenyi Biotec), according to the manufacturer's protocol. CD14$^+$ mononuclear cells were incubated for 5 days on 6 well plates at 5x10^5 cells/ml in the presence of 50U/ml IL-4 (200-4, Peprotech, Rocky Hill, NJ, USA) and 50ng/ml GM-CSF (300-3, Peprotech) in complete media supplemented with 10% Foetal Calf Serum (FCS) (10270-098, Gibco, UK) (heat-inactivated for 20min at 56^{o}C). After 5 days of incubation, monocyte derived DCs (moDCs) were harvested and stored in liquid nitrogen for later use.

2.1.4. Cryopreservation and thawing of human leukocytes

Cells were resuspended in freezing medium (45% RPMI, 45% FCS, 10% DMSO). Cells were frozen in 2ml cryovials as 500µl aliquots in freezing boxes at -80°C, before being transferred to -180°C for long-term storage. Frozen vials of cells were transferred to -80°C for one hour before thawing at 37°C. Thawed cell suspensions were immediately washed in 10ml RPMI, added dropwise.

2.2. Flow cytometry analyses

Flow cytometric data were acquired using a BD FACSAria II or BD Canto II (BD Biosciences, UK), and analysed using FlowJo software (Flowjo Enterprise, USA). All fluorochrome-coupled mAbs used are summarised in Table 2.1.

2.2.1. Cell surface staining

Cells, washed in PBS or FACS buffer, were incubated with the appropriate fluorochrome-coupled mAbs for 30-45 minutes at 4°C in the dark. 7-AAD (eBioscience) was stained concurrently with antibodies in all flow cytometry assays. Excess of antibodies was washed by adding PBS or FACS buffer, centrifuging samples at 500g for 5 min at 4°C and then removing the supernatant. Samples were fixed in a 100µl 1% paraformaldehyde (PFA) before flow cytometry analysis in FACSCanto II instrument (BD). Unstained, isotype and fluorescence minus one (FMO) controls were used as standard controls to permit accurate gating of positive and negative populations.

2.2.2. Intracellular immunostaining

Following cell-surface staining, cells which were to undergo intracellular staining were fixed and permeabilised using FOXP3 staining buffers (00-5523-00, eBiosciences, UK) for 1 hour or overnight at 4°C in accordance with manufacturer's guidelines. Cells were

then washed twice with permeabilization buffer. 2% mouse or rat serum was added for 15min prior incubation with either the fluorochrome-coupled mAb under interrogation or the appropriate isotype control for 45min at 4°C in the dark. Cells were subsequently washed and fixed in 1% PFA as for cell surface staining (section 2.2.1).

2.2.3. Staining with cell proliferating dyes

For staining with Violet Proliferation Dye 450 (VPD) (562158, BD Biosciences), cells were washed in PBS and then resuspended at at least $30x10^6$ cells/ml in PBS. Cells were incubated with 1μM VPD (562158, BD Biosciences) for 10min at 37°C before being washed in media with FCS. To stain with carboxyfluorescein succinimidyl ester (CFSE) (65-0850-84, eBioscience), cells were incubated in 2ml pure RPMI with 10μM CFSE for 10min at 37°C, then washed with RPMI supplemented with 10% FCS.

2.2.4. Intracellular cytokine staining

Expanded Tregs were stimulated with 100ng/ml phorbol myristate acetate (PMA) (P1585, Sigma Aldrich) and 1μg/ml Ionomycin (I0634, Sigma Aldrich) in the presence of Golgi protein inhibitor (55029, BD Biosciences or 00-4505-51, eBioscience) for 5h at 37^0C. Cells were washed, fixed and permeabilized using FOXP3 staining kit (eBioscience) as described in section 2.2.2, and stained with anti-IL-17 FITC, anti-IL-17 PE, anti-IL-10 eFluor660 or anti-IFN-γ FITC (eBioscience).

2.2.5. Antibodies

All antibodies for flow cytometry are reactive against human antigens, unless otherwise stated.

Table 2.1. Flow Cytometry Antibodies

Antigen	Fluorochrome	Clone	Species of origin	Supplier	Catalog number
4-1BB	PE	4B4-1	mouse	eBioscience	12-1379
CD127	PE	HIL-7R-M21	mouse	BD Biosciences	557938
CD14	PE-Cy7	M5E2	mouse	BD Biosciences	557742
CD25	PE-Cy7	M-A251	mouse	BD Biosciences	557741
CD25	APC-Cy7	M-A251	mouse	BD Biosciences	557753
CD27	eFluor 450	O323 (used for FACS staining)	mouse	eBioscience	40-0279
CD27	PE-Cy7	MT271 (used for FACS staining and FACS sorting)	mouse	Biolegend	356411
CD27	FITC	M-T271 (used for FACS staining)	mouse	BD Biosciences	557329
CD27	PE	O323 (used for MACS sorting)	mouse	Biolegend	302808
CD3	PE-Cy7	SK7	mouse	BD Biosciences	557851
CD39	PE	eBioA1	mouse	eBioscience	12-0399
CD4	PE-eFluor 610	RPA-T4	mouse	eBioscience	61-0049
CD40L	FITC	24-31	mouse	Biolegend	310804
CD45	APC	HI30	mouse	eBioscience	17-0459
CD45RA	FITC	HI100	mouse	Biolegend	304106
CD62L	APC-Alexa Fluor70	Dreg-56	mouse	Invitrogen	MHCD62L27
CD70	APC	113-16 (used for FACS staining)	mouse	Biolegend	355110
CD70	PE	Ki-24 (used for MACS sorting)	mouse	BD Biosciences	555835
CD70	PE	113-163 (used for MACS sorting and FACS staining)	mouse	Biolegend	355104

CD73	APC	AD2	mouse	eBioscience	17-0739
CD8	APC-Cy7	SK1	mouse	BD Biosciences	557834
CTLA-4	PE	BNI3	mouse	BD Biosciences	555853
FOXP3	FITC	PCH101 (used for FACS staining)	rat	eBioscience	11-4776
FOXP3	Alexa Fluor 647	259D (used for FACS staining)	mouse	Biolegend	320213
GATA-3	eFluor 660	TWAJ	rat	eBioscience	50-9966
GITR	FITC	110416	mouse	R&D	FAB689F-025
Helios	Alexa Fluor 647	22F6	hamster	Biolegend	137218
Helios	PE	22F6	hamster	Invitrogen	12-9883
HLA-ABC	APC	W6/32	mouse	eBioscience	17-9983
HLA-ABC	PE-Cy7	W6/32	mouse	eBioscience	25-9983
HLA-DR	ECD	Immu-357	mouse	Beckman Coulter	IM3636
ICOS	FITC	ISA-3	mouse	eBioscience	11-9948
IFN-γ	FITC	4S.B3	mouse	eBioscience	11-7319
IL-10	eFluor660	JES3-9D7	rat	eBioscience	50-7108
IL-17A	PE	eBio4CAP17	mouse	eBioscience	12-7178
IL-17A	FITC	eBio64DEC17	mouse	eBioscience	11-7179
mouse CD45	FITC	30-F11	rat	BD Biosciences	553080
OX40	FITC	ACT-35	mouse	Invitrogen	11-1347
PD-1	FITC	EH12.2H7	mouse	Biolegend	329904
RORyt	PE	AFKJS-9	rat	eBioscience	12-6988
T-bet	PE-Cy7	eBio4B10	mouse	eBioscience	25-5825
TIGIT	PE	MBSA43	mouse	eBioscience	12-9500
TIM-3	PE	F38-2E2	mouse	Biolegend	345005

2.2.6. Cytokine bead array

Supernatants were collected from cell cultures, after 72hrs stimulation, unless otherwise stated, and stored at -80°C until use. Thawed supernatants were probed using a multiplex bead-based immunoassay. A LEGENDplex™ Human Th Cytokine Panel flow cytometric bead array kit (740721, BioLegend) was used to analyse supernatants from Treg cultures and from suppression assays. Samples were acquired using FACSCanto II instrument (BD) and analysis was done using LEGENDplex™ software (BioLegend).

2.3. *In vitro* cell activation assays

2.3.1. CD27 and CD70 expression time course

Freshly isolated Tregs and $CD4^+$ Tconv cells were activated with anti-CD3/anti-CD28 coated beads (11132D, Thermo Fisher Scientific) at 1bead : 5cells ratio and IL-2 (250U/mL for Treg or 25U/ml for Tconv activation) for 7 days. Aliquots of cells were stained with 7-AAD (eBioscience), anti-CD27 and anti-CD70 antibodies (BioLegend, San Diego, CA, USA) on day 0, 3, 5 and 7 of culture and analysed by flow cytometry.

2.3.2. Treg activation upon diverse stimuli

Freshly isolated Tregs were activated with 100ng/ml PMA (Sigma Aldrich) and 1µg/ml Ionomycin (Sigma Aldrich) or anti-CD3/anti-CD28 coated beads (1bead : 5cells) and IL-2 (250U/mL) for 5 days. A mix of viral Toll-like receptor (TLR) ligands [imiquimod (5µg/ml), ssRNA40/LyoVec (5µg/ml), ODN2006 (5µM), Poly(I:C) (10µg/ml) and Poly(I:C)-LMW (10µg/ml)] or bacterial TLR ligands [Pam3CSK4 (1µg/ml), HKLM (10^8 cells/well), FSL1 (1µg/ml), LPS (0.1µg/ml) and flagellin (1µg/ml)] was added together with stimulating anti-CD3/anti-CD28 beads. TLR ligands were purchased as a human TLR1-9 Agonist Kit from InvivoGen (tlrl-kit1hw). Alternatively, cells were activated with stimulating anti-CD3/anti-

CD28 beads in the presence of human IL-1β, IL-6, TNF-α, IFN-γ and IL-23 cytokines (PeproTech EC Ltd) at a concentration of 10ng/ml for each cytokine. Cells were stained with 7-AAD (eBioscience), anti-CD27 and anti-CD70 antibodies (BioLegend) and analysed by flow cytometry.

2.4. *In vitro* Treg functional assays

The ability of Tregs to regulate autologous T cell proliferation was assessed *in vitro* using $CD3^+CD25^-$ cells as responder T cells (Tresp). Tresp were isolated from frozen PBMCs by depletion of $CD25^+$ cells, by incubating with $CD25^+$ Microbeads (Miltenyi Biotec), followed by the positive selection of $CD3^+$ T cells by $CD3^+$ Microbeads (Miltenyi Biotec). Both procedures were performed according to the manufacturer's protocol.

Calibrate beads (340486, BD Biosciences) were used as counting beads to determine absolute number of cells in co-cultures of Tregs and Tresp by flow cytometry.

2.4.1. *In vitro* mixed lymphocyte reaction (MLR)

Variable numbers of Tregs were incubated with $2x10^4$ allogenic monocyte-derived dendritic cells (allo moDCs) as stimulators and $10x10^4$ autologous $CD3^+CD25^-$ T cells (Tresp) labelled with 1μM VPD (562158, BD Biosciences) proliferation dye as responder cells in triplicate wells. Labelled Tresp cultured alone or in the presence of allo moDCs (without Tregs) were used as a negative and positive control, respectively. Following 80-96 hours of incubation, co-cultures were stained with 7-AAD viability dye (eBioscience), anti-CD4 PE-eFluor 610 (eBioscience), anti-CD8 APC-Cy7 (BD Biosciences), anti-CD27 PE-Cy7 (Biolegend) and anti-CD70 APC (Biolegend) antibodies and analysed by flow cytometry. To quantify Tresp cell proliferation from VPD dilution profiles, division indeces were calculated using FlowJo software. The software calculates

division index as the average of cell divisions that a cell in the original population has undergone, according to the following formula:

Division index = # cell divisions/ # precursor cells =
= {1(# cells division1/2^1) + 2(# cells division 2/2^2)+...+ n(# cells division n/2^n)} /
{(# cells division 0/2^0)+(# cells division 1/2^1)+...+(# cells division n/2^n)}

Percentage of suppression was calculated by using division index of co-cultures containing Tregs, Tresp and DCs compared to division index of Tresp with DCs alone, according to the following formula:

Percentage of suppression = (1 - (div.index Treg+Tresp / div.index Tresp)) x 100

2.4.2. *In vitro* Treg co-stimulation test

$CD3^+CD25^-$ T responder cells (Tresp) were labelled with 1uM VPD (562158, BD Biosciences). VPD-stained Tresp were cultured in plates coated with 1µg/ml anti-CD3 mAb (cat: 317315, clone: OKT3, BioLegend) and in the presence of 4 weeks *in vitro* expanded Tregs or $CD4^+$ Tconv cells. Assays were performed in triplicate wells. After 5 days of culture, cells were stained with 7-AAD viability dye (eBioscience), anti-CD4 PE-eFluor 610 (eBioscience), anti-CD8 APC-Cy7 (BD Biosciences), anti-CD27 PE-Cy7 (Biolegend) and anti-CD70 APC (Biolegend) antibodies and analysed by flow cytometry. Proliferation of responder $CD4^+$ and $CD8^+$ T cells was calculated as division index using FlowJo software as described in section 2.4.1.

2.4.3. Mechanistic *in vitro* blockade

Anti-CD70 blocking mAb (clone BU.69) was purchased from Abcam (UK) as mouse antihuman antibody or from Absolute Antibody Ltd as fully human Ab. Fully human anti-CD27 mAb and its Fc-mutated version (1F5N297S) were provided by Celldex Therapeutics. Isotype control antibodies were mouse IgG1 (400124, BioLegend), fully

human IgG1 (BE0297, BioXcell) and human IgG1 Fc-silent (Ab00178-10.3, Absolute Antibody Ltd). Secondary goat anti-human antibody for crosslinking was purchased from Abcam (UK) (cat: ab97223).

Anti-CD40L (cat: MAB617) and anti-PD-1 (cat: MAB10861) blocking mAbs and their respective isotypes, mouse IgG_{1k} (cat: MAB002) and mouse IgG_{2b},(cat: MAB004) were obtained from R&D Systems.

Where indicated, Tregs were pre-incubated with 20µg/ml anti-CD70, anti-CD27, anti-CD40L, anti-PD-1 or control isotype antibodies for 1 hour at 37^{o}C. Excess antibodies were washed out before assessing functionality of pre-incubated Tregs. Alternatively, 20µg/ml anti-CD70, anti-CD27 blocking mAb or corresponding isotype antibody was added to the functional assay. Blocking antibodies were added to both control and experimental conditions and Treg function was calculated relative to the control condition which had also been exposed to the antibody.

2.4.4. MLR assay in a transwell system

Transwell experiments were performed in 96-well plates with pore size 1.0 µm (CLS3380, Sigma Aldrich). VPD-stained $CD3^{+}CD25^{-}$ Tresp (10×10^{4}) were cultured in the bottom chamber (receiver wells) of the 96-well plates in medium containing 2×10^{4} allo moDCs. 10×10^{4} *in vitro* expanded $CD27^{-}CD70^{+}$ Tregs or CFSE-labelled Tresp were cultured in the top chamber (insert wells) along with 2×10^{4} allo moDCs. After 5 days in culture, insert wells were removed and cells in both insert and receiver wells were harvested and stained to differentiate $CD4^{+}$ and $CD8^{+}$ T cells. Dilution of the proliferation dye within $CD4^{+}$ and $CD8^{+}$ Tresp was studied by flow cytometry and used to calculated division indeces by FlowJo software as explained in section 2.4.1.

2.5. *In vivo* Treg functional assay

2.5.1. Mice

BALB/c Rag2$^{-/-}$cγ$^{-/-}$ mice (The Jackson Laboratory, Bar Harbor, ME, USA) were maintained in individually-ventilated cages under specific pathogen-free in the Biomedical Service Unit of the University of Oxford (Oxford, United Kingdom). All mouse experiments were performed using protocols approved by the Committee on Animal Care and Ethical Review at the University of Oxford and in accordance with the UK Animals (Scientific Procedures) Act 1986 and under PPL number P8869535A. Experiments using donated human cells *in vivo* were performed with ethical approval from the Oxfordshire Research Ethics Committee (REC B), study number 07/H0605/130.

2.5.2. Adoptive transfer of human leukocytes

Female mice were aged between 8 and 12 weeks at the time of the experimental procedure. Mice received an intraperitoneal injection of 5×10^6 cryopreserved and thawed PBMCs labelled with 1μM VPD (562158, BD Biosciences) together with 1x10^6 cryopreserved and thawed 4-week expanded CD27$^+$CD70$^-$ or CD27$^-$CD70$^+$ Tregs. Mice were injected with different Treg subsets or no Tregs in a blind way and allocated randomly between different cages.

2.5.3. Flow cytometry analysis

Cells were extracted by peritoneal lavage at day 4 after transfer, stained with 7-AAD viability dye (eBioscience), mouse anti-CD45 FITC (BD Biosciences), human anti-CD45 APC (eBioscience), anti-CD3 PE-Cy7 (BD Biosciences), anti-CD4 PE-eFluor 610 (eBioscience), anti-CD8 APC-Cy7 (BD Biosciences) and anti-CD27 PE (Biolegend), and analysed by flow cytometry. On analysis, lavage fluid was procured and analysed in a

blinded fashion before unblinding for statistical analysis. VPD dilution was assessed to calculate proliferation index with FlowJo software. Proliferation index takes into account the cells that underwent at least one division, according to the following formula:

> Proliferation index = # cell divisions / (# precursor cells - # undivided cells)=
> = {1(# cells division1/2^1) + 2(# cells division 2/2^2)+...+ n(# cells division n/2^n)} /
> {((# cells division 0/2^0)+(# cells division 1/2^1)+...+(# cells division n/2^n)) - #undivided cells}

2.6. RNA sequencing analysis

RNA sequencing (RNA-seq) analysis was performed in 4 weeks expanded $CD27^+CD70^-$ and $CD27^-CD70^+$ Tregs as depicted in Figure 3.8A for 4 independent donors. Before analysis, expanded cell products were resorted according to CD27 and CD70 expression for higher purity. RNA-seq was performed and analysed by Dr. Peng Hua at the Weatherall Institute of Molecular Medicine (Oxford). RNA was isolated from 300,000 $CD27^+CD70^-$ and $CD27^-CD70^+$ Tregs cells using RNeasy Plus Mini Kit (74136, QIAGEN) according to the manufacturer's protocol. mRNA capture and cDNA synthesis were performed using KAPA mRNA Hyper Kit for Illumina platform (Roche) according to the manufacturer's protocol. After quality check using Qubit High-sensitivity kit (Life Technologies), 16 cycles of PCR were carried out for amplifying each library. Each experiment starting from RNA isolation was performed in triplicate using cells from four different donors. Amplified cDNA libraries were sequenced on an Illumina HiSeq4000 machine using paired end reads (2 x 150 bp) at Novogene, China. Forty million reads per sample were gained and aligned using STAR against the human genome (UCSC hg38). The non-adjusted read counts for each gene were assessed statistically for global differential expression between the specified populations using the edgeR package. Genes that are significant at a 1% false discovery rate (calculated using a Benajmini-Hochberg adjusted p-value) were considered differentially expressed between populations as described previously (*313*). Gene ontology enrichment was assessed

using the topGO package and pathway enrichment was analysed on the ReactomePA package. R programme was used for the design of volcano plots.

2.7. Treg expansion according to GMP requirements

2.7.1. Magnetic isolation of human Tregs for GMP-like culture

PBMCs were isolated from blood cones obtained from healthy donors (NHS Blood and Transplant [NHSBT] UK) by LSM1077 (GE Healthcare, Chicago, IL, USA) gradient centrifugation. $200x10^6$ PBMCs were depleted for $CD8^+$ cells by incubation with $CD8^+$ Microbeads (130-045-201, Miltenyi Biotec) and separation in a LD depletion column (cat: 130-042-901, Miltenyi Biotech), according to manufacturer's protocol. CD8 depleted cells were then enriched in $CD25^+$ T cells using CD25 Microbeads (130-092-983, Miltenyi Biotec) and run twice in a LS separation column (130-042-401, Miltenyi Biotec), following manufacturer's guidelines.

Tregs were separated according to CD70 expression after 2 or 3 cycles of *in vitro* expansion. For this, Tregs were incubated with anti-CD70 PE mAb (Biolegend) (0.5 µl mAb + 10 µl PBS per 10^6 Tregs) for 30min at 4ºC. Excess of mAb was washed and Tregs were incubated with anti-PE Microbeads (cat: 130-048-801, Miltenyi Biotec) for 15min at 4ºC. Cells were washed and separated according to CD70 expression using a LD depletion column (130-042-901, Miltenyi Biotec). Purity of isolated cells was determined by flow cytometry.

2.7.2. *In vitro* expansion of Tregs in the presence of rapamycin

Isolated cells were plated at $5x10^5$ cells/ml in 6 well plates in complete media supplemented with 10% human antibody pooled serum (Life Science Production) (heat-inactivated for 20min at 56ºC). Cells were cultured in the presence of 100nM rapamycin (GMP-approved) (cat: 170-076-308, Miltenyi Biotec, Bergisch Gladbach, Germany), and

activated with Dynabead Human T-activator anti-CD3/anti-CD28 beads (cat: 11132D, Thermo Fisher Scientific, MA, USA) at a bead:cell ratio of 3:1 at day 0 and 1:1 at days 12 and 24 of culture. 500U/ml rhIL-2 (Proleukin, Novartis, Frimley, UK) was added at day 3 and replenished every 2-3 days. Prior each re-stimulation, cells were rested for 2 days in the absence of rhIL-2.

2.7.3. Assessing suppressive capacity of rapamycin-expanded Tregs

Treg suppressive capacity was assessed by MLR suppression assays as described in section 2.4.1. Alternatively, Treg activity was studied by *in vitro* suppression assay driven by anti-CD3/anti-CD28 stimulating beads. Variable numbers of Tregs were incubated with $10x10^4$ autologous $CD25^-CD3^+$ Tresp cells labelled with 10μM CFSE (65-0850-84, eBioscience) proliferation dye in triplicate wells containing anti-CD3/anti-CD28 coated beads (1:42 bead:cell ratio) (11132D, Thermo Fisher Scientific). Following 5 days of expansion, co-cultures were stained to distinguish $CD4^+$ and $CD8^+$ T cells and analysed by flow cytometry. CFSE dilution was studied to calculate division index and percentage of suppression using FlowJo software as described in section 2.4.1.

2.8. TSDR DNA methylation analysis

2.8.1. Assessment of the methylation status of TSDR in CD27/CD70 Treg subsets

Methylation at the Treg-Specific Demethylated Region (TSDR) was studied in $CD27^+CD70^-$ and $CD27^-CD70^+$ Treg cell subsets from matched donors sorted from $CD4^+CD25^+CD127^{-/low}$ Tregs either freshly isolated or after 2 weeks of *in vitro* expansion. Methylation analysis was conducted by EpigenDx by pyrosequencing of bisulphite-modified DNA purified from flow sorted frozen cell pellets ($0.12\text{-}5x10^5$ cells). 9

representative CpG residues in the TSDR were analysed using assay ADS783-FS2 for human *foxp3*.

2.8.2. Assessment of the methylation status of TSDR in CD25/CD45RA Treg subsets

The methylated status of the TSDR region in CD25/CD45RA Treg cell subsets was analysed by bisulfite conversion and PCR at Dr. Sawitzki's lab (Charité, Berlin, Germany). Genomic DNA was isolated from freshly sorted or expanded Tregs using the DNeasy blood and tissue kit (51306, Qiagen) following the protocol for cultured animal cells. Bisulfite treatment of DNA was performed with EpiTect bisulfite kit (59104, Qiagen) following the protocol suggested. PCR was performed in a final volume of 20 µl containing 10µL FastStart universal probe master (4913957001, Roche Diagnostics, Mannheim, Germany), 50ng/µL lambda DNA (N3013S, New England Biolabs, Frankfurt, Germany), 5pmol/µL methylation or nonmethylation-specific probe, 30pmol/µL methylation or nonmethylation-specific primers, and 60ng bisulfite-treated DNA or a respective amount of plasmid standard. The samples were analysed in triplicates on an ABI 7500 cycler.

2.9. Genetic engineering of human Tregs

2.9.1. Generation of lentiviral vectors

A third-generation self-inactivating 'terminal' lentiviral vector expressing GFP and single guide RNA (sgRNA) was generated as described previously (*314*) and obtained from Prof. Qasim's laboratory (UCL, London). The vector incorporates guide sequences into the ΔU3 region of the 3'LTR, thereby coupling transgene expression and CRISPR effects after subsequent Cas9 delivery by electroporation. The VSV-G envelope plasmid pMD2.G, P8.74 plasmid containing gag and pol, and Rev plasmid were a gift from Prof. Qasim's laboratory.

Concentrated vector preparations were produced by transient transfection of 293T cells. 293T cultures were maintained in Dulbecco's Modified Eagle's Medium (DMEM) supplemented with 10% FCS, 4mM L-Glutamine, 100U/mL penicillin and 10mg/mL Streptomycin in T175 flasks. 293T cells were transfected using polyethylenimine (44, 872-7, Sigma Aldrich). GFP/sgRNA vector was packaged using pMD.G2 (17.5µg/flask), p8.74 (32.5µg/flask), Rev (25µg/flask) and GFP/sgRNA (25µg/flask) plasmids.

Medium was replaced 4 and 24 hours after transfection and supernatant was collected 48 hours post-transfection. Lentivirus-containing supernatant was centrifuged at 500g for 5min and filtered through 0.45µm filters. Lentiviral particles were concentrated by centrifugation for 2h at 90000 to 100000g (23000rpm in a TH-641 rotor) at 4°C and resuspended in 110µl of pure DMEM. After 30min incubation at room temperature, lentiviral particles were aliquoted and frozen at -80°C.

2.9.2. Titration of lentiviral vector

293T cells were seeded at 10^5 cells per well in a 24-well plate 24h prior to addition of lentiviral particles at varying concentrations. 4 days after addition of the virus, cells were harvested and the proportion of GFP^+ cells was studied by flow cytometry. The concentration of the viral stock was calculated as infection units (IU) per millilitre according to the following formula:

> Titre (IU/ml) = ((%GFP^+ cells - %GFP^+ cells in unstransduced control) x #293T cells seeded) / (volume of virus (ml) x viral dilution)

2.9.3. Transduction of human Tregs

10 days-*in vitro* expanded-$CD4^+CD25^+CD127^{-/low}$ Tregs were transduced with lentiviral vectors at a multiplicity of infection (MOI) of 5, three days after re-stimulation with anti-

CD3/anti-CD28 coated beads in the presence of rhIL-2 (1000 U/ml). The volume of concentrated lentivirus needed was calculated following the formula:

Volume of virus (ml) = (MOI 5 x #cells to be transduced) / titre

On day 13 of expansion (3 days post transduction) cells were electroporated with Cas9 mRNA (see section 2.9.7). Tregs were further expanded *in vitro* and positively transduced GFP^+ cells were isolated by FACS 10 days post-transduction.

2.9.4. CRISPR/Cas9 single guide RNA (sgRNA) design

4 sgRNAs sequences targeting CD70 were studied, 3 sgRNAs targeting exon 3 and 1 sgRNA targeting exon 1. All sgRNAs targeting exon 3 of CD70 (named as 1_3, 2_3 and 3_3) were previously described (*315*). sgRNA targeting exon 1 of CD70 (1_1) was designed using Benchling software (https://benchling.com/crispr) with a predicted on-target score of 51.1 and off-target score of 48.8. Optimised score ranges from 0 to 100 (higher is better). A sgRNA sequence targeting B_2M, validated in Prof. Qasim's laboratory, was used as a positive control of gene editing. sgRNA sequences were: 1_3: GCTACGTATCCATCGTGA, 2_3: GTACACATCCAGGTGACGC, 3_3: GCAGGCTGATGCTACGGG, 1_1: TCACCAAGCCCGCGACCAAT and B2M: GAGTAGCGCGAGCACAGCTA.

2.9.5. Streptococcus pyogenes Cas9 (spCas9)

Streptococcus pyogenes Cas9 (spCas9) was delivered as mRNA or as a protein. CleanCap™ spCas9 mRNA (cat: L-7606, TriLink Biotechnologies, San Diego, USA) was a kind gift from Prof. Qasim's group. spCas9 protein was purchased as Alt-R S.p. HiFi Cas9 Nuclease from Integrated DNA Technologies, Inc (cat: 1081061) or produced at the Oxford Protein Facility by Dr. Nettleship. In brief, Cas9 DNA tagged with histidine residues was produced in Rosetta cells and Cas9 expression was verified by Western Blot,

corroborating that a band could be seen on the gel at the correct molecular weight (160kDa). For verification, Cas9 was pulled down using a Ni-NTA purification system (nitrilotriacetic acid agarose resin loaded with nickel). Rosetta cells were then lysed and Cas9 was purified via Histidine-Gel filtration chromatography. Cas9 protein was stored at -80°C until its usage.

2.9.6. Formation of ribonucleoprotein (RNP) complexes

Gene-specific CRISPR RNAs (crRNAs) and tracer RNA (tracrRNA) were obtained from Integrated DNA Technologies, Inc. RNP complexes were prepared according to the manufacturer's instruction. crRNA and tracrRNA were reconstituted to 200µM with Nuclease-Free Duplex Buffer (Integrated DNA Technologies, Inc) and mixed at equimolar concentrations. Oligos were annealed by heating at 95°C for 5min in a PCR thermocycler and slowly cooled to room temperature. RNPs complexes were performed by addition of Cas9 Nuclease to crRNA:tracrRNA duplex in Resuspension Buffer R (Neon System Kit, ThermoFisher Scientific). RNP complexes were incubated for 10min at room temperature before electroporation. For each electroporation reaction, RNP complexes were prepared using 3µl of 62µM (10µg/ml) Cas9 from Integrated DNA Technologies or 5µl of 62µM (10µg/ml) Cas9 from Oxford Protein Facility, along with 5ul of 44µM crRNA:tracrRNA duplex in a final volume of 10µl.

2.9.7. Electroporation

CleanCap™ spCas9 mRNA and RNP (as described in section 2.9.6) electroporation was performed in 100µl tips using an optimised protocol consisted of 3 pulses at 1600V and 10ms on the Neon Transfection System (ThermoFisher Scientific) in accordance with manufacturer's instructions.

Each electroporation reaction contained $2x10^6$ Tregs washed in PBS and 100µg/ml of Cas9 mRNA or RNP complexes prepared as described in sections 2.9.4 and 2.9.6 in 100ul of buffer T (MPK10025, Neon System Kit, ThermoFisher Scientific).

2.9.8. Knockout efficiency analysed by FACS

Knockout (KO) efficiency was calculated as percentage of $CD70^+$ or $HLA\text{-}ABC^+$ cells in KO-Tregs compared to control-Tregs, according to the following formula:

%KO = (100 - (% positive cells in KO-Tregs * 100 / % positive cells in control-Tregs))

For lentiviral coupled to Cas9 mRNA experiments, KO-Tregs refer to transduced Tregs electroporated with Cas9 mRNA while control-Tregs were transduced but not electroporated with Cas9 mRNA. When CRISPR editing was performed using RNPs, KO-Tregs were electroporated with crRNA:tracrRNA:Cas9 and control-Tregs were electroporated only with Cas9.

2.9.9. Detection of genetic modifications by ICE algorithm

Genetic modifications at the *CD70* locus were analysed using ICE protocols *(*https://ice.synthego.com/). Genomic DNA extraction was performed using DNeasy Blood and Tissue Kit (cat: 69504, Qiagen, Hilden, Germany) and amplification of 700bp around sites of predicted Cas9 scission was performed by PCR. Primers used for PCR and sequencing were 1_3 forward: CACCGGCTACGTATCCATCGTGA and 1_3 reverse: AAACTCACGATGGATACGTAGCC. Primers were designed using Benchling software. PCR products were sequenced and analysed using ICE algorithm.

2.10. Statistical analysis software

Graphs were produced and statistical analyses performed using Graph Prism software (GraphPad Software, San Diego, CA, USA). Statistical significance was determined as

indicated in the figure legends. Standard deviation (SD) is represented in graphs with data from multiple donors, when each data point displays the data of one donor, or in graphs showing replicates from 1 representative donor. Standard Error of the Mean (SEM) is used in graphs displaying Median Fluorescence Intensity (MFI), or in graphs with data from multiple donors, with each data point showing the average of replicates for each donor. Unpaired tests were performed to compare between cell subsets. Paired tests were used when comparing a specific cell subset over time or upon treatments, and for a comparison between knockout and control cells.

Chapter 3:
Generation and characterisation of *in vitro* expanded CD27$^+$CD70$^-$ and CD27$^-$CD70$^+$ Treg subpopulations

3.1. Introduction

The understanding of Treg cell biology has expanded considerably over the last two decades and their potential therapeutic benefit for the treatment of autoimmune diseases and allograft rejection is currently under evaluation (*280, 316, 317*). In particular, adoptive transfer of polyclonally expanded Tregs into transplanted patients is a promising approach to induce tolerance towards alloantigens and Phase I/II clinical trials are already underway (ONE Study, NCT02129881) (ThRIL, NCT02166177). Treg treatment has shown to be feasible and safe for prevention of allogenic solid organ transplantation (*318*), GvHD (*217, 222, 319*) and autoimmune diseases (*226, 320*).

Improved Treg-based therapies significantly rely on efficient strategies for isolation, *in vitro* expansion and manipulation of Treg functional properties to maintain stable and potent suppressive function. Essentially, Tregs require high and continuous FOXP3 expression for their stability and suppressive function (*24*). Although it is not possible to isolate viable Tregs based on intracellular expression of FOXP3, surrogate cell surface markers that directly correlate with FOXP3 expression have been identified. CD127 inversely correlates with FOXP3 expression and Tregs isolated based on CD25 in combination with low or absent CD127 expression have demonstrated higher levels of FOXP3 and superior suppressive potency and stability as compared with CD4$^+$CD25$^+$-isolated Tregs (*167, 168*).

Tregs need to be expanded *ex vivo* post-isolation in order to achieve an optimal Treg dosing for therapeutic effect. *In vitro* expansion of Tregs using allogenic B cells or polyclonal stimulation via anti-CD3/anti-CD28 in the presence of recombinant human IL-2 (rhIL-2) has proved effective in reaching clinically relevant numbers (*217, 226, 297, 304*). While some groups have demonstrated that FACS-isolated CD4^{+}CD25^{high}CD127$^{-/low}$ Tregs maintain stable phenotype and potent suppressive activity upon *in vitro* expansion (*308, 321*), other studies have shown that repeated *in vitro* stimulation may result in increased methylation within the TSDR region and decreased levels of FOXP3 expression (*307, 308*), highlighting instability of the Treg lineage. On the other hand, activated human Tconv cells can transiently upregulate FOXP3 expression (*322*), which may also count for impurity of the expanded Treg population. Therefore, either Treg instability and/or contamination of the starting population with Teff cells may contribute to decreased FOXP3 levels within the expanded cell product.

Tregs are either produced in the thymus (tTregs) or generated from naive CD4^{+} T cells in peripheral sites (pTregs). The demethylation status of the Treg-specific demethylated region (TSDR) at the *foxp3* locus allows the differentiation between these Treg subsets (*173, 323, 324*), but there are no cell surface markers identified so far able to distinguish tTregs from pTregs. While unstable FOXP3 expression in pTregs has been widely observed, tTregs have been traditionally considered a terminally differentiated population with the only function to suppress T cell responses. However, accumulating data in recent years suggest that tTregs possess some degree of instability and plasticity under certain inflammatory conditions (*243-245*). Importantly, the molecular mechanisms and environmental triggers that drive Tregs to lose their suppressive identity and acquire effector-like functions require further investigation and will have clear consequences for the development of new therapeutic interventions using Treg cell therapy.

Immune phenotyping by mass cytometry for over 40 markers have highlighted the heterogeneity of the CD4^{+}CD25^{+}CD127$^{-/low}$ Treg population (*185, 325*), raising the

opportunity to find definitive functional markers that control stability and function of Tregs. An important regulatory mechanism for Treg stability is co-stimulation, since it provides important signalling for Treg activation, survival, expansion and acquisition of effector functions upon antigen recognition (*62, 82*). In this regard, expression of the co-stimulatory receptor CD27 has been shown to closely correlate with suppressive potency on human *in vitro* expanded Tregs (*179, 180, 311*). The CD27-CD70 costimulatory receptor-ligand pair belongs to the TNFR superfamily. CD27 is constitutively expressed on NK cells, B cells and resting CD8$^+$ and CD4$^+$ T cells, including CD4$^+$FOXP3$^+$ Tregs (*70, 101*). Expression of CD70, the unique ligand for CD27, is tightly controlled and upregulated exclusively upon activation on T cells, B cells, NK cells and certain subsets of DCs (*73, 74*). Moreover, several transcriptomic studies have demonstrated an increased expression of CD70 mRNA in human Tregs compared with CD4$^+$ Tconv cells (*175*). Hence, CD27 signalling is regulated by the restricted expression of its ligand CD70.

In this chapter we firstly sought to demonstrate that CD27 cell surface marker identifies potent and stable Tregs. Secondly, we aimed to characterise in more detail functional differences between CD27$^+$ and CD27$^-$ Treg cell products. In order to do this, it was necessary to study the dynamic expression of CD27 and its ligand CD70 in Tregs upon different *in vitro* stimulation and identify the optimal expansion protocol to generate CD27$^+$ and CD27$^-$ enriched Treg populations. Since we demonstrated that activated Tregs upregulate CD70, the unique ligand for CD27, we decided to generate CD27$^+$CD70$^-$ and CD27$^-$CD70$^+$ cell products to control potential CD27/CD70 ligation during Treg expansion. Once the protocol was established, enriched CD27$^+$CD70$^-$ and CD27$^-$CD70$^+$ Treg populations where extensively characterised for further functional differences.

3.2. Objectives and hypotheses

Objective 1: To study the expression pattern of CD27 and CD70 in freshly isolated and *in vitro* stimulated Tregs.

Hypothesis 1: Upon stimulation, Tregs will differentially express CD27 and CD70 at the cell surface, allowing the discrimination between CD27$^+$CD70$^-$ and CD27$^-$CD70$^+$ cells.

Objective 2: To optimise a protocol for generating CD27$^+$CD70$^-$ and CD27$^-$CD70$^+$ enriched Treg cell products.

Hypothesis 2: CD27 and/or CD70 cell surface expression will identify a more potent and stable regulatory cell product after *in vitro* Treg expansion.

Objective 3: To extensively characterise expanded CD27$^+$CD70$^-$ and CD27$^-$CD70$^+$ Treg subsets.

Hypothesis 3: CD27$^+$CD70$^-$ and CD27$^-$CD70$^+$ Tregs will differ in their regulatory phenotype, suppressive activity and transcriptome profile.

3.3. Results

3.3.1. CD27 and CD70 expression defines distinct *ex vivo* human Treg subpopulations

We assessed expression levels of CD27 and CD70 on flow-sorted CD4$^+$CD25$^+$CD127$^{-/low}$ human Tregs isolated at high purity levels from healthy donor PBMCs. Most of *ex vivo* Tregs were CD27$^+$CD70$^-$ (64.4-92.7%), with a variable, but minor, subpopulation expressing CD70 (Figure 3.1A). Distinct CD27 and CD70 expression patterns were associated with different levels of FOXP3 expression (Figure 3.1B). When normalised to the total Treg population, CD27$^+$CD70$^+$ and CD27$^-$CD70$^+$ cell subsets displayed a higher

intensity of FOXP3 expression, while CD27⁻CD70⁻ and CD27⁺CD70⁻ cell subsets had a lower or similar level of FOXP3 expression (Figure 3.1B; right panel).

Figure 3.1

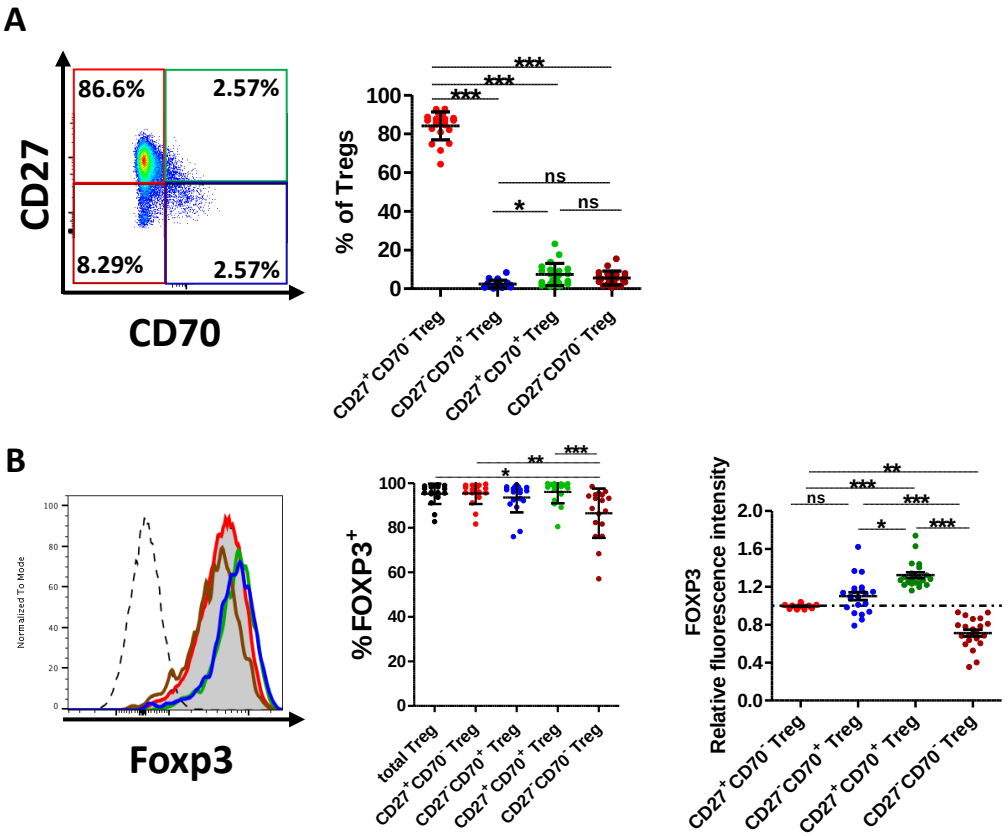

3.1. CD27 and CD70 expression defines distinct *ex vivo* human Treg subpopulations.

(A) Expression of CD27 and CD70 was analysed on freshly isolated CD4⁺CD25⁺CD127⁻/low Tregs (total Tregs). Left panel: Representative FACS plots from one donor. Right panel: Statistical analysis of several donors (n= 21 independent donors). Data were analysed using Kruskal-Wallis test with Dunn's post-test for multiple comparisons and are represented as mean ± SD.

(B) FOXP3 expression was measured within the total Tregs or within different Treg subsets defined by CD27 and CD70 expression. Left panel: Representative FACS plots from one donor. Middle panel: Percentage of FOXP3⁺ cells in different CD27/CD70 Treg subsets. Mean ± SD is represented. Right panel: FOXP3 fluorescence intensity normalised to the total Treg population in different Treg subsets (n= 21 independent donors). Errors bars represent mean ± SEM. Kruskal-Wallis test with Dunn's post-test for multiple comparisons was conducted.

ns= non-significant, *P<0.05, **P<0.01, ***P < 0.001.

3.3.2. Dynamic CD27 and CD70 expression on human Tregs and CD4$^+$ Tconv cells following *in vitro* stimulation

We then studied changes in CD27 and CD70 expression upon activation. Sorted CD4$^+$CD25$^+$CD127$^{-/low}$ Tregs or CD4$^+$CD25$^-$ Tconv cells were activated with anti-CD3/anti-CD28 coated beads (1 bead: 5 Tregs) and rhIL-2 (250 U/ml) over a short time frame. Analysis of expression patterns revealed a reciprocal relationship between CD27 and CD70 on activated Treg and Tconv cells (Figure 3.2A). CD27 expression was highly upregulated by Tregs after 3 days of stimulation and largely downregulated afterwards. A similar trend in CD27 expression was observed in activated Tconv, although lower CD27 upregulation compared to Tregs was observed (Figure 3.2B). In both Tregs and Tconv cells, CD70 expression was increased after 3 and 5 days of stimulation (Figure 3.2B).

Figure 3.2

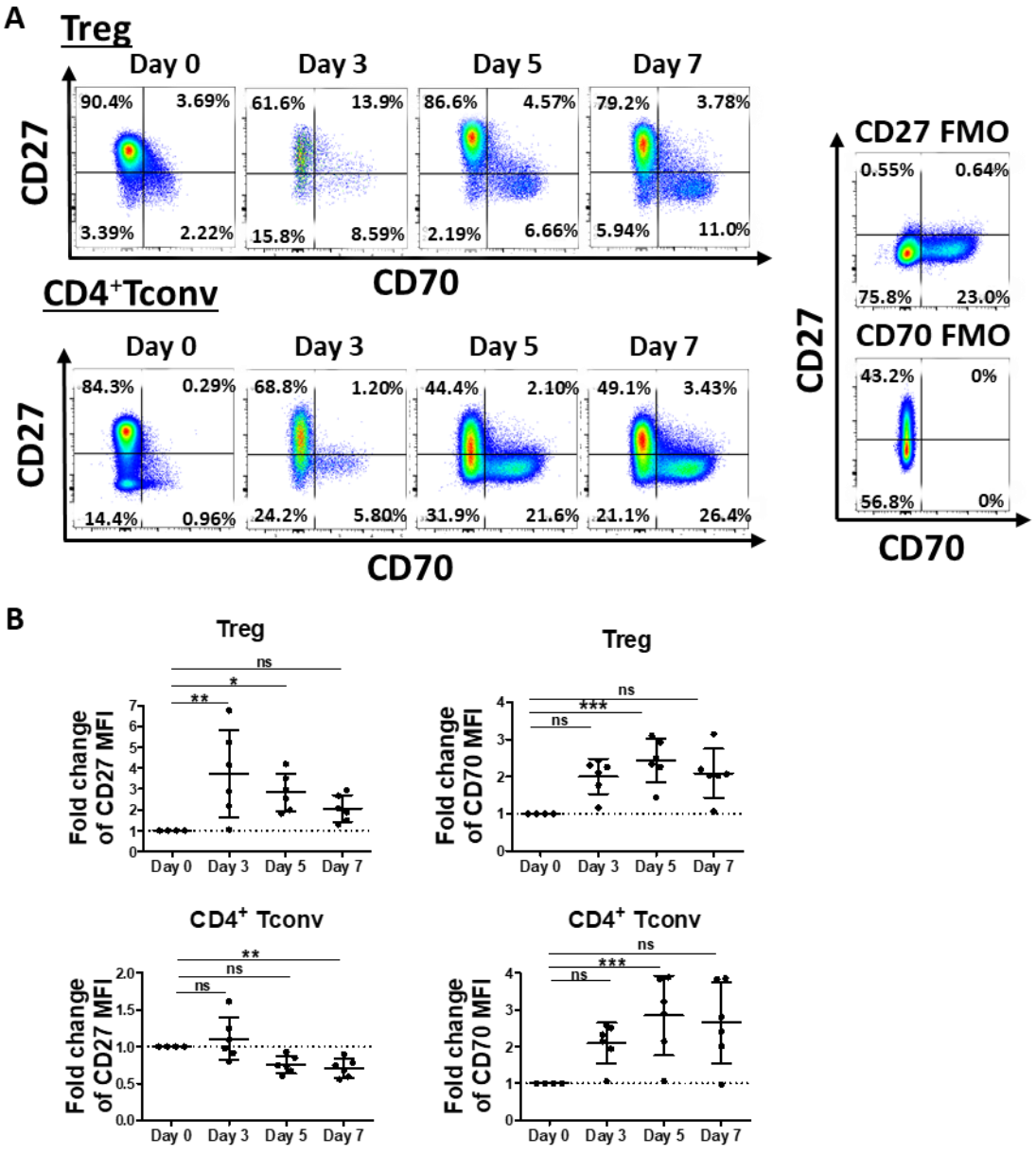

3.2. Dynamic CD27 and CD70 expression on human Tregs and CD4⁺ Tconv following *in vitro* activation.

CD27 and CD70 expression was measured at different time points in (top) $CD4^+CD25^+CD127^{-/low}$ sorted Tregs (Treg) or (bottom) $CD4^+CD25^-$ conventional T cells ($CD4^+$ Tconv) stimulated polyclonally with anti-CD3/anti-CD28 coated beads (1:5 beads:cells) in the presence of rhIL-2 (250U/ml for Tregs and 25U/ml for $CD4^+$Tconv).

(A) Dot plots from one representative donor.

(B) CD27 and CD70 fluorescence intensity was analysed within the $CD27^+CD70^-$ or the $CD27^-CD70^+$ gate respectively in both Tregs and $CD4^+$ Tconv at different time points and normalised to levels prior stimulation. Data represented as mean ± SD. (n=6 independent donors with 1-3 replicates per donor). Statistical significances were analysed using Friedman test with Dunn's post-test for multiple comparisons. ns= non-significant, *P<0.05, **P<0.01, ***P < 0.001.

It is well known that the microenvironment plays a crucial role in the expansion, differentiation and function of Tregs. Toll-like receptors (TLR) ligands are potent activators of the innate immune system, which will promote an adaptive immune response. Recent studies have shown that Tregs express TLRs, and TLR ligands can also act directly on Tregs and modulate Treg expansion and function (*326*). Likewise, it is well known that cytokines are crucial for Treg development, their stability and function (*327*).

In order to find environmental cues that affect CD27/CD70 expression, Tregs were activated under different stimuli. Tregs were cultured in the presence of rhIL-2 and activated with phorbol myristate acetate (PMA) and ionomycin or anti-CD3/anti-CD28 coated beads. In addition, a combination of TLR ligands or pro-inflammatory cytokines were added along with stimulating beads. After 5 days of culture, PMA and ionomycin treatment did not result in significant changes, but both CD27 and CD70 were significantly upregulated upon activation with anti-CD3/anti-CD28 coated beads (Figure 3.3A). In comparison to activation via CD3 and CD28, additional stimulation using a combination of viral TLR ligands (imiquimod, ssRNA40/LyoVec, ODN2006, Poly(I:C) and Poly(I:C)-LMW for activation of TLR7, TLR8, TLR9 and TLR3) or bacterial TLR ligands (Pam3CSK4, HKLM, FSL1, LPS and flagellin for triggering TLR1/2, TLR2, TLR6/2 and TLR5) did not result in significant differences in CD27 or CD70 expression (Figure 3.3A).

CD27 and CD70 expression was affected when pro-inflammatory cytokines were added into Treg cultures stimulated with anti-CD3/anti-CD28 coated beads (Figure 3.3B). Whereas reduced intensity of CD27 expression was observed when Tregs were stimulated in the presence of a combination of IL-1β, IL-6 and TNF-α pro-inflammatory cytokines, CD70 expression was increased (Figure 3.3B). When the effect of each cytokine was analysed individually, we observed that IL-1β and IL-6 tended to reduce CD27 but to increase the intensity of CD70 expression (Figure 3.3B). On the other hand, TNF-α, IFN-γ and IL-23 alone did not affect CD27 nor CD70 expression (Figure 3.3B).

Since the major difference was observed when Tregs were activated via anti-CD3/anti-CD28 compared to PMA and ionomycin or TLR ligands, we tested whether levels of CD27 and CD70 expression was dependent on the strength of this stimulation. Tregs were activated with anti-CD3/anti-CD28 coated beads at ratios 1:5 or 1:1 bead:Treg in the absence or presence of IL-1β, IL-6 and TNF-α. Following 5 days of culture, similar expression patterns of CD27 and CD70 were observed regardless of the bead:Treg ratio (Figure 3.3C).

Altogether, these results show that, among the tested stimuli, signalling via CD3 and CD28 is the main driver for CD27 and CD70 upregulation in Tregs.

Figure 3.3

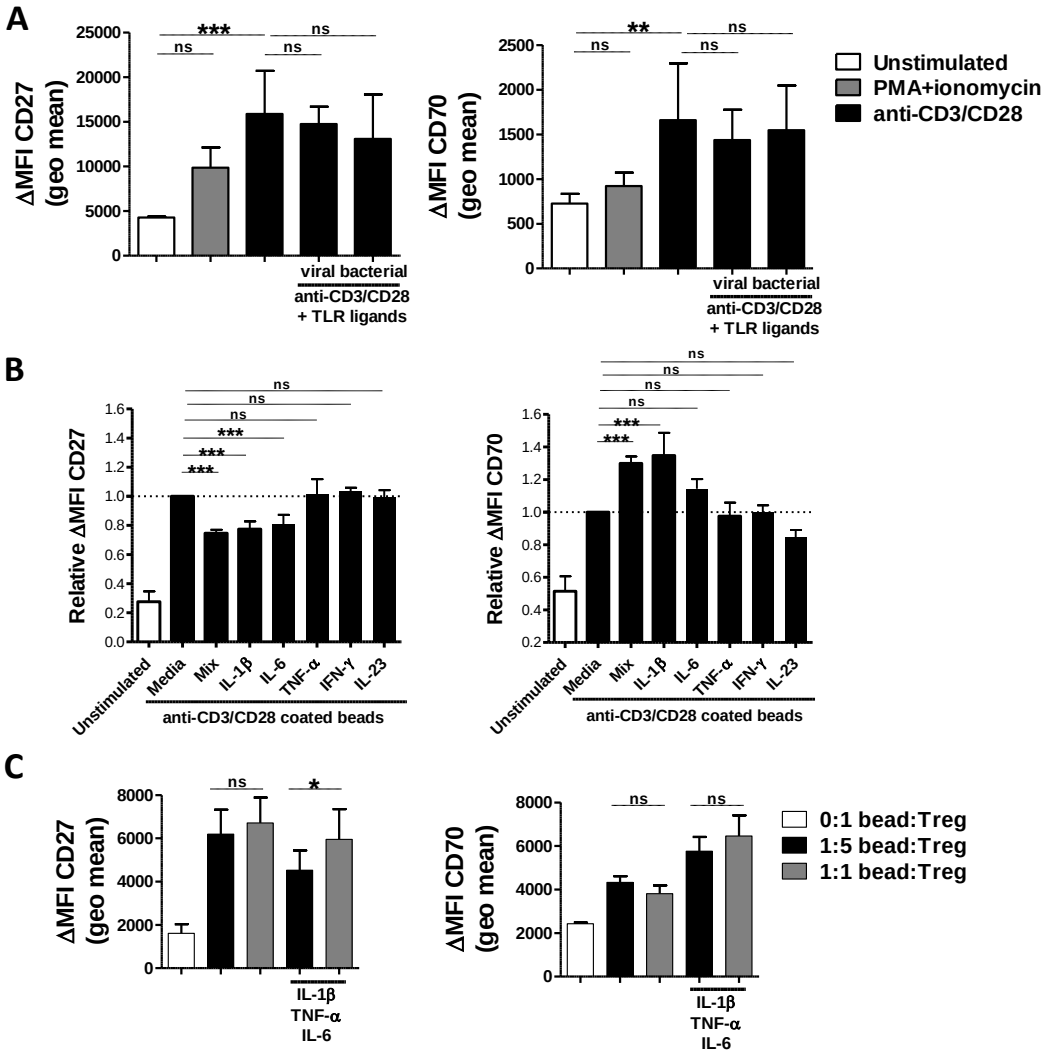

3.3. CD27 and CD70 expression under different activation stimuli.

CD27 and CD70 expression was measured on sorted and stimulated $CD4^+CD25^+CD127^{-/low}$ Tregs. CD27 and CD70 fluorescence intensity was analysed within $CD27^+CD70^-$ or $CD27^-CD70^+$ gate respectively. Tregs were stimulated for 5 days in the presence of 250U/ml rhIL-2 with different stimuli as follow.

(A) 100ng/ml phorbol myristate acetate (PMA) and 1µg/ml ionomycin or anti-CD3/anti-CD28 coated beads (1:5 beads:cells) along with a mix of viral or bacterial TLR ligands. (Viral TLR ligand mix contains: imiquimod (5µg/ml), ssRNA40/LyoVec (5µg/ml), ODN2006 (5µM), Poly(I:C) (10µg/ml) and Poly(I:C)-LMW (10µg/ml). Bacterial TLR ligand mix contains: Pam3CSK4 (1µg/ml), HKLM (10^8 cells/well), FSL1 (1µg/ml), LPS (0.1µg/ml) and flagellin (1µg/ml)).

(B) Anti-CD3/anti-CD28 coated beads (1 bead: 5 cells) and cytokines as indicated in the figure at a concentration of 10ng/ml for each cytokine. Data is displayed as relative to stimulation via anti-CD3/anti-CD28 in the absence of cytokines. (Mix of cytokines contains: IL-1β, IL-6 and TNF-α).

(C) Anti-CD3/anti-CD28 coated beads (1:5 or 1:1 beads:cells) and combination of cytokines (10ng/ml) as indicated.

Data represent mean ± SD of 3-6 independent donors with 1-3 replicates per donor. Data were analysed using one way-ANOVA with Bonferroni post-test for multiple comparisons. ns= non-significant, *P<0.05, **P<0.01, ***P < 0.001.

3.3.3. *In vitro* expanded Tregs and Tconv cells can be separated into cell subsets by the expression of CD27 and CD70

To investigate how prolonged stimulation may alter CD27 and CD70 expression, the phenotype of Tregs was examined following stimulation and expansion for 2 to 4 weeks, using anti-CD3/anti-CD28 coated beads (1 bead: 1 cell) and rhIL-2 (1000U/ml). While initial levels of CD27 expression were high in freshly isolated cells, after expansion there was a progressive reduction of expression in most of the donors (Figure 3.4A). Conversely, CD70 expression levels were initially low and then increased after expansion (Figure 3.4A). By 2 weeks of expansion, two distinct Treg subpopulations could be identified by their pattern of CD27 and CD70 expression: CD27$^+$CD70$^-$ or CD27$^-$CD70$^+$ Tregs (Figure 3.4B). A variable proportion of CD27$^+$CD70$^+$ cells was also observed for some of the donors.

We then studied whether Tconv and Tregs may differ in their CD27/CD70 phenotype upon expansion. Levels of CD27 expression were similar between both subsets before and after 2 or 4 weeks of *in vitro* expansion, while the Treg population had higher percentage of CD70$^+$ cells at all time points (Figure 3.4C).

Figure 3.4

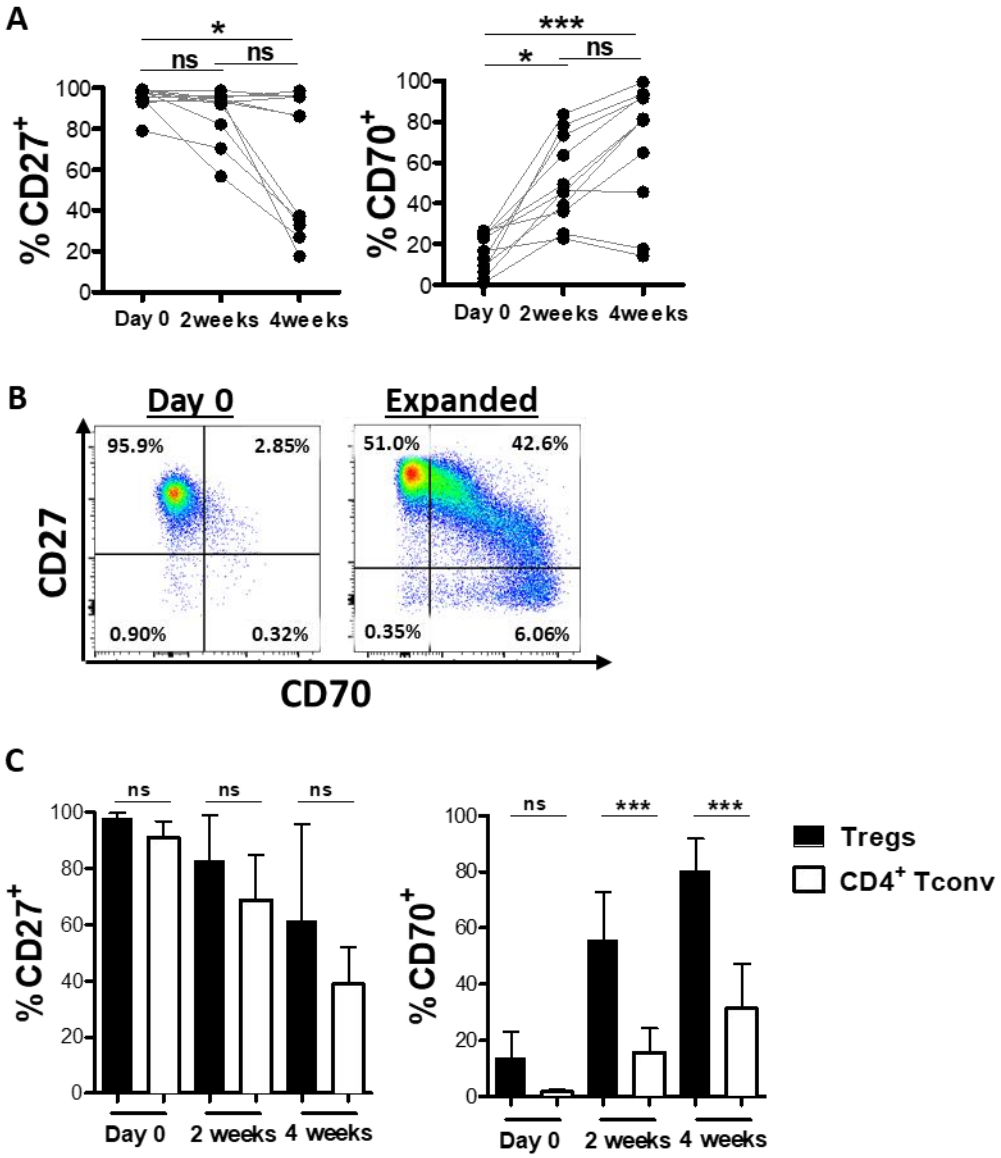

3.4. *In vitro* expanded Tregs and Tconv can be separated into cell subsets by the expression of CD27 and CD70.

(A-B) CD27 and CD70 expression was analysed on freshly isolated *ex vivo* Tregs or Tregs expanded for 2 or 4 weeks with anti-CD3/anti-CD28 coated beads at a ratio of 1:1 beads to cells in the presence of rhIL-2 (1000 U/ml). **(A)** Data show n=11 independent donors analysed using a Friedman test with Dunn's post-test for multiple comparisons. **(B)** Representative dot plot from one donor; expanded cells shown at 2 weeks.

(C) CD27 and CD70 expression was analysed in Tregs or $CD4^+CD25^-$ Tconv cells on freshly isolated *ex vivo* cells (day 0) or cells expanded for 2 or 4 weeks with anti-CD3/anti-CD28 coated beads at a ratio of 1:1 beads to cells in the presence of rhIL-2. 4-6 independent donors analysed using a one-way ANOVA with Bonferroni post-test.

ns= non-significant, *P<0.05, **P<0.01, ***P < 0.001.

3.3.4. Prolonged *in vitro* expansion reduces suppressive capacity of human Tregs

Since Tregs represent 1%-10% of the total CD4$^+$ T lymphocytes in peripheral blood, it is required to expand them *ex vivo* for therapeutic application. When CD4$^+$CD25$^+$CD127$^{-/low}$ Tregs were *in vitro* stimulated with anti-CD3/anti-CD28 coated beads and rhIL-2, we found an average expansion rate of 82.86 ± 45.93 during 2 weeks of expansion (Figure 3.5A; left panel). For most of the donors, some Tregs died during a resting period of 2 days in 250 U/ml rhIL-2 in the absence of anti-CD3/anti-CD28 stimulation; with an average of cell recovery after resting of 86.70% ± 49.43% (Figure 3.5A; right panel). Treg expansion rate was highly variable among donors, underlining the need of longer *in vitro* expansion to ensure good yield for clinical therapy. If Tregs were expanded for 2 further weeks, an average expansion rate of 155.9 ± 353.8 and cell recovery after rest of 70% ± 48.28% was observed (Figure 3.5B). Therefore, a 32 days expansion protocol (4 weeks expansion and 4 days resting) leaded to 9960 ± 12454 fold expansion, ensuring enough cell yield for clinical application (Figure 3.5C).

Figure 3.5

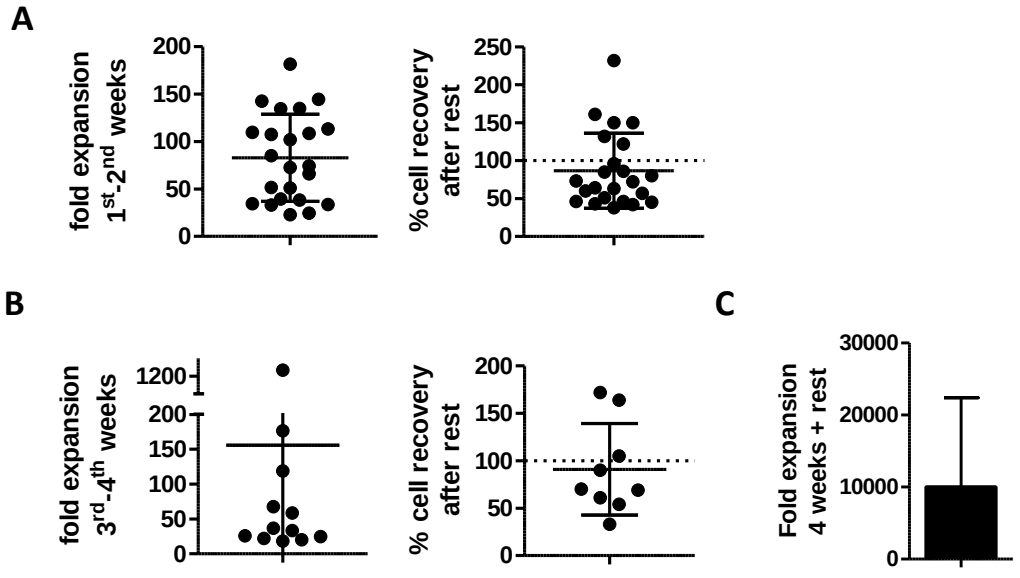

3.5. Treg proliferation rate during the expansion procedure.

(A) CD4^{+}CD25^{+}CD127$^{-/low}$ total Tregs were expanded *in vitro* with anti-CD3/anti-CD28 coated beads (1 bead to 1 cell) in the presence of 1000 U/ml rhIL-2. Left panel: Treg fold expansion was studied over 2 weeks of *in vitro* culture. Right panel: After 2 weeks of expansion, Tregs were rested for 2 days in 250U/ml rhIL-2 in the absence of stimulating beads. Percentage of cell recovery after resting is shown. n= 23 independent donors. Error bars represent mean ± SD.

(B) After 2 weeks of expansion and 2 resting days, Tregs were expanded for 2 further weeks. Left panel: Treg fold expansion during 3rd and 4th expansion weeks**.** Right panel: Percentage of cell recovery after 2 resting days following 4 weeks of expansion. n= 9-12 independent donors. Mean ± SD.

(C) Cumulative Treg fold expansion during 4 weeks of expansion and 2 resting periods of 2 days every 2 expansion weeks. n= 6 independent donors. Error bars represent mean ± SD.

We then analysed the regulatory phenotype of Tregs following *in vitro* expansion for 2 to 4 weeks with anti-CD3/anti-CD28 coated beads and rhIL-2. Tregs pre-expansion expressed high levels of FOXP3, and while this was largely maintained during the first 2 weeks of expansion, after 4 weeks there was a significant reduction in FOXP3 expression; from 96.53% (mean +/- 4.80% SD) on freshly sorted Tregs to 92.35% (mean +/- 5.86% SD) after 2 weeks and to 58.54% (mean+/- 18.85% SD) after 4 weeks (Figure 3.6A). Although not being statistically significant, there was a trend towards a negative correlation between fold expansion and FOXP3 expression in 4 weeks expanded Tregs (Figure 3.6B). On functional assessment of these Tregs using an *in vitro* MLR suppression assay, suppressive potency was maintained after 2 weeks of expansion but reduced after 4 weeks (Figure 3.6C,D). Neither FOXP3 nor CD70 expression correlated with Treg suppressive potency at 4 weeks of expansion (Figure 3.6E,F).

Figure 3.6

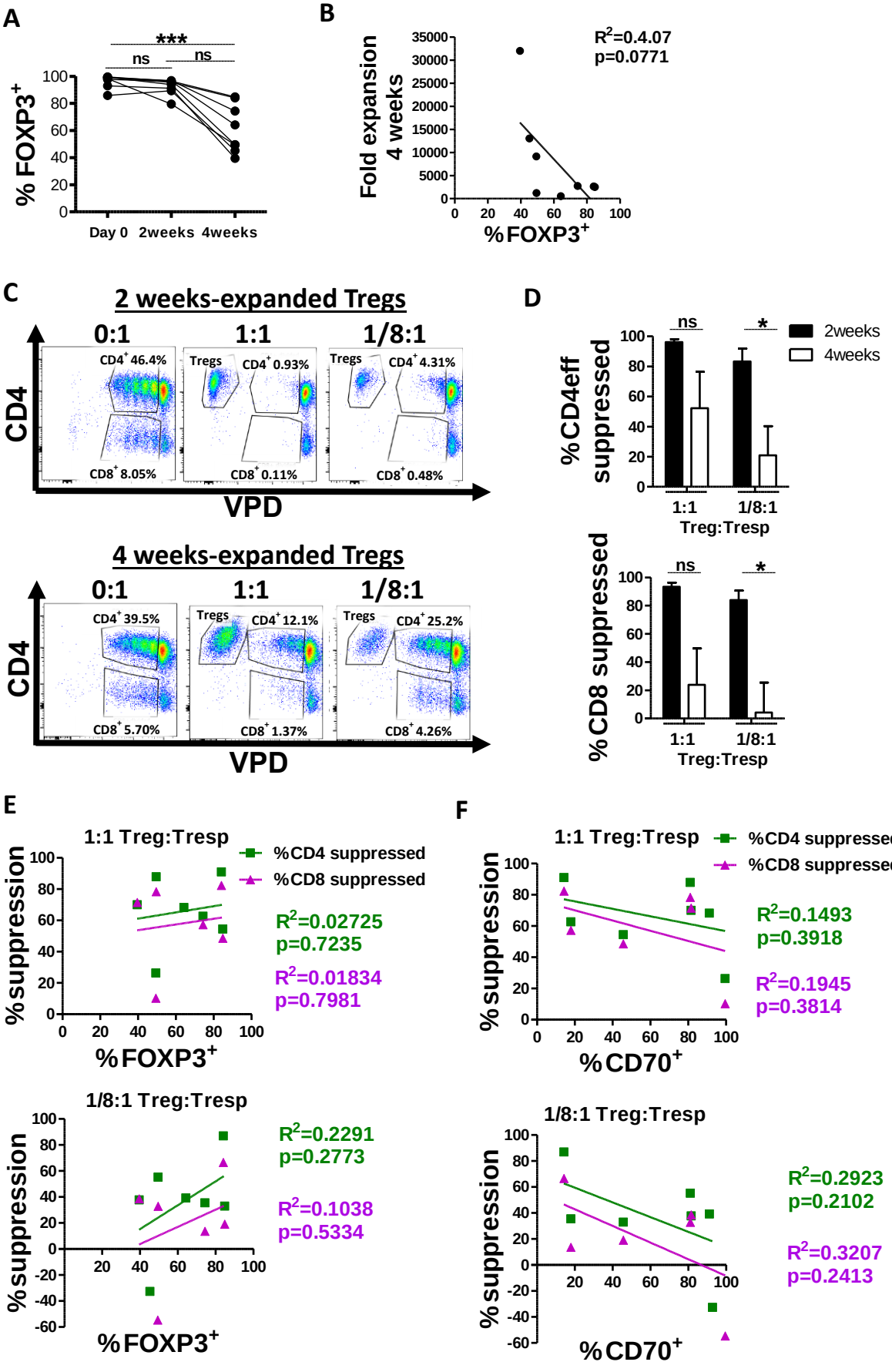
A
***
ns
ns
% FOXP3+
Day 0
2weeks
4weeks
B
R2=0.4.07
p=0.0771
Fold expansion 4 weeks
%FOXP3+
C
2 weeks-expanded Tregs
0:1
1:1
1/8:1
CD4
VPD
CD4+ 46.4%
CD8+ 8.05%
Tregs
CD4+ 0.93%
CD8+ 0.11%
CD4+ 4.31%
CD8+ 0.48%
4 weeks-expanded Tregs
CD4+ 39.5%
CD8+ 5.70%
CD4+ 12.1%
CD8+ 1.37%
CD4+ 25.2%
CD8+ 4.26%
D
%CD4eff suppressed
%CD8 suppressed
2weeks
4weeks
1:1
1/8:1
Treg:Tresp
E
1:1 Treg:Tresp
%CD4 suppressed
%CD8 suppressed
R2=0.02725
p=0.7235
R2=0.01834
p=0.7981
%suppression
%FOXP3+
1/8:1 Treg:Tresp
R2=0.2291
p=0.2773
R2=0.1038
p=0.5334
F
1:1 Treg:Tresp
R2=0.1493
p=0.3918
R2=0.1945
p=0.3814
%CD70+
1/8:1 Treg:Tresp
R2=0.2923
p=0.2102
R2=0.3207
p=0.2413

3.6. Prolonged *in vitro* expansion reduces the suppressive capacity of human Tregs.

CD4$^+$CD25$^+$CD127$^{-/low}$ total Tregs were expanded *in vitro* with anti-CD3/anti-CD28 coated beads (1 bead to 1 cell) in the presence of 1000 U/ml rhIL-2 for 2 to 4 weeks.

(A) FOXP3 expression was analysed in 8 independent donors at different time points. Statistical significance was calculated by Friedman test with Dunn's post-test for multiple comparisons.

(B) Fold expansion is plotted against FOXP3 expression in the same samples at 4 weeks culture.

(C-D) Treg suppressive capacity was assessed *in vitro* using a MLR suppression assay consisted of VPD-labelled CD3$^+$CD25$^-$ responder T cells (Tresp) stimulated with allogenic DCs in the presence of Tregs. **(C)** Percentage of dividing CD4$^+$ or CD8$^+$ Tresp in the absence of Tregs (0:1) and in the presence of Tregs at a 1:1 or 1/8:1 Treg:Tresp ratios (Percentage of dividing CD4$^+$ or CD8$^+$ Tresp is calculated after exclusion of Treg gate as shown). **(D)** Percentage suppression of CD4$^+$ and CD8$^+$ Tresp calculated based in division index according to the formula described in Materials and Methods. Data represent mean ± SEM of 3 independent donors (with 3 replicate wells in the suppression assay of each donor). Statistics are derived from a two-way ANOVA with Bonferroni post-tests. ns= non-significant, *P<0.05.

(E-F) Percentage of suppression is plotted against **(E)** FOXP3 and **(F)** CD70 expression in the same samples at 4 weeks culture for (top) 1:1 and (bottom) 1/8:1 Treg:Tresp ratios.

We hypothesised that the loss in suppression observed in expanded Tregs was secondary to the expansion-related changes in CD27 and CD70 expression. On examination of the specific function of CD27$^+$CD70$^-$ or CD27$^-$CD70$^+$ Tregs sorted from bulk Treg culture after 2 weeks of expansion, both populations were capable to suppress CD4$^+$ and CD8$^+$ T cell proliferation, although the CD27$^+$CD70$^-$ Treg subset appeared as a more potent suppressor than CD27$^-$CD70$^+$ Tregs (Figure 3.7A). This was largely unrelated to any differences in FOXP3 expression levels (Figure 3.7B). The activity of CD27$^+$CD70$^+$ Tregs was not analysed since the presence of this double positive population in expanded Tregs appeared to be donor-dependet and was not present for all donors analysed.

To investigate differential stability of CD27/CD70 Treg subsets on an epigenetic level, we analysed the methylation state of the TSDR region in sorted CD27$^+$CD70$^-$ and CD27$^-$CD70$^+$ Treg subsets from freshly isolated or 2 weeks expanded total Tregs. In freshly isolated Tregs, both Treg subsets had low methylated TSDR, confirming their high degree of purity (Figure 3.7C). Upon 2 weeks of expansion, TSDR remained largely demethylated in CD27$^+$CD70$^-$ Tregs, whereas CD27$^-$CD70$^+$ Tregs had hypermethylated TSDR (Figure 3.7C). At this time, disparity in TSDR demethylation did not relate to differences in FOXP3

expression (Figure 3.7B,C). Interestingly, the methylation pattern in expanded CD27⁻CD70⁺ Tregs was not equal across different CpG motifs (Figure 3.7D and Table 3.1).

Figure 3.7

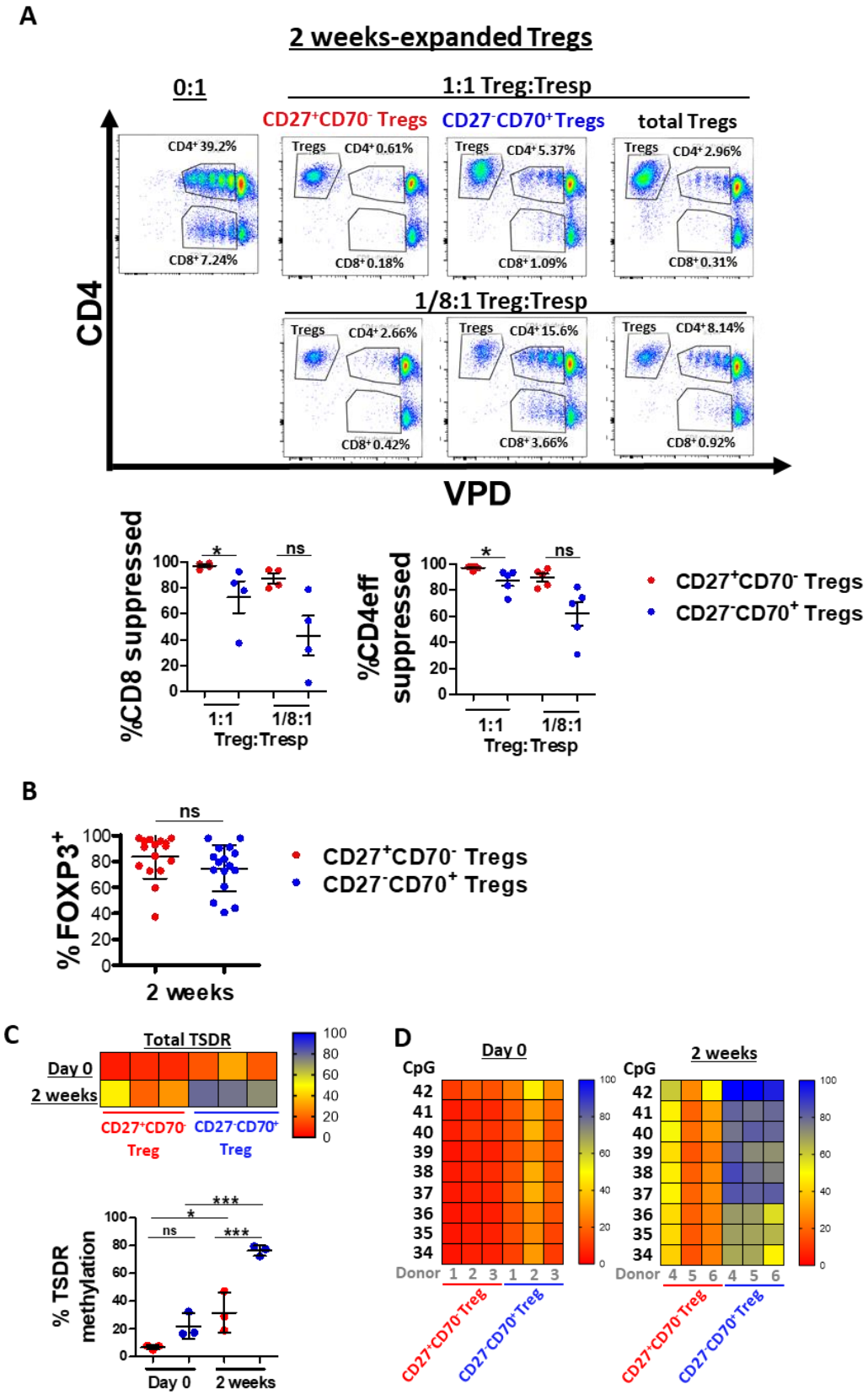

3.7. After 2 weeks of *in vitro* expansion, both CD27$^+$CD70$^-$ and CD27$^-$CD70$^+$ Treg subsets suppress T cell proliferation.

After 2 weeks of expansion, suppressive capacity of CD27$^+$CD70$^-$ and CD27$^-$CD70$^+$ sorted Tregs was assessed using a MLR *in vitro* suppression assay. CD3$^+$CD25$^-$ responder T cells (Tresp) were labelled with VPD and stimulated with allogenic DCs in the presence of absence of CD27/CD70 Treg subsets sorted from bulk Treg expanded population.

(A) Top panel: Data from one representative donor. Numbers in the plots refer to the percentage of dividing CD4$^+$ or CD8$^+$ Tresp in the absence of Tregs (0:1) and in the presence of different CD27/CD70 Treg subsets at a (top) 1:1 or (bottom) 1/8:1 Treg:Tresp ratios. Bottom panel: Percentage suppression of CD4$^+$ and CD8$^+$ Tresp for 4-5 independent donors with each data point showing the mean of 3 replicate wells for each donor; calculated based on division index. Mean ± SEM is depicted. Red: CD27$^+$CD70$^-$ Tregs; Blue: CD27$^-$CD70$^+$ Tregs, both sorted after 2 weeks of expansion. A Kruskal-Wallis test with Dunn's post-test for multiple comparisons was conducted.

(B) FOXP3 levels were analysed in CD27$^+$CD70$^-$ and CD27$^-$CD70$^+$ Treg subsets after 2 weeks of expansion (n=16 independent donors, Mann-Whitney test). Data are represented as mean ± SEM.

(C-D) DNA methylation pattern of the Treg-Specific Demethylation Region (TSDR) was studied in CD27$^+$CD70$^-$ and CD27$^-$CD70$^+$ Treg subsets from matched donors, sorted from freshly isolated and 2 weeks *in vitro* expanded CD4$^+$CD25$^+$CD127$^{-/low}$ Tregs. **(C)** The average methylation rate for 9 CpG motifs of the TSDR is shown for 6 different donors. Top panel: Each box represents the percentage of methylation for each cell donor. Bottom panel: each dot denotes a donor and error bars indicate mean ± SD. Statistical significance was determined by one-way ANOVA with Bonferroni post-test. **(D)** Each box represents the percentage of methylation of a single CpG residue for each different donor at each time point (Left panel: day 0; right panel: 2 weeks) (n=3 donors matched for each CD27/CD70 Treg subset). Bar colours designate: red: 0% methylation; yellow: 50% methylation; blue: 100% methylation.

ns= non-significant, *P<0.05, ***P < 0.001.

Table 3.1 DNA methylation analysis of the Treg-Specific Demethylated Region (TSDR).

													Overall Region			
			From ATG	-2330	-2322	-2312	-2309	-2303	-2299	-2291	-2282	-2263	-2330 to -2263			
			From TSS	3992	4000	4010	4013	4019	4023	4031	4040	4059	+3992 to +4059			
			GRCh38, ChrX	49260835	49260827	49260817	49260814	49260808	49260804	49260796	49260787	49260768	chrX:49260835-49260768			
	Donor	Subset	**CpG#**	**-42**	**-41**	**-40**	**-39**	**-38**	**-37**	**-36**	**-35**	**-34**	**Mean**	St Dev	Min	Max
Day 0	1	$CD27^+CD70^-$ Treg		11.2	4.8	5.4	3.5	4.7	4.5	3.8	3.8	3.7	**5.0**	2.4	3.5	11.2
	1	$CD27^-CD70^+$ Treg		24.8	16.4	15.5	14.5	15.7	18.5	15.6	14.9	12.5	**16.5**	3.5	12.5	24.8
	2	$CD27^+CD70^-$ Treg		18.0	7.4	10.7	6.5	6.8	6.0	4.9	5.2	5.8	**7.9**	4.2	4.9	18.0
	2	$CD27^-CD70^+$ Treg		46.8	31.7	35.0	25.9	33.8	34.4	27.3	26.8	30.0	**32.4**	6.4	25.9	46.8
	3	$CD27^+CD70^-$ Treg		15.7	7.3	9.5	5.7	7.9	6.7	5.3	6.0	5.7	**7.7**	3.2	5.3	15.7
	3	$CD27^-CD70^+$ Treg		27.7	18.9	16.8	16.1	17.0	19.0	16.0	13.0	11.2	**17.3**	4.6	11.2	27.7
2 weeks expansion	4	$CD27^+CD70^-$ Treg		60.4	47.4	51.2	43.5	46.8	47.8	43.0	42.6	40.6	**47.0**	6.0	40.6	60.4
	4	$CD27^-CD70^+$ Treg		100.0	80.7	77.3	80.7	85.9	83.5	69.9	68.7	66.7	**79.3**	10.3	66.7	100.0
	5	$CD27^+CD70^-$ Treg		26.6	19.0	20.6	16.2	18.1	19.1	18.4	16.7	15.5	**18.9**	3.3	15.5	26.6
	5	$CD27^-CD70^+$ Treg		100.0	77.4	81.9	73.0	78.4	80.9	69.3	67.7	67.1	**77.3**	10.2	67.1	100.0
	6	$CD27^+CD70^-$ Treg		48.1	31.2	29.6	24.5	26.9	27.1	25.2	24.2	24.6	**29.0**	7.5	24.2	48.1
	6	$CD27^-CD70^+$ Treg		94.1	79.5	79.9	71.6	74.9	81.8	56.5	64.2	47.5	**72.2**	14.2	47.5	94.1
Methylation Controls		Low		18.7	4.4	6.7	2.1	3.9	2.1	4.5	2.9	4.4	**5.5**	5.2	2.1	18.7
		Med		59.0	46.7	42.2	37.4	42.4	43.9	42.4	36.1	44.1	**43.8**	6.6	36.1	59.0
		High		100.0	94.6	100.0	92.2	91.3	92.3	81.7	77.8	93.6	**91.5**	7.4	77.8	100.0
Negative control				-	-	-	-	-	-	-	-	-				

3.3.5. Upon prolonged expansion, the CD27$^+$CD70$^-$ phenotype discriminate Tregs with potent suppressive activity

We therefore investigated whether re-sorting cells based on CD27 and CD70 expression 2 weeks following expansion would address the loss of suppressive potency that developed between weeks 2 and 4 of expansion. Total Tregs were expanded for 2 weeks and then flow sorted into CD27$^+$CD70$^-$ and CD27$^-$CD70$^+$ populations before continuing expansion for a further 2 weeks (Figure 3.8A). While sorted CD27$^-$CD70$^+$ Tregs maintained their phenotype for the 2 subsequent weeks of expansion, CD27$^+$CD70$^-$ Tregs downregulated CD27 and upregulated CD70 (Figure 3.8B). FOXP3 expression was significantly higher in 4 weeks expanded CD27$^+$CD70$^-$ cells than CD27$^-$CD70$^+$ cells (67.6% mean ± 21.23 SD and 44.39% mean ± 25.88 SD respectively) (Figure 3.8B).

Figure 3.8

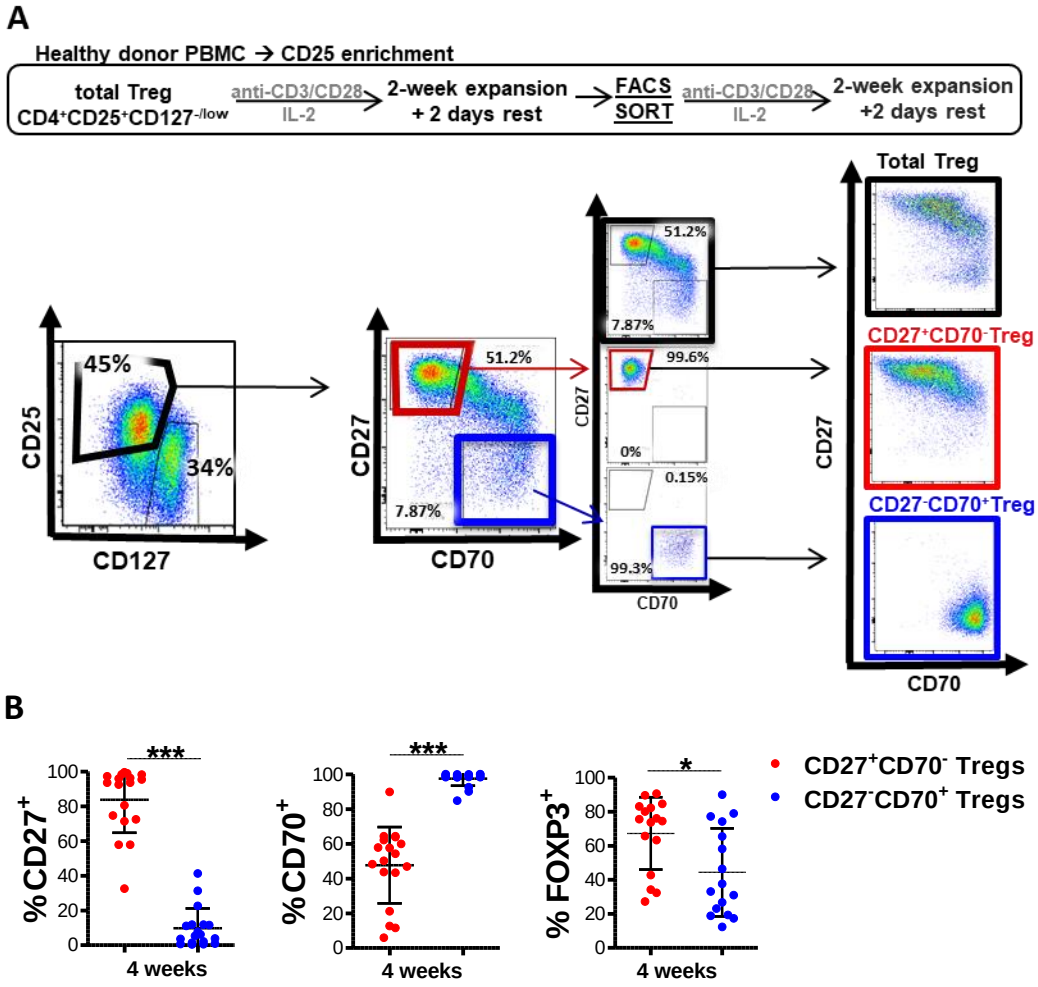

3.8. Expansion strategy for prolonged CD27⁺CD70⁻ and CD27⁻CD70⁺ Treg culture.

(A) Schematic overview of Treg expansion strategies. CD4⁺CD25⁺CD127⁻/low Tregs were flow sorted from healthy donor PBMCs, expanded *in vitro* over two rounds of 7 days, stimulated with anti-CD3/anti-CD28 coated beads (at a ratio of 1 bead to 1 cell) and rhIL-2 (1000U/ml) and rested for 2 days with a low concentration of rhIL-2 (250U/ml) and without stimulating beads. Tregs expanded for 2 weeks were next flow sorted into CD27⁺CD70⁻ and CD27⁻CD70⁺ subsets. Total Tregs (black), flow sorted CD27⁺CD70⁻ Tregs (red) and flow sorted CD27⁻CD70⁺ Tregs (blue) were then cultured for a further 16 days before analysis. Dot plots from one representative donor are shown.

(B) FOXP3, CD27 and CD70 expression levels on expanded and then flow sorted CD27⁺CD70⁻ and CD27⁻CD70⁺ Tregs after further 2 weeks of expansion. n=16-18 independent donors, analysed using a Mann-Whitney test. Data are represented as mean ±SD. *p<0.05, *** p<0.001.

When we measured suppressive activity after 4 weeks of expansion using an MLR assay, the CD27$^+$CD70$^-$ Treg subset was more potent at inhibiting CD4$^+$ and CD8$^+$ T cell proliferation than CD27$^-$CD70$^+$ expanded cells at all ratios tested (Figure 3.9A). Moreover, in 11 out of 14 of the donors analysed, CD27$^-$CD70$^+$ Tregs actively promoted T cell proliferation (Figure 3.9B). Reduced suppression by CD27$^-$CD70$^+$ Tregs was not due to impaired Treg survival or proliferation, since for most of the donors analysed, similar or higher numbers of CD27$^-$CD70$^+$ Tregs were observed at the end of the MLR assay compared to numbers of CD27$^+$CD70$^-$ Tregs (Figure 3.9C).

When analysing CD27 and CD70 expression in Tregs and responder T cells (Tresp) at the end of the suppression test, we found high levels of CD27 and low CD70 expression in both CD4$^+$ and CD8$^+$ Tresp cells (Figure 3.9D). CD27 expression was maintained at high levels upon T cell activation, reflected by VPD dilution, and this was also true in the presence of CD27$^+$CD70$^-$ or CD27$^-$CD70$^+$ Tregs (Figure 3.9D). No major difference was detected in CD70 expression in Tresp when co-cultured with CD27$^+$CD70$^-$ or CD27$^-$CD70$^+$ Tregs (Figure 3.9D).

Figure 3.9

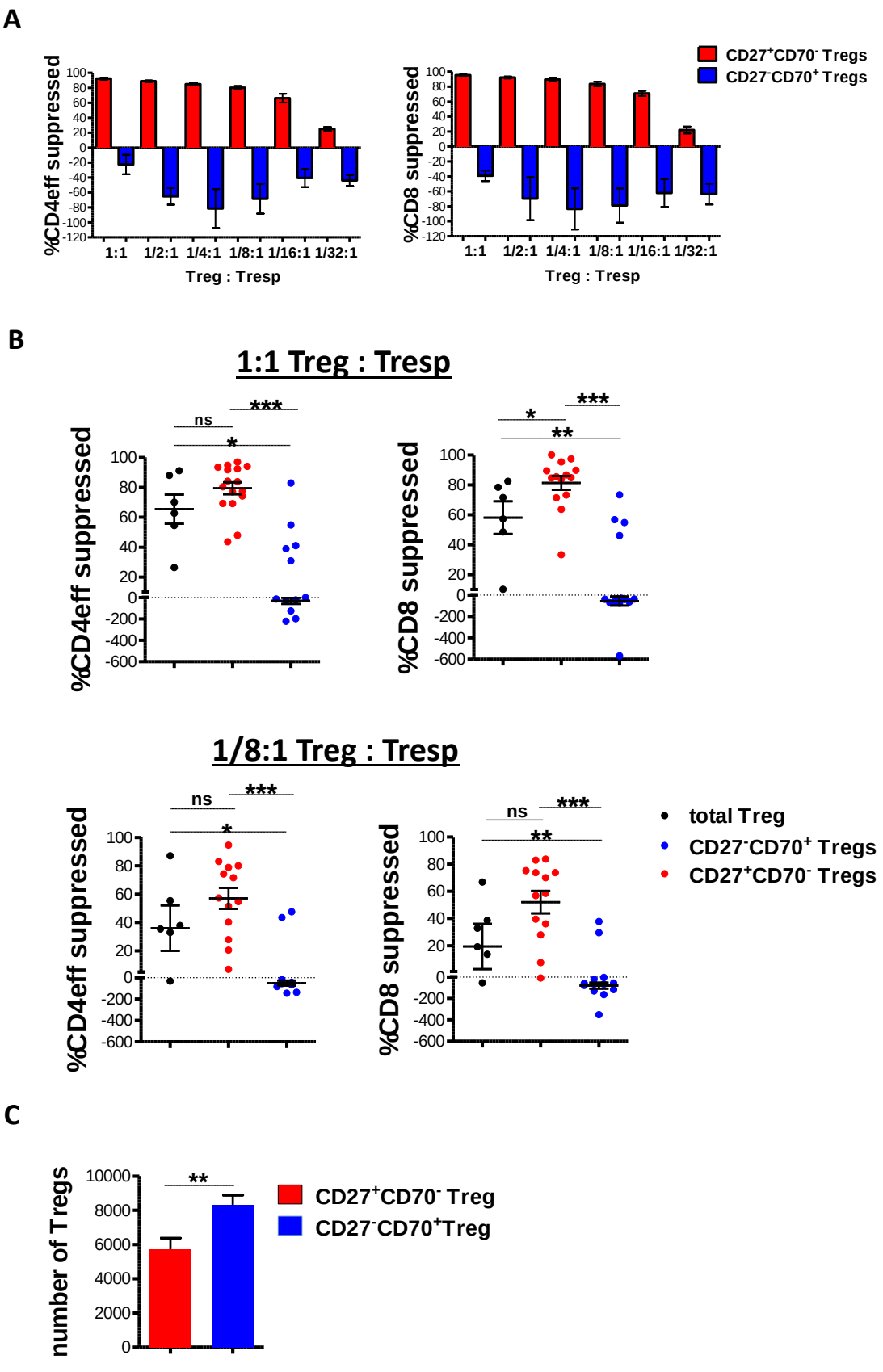
A
%CD4eff suppressed
%CD8 suppressed
1:1
1/2:1
1/4:1
1/8:1
1/16:1
1/32:1
Treg : Tresp
CD27⁺CD70⁻ Tregs
CD27⁻CD70⁺ Tregs
B
1:1 Treg : Tresp
1/8:1 Treg : Tresp
ns
*
**
***
total Treg
C
number of Tregs
CD27⁺CD70⁻ Treg
CD27⁻CD70⁺Treg

Figure 3.9

D

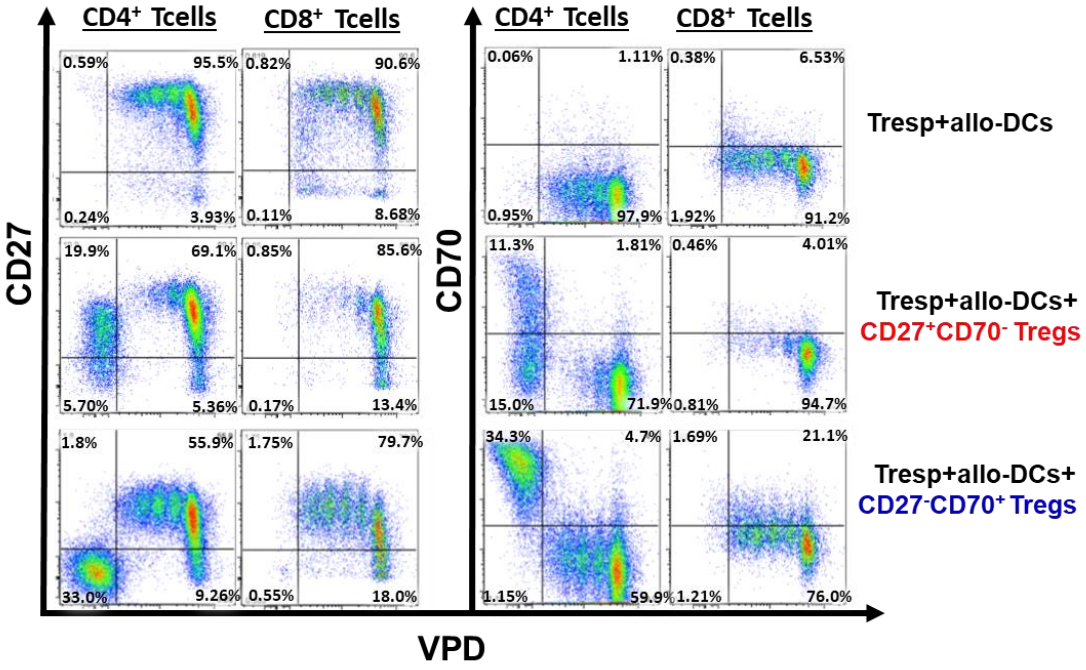

3.9. Upon prolonged expansion, the CD27⁺CD70⁻ phenotype discriminate Tregs with potent suppressive activity.

(A-B) Suppressive capacity of 4 week-expanded CD27⁺CD70⁻ and CD27⁻CD70⁺ Treg subsets (according to Figure 3.8A) was assessed in an *in vitro* MLR suppression test, where VPD-stained CD3⁺CD25⁻ responder T cells (Tresp) were stimulated with allogenic DCs in the presence of Tregs. **(A)** Graph for one representative donor showing 3 replicate wells in the assay (data displayed as mean ± SD). **(B)** Cumulative data of 14 independent donors at 1:1 (top) and 1/8:1 (bottom) ratios of Treg to Tresp. Each data point represents the mean of 3 replicate wells from each donor. Mean ± SEM is depicted. Red: CD27⁺CD70⁻; Blue: CD27⁻CD70⁺ Tregs. Data were analysed using a Mann-Whitney test.

(C) Number of Tregs at the end of the MRL assay for one representative donor (3 replicate wells). Statistical difference was studied by unpaired t test.

(D) (Left panel) CD27 and (right panel) CD70 expression was analysed in Tregs, CD4⁺ Tresp and CD8⁺ Tresp at the end of the MLR assay. Tregs are distinguished from CD4⁺ Tresp by VDP staining, Tregs being CD4⁺VDP⁻ cells.

ns= non-significant, **p*<0.05, ** *p*<0.01, *** *p*<0.001.

Although being consistently more suppressive than CD27⁻CD70⁺ Tregs, there was some donor-related heterogeneity in the suppressive activity of expanded CD27⁺CD70⁻ Tregs (Figure 3.9B). We considered whether differences in suppression by the expanded CD27⁺CD70⁻ cells were due to the presence of cells that had downregulated CD27 and upregulated CD70. In support of this hypothesis, re-sorted CD27^{high}CD70⁻ cells

demonstrated significantly enhanced suppressive activity than the total population of CD27+CD70- expanded cells (Figure 3.10). These data show that CD27+CD70- Tregs are not a fully stable population and repeated cell stimulation may lead to their progressive conversion into CD27-CD70+ cells.

Figure 3.10

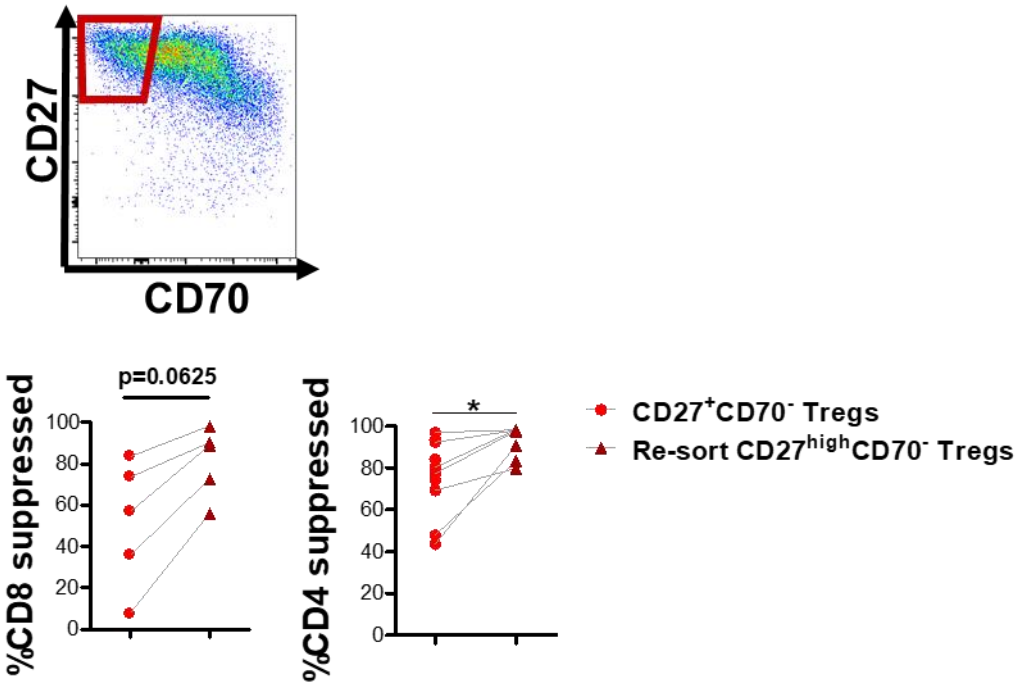

3.10. The CD27highCD70- phenotype identifies Tregs with potent suppressive activity

Suppressive capacity of re-sorted CD27highCD70- Tregs within 4 week-expanded CD27+CD70- expanded cells that upregulated CD70 and downregulated CD27. Top panel: Sorting strategy. Bottom panel: Treg suppressive activity was assessed in an *in vitro* MLR suppression test. Each data point represents the mean of 3 replicate wells for each of 5-7 independent donors. Data were analysed using a Wilcoxon matched-pairs test, *p<0.05.

Furthermore, to assess the increased potency of the CD27+CD70- Treg subset *in vivo*, we performed a human leukocyte proliferation assay in immunodeficient mice. VPD-labelled human PBMCs were transferred into mice together with human CD27+CD70- or CD27-CD70+ Tregs expanded *in vitro* for 4 weeks. CD27+CD70- Tregs, but not CD27-CD70+ Tregs were able to suppress CD4+ and CD8+ T cell proliferation *in vivo* in 2 independent donors (Figure 3.11). It should be noted that this *in vivo* model reflects Tregs controlling

homeostatic proliferation of responder T cells, which might differ from the allotransplantation scenario, when responder T cells are activated towards allo-antigens.

Figure 3.11

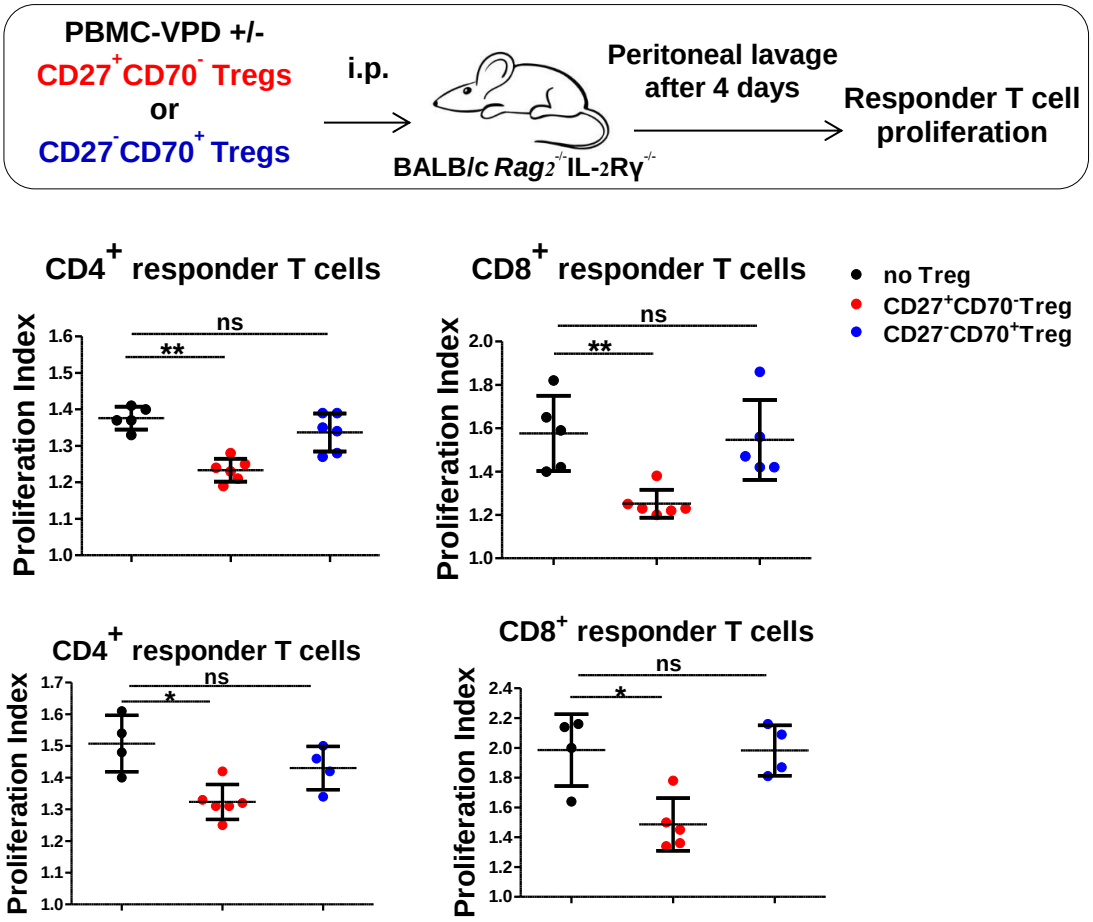

3.11. Upon long-term expansion, the CD27⁺CD70⁻ Treg subset, but not CD27⁻CD70⁺ Tregs, suppress T cell proliferation *in vivo*.

The *in vivo* suppressive capacity of CD27⁺CD70⁻ and CD27⁻CD70⁺ Treg subsets was assessed by injecting VPD-labelled PBMCs together with 4-week expanded CD27⁺CD70⁻ or CD27⁻CD70⁺ Treg subsets (5:1 PBMC:Treg ratio) into the peritoneal cavity of immunodeficient mice. Top: Schematic representation of the experimental plan. Bottom: The proliferation index of CD4⁺ and CD8⁺ responder T cells was studied by flow cytometry in 2 independent experiments (4-6 mice per group per experiment, each mouse is represented as a data point). Data were analysed using a Kruskal-Wallis test with Dunn's post-test for multiple comparisons and are represented as mean ±SD.

ns= non-significant, *p<0.05, ** p<0.01.

3.3.6. Global gene expression differs between CD27$^+$CD70$^-$ Tregs and CD27$^-$CD70$^+$ Tregs

Having shown differential functionality of expanded CD27$^+$CD70$^-$ and CD27$^-$CD70$^+$ Treg subsets, we sought to compare gene signatures between the two Treg populations. To this end, CD27$^+$CD70$^-$ and CD27$^-$CD70$^+$ Tregs expanded for 4 rounds of stimulation (as depicted in Figure 3.8A), were re-sorted as CD27$^+$CD70$^-$ and CD27$^-$CD70$^+$ cells and subjected to RNA-seq analysis to investigate the protein-coding transcriptome from 4 independent blood donors.

Global examination of the data by principal component analysis (PCA) revealed the existence of two separated clusters identifying the CD27$^+$CD70$^-$ and CD27$^-$CD70$^+$ Treg subsets (Figure 3.12A). In total 1568 genes were differentially expressed between both Treg subsets (absolute Log2FC ≥2 and adjusted p-Value<0.01); 681 transcripts were up- and 887 down-regulated in CD27$^+$CD70$^-$ Tregs compared to CD27$^-$CD70$^+$ Tregs. Figure 3.12B contains the top 64 most differentially expressed genes between both CD27/CD70 Treg subsets (absolute Log2FC≥6).

Interestingly, *IL-17A* and *IL-17F,* effector cytokines for Th17 function, appeared among these highly differentially expressed genes (Figure 3.12B). Accumulating evidence for Treg plasticity, especially between Treg and Th17 cells (*248, 328, 329*), led us to examine the expression of Th lineage-specific transcription factors FOXP3, RORγt, GATA-3 and T-bet – master transcription factors for Tregs, Th17, Th2 and Th1 cells respectively. No difference in GATA-3 or T-bet mRNA or protein expression was found between CD27/CD70 Treg subsets (Figure 3.12C). At mRNA levels, *FOXP3* was overexpressed in CD27$^+$CD70$^-$ Tregs and *RORC* in CD27$^-$CD70$^+$Tregs. It is known that FOXP3 physically binds to RORγt and antagonize its transcriptional function to induce IL-17 production (*330*). However, we did not find higher levels of RORγt protein expression in CD27$^-$CD70$^+$ Tregs compared to CD27$^+$CD70$^-$ Tregs in 2 donors analysed (Figure 3.12C). From these

results, we cannot infer a regulatory mechanism between FOXP3 and RORγt for controlling Treg stability or IL-17 expression and more donors should be studied before reaching a conclusion.

Figure 3.12

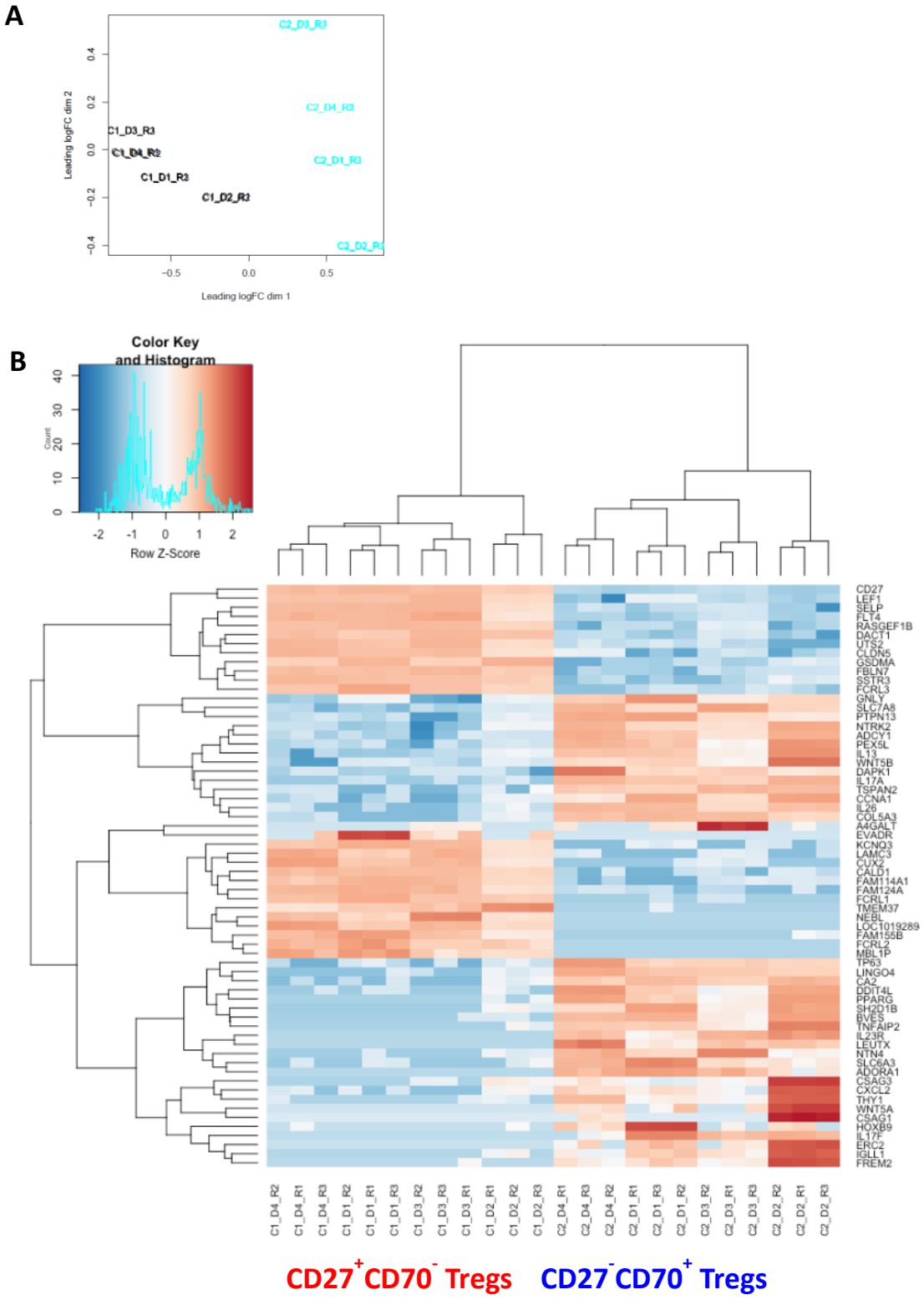

Figure 3.12

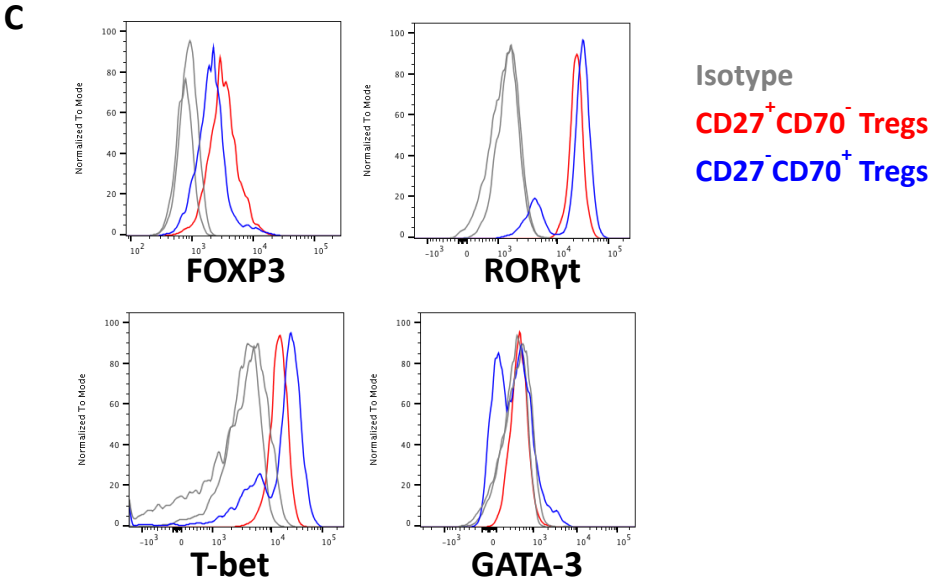

3.12. Global gene expression differs between CD27⁺CD70⁻ Tregs and CD27⁻CD70⁺ Tregs.

(A) Principal component analysis (PCA) of RNA-seq data from CD27⁺CD70⁻ and CD27⁻CD70⁺ Treg subsets isolated from 4 independent donors. Each sample was run in triplicate. Data was analysed using the edgeR package.

(B) Heatmap and hierarchical clustering from RNA-seq data with Log2FC≥6. The top 64 differentially expressed genes are shown. Data was analysed using the edgeR package.

(C) FOXP3, RORγt, T-bet and GATA-3 intracellular expression was analysed by flow cytometry in 4 weeks expanded CD27⁺CD70⁻ and CD27⁻CD70⁺ Tregs. 1 donor out of 2 is shown.

We then sought to investigate further functional differences between CD27/CD70 Treg subsets. Gene Ontology (GO) term enrichment analysis of genes differentially expressed identified specific molecular pathways altered between both Treg subsets (Figure 3.13A). A large proportion of highly differentiated expressed loci related to cytokine and chemokine signalling. Differences in cytokine expression are addressed in Chapter 4. Both Treg subsets expressed chemokine receptors; CD27⁺CD70⁻ Tregs expressed higher levels of *CXCR5, CCR8, CCR7* and *CXCR6*, whereas CD27⁻CD70⁺ Tregs overexpressed *CCR9, CCR1, CCR6* and *CCR5* (Figure 3.13B). During an immune response, trafficking of Tregs from peripheral tissue to draining lymph nodes (LNs) and to inflammatory sites is essential for their optimal suppressive capacity (*331, 332*). Although no difference was observed at mRNA levels, a significantly higher proportion of CD27⁺CD70⁻ Tregs

expressed CD62L protein compared to the CD27$^-$CD70$^+$ Treg population (Figure 3.13C). CD62L expression is required for homing to LN and has been also associated with Treg phenotypic stability (*177, 333*). Differences observed in the expression of chemokine and homing receptors suggest that CD27/CD70 Treg subsets might have different migratory capacity to LN and inflamed tissues.

Moreover, Patterson *et al*., has proposed secretion of chemokines as a new suppressive mechanism for Tregs (*191*). RNA-seq data showed that CD27$^-$CD70$^+$ Tregs expressed high levels of a wide range of chemokines (*CXCL2, CXCL3, CCL23, CCL17, CXCL5, CXCL10, CXCL8, CCL20, CCL3L1, CCL4L1, CXCL1, CXCL6* and *CCL4L2*), whereas only *CCL27* was found overexpressed in CD27$^+$CD70$^-$ Tregs (Figure 3.13B). Hence, the disparity observed in the function of CD27/CD70 Treg subsets might be explained by a different ability to interact with DCs or responder T cells and additional experiments are needed to corroborate this hypothesis.

Our RNA-seq results also showed differences in pathways related to cell cycle and cell proliferation (Figure 3.13A). CD27 signalling is not required for entry into the cell cycle upon cell activation, but it promotes the survival of activated Tconv cells throughout successive rounds of division (*72*). Whether similar proliferation signals occur in Tregs is unclear. We analysed cell proliferation during 3rd and 4th expansion weeks in total Tregs, and sorted CD27$^+$CD70$^-$ or CD27$^-$CD70$^+$ Tregs. No significant difference was found in fold expansion between Treg subsets (Figure 3.13D; left panel). However, when analysing cell recovery after 2 days of resting in 250 U/ml rhIL-2 in the absence of anti-CD3/anti-CD28 stimulation, some Tregs died within total and CD27$^+$CD70$^-$ Treg cell products, whereas CD27$^-$CD70$^+$ Tregs were still proliferative and increased in numbers for most of the donors (Figure 3.13D; right panel). Since RNA-seq analysis was performed in 4 weeks expanded and 2 days rested Treg subsets, differential expression of genes related to cell cycle between Treg subpopulations might reflect their proliferating status during resting.

Figure 3.13

A

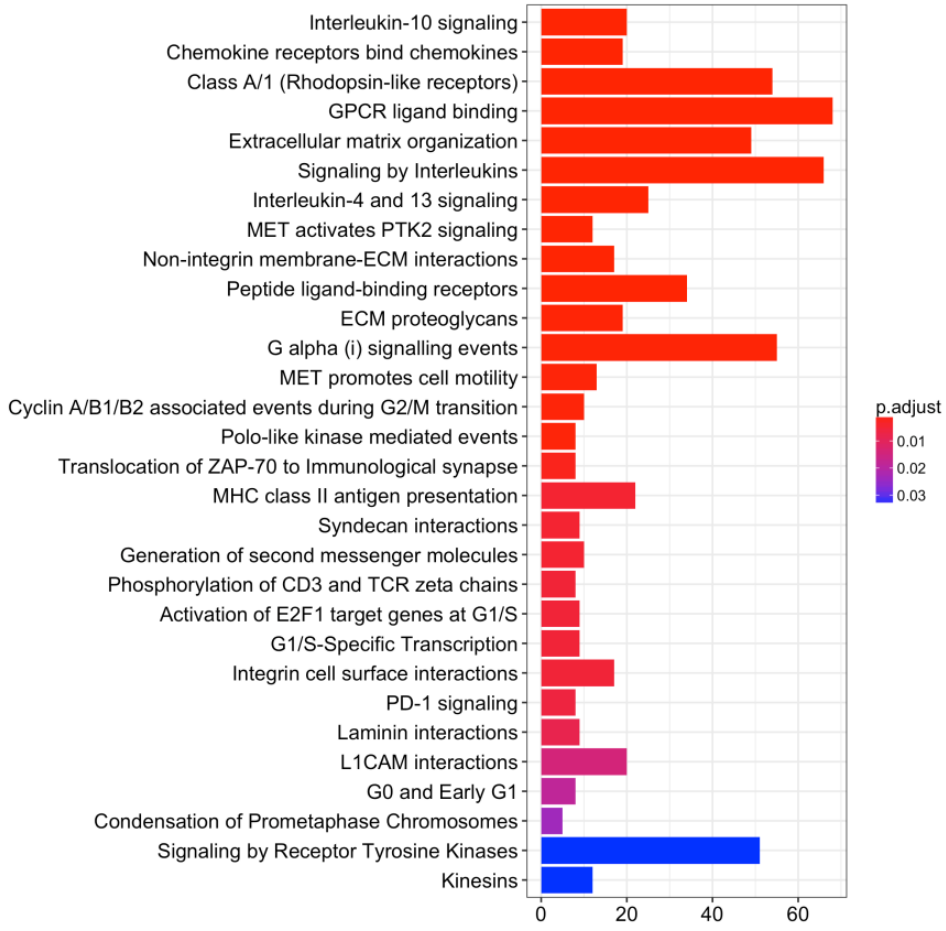

B

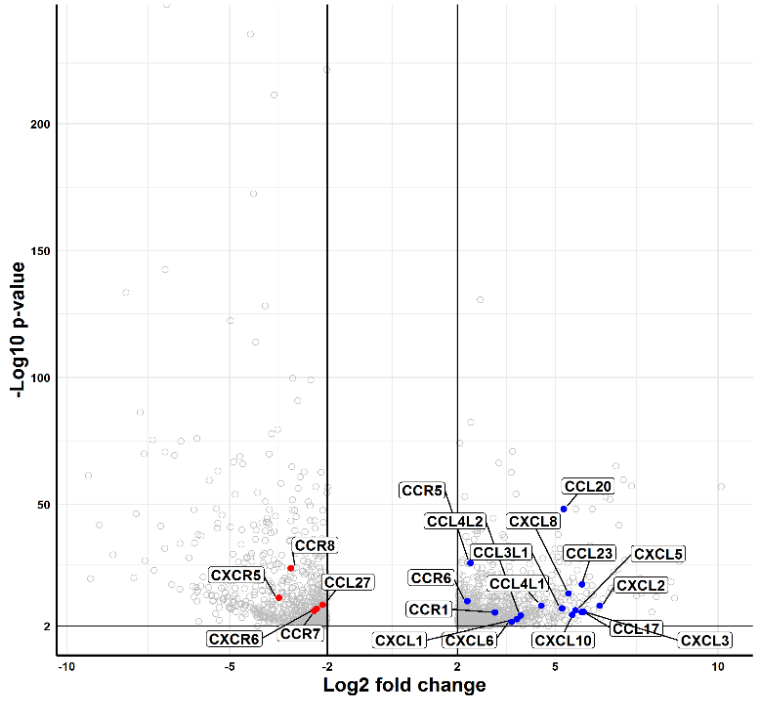

p<0.01

Figure 3.13

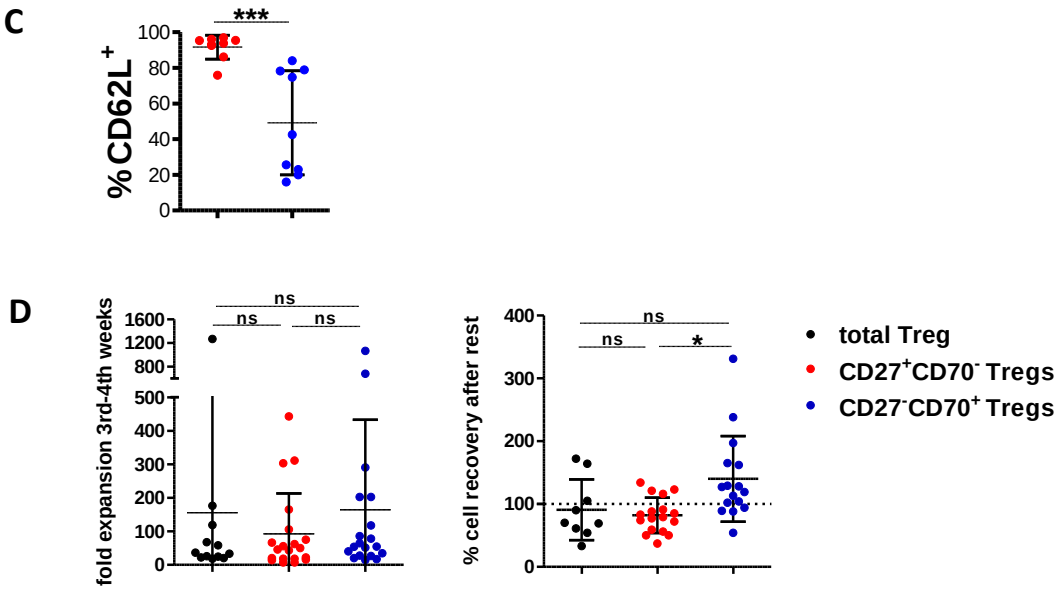

3.13. Global gene ontology analysis.

(A) Gene ontology (GO) enrichment plot obtained using the topGO R package. x axis shows the number of genes for each gene ontology term (y axis).

(B) Volcano plot of differentially expressed genes (each grey circle represents a gene) with p<0.01 (horizontal line) and log2FC>2 or <-2 (vertical lines). Genes encoding for chemokines and chemokine receptors are highlighted in red if overexpressed in $CD27^{+}CD70^{-}$ Tregs or blue if overexpressed in $CD27^{-}CD70^{+}$ Tregs.

(C) Surface expression of CD62L was analysed by flow cytometry in 4 weeks expanded $CD27^{+}CD70^{-}$ and $CD27^{-}CD70^{+}$ Tregs in 9 independent donors. Data were analysed by Mann-Whitney test and represented as mean ± SD.

(D) Left panel: Treg fold expansion was studied in total Tregs, $CD27^{+}CD70^{-}$ and $CD27^{-}CD70^{+}$ sorted Tregs during the second 2 weeks of the expansion protocol (refer to Figure 3.8A). Right panel: After 4 weeks of expansion, Tregs were rested for 2 days in 250U/ml rhIL-2 in the absence of stimulating beads. Percentage of cell recovery after resting is shown. N= 9-20 independent donors. Statistical significance was calculated by Kruskal-Wallis test with Dunn's post-test. Error bars represent mean ± SD.

ns= non-significant, *P<0.05, ***P < 0.001.

3.3.7. Comparison of the transcriptome profile of CD27/CD70 Treg subsets with the canonical Treg-gene signature

Previous studies analysing genes differentially expressed between human Tregs and Tconv have identified a "Treg gene signature" that helps to define the human Treg cell identity at the molecular level (*174, 175*).

We compared the transcriptome profile of CD27/CD70 Treg subsets with the Treg-specific gene signature previously described by Ferraro *et al*. (*174*). It is important to stress that there are limitations in this comparison since we are studying the transcriptional signature of *in vitro* expanded Tregs while Ferraro *et al*. defined their *ex vivo* profile. In this study, 368 genes were differentially expressed between Tregs and Tconv; with 187 and 181 genes being upregulated in Tregs or Tconv respectively (*174*). From 187 genes specifically upregulated in Tregs, we found 31 genes that were overexpressed in CD27$^+$CD70$^-$ Tregs (and included *FOXP3, IKZF2, TIGIT, FCRL2* and *UTS2*) and 12 genes in CD27$^-$CD70$^+$ Tregs (Figure 3.14A; left panel). On the other hand, among the 181 genes upregulated in Tconv, 18 were overexpressed in CD27$^+$CD70$^-$ Tregs and 37 in CD27$^-$CD70$^+$ Tregs (including *CD40L*, *IL7R, THEMIS* and *TMEM71*) (Figure 3.14A, right panel). When analysing other genes of the so called Treg-specific gene signature, *CTLA-4*, *IL2RA*, *GITR* and *ENTPD1* (CD39) were not differentially expressed between CD27/CD70 Treg subsets. Genes that were found upregulated in both Tregs or Tconv and CD27$^+$CD70$^-$ or CD27$^-$CD70$^+$ Tregs are shown in Table 3.2.

Canonical Treg-signature genes found increased in the CD27$^+$CD70$^-$ cell population included typical markers associated with Treg biology such as *FOXP3, IKZF2* (HELIOS) and *TIGIT* and some genes with yet unknown function (*FCRL3* and *UTS2*) (Figure 3.14A) (*175*). Higher FOXP3 expression in CD27$^+$CD70$^-$ Tregs was also found at a protein level (Figure 3.8B), however CD27$^+$CD70$^-$ and CD27$^-$CD70$^+$ Tregs expressed similar levels of TIGIT protein (Figure 3.14B). According to previous studies, HLA-DR expression pattern

is different between Tregs and Tconv, being temporarily expressed by both populations upon activation but with Tregs preserving HLA-DR expression for longer time (*182*). Hence, higher HLA-DR transcription has been identified in Tregs over Tconv (*174*). HLA-DR also identifies a subset of terminally differentiated Tregs with enhanced suppressive potency compared to HLA-DR$^-$ Tregs (*182*). Here, we found higher mRNA and protein expression of HLA-DR in CD27$^-$CD70$^+$ Tregs over CD27$^+$CD70$^-$ Tregs (Figure 3.14A,B and Table 3.2). On the other hand, within genes typically overexpressed in Tconv over Tregs, *CD40L, IL-7R* (CD127), *THEMIS* and *TMEM71* were overexpressed in CD27$^-$CD70$^+$ Tregs (Figure 3.14A and Table 3.2). CD40L, but not CD127, was also found at higher protein levels in CD27$^-$CD70$^+$ Tregs compared to CD27$^+$CD70$^-$ Tregs (Figure 3.14B).

The transcription factor *IKZF2* (HELIOS), typical marker of Treg gene signature, was also overexpressed in CD27$^+$CD70$^-$ Tregs (Table 3.2). HELIOS has been considered a marker to discriminate between thymic Tregs (tTreg) and peripheral Tregs (pTregs) (*157, 158*). However, more recent publications have proven that HELIOS can be induced in pTregs and that the tTreg population contain HELIOS$^-$ cells (*161-163*). Beyond its potential ability to identify tTregs, loss of HELIOS expression results in increased IL-2 secretion and proliferation and decreased suppressive potency in Tregs, highlighting the requirement of HELIOS for stable Treg activity (*165, 246, 334, 335*). We found that, in freshly isolated Tregs, HELIOS protein expression was significantly lower in the CD27$^-$CD70$^+$ Treg subset than in CD27$^+$CD70$^-$ Tregs (Figure 3.14C). Same trend in HELIOS protein expression was observed in 2 weeks *in vitro* expanded Treg subsets (Figure 3.14D).

Taken together, our transcriptional analysis showed that expanded CD27$^+$CD70$^-$ Tregs display a gene profile which closely relates to the previously described “Treg gene signature”, whereas CD27$^-$CD70$^+$ Tregs express some genes associated with Treg gene signature and some genes overexpressed in Tconv.

Figure 3.14

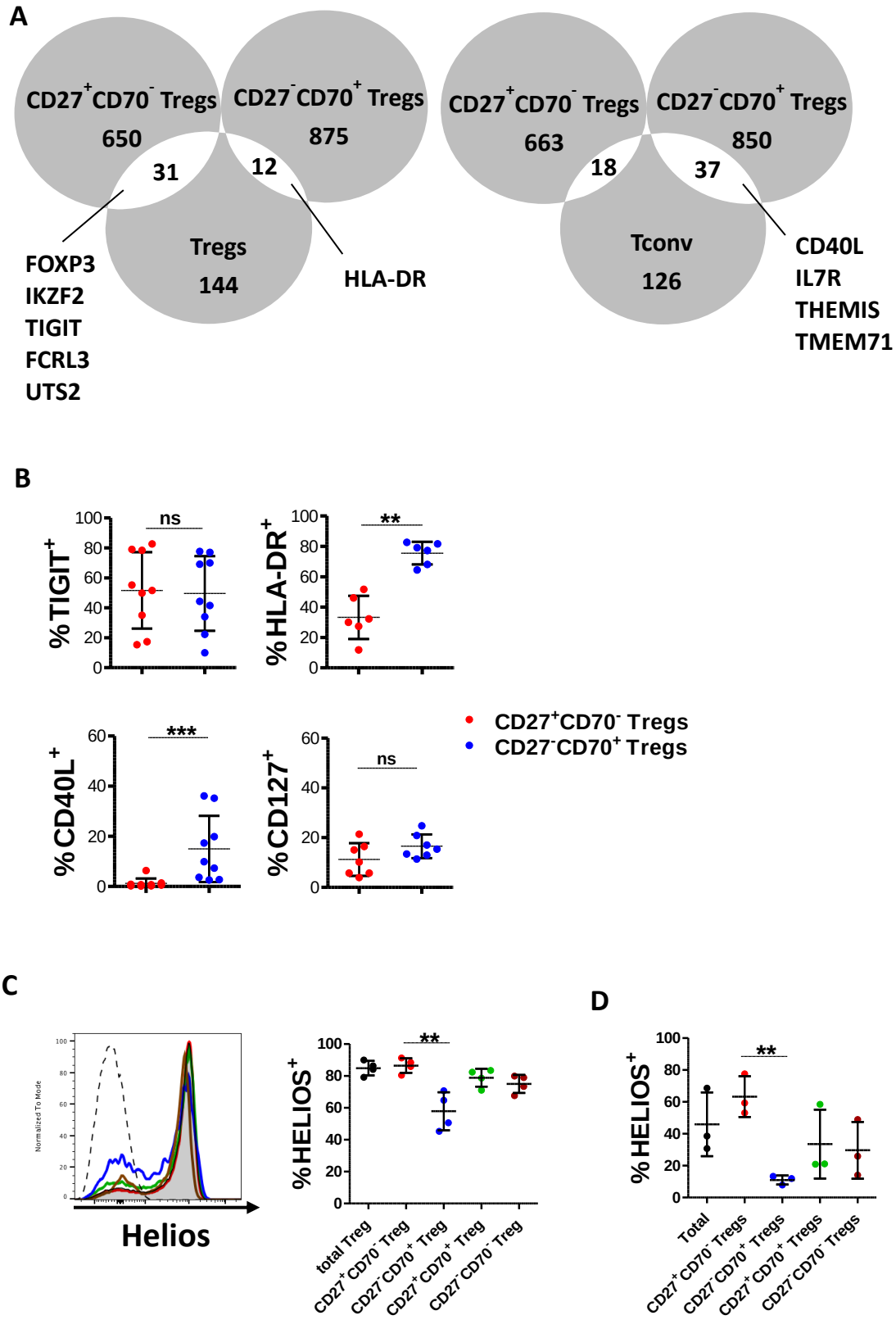
A
CD27+CD70- Tregs
650
31
CD27-CD70+ Tregs
875
12
Tregs
144
FOXP3
IKZF2
TIGIT
FCRL3
UTS2
HLA-DR
CD27+CD70- Tregs
663
18
CD27-CD70+ Tregs
850
37
Tconv
126
CD40L
IL7R
THEMIS
TMEM71
B
%TIGIT+
ns
%HLA-DR+
**
%CD40L+
***
%CD127+
ns
CD27+CD70- Tregs
CD27-CD70+ Tregs
C
Normalized To Mode
Helios
%HELIOS+
**
total Treg
CD27+CD70- Treg
CD27-CD70+ Treg
CD27+CD70+ Treg
CD27-CD70- Treg
D
%HELIOS+
**
Total
CD27+CD70- Tregs
CD27-CD70+ Tregs
CD27+CD70+ Tregs
CD27-CD70- Tregs

3.14. Comparison of the transcriptome profile of CD27/CD70 Treg subsets with the canonical Treg-gene signature.

(A) Venn diagrams showing the overlap between genes overexpressed in CD27^{+}CD70^{-} Tregs or CD27^{-}CD70^{+} Tregs and genes upregulated in (left panel) Tregs or (right panel) conventional T cells (Tconv) (comparison with data from (*174*)).

(B) TIGIT, HLA-DR, CD40L and CD127 protein expression was analysed in 4 weeks expanded CD27^{+}CD70^{-} Tregs or CD27^{-}CD70^{+} Tregs. N= 6-9 independent donors. Data were analysed by Mann-Whitney test and represented as mean ± SD.

(C-D) (C) HELIOS expression was measured in freshly isolated total Tregs or within different Treg subsets defined by CD27 and CD70 expression. Left panel: Representative FACS plot from one donor. Right panel: Percentage of HELIOS^{+} cells in different CD27/CD70 Treg subsets. Mean ± SD is represented. **(D)** HELIOS expression was analysed in 2 weeks expanded total Tregs or within different Treg subsets defined by CD27 and CD70 expression. Mean ± SD is represented. N= 3-4 independent donors. Kruskal-Wallis test with Dunn's post-test for multiple comparisons was conducted.

ns= non-significant, **P<0.01, ***P < 0.001.

Table 3.2. Comparison of the transcriptome profile of CD27/CD70 Treg subsets with the canonical Treg-gene signature.

	Upregulated in Tregs and CD27$^+$CD70$^-$Tregs	**Upregulated in Tregs and CD27$^-$CD70$^+$Tregs**	**Upregulated in Tconv and CD27$^+$CD70$^-$Tregs**	**Upregulated in Tconv and CD27$^-$CD70$^+$Tregs**
1	FCRL3	ARHGEF12	DACT1	ID2
2	FCRL1	ITGB1	NELL2	TARP
3	SELP	CCR6	SCML1	USP46
4	UTS2	HIST1H3B	ZNF204P	PTPRM
5	RTKN2	MKI67	NEFL	ST6GALNAC1
6	GCNT4	AIM2	MID2	CD200R1
7	CEACAM4	HLA-DRA	HOOK1	GPR160
8	VAV3	NEDD4L	ANKRD55	ANXA1
9	CDK14	HIST1H3F	PECAM1	STOM
10	METTL7A	HRH4	DHRS3	GZMA
11	GPA33	MYB	SLC40A1	ABCB1
12	ID3	CCR9	TCF7	CD40LG
13	ZCCHC14		SBF2	APBA2
14	ATP1B1		NAP1L3	B3GALT2
15	LPAL2		PVRL3	TMEM71
16	SGPP2		EPHX2	PDZD4
17	FOXP3		FHIT	IL7R
18	SMPD3		PCSK5	SYTL2
19	CCR8			THEMIS
20	SLC14A1			CR1
21	F5			PRR5L
22	FAM19A2			NEO1
23	CSF2RB			ADAM23
24	PI16			PLEK
25	CXCR6			AOAH
26	TIMD4			IFI44L
27	IKZF2			CD300A
28	SESTD1			NKG7
29	RBMS3			MCOLN2
30	IKZF4			CX3CR1
31	TIGIT			HDGFRP3
32				KLRB1
33				CFH
34				CYB561
35				GNLY
36				TSPAN2
37				PTPN13

3.3.8. CD27$^-$CD70$^+$ Tregs are not enriched within the previously reported CD4$^+$FOXP3$^+$CD45RA$^-$CD25^{int} non-suppressive Treg population

Miyara *et al.* described six CD4$^+$ T cell fractions defined by surface expression of CD45RA and CD25; 3 of which were FOXP3$^+$ cells and 3 did not express FOXP3 (*336*). We were able to identify the six CD4$^+$ T cell subsets in healthy donor PBMCs (as depicted in Figure 3.15A). FOXP3$^+$ cells comprised naive Tregs (CD45RA$^+$CD25^{int}), memory Tregs (CD45RA$^-$CD25^{hi}) and a non-suppressive T cell population (CD45RA$^-$CD25^{int}); which were characterized and showed different gene expression profiles, phenotype and function (*336*). We examined whether unstable CD27$^-$CD70$^+$ Tregs might reflect the non-suppressive T cell population described by Miyara *et al*. as CD4$^+$CD45RA$^-$CD25^{int} cells (fraction III in Figure 3.15A). When analysing the proportion of CD27$^+$CD70$^-$, CD27$^-$CD70$^+$, CD27$^+$CD70$^+$ and CD27$^-$CD70$^-$ cells of freshly isolated Tregs within these CD4$^+$ human T cell subsets, CD27$^-$CD70$^+$ Tregs were not predominantly found within the non-suppressive CD45RA$^-$CD25^{int} cell population (fraction III), nor in any of the FOXP3$^-$ Tconv cell subsets (fractions IV, V or VI) (Figure 3.15B,C).

Figure 3.15

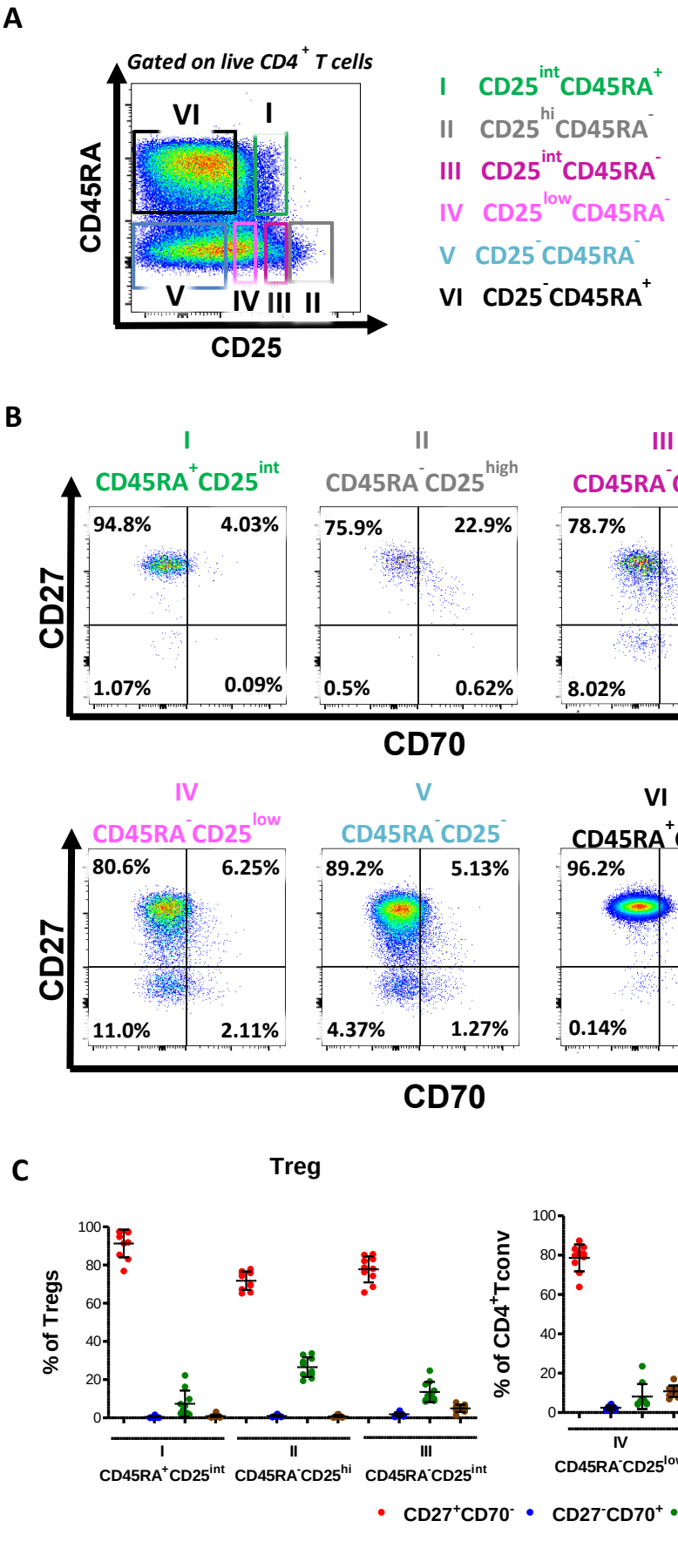
A
Gated on live CD4+ T cells
CD45RA
CD25
VI
I
V
IV III II
I CD25intCD45RA+
II CD25hiCD45RA-
III CD25intCD45RA-
IV CD25lowCD45RA-
V CD25-CD45RA-
VI CD25-CD45RA+
B
I
CD45RA+CD25int
II
CD45RA-CD25high
III
CD45RA-CD25int
94.8%
4.03%
1.07%
0.09%
75.9%
22.9%
0.5%
0.62%
78.7%
11.5%
8.02%
1.78%
CD27
CD70
IV
CD45RA-CD25low
V
CD45RA-CD25-
VI
CD45RA+CD25-
80.6%
6.25%
11.0%
2.11%
89.2%
5.13%
4.37%
1.27%
96.2%
3.67%
0.14%
0.03%
CD27
CD70
C
Treg
CD4+ Tconv
% of Tregs
% of CD4+Tconv
100
80
60
40
20
0
I
CD45RA+CD25int
II
CD45RA-CD25hi
III
CD45RA-CD25int
IV
CD45RA-CD25low
V
CD45RA-CD25-
VI
CD45RA+CD25-
CD27+CD70-
CD27-CD70+
CD27+CD70+
CD27-CD70-

3.15. CD27^{-}CD70^{+} Tregs are not enriched within the previously defined CD4^{+}CD45RA^{-}CD25^{int} non-Treg population.

(A) Gating strategies to isolate CD4^{+} cell fractions I (CD25^{int}CD45RA^{+}); II (CD25^{hi}CD45RA^{-}); III (CD25^{int}CD45RA^{-}); IV (CD25^{low}CD45RA^{-}); V (CD25^{-}CD45RA^{-}); and VI (CD25^{-}CD45RA^{+}) from healthy donor PBMCs.

(B-C) CD27 and CD70 expression was analysed within the CD4^{+} T cell populations. **(B)** Dot plots from 1 representative donor. **(C)** Cumulative data of 10 independent donors. Error bars represent mean ± SD.

It is known that although CD45RA^{-}CD25^{+} cells display a Treg phenotype just after isolation, only the naive Treg population remains highly potent and retain stable FOXP3 expression upon expansion (*178, 307, 310, 336, 337*). CD25^{hi} memory Tregs (fraction II) are highly suppressive but terminally differentiated and do not expand *in vitro* sufficiently to perform experiments (*184*). Therefore, for subsequent experiments, only *in vitro* expanded CD25^{int} memory and naive Treg subsets were evaluated. In order to investigate whether CD27/CD70 expression relates to differences in the stability of CD25^{int} memory and naive Tregs upon expansion, we FACS sorted the CD25^{int}CD45RA^{+} naive Treg and CD25^{int}CD45RA^{-} memory Treg subsets from CD4^{+}CD25^{+}CD27$^{-/low}$ Tregs (Figure 3.16A). Despite showing similar levels of TSDR demethylation and FOXP3 expression prior expansion, CD25^{int} memory Tregs had reduced FOXP3 expression and TSDR demethylation after 2 weeks of *in vitro* expansion (Figure 3.16B). Interestingly, CD25^{int} memory Tregs were more prone to acquire the CD27^{-}CD70^{+} pro-inflammatory phenotype than naive Tregs (Figure 3.16C). Despite differences in TSDR demethylation, FOXP3 and CD27/CD70 phenotype, both CD25^{int} memory and naive Tregs were highly suppressive when expanded for 2 weeks (Figure 3.16D).

To explore the role of CD27/CD70 upon prolonged expansion, CD27^{+}CD70^{-} and CD27^{-}CD70^{+} cells were isolated from 2 weeks expanded CD25^{int} naive and memory Tregs (Figure 3.16E). As shown previously in total Treg cultures, the CD27^{+}CD70^{-} phenotype is not stable and CD27^{+}CD70^{-} cells downregulated CD27 and upregulated CD70 upon activation, especially in CD25^{int} memory expanded Tregs (Figure 3.16F). Thus, more than

90% of the CD27^{+}CD70^{-} cells isolated from memory expanded Tregs converted to a CD27^{-}CD70^{+} phenotype, appearing almost undistinguishable from the CD27^{-}CD70^{+} cell product after further 2 weeks of expansion (Figure 3.16F, top panel). When analysing their suppressive activity in an MLR assay, both expanded CD27^{+}CD70^{-} and CD27^{-}CD70^{+} isolated from CD25^{int} memory Tregs induced T cell proliferation to the same extent (Figure 3.16G, left panel), which correlates with their similar CD27/CD70 phenotype post expansion. On the other hand, 31% of isolated CD27^{+}CD70^{-} cells from naive expanded Tregs remained as CD27^{+}CD70^{-} cells while 32% were CD27^{-}CD70^{+} after 2 weeks of expansion (Figure 3.16F, bottom panel). On functional analysis, the expanded CD27^{-}CD70^{+} population, but not the CD27^{+}CD70^{-} population, induced T cell proliferation (Figure 3.16G, right panel).

In addition, when comparing their transcriptome profile with previous studies, 4 weeks expanded CD27^{+}CD70^{-} Tregs shared some of the Treg genetic signature of naive Tregs (e.g. *IKZF2*) but also some of memory Tregs; especially of highly suppressive CD45RA^{-}CD25^{hi} memory/effector Tregs (such as *ITGB8*, *CCR8*, *CXCR6*). CD27^{-}CD70^{+} Tregs resembled CD45RA^{-}CD25^{hi}FOXP3^{+} and CD45RA^{-}CD25^{int}FOXP3^{+} cells, showing upregulation of *LAG3, IL10, RORC, TNFRSF8* and *IL12A* (*336*).

Overall, our data suggest that in freshly isolated Tregs CD27^{+}CD70^{-} and CD27^{-}CD70^{+} cell subsets do not correspond to the CD45RA^{+}CD25^{int}, CD45RA^{-}CD25^{int} and CD45RA^{-}CD25^{hi} Treg populations described by Miyara *et al*. However, upon prolonged expansion, CD27^{-}CD70^{+} cells are much faster generated from CD25^{int} memory Tregs than from CD25^{int} naive Tregs.

Figure 3.16

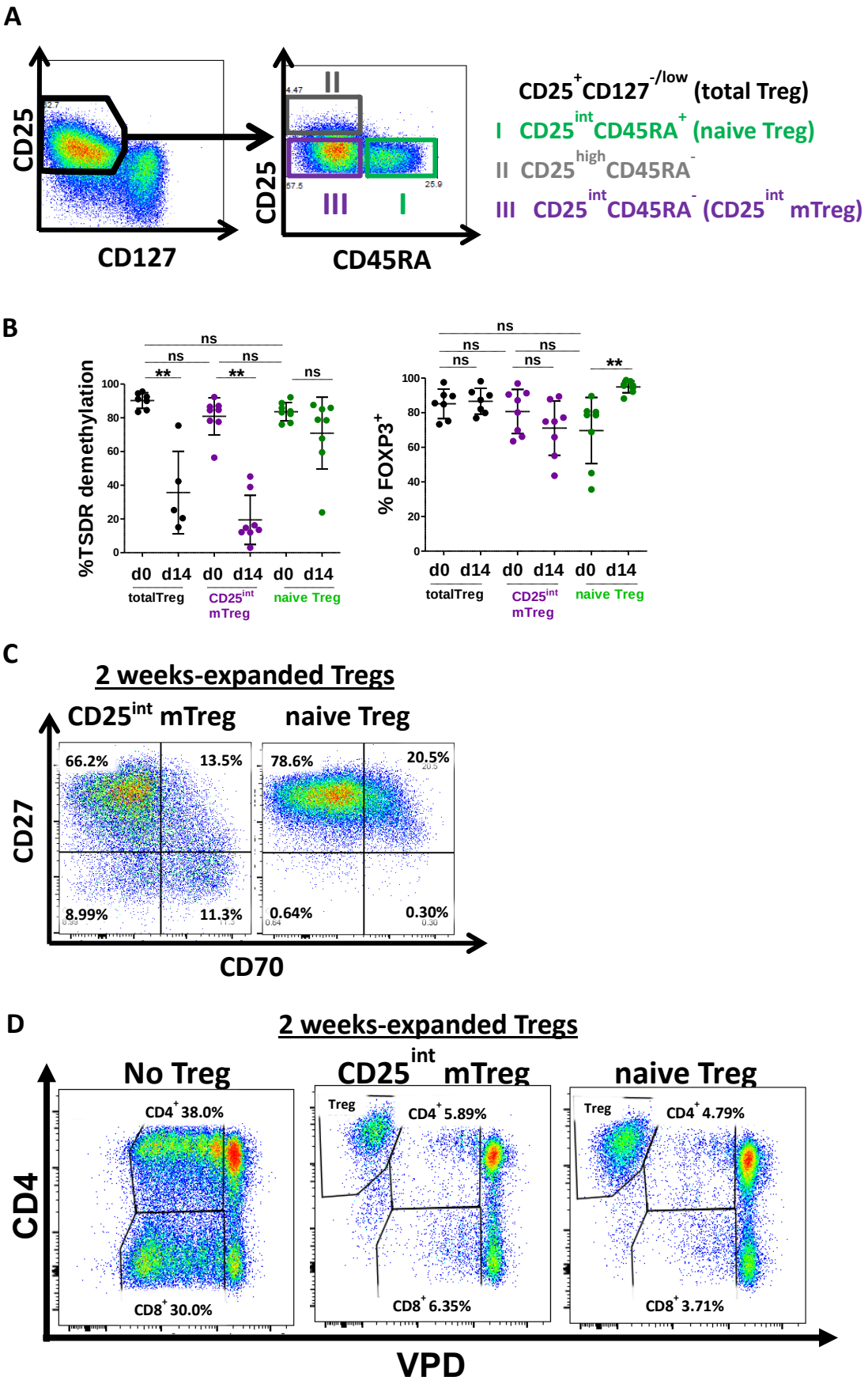
A
CD25
CD127
CD25
CD45RA
II
III
I
CD25+CD127-/low (total Treg)
I CD25int CD45RA+ (naive Treg)
II CD25high CD45RA-
III CD25int CD45RA- (CD25int mTreg)
B
%TSDR demethylation
% FOXP3+
ns
**
d0 d14
totalTreg
CD25int mTreg
naive Treg
C
2 weeks-expanded Tregs
CD25int mTreg
naive Treg
66.2%
13.5%
8.99%
11.3%
78.6%
20.5%
0.64%
0.30%
CD27
CD70
D
2 weeks-expanded Tregs
No Treg
CD25int mTreg
naive Treg
CD4+ 38.0%
CD8+ 30.0%
Treg
CD4+ 5.89%
CD8+ 6.35%
CD4+ 4.79%
CD8+ 3.71%
CD4
VPD

Figure 3.16

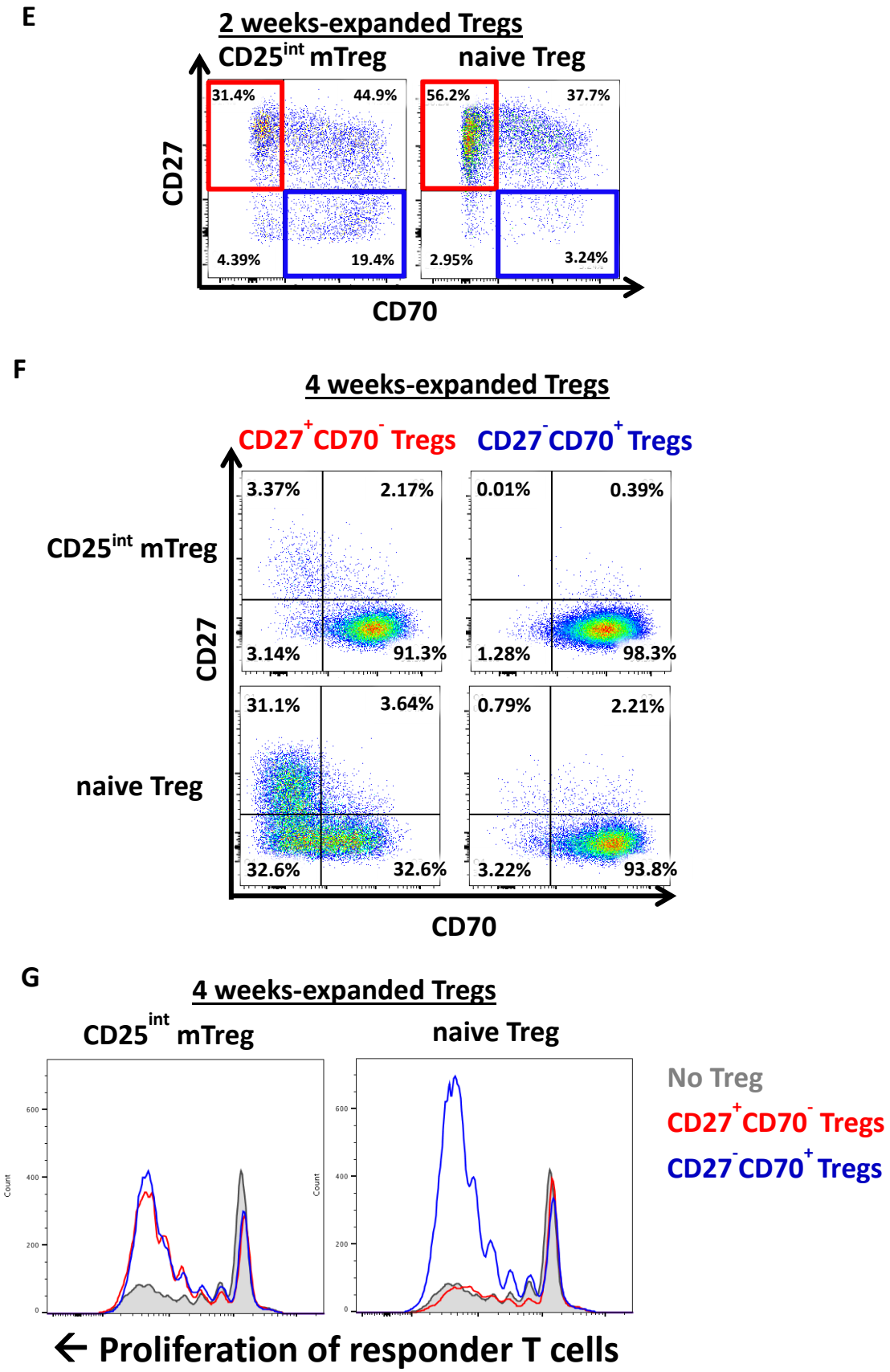
E
2 weeks-expanded Tregs
CD25int mTreg
naive Treg
31.4%
44.9%
56.2%
37.7%
4.39%
19.4%
2.95%
3.24%
CD27
CD70
F
4 weeks-expanded Tregs
CD27+CD70- Tregs
CD27-CD70+ Tregs
CD25int mTreg
naive Treg
3.37%
2.17%
0.01%
0.39%
3.14%
91.3%
1.28%
98.3%
31.1%
3.64%
0.79%
2.21%
32.6%
32.6%
3.22%
93.8%
CD27
CD70
G
4 weeks-expanded Tregs
CD25int mTreg
naive Treg
Count
600
400
200
0
No Treg
CD27+CD70- Tregs
CD27-CD70+ Tregs
← Proliferation of responder T cells

3.16. The CD27^{-}CD70^{+} Treg subset, but not CD27^{+}CD70^{-} Tregs, has pro-inflammatory capacity following *in vitro* expansion of naive Tregs.

(A) Gating strategies to isolate total Tregs (CD4^{+}CD127^{-}CD25^{+}); naive Tregs (CD127^{-}CD25^{int}CD45RA^{+}) and CD25^{int} memory Tregs (CD25^{int}mTreg)(CD127^{-}CD25^{int}CD45RA^{-}).

(B) Percentage of TSDR demethylation and cells expressing FOXP3 was analysed in different Treg subsets before and after 14 days of *in vitro* expansion (n= 8 independent donors). Errors bars represent mean ± SD. Kruskal-Wallis test with Dunn's post-test for multiple comparisons was conducted. ns= non-significant, **P < 0.01, ***P < 0.001.

(C) CD27 and CD70 expression within naive and CD25^{int} mTreg populations at day 14 of expansion is shown for 1 donor.

(D) After 2 weeks of expansion, suppressive capacity of naive and CD25^{int} mTregs was assessed in an MLR suppression assay, consisted of VPD-labelled CD3^{+}CD25^{-} responder T cells (Tresp) stimulated with allogenic DCs (5 Tresp: 1 DC) in the presence or absence of Tregs. FACS plots from 1 donor are represented. VPD dilution indicates cell division in CD4^{+} and CD8^{+} Tresp.

(E) After 2 weeks of expansion, naive and CD25^{int} mTregs were FACS-sorted as CD27^{+}CD70^{-} (red gate) and CD27^{-}CD70^{+} (blue gate) cells.

(F-G) CD27^{+}CD70^{-} and CD27^{-}CD70^{+} cells, sorted from 2 weeks expanded CD25^{int} memory or naïve Tregs were expanded for 2 further weeks and analysed for **(F)** CD27 and CD70 expression and **(G)** suppressive capacity. Treg activity was assessed *in vitro* by MLR suppression assay. Histograms from one donor depict VPD dilution by CD8^{+} Tresp when stimulated with allogenic DCs in the absence of Tregs (grey histogram) or when co-culture with expanded CD27^{+}CD70^{-} (red) or CD27^{-}CD70^{+} (blue) Tregs isolated from CD25^{int} memory Tregs (left panel) or naive Tregs (right panel).

3.4. Discussion

Several studies have described that *in vitro* expansion of human CD4^{+}CD25^{+} Tregs leads to cell subsets with differential CD27 expression and that CD27 correlates with suppressive potency within the expanded Treg cell product (*179, 180, 311*). However, a further characterisation of CD27 in relationship with CD127 was missing. Here, we showed that freshly isolated CD4^{+}CD25^{+}CD127$^{-/low}$ Tregs had high CD27 and low CD70 expression and that both markers were upregulated following activation (Figure 3.1A and 3.2). However, upon prolonged stimulation, some cells downregulated CD27 while retained high CD70 expression on the cell surface, resulting in two distinct subpopulations: CD27^{+}CD70^{-} and CD27^{-}CD70^{+} (Figure 3.4).

In kidney transplant patients, up to 10x10^{6} Tregs/kg have been administered with no adverse effects reported (ONE Study, NCT02129881). Upon polyclonal stimulation in the

presence of high doses of rhIL-2, we observed that Treg expansion rate was highly variable among donors; with figures ranging from 13 to 172 fold expansion over 2 weeks of expansion (Figure 3.5A). To ensure that a 10x10^6 Tregs/kg dose is reached for as many patients as possible, Tregs would need to be expanded longer. In a 32 days expansion protocol, we reported a minimum of 223 and maximum of 32120 expansion rate among individuals, ensuring enough yield for clinical application (Figure 3.5C). However, consistent with previous reports (*307, 308*), our data showed that *in vitro* stimulation and expansion of flow-sorted CD4$^+$CD25$^+$CD127$^{-/low}$ Tregs results in a final cell product that contains cells with unstable regulatory activity (Figure 3.6). Importantly, within this population, the CD27$^+$CD70$^-$ phenotype identifies a Treg subset that retains potent suppressive activity upon long-term stimulation *in vitro*. By contrast, CD27$^-$CD70$^+$ Tregs have significantly impaired suppressive capacity after prolonged *in vitro* expansion and, conversely, the ability to induce T cell proliferation (Figure 3.9A,B).

Moreover, our transcriptomics analyses revealed that the gene profile of CD27$^+$CD70$^-$ and CD27$^-$CD70$^+$ cells were clearly distinct (Figure 3.12A), suggesting a differential regulation at the transcriptional level. Indeed, the CD27$^+$CD70$^-$ Treg subset shared important elements of transcriptome profile with a previously identified Treg-gene signature, whereas CD27$^-$CD70$^+$ expanded Tregs shared some gene expression with Tconv cells (Figure 3.14A) (*174, 175*). For instance, FOXP3 and HELIOS were differentially expressed in our system (Figures 3.8B and 3.14D), which is linked to the increased stability and suppressive capacity of CD27$^+$CD70$^-$ cells compared to CD27$^-$CD70$^+$ cells. However, expression of other markers associated to Treg suppressive potency (such as *CTLA-4*, *TIGIT*, *CD39*, *CD25* or *GITR*) was similar between CD27/CD70 Tregs subsets, and the CD27$^-$CD70$^+$ Treg phenotype did not completely correspond to that from Tconv (e.g. HLA-DR overexpression). Still, an uncomplete regulatory transcriptional profile might be responsible for defective suppressive stability upon long-term expansion.

TNFR family molecules provide signals that, besides promoting survival and proliferation, also influence Th cell differentiation and cytokine production (*99*). Several studies have implicated CD27 intracellular signalling in regulating CD4$^+$ T cell subset differentiation; inducing Th1 development (*119, 338-340*) and repressing Th17 effector cell function (*312*). Whether CD27/CD70 signalling regulates Treg stability and its conversion into other Th cell subsets is not known.

In human CD4$^+$ T cells, CD27 stimulation leads to up-regulation of T-bet, main transcription factor for Th1 cell development, and subsequent overexpression of IL-12Rβ2 chain that results in preferential proliferation of Th1 cells expressing IFN-γ in the presence of IL-12 (*338*). In the mouse system, an IL-12 independent pathway for CD70-mediated induction of IFN-γ-expressing CD4$^+$ T cells has also been described (*339*). No differences were observed in T-bet expression, at mRNA or protein levels, between CD27$^+$CD70$^-$ and CD27$^-$CD70$^+$ Tregs (Figure 3.12C), indicating that CD27$^-$CD70$^+$ Tregs do not convert into Th1 cells.

CD27$^-$CD70$^+$ Tregs overexpressed *RORC* which encodes RORγt, master transcription factor of Th17 cell development, suggesting potential conversion into Th17 cells. However, it should be noted that RORγt expression in FOXP3$^+$ Tregs is associated with both suppressive and pro-inflammatory properties (*341*). Indeed, recent findings indicate that acquisition of Th-lineage specific transcription factors is required for the development of functionally unique properties within highly specialised Treg subsets. Thus, co-expression of T-bet, GATA-3 or RORγt induces particular transcriptional modules that enables for specific migration and suppressive mechanisms to control Th1, Th2 and Th17 responses (*342-344*). Therefore, overexpression of RORγt by CD27$^-$CD70$^+$ Tregs may indicate conversion towards Th17 cells or dedicated function for regulation of Th17 cells.

Our RNA-seq data also pointed out differences in many chemokine transcripts and their receptors (Figure 3.13B). Given that cellular migration and recruitment represent a

fundamental aspect of the immune response and are important for Treg function (*331, 332*), we could reason that CD27$^+$CD70$^-$ and CD27$^-$CD70$^+$ cells possess different chemokine sensing or production machinery, which make them differentially equipped and prompt to migration and cell recruitment. In this regard, patients with type 1 diabetes present Tregs with defective chemokine secretion compared to those from healthy individuals (*191*), supporting a role for chemokine production in Treg-related pathologies. Nonetheless, from our suppression assays, we cannot infer whether the suppressive or pro-inflammatory abilities of CD27/CD70 Treg subsets derive, at least partially, from their capacity to migrate or recruit other cell types. Further experiments are needed to answer these questions and are discussed in Chapter 6.

Taken together, our findings may indicate the presence of contaminant CD4$^+$ Teff cells within the isolated CD4$^+$CD25$^+$CD127$^{-/low}$ Tregs or the potential for Treg instability after prolonged stimulation. Importantly, the same trend towards downregulation of CD27 and upregulation of CD70 was observed in CD4$^+$CD25$^-$ Tconv cells upon expansion, although percentage of CD70$^+$ cells was lower than in Tregs (Figure 3.2A,B and 3.4C). While contamination with Teff cells within CD70$^+$ Tregs may be possible, Tregs were sorted based on negative expression of CD127 and high CD25 expression as cell surface makers to isolate functional Tregs with high purity (*167, 168*). CD27$^-$CD70$^+$ cells were already represented within these highly pure freshly isolated Tregs, had similar levels of TSDR demethylation than CD27$^+$CD70$^-$ Tregs and expressed high FOXP3 levels (Figure 3.1 and Figure 3.7C,D). Moreover, CD27$^-$CD70$^+$ Tregs suppressed T cell proliferation after 2 weeks of expansion, but lost this ability after 4 weeks (Figure 3.7A and 3.9A,B). In addition, we found that repeated cell stimulation of highly pure isolated CD27^{high}CD70$^-$ Tregs leads to their progressive conversion into CD27$^-$CD70$^+$ cells, implying intrinsic phenotypic instability (Figure 3.8A,B). On the other hand, re-sorted CD27^{high}CD70$^-$ Tregs (see gating in Figure 3.10) showed increased suppressive ability compared to the expanded CD27$^+$CD70$^-$ bulk population (Figure 3.10). All factors considered, our data

suggest that loss of suppressive potency upon prolonged stimulation is due to Treg instability.

Given their improved stability upon *ex vivo* expansion, selection of CD45RA$^+$ naive Tregs is considered a better option for cellular therapy than the whole Treg population. CD45RA$^+$ naive Tregs represent a particularly stable Treg subset that maintains a Treg phenotype and suppressive activity upon *in vitro* expansion (*178, 307, 345*). On the other hand, CD45RA$^-$ memory Tregs are more prone to lose FOXP3 expression, gain methylation in TSDR, and express pro-inflammatory cytokines (*178, 307, 310, 337, 346*). Within the CD45RA$^-$ Treg population, Miyara *et al*. distinguished two CD4$^+$FOXP3$^+$ cell subsets: activated Tregs with high CD25 expression, and non-suppressive T cells with intermediate levels of CD25 (*336*). Importantly, we have shown that in freshly isolated Tregs, the CD27$^-$CD70$^+$ Treg subset did not correspond to CD45RA$^-$CD25^{int} non-suppressive Treg population (Figure 3.15). However, upon *in vitro* expansion, CD27$^-$CD70$^+$ cells were predominant within the CD25^{int} memory Treg expanded population over the naive Treg population (Figure 3.16C,E). Moreover, expanded CD27$^+$CD70$^-$ cells showed a mixed gene signature similar to that of naive and CD25^{hi} memory Tregs, whereas expanded CD27$^-$CD70$^+$ cells displayed a shared transcriptome of CD25^{hi} and CD25^{int} memory Tregs. As in the “whole” Treg cultures, naive and memory Tregs showed similar suppressive capacity when expanded for 2 weeks, but, after 4 weeks of expansion, only the CD27$^-$CD70$^+$ cells within memory or naive expanded Tregs had a pro-inflammatory function (Figure 3.16D,G).

In conclusion, the data presented in this chapter demonstrate that the CD27$^+$CD70$^-$ phenotype allows for the identification and isolation of potent human Tregs within expanded CD4$^+$CD25$^+$CD127$^{-/low}$ Treg cultures. Upon expansion, human Tregs gradually increase CD70 and lose CD27 expression, which correlates with a gene signature that shares some elements with Teff cells, and a decrease in suppressive capacity, FOXP3 expression and TSDR demethylation. It is worth mentioning that our overall Treg purity

after long term *in vitro* expansion is lower than what other laboratories have described (*217, 293, 308*), and the CD27^{+}CD70^{-} phenotype might be less relevant in these protocols achiving greater purity.

In order to produce a homogenous, potent and stable Treg cell product for cellular therapy, diverse strategies have been explored, such as pre-enrichment based on expression of CD45RA (*345*). Here, we show that naive and memory Tregs differentially regulate CD27 and CD70 expression upon expansion. The use of CD27 and CD70 phenotype further improves the identification of Tregs with stable suppressive activity beyond isolation by CD45RA. The role of CD27 and/or CD70 and their active influence on the suppressive mechanisms of Tregs is discussed in Chapter 4.

Chapter 4:
Investigation into the role of CD27 and CD70 in immune regulation mediated by human regulatory T cells

4.1. Introduction

Although the mechanisms by which Tregs control immune responses have been widely researched with numerous pathways described, the details of the suppressive mechanisms of Tregs are still not completely understood. Tregs can target multiple cell subsets (e.g. specialised T cell populations or APCs) and suppress by cell-contact-dependent and contact-independent pathways (*183, 251, 347*). Contact-dependent mechanisms require the interaction of cell surface molecules between Tregs and target cells. CTLA-4 is probably the most-well studied co-inhibitory receptor, known to act on DCs and Tregs. Additional cell surface functional makers for Treg suppression are CD25, CD39 and CD73; which are involved in IL-2 deprivation, ATP consumption and adenosine production respectively (*176, 192, 194*). Contact-independent regulatory mechanisms include production of chemokines (discussed in Chapter 3) (*191*) and release of inhibitory cytokines, such as IL-10, TGF-β and IL-35 (*190*).

Despite numerous reports stating a strong correlation between CD27 expression and suppressive potency of *in vitro* expanded human Tregs, a critical role for CD27/CD70 signalling in Treg stability or regulatory function has not been stablished. Studies in mouse models using knockout or transgenic mice have provided insight into the role of the CD27/CD70 pathway in T cell function and have demonstrated that CD27 is essential for the generation of memory T cell immunity by enhancing survival of activated T cells (*71, 72, 119, 126*). However, the interpretation of these data is complicated by the fact that the effects of CD27-CD70 stimulation appear to be dependent on the context and intensity of

the signal (*125*). Hence, different outcomes have been reported in different mouse models. In CD70-transgenic mice, CD70 expression on B cells or DCs increases the antigen-specific T cell response (*119, 120*), whereas CD70 expression on T cells results in T cell exhaustion (*122*), although this may also depend on whether T cells are being transiently or constitutively activated. Supporting these data, an immune-inhibitory function for T cell–derived CD70 signalling has been identified in mouse models of autoinflammatory bowel disease and allogenic GvHD using $CD70^{-/-}$ mice (*123*). Importantly, the role of CD70 expressed on Tregs has not been explored yet.

In Chapter 3 we described an inverse expression pattern between CD27 and CD70 upon Treg expansion. High CD27 and low CD70 expression on the cell surface identifies cells with potent suppressive activity, whereas loss of CD27 and acquisition of CD70 distinguish unstable Tregs. In this chapter we sought to elucidate whether CD27 or CD70 has an active role in Treg functionality and whether modulation of the CD27/CD70 signalling could be targeted to enhance Treg stability and suppressive potency upon long-term *in vitro* expansion.

4.2. Objectives and hypothesis

Objective 1: To determine whether the co-stimulatory molecule CD27 and its ligand CD70 contributes to the stability and regulatory function of human Tregs.

Hypothesis 1: Blocking or stimulating CD27 or CD70 in Tregs will affect Treg stability and regulatory function.

Objective 2: Should the CD27/CD70 co-stimulatory pathway prove to have an active role in human Treg function, to identify the mechanisms by which CD27 and CD70 influences Treg physiology.

Hypothesis 2.1: CD27 and CD70 expressed on Tregs can bind to CD70 and CD27 respectively on other cell types and provide co-stimulatory or co-inhibitory signals.

Hypothesis 2.2: CD27 and CD70 transduce intracellular signals into Tregs that control cytokine production and Treg stability.

4.3. Results

4.3.1. $CD27^+CD70^-$ Treg suppressive function does not rely on CD27 signalling

After reporting that CD27 expression constitutes a marker of human Tregs with potent and stable suppressive activity, we sought to determine whether CD27 has an active role in the suppressive mechanism of Tregs. It has been proposed that $CD27^+$ Tregs may compete for CD70 binding on DCs, thus preventing DCs to provide CD70 co-stimulation to $CD27^+$ Tconv cells (*188*). Besides, several studies have shown that CD27 signalling influences $CD4^+$ Th subset differentiation, promoting Th1 responses and inhibiting Th17 function (*119, 312, 338-340*). Given its effect in $CD4^+$ Tconv cells, CD27 intracellular signalling might also play a role in regulating Treg activity.

We therefore hypothesised that stimulating or blocking CD27 signalling on Tregs might enhance or impair Treg suppressive potency respectively. For these studies, we used anti-CD27 monoclonal antibodies (mAbs) where the precise function depends on the presence or absence of cross-linking, which can be provided by Fc receptors or artificially (*348, 349*). Using these antibodies cross-linked with goat anti-human IgG results in agonist function, whereas an Fc-mutated anti-CD27 mAb in which cross-linking by Fc receptors is prevented results in an antagonist activity (*348*) (Figure 4.1A).

$CD27^+CD70^-$ Tregs were pre-incubated with Fc-mutated (1F5N297S) or non-mutated anti-CD27 mAb (varlilumab) and anti-human IgG antibody, as blocking or activating

conditions respectively. Pre-incubated Tregs were assessed for their capacity to suppress T cell proliferation in an *in vitro* MLR assay using allo moDCs as stimulators. The comparison between Tregs pre-incubated with varlilumab with or without anti-human IgG antibody could inform us whether DCs are able to provide crosslinking. Percentage of suppression by Tregs was calculated based on division index of $CD4^+$ or $CD8^+$ responder T cells (Tresp). Tregs pre-incubated in media, isotype control, agonist anti-CD27 or blocking anti-CD27 conditions showed similar suppressive potency (Figure 4.1B,C). This indicated that stimulation or blocking CD27 signalling on Tregs does not have a significant effect on Treg suppressive activity *in vitro*. When looking at number of Tregs at the end of the MLR assay, targeting CD27 signalling did not affect the survival of Tregs during the suppression test, as similar numbers of Tregs were found across different pre-incubation conditions (Figure 4.1D). We proved the ability of anti-CD27 mAbs to bind to CD27 by incubating conventional T cells with Fc mutated anti-CD27 mAb (see sections 4.3.4 and 4.3.5).

These results show that Treg-suppression could not be enhanced or reduced by antibodies directed against CD27, suggesting that CD27 does not have a crucial role in the suppressive mechanism of Tregs.

Figure 4.1

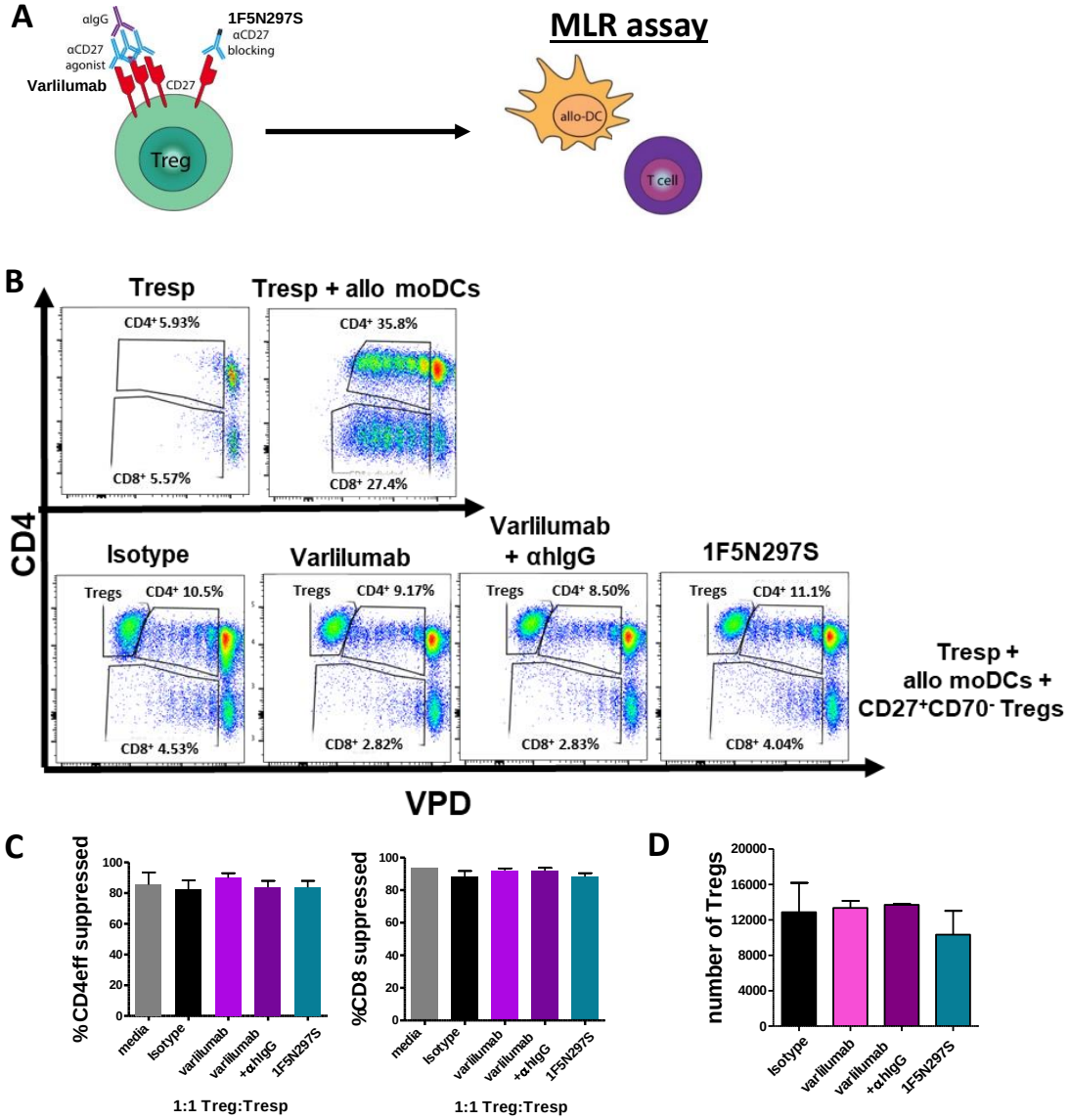

4.1. CD27$^+$CD70$^-$ Treg suppressive function does not rely on CD27 signalling.

(A) Cartoon depicting Treg CD27 targeting strategies. Tregs were pre-incubated for 1 hour with non-mutated anti-CD27 mAb (varlilumab) or Fc-mutated blocking anti-CD27 mAb (1F5N297S) (20µg/ml). Anti-human IgG antibody (20µg/ml) was added for an extra hour for cross-linking to non-mutated anti-CD27 antibody. As a control, cells were incubated with isotype matched antibodies. *In vitro* suppressive capacity was assessed afterwards in a MLR assay co-culturing anti-CD27 pre-incubated Tregs with VPD stained-CD3$^+$CD25$^-$ responder T cells (Tresp) in the presence of allogenic monocyte derived-DCs (allo moDC).

(B) Numbers in the plots refer to the percentage of indicated Tresp cells (CD4$^+$ or CD8$^+$) that are dividing as reflected by VPD staining (top) in the absence of Tregs and (bottom) in the presence of Tregs treated as indicated at 1:1 Treg:Tresp ratio for 1 representative donor out of 3.

(C) Percentage suppression of CD4$^+$ and CD8$^+$ T cell proliferation by Tregs pre-incubated with anti-CD27 mAbs. Bars indicate mean ± SEM for 3 independent cell donors. The average of 3 replicate wells in the suppression assay of each donor is represented. Percentage of suppression was calculated relative to division index of DC-stimulated Tresp in the absence of Tregs.

(D) Number of Tregs at the end of the assay for one representative donor out of 3 is shown as mean ± SD.

4.3.2. Blocking the CD27-CD70 pathway increases Treg suppressive potency *in vitro*

To establish whether the CD27/CD70 pathway is decisive in Treg suppression, an anti-CD70 blocking mAb was used during *in vitro* MLR assays. Blocking mAb (10-20µg/ml) was added to both stimulated T cells positive control condition and to stimulated T cells co-cultured with Tregs. Surprisingly, blockade of CD70 tended to enhance the proliferation of both $CD8^+$ and $CD4^+$ T cells when stimulated with allo moDCs. However, in the presence of $CD27^-CD70^+$ Tregs, the addition of an anti-CD70 blocking mAb substantially enhanced Treg suppressive capacity (Figure 4.2A,B). Increased suppressive potency was unrelated to any effect in Treg proliferation or survival, since no difference was observed in numbers of Tregs at the end of the suppression test between anti-CD70 and isotype control (Figure 4.2C).

When analysing CD70 expression in Tregs and Tresp at the end of the suppression test, we found low levels of CD70 expression in both $CD4^+$ and $CD8^+$ Tresp (Figure 4.2D). CD70 expression was higher in $CD8^+$ than in $CD4^+$ Tresp, but still substantially lower than in $CD70^+$ Tregs. Upon addition of anti-CD70 blocking mAb to the suppression test and subsequent staining with a competitive fluorophore-bound anti-CD70 mAb, lower percentage of $CD70^+$ cells were found in all T cells populations (Tregs, $CD4^+$ and $CD8^+$ Tresp), suggesting that anti-CD70 blocking mAb remained bound to CD70 until the end of the assay (Figure 4.2D). These data also indicated that $CD70^+$ Tregs were the cell population more affected by CD70 blockade, although some binding of anti-CD70 blocking mAb to CD70 expressed on Tresp or DCs cannot be excluded within this setting.

Figure 4.2.

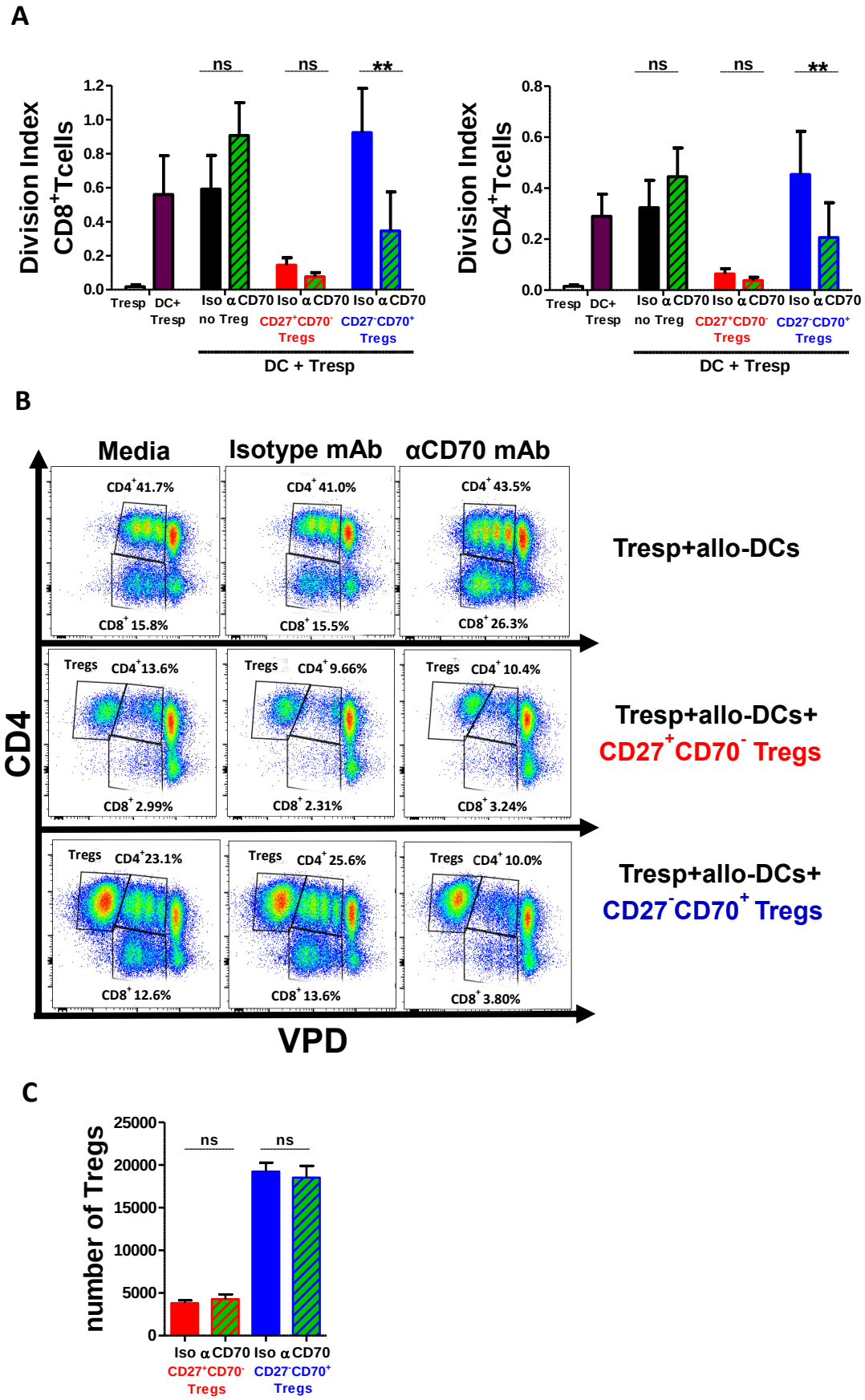
A
Division Index CD8+Tcells
Division Index CD4+Tcells
ns
ns
**
Tresp
DC+ Tresp
Iso αCD70 no Treg
Iso αCD70 CD27+CD70- Tregs
Iso αCD70 CD27-CD70+ Tregs
DC + Tresp
B
Media
Isotype mAb
αCD70 mAb
CD4+41.7%
CD8+15.8%
CD4+41.0%
CD8+15.5%
CD4+43.5%
CD8+26.3%
Tresp+allo-DCs
Tregs
CD4+13.6%
CD8+2.99%
CD4+9.66%
CD8+2.31%
CD4+10.4%
CD8+3.24%
Tresp+allo-DCs+ CD27+CD70- Tregs
CD4+23.1%
CD8+12.6%
CD4+25.6%
CD8+13.6%
CD4+10.0%
CD8+3.80%
Tresp+allo-DCs+ CD27-CD70+ Tregs
CD4
VPD
C
number of Tregs
25000
20000
15000
10000
5000
0
ns
ns
Iso αCD70 CD27+CD70- Tregs
Iso αCD70 CD27-CD70+ Tregs

Figure 4.2

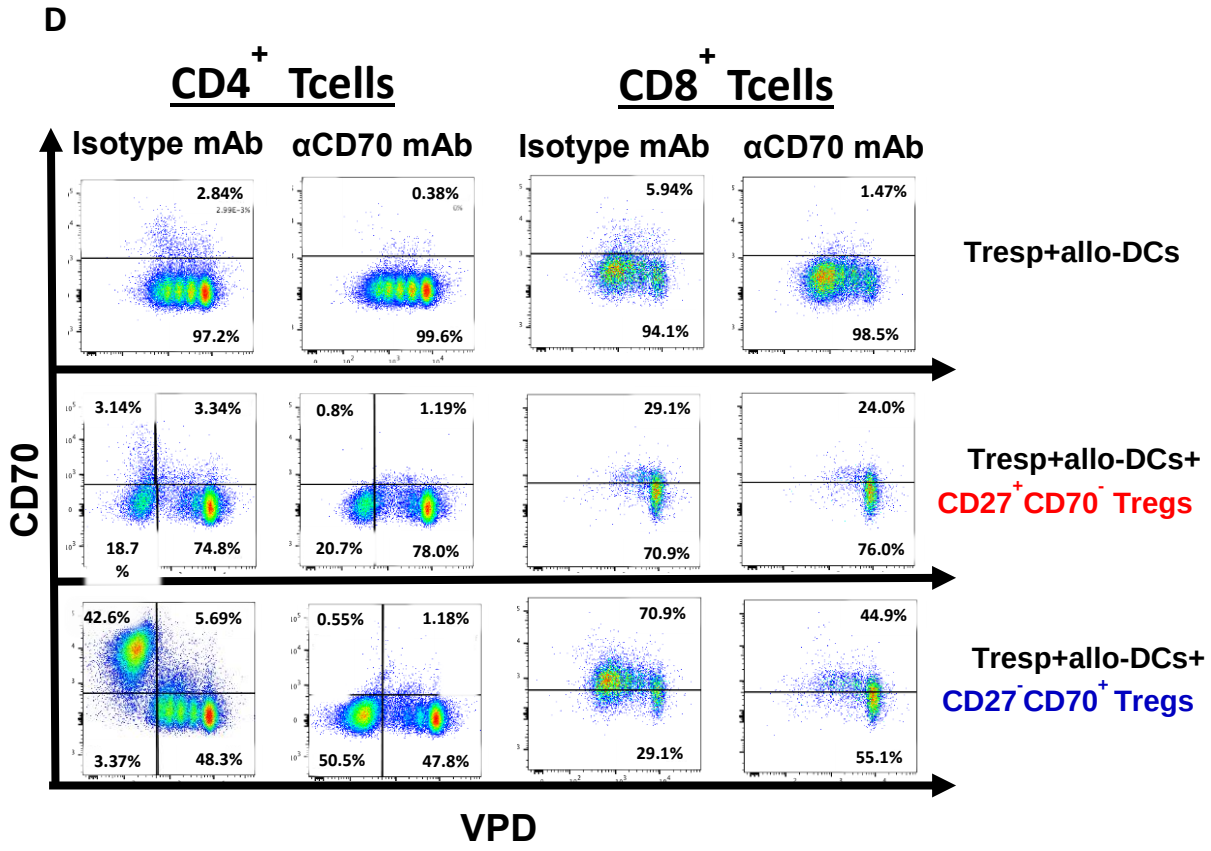

4.2. Blocking the CD27-CD70 pathway during a suppression test enhances Treg suppressive potency.

$CD3^+CD25^-$ responder T cells (Tresp) were stained with VPD and stimulated with allogenic monocyte derived-DCs in the absence of Tregs (black) or in the presence of $CD27^+CD70^-$ Tregs (red) or $CD27^-CD70^+$ Tregs (blue). Isotype control antibody or anti-CD70 mAb (10-20µg/ml) was added to the MLR co-culture assays. Proliferation of Tresp was assessed by VPD dilution and measured by flow cytometry.

(A) Proliferation of responder $CD8^+$ or $CD4^+$ T cells is represented as division index. Bars indicate mean ± SEM for 4 independent cell donors. The average of 3 replicate wells in the suppression assay of each donor is represented. Statistics are derived from a two-way ANOVA with Bonferroni post-test.

(B) Numbers in the plots refer to the percent of indicated Tresp cells ($CD4^+$ or $CD8^+$) that are dividing as reflected by VPD staining (top) in the absence of Tregs and (bottom) in the presence of Tregs and mAbs as indicated.

(C) Number of Tregs at the end of the MLR assay for 1 representative donor out of 4. Error bars represent mean ± SD. Statistical analysis was conducted by one-way ANOVA with Bonferroni post-test.

(D) CD70 expression was studied in (left) $CD4^+$ T cells and (right) $CD8^+$ T cells at the end of the MLR assay when isotype or anti-CD70 mAb was added to the test.

ns= non-significant, **P<0.01.

4.3.3. Blocking CD70 on Tregs enhances suppressive potency

It is unclear how CD70 expressed on different cell types such as APCs, Teff cells or Tregs, affects T cell function (*125*). We sought to investigate the role of CD70 expressed on Tregs, however, the interpretation of the previous results by addition of anti-CD70 mAb into the suppression test (Figure 4.2) could be misleading if blocking CD70 on Tresp or DCs might negate the effect of blocking CD70 on Tregs. Therefore, in a new set of experiments, Tregs were pre-incubated with anti-CD70 blocking mAb or matched isotype and assessed in an *in vitro* MLR test. Tregs were pre-incubated at saturating doses of 20µg/ml for 1 hour at 37°C. Excess of mAbs was washed out before assessing functionality of pre-incubated Tregs (Figure 4.3A). The effective binding of anti-CD70 blocking mAb was confirmed by FACS using competitive anti-CD70 mAb for staining (Figure 4.3B).

Figure 4.3

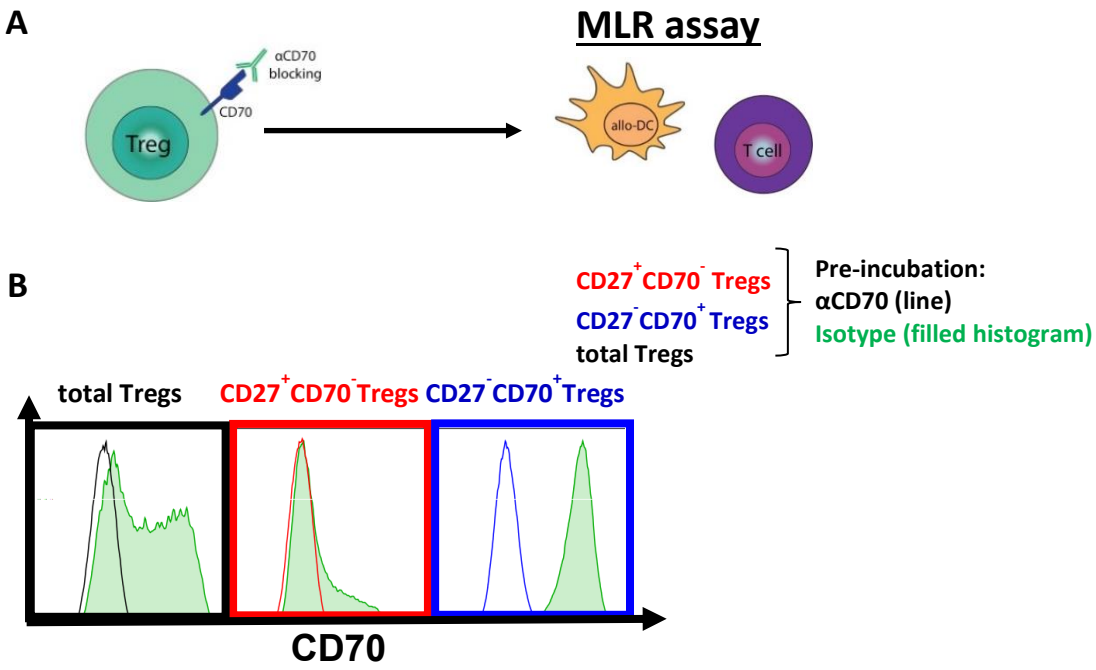

4.3. Anti-CD70 blocking mAb effectively binds to CD70 expressed on Tregs.

(A) $CD27^{-}CD70^{+}$ Tregs were incubated for 1 hour with anti-CD70 blocking mAb or matched isotype antibody, before assessing their suppressive activity in a MLR assay.

(B) Effective anti-CD70 mAb binding was confirmed by flow cytometry using a competitive anti-CD70-fluorochrome mAb. CD70 expression is shown by green filled histogram on isotype-incubated Tregs and by solid lines on anti-CD70-incubated Tregs.

Blocking CD70 on Tregs inhibited the pro-inflammatory effect of $CD27^{-}CD70^{+}$ Tregs and enhanced suppressive potency of total unsorted Tregs without affecting the activity of $CD27^{+}CD70^{-}$ Tregs (Figure 4.4A). The effect on Treg suppressive potency upon CD70 blockade was not due to differences in Treg survival or proliferation, since similar numbers of Tregs were found at the end of the MLR assay regardless of pre-incubation conditions (Figure 4.4B).

Figure 4.4

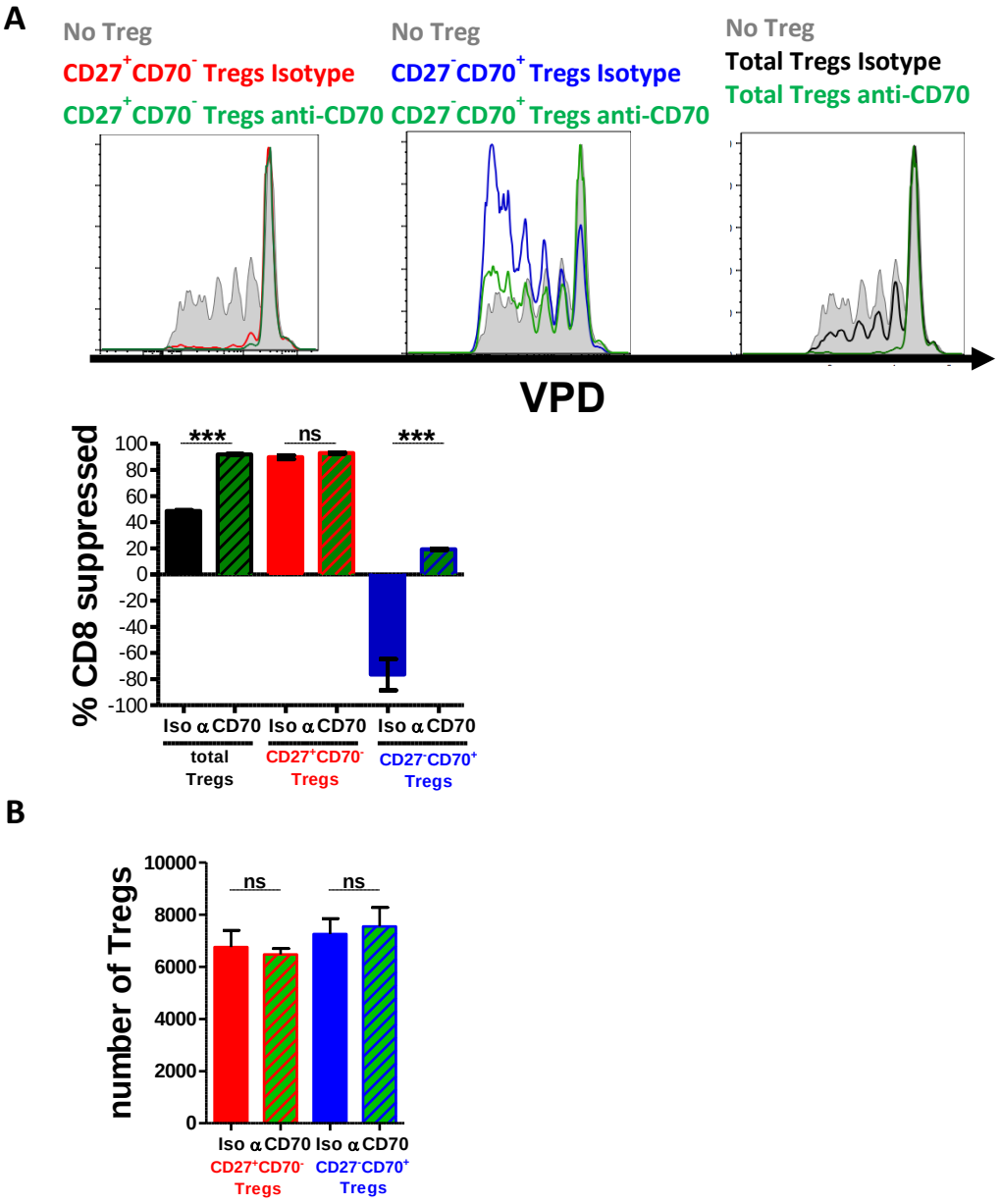

4.4. Blocking CD70 on Tregs enhances their suppressive capacity.

4 weeks expanded Treg subsets (total Tregs, $CD27^+CD70^-$ Tregs and $CD27^-CD70^+$ Tregs) were pre-incubated for 1 hour with anti-CD70 blocking mAb or matched isotype antibody before assessing their suppressive capacity in a MLR assay, which consisted of $CD3^+CD25^-$ responder T cells (Tresp) labelled with VPD and stimulated with allogenic monocyte derived-DCs.

(A) Top panel: Proliferation of VPD-labelled $CD8^+$ Tresp co-cultured with different Treg subsets pre-incubated with isotype or anti-CD70 mAb. Bottom panel: Percentage suppression of $CD8^+$ Tresp cell proliferation by Tregs pre-incubated with anti-CD70 mAb or isotype antibody based on division index. One representative donor out of 6 is shown as mean ± SD. Statistical significances were analysed using one way-ANOVA with Bonferroni post-test for multiple comparisons.

(B) Number of Tregs at the end of the MLR assay for 1 representative donor out of 6. Errors bars represent mean ± SD. Statistics are derived from a one way-ANOVA with Bonferroni post-test.

ns= non-significant, ***P < 0.001.

In 2 out of 5 donors, $CD27^-CD70^+$ Tregs showed suppressive activity when CD70 was blocked (Figure 4.5A). In chapter 3 we demonstrated that 2 weeks expanded $CD27^-CD70^+$ Tregs are able to suppress T cell proliferation, although to less extent than $CD27^+CD70^-$ Tregs (Figure 3.7A), and show pro-inflammatory activity only after been expanded for 4 weeks (Figure 3.9A,B). We then investigated if CD70 blocking in 2 weeks expanded $CD27^-CD70^+$ Tregs may enhance their suppressive capacity. 2 weeks *in vitro* expanded total Tregs ($CD4^+CD25^+CD127^{-/low}$) were sorted as $CD27^+CD70^-$ and $CD27^-CD70^+$ Tregs. $CD27^-CD70^+$ Tregs were pre-incubated with isotype or anti-CD70 blocking mAbs and their suppressive capacity was assessed by MLR. CD70 blockade completely restores suppressive potency of $CD27^-CD70^+$ Tregs to similar levels as $CD27^+CD70^-$ Tregs (Figure 4.5B).

These data identify a pro-inflammatory role for CD70 in expanded Tregs, that can be reversed by blocking CD70 using monoclonal antibodies.

Figure 4.5

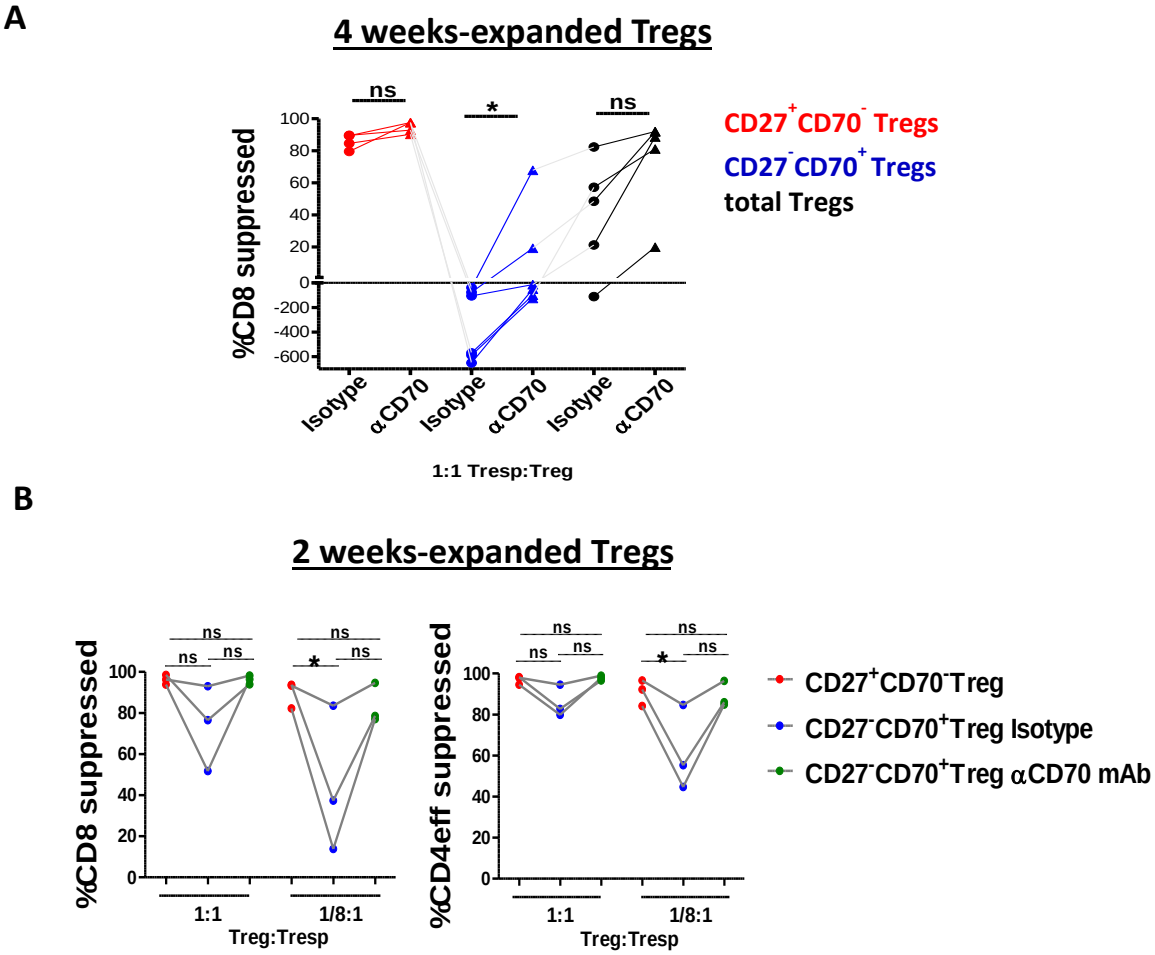

4.5. CD70 blockade fully restores suppressive potency of 2 week-expanded CD27$^-$CD70$^+$ Tregs.

(A) 4 week-expanded total Tregs, CD27$^+$CD70$^-$ Tregs and CD27$^-$CD70$^+$ Tregs were pre-incubated with anti-CD70 blocking mAb or isotype antibody before assessing their suppressive capacity in a MLR test. Percentage of suppression of CD8$^+$ Tresp proliferation is shown for 6 independent donors. Each data point represents the mean of 3 replicate wells for each donor. Data were analysed using a Wilcoxon matched-pairs test.

(B) 2 weeks expanded CD4$^+$CD25$^+$CD127$^{-/low}$ Tregs were flow sorted into CD27$^+$CD70$^-$ and CD27$^-$CD70$^+$ cells subsets. CD27$^-$CD70$^+$ Tregs were pre-incubated with anti-CD70 blocking mAb or isotype antibody before assessing their suppressive potency in a MLR assay. Percentage of suppression of CD8$^+$ and CD4$^+$ responder T cell proliferation is shown for 3 independent donors. Each dot shows the average of 3 replicate wells in the suppression assay of each donor and each line represents a separate donor. A one way-ANOVA with Bonferroni post-test was used for statistical significance.

MLR test consisted of CD3$^+$CD25$^-$ responder T cells (Tresp) stained with VPD and stimulated with allogenic monocyte derived-DCs in the presence or absence of Tregs. Percentage of suppression was calculated based on division index of Tresp.

ns= non-significant, *P<0.05.

4.3.4. CD70 on Tregs provides co-stimulation to CD27$^+$ conventional T cells

In order to further explore the mechanism underlying differences in suppressive potency between CD27$^+$CD70$^-$ and CD27$^-$CD70$^+$ Tregs, we investigated whether this was a result of CD70-mediated co-stimulation. To this end, we impeded CD27-CD70 interaction by blocking CD70 expressed in Tregs or CD27 expressed in Tresp. As in section 4.3.3, CD27$^-$CD70$^+$ Tregs were pre-incubated with anti-CD70 blocking mAb before being assessed for their suppressive capacity. Alternatively, anti-CD27 blocking mAb (1F5N297S) was added to the suppression assay, with the intention to bind to Tresp. Suppressive activity was measured by MLR assay, which consisted of VPD-stained CD25$^-$CD3$^+$ Tresp stimulated with allo moDCs in the presence or absence of CD27$^-$CD70$^+$ Tregs (Figure 4.6A).

Addition of anti-CD27 blocking mAb did not affect the proliferation of Tresp when stimulated with allo moDCs (Figure 4.6B). Blocking CD27 on Tresp in the presence of CD27$^-$CD70$^+$ Tregs resulted in suppression of proliferation to a similar extent as blocking CD70 on Tregs (Figure 4.6C,D). As in previous experiments, the number of Tregs at the end of the suppression assay was similar between different antibody treatments (Figure 4.6E).

Figure 4.6

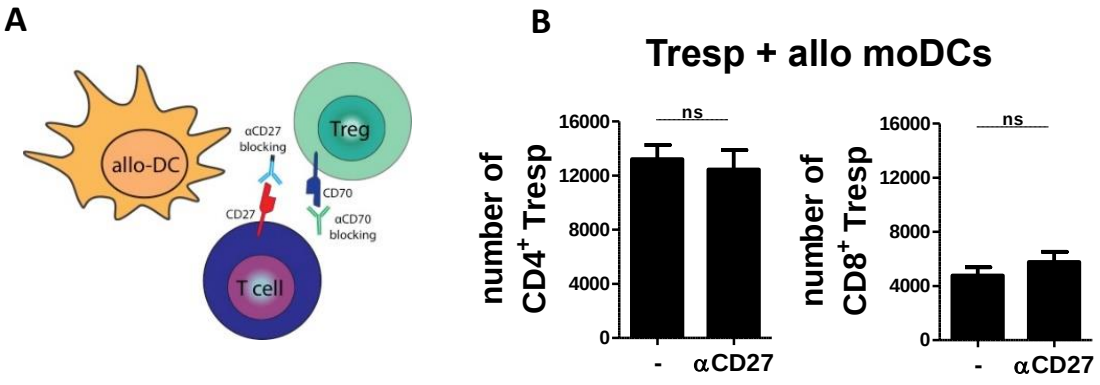

Figure 4.6

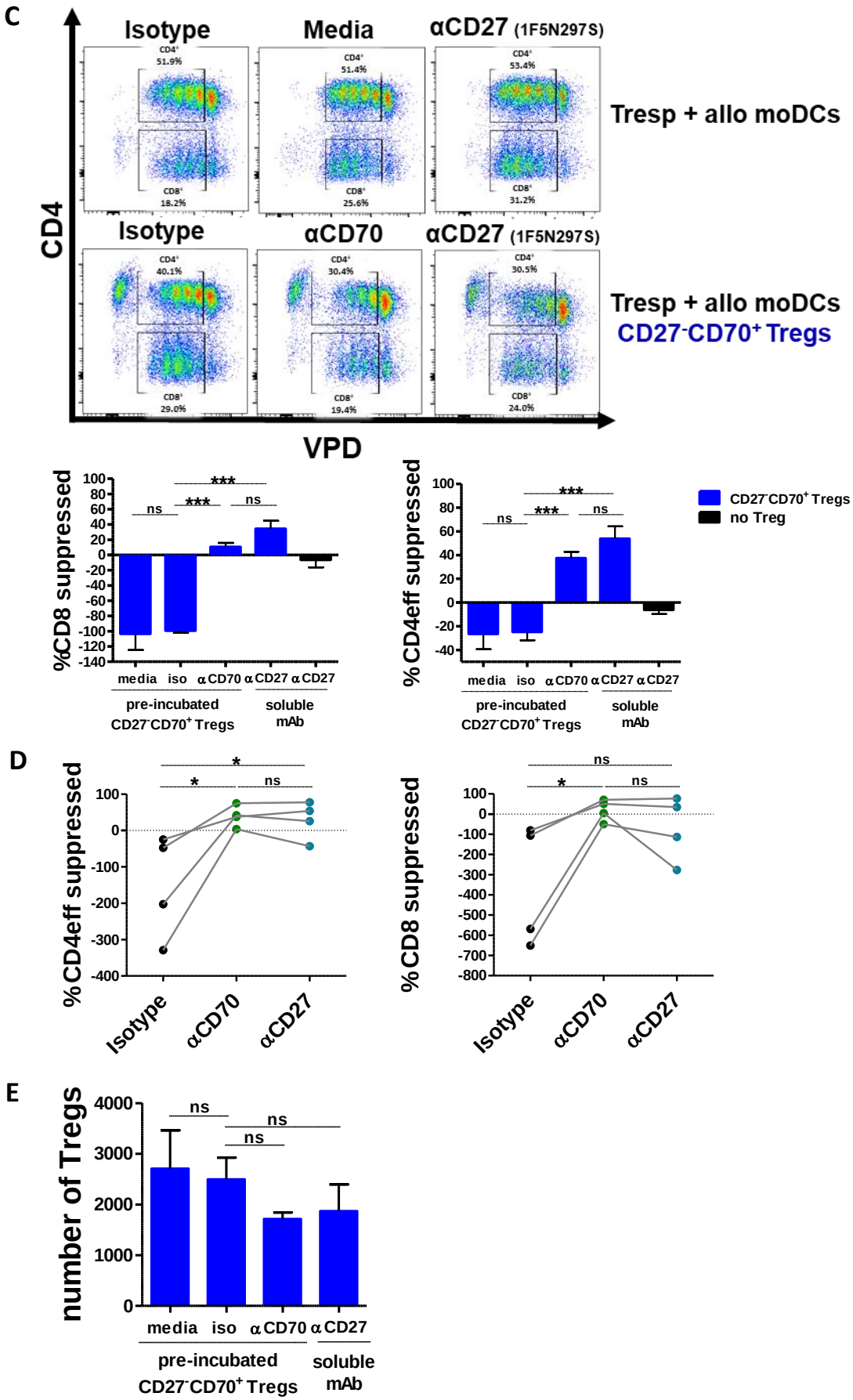
C
Isotype
Media
αCD27 (1F5N297S)
Tresp + allo moDCs
Isotype
αCD70
αCD27 (1F5N297S)
Tresp + allo moDCs
CD27-CD70+ Tregs
CD4
VPD
%CD8 suppressed
%CD4eff suppressed
CD27-CD70+ Tregs
no Treg
media
iso
αCD70
αCD27
αCD27
pre-incubated CD27-CD70+ Tregs
soluble mAb
D
%CD4eff suppressed
%CD8 suppressed
Isotype
αCD70
αCD27
E
number of Tregs
media
iso
αCD70
αCD27
pre-incubated CD27-CD70+ Tregs
soluble mAb

4.6. CD70 on Tregs provides co-stimulation to CD27$^+$ conventional T cells.

(A) Cartoon depicting CD27/CD70 blocking strategies on CD3$^+$CD25$^-$ responder T cells (Tresp) or Tregs during MLR suppression assays. CD27$^-$CD70$^+$ Tregs were pre-incubated with anti-CD70 blocking mAb or matched isotype antibody (20µg/ml) prior to subsequent culture with Tresp. Alternatively, soluble Fc-mutated blocking anti-CD27 mAb (1F5N297S) (20µg/ml) was added to the suppression assay to block CD27 on Tresp.

(B) Numbers of CD4$^+$ and CD8$^+$ Tresp when stimulated with allogenic DCs in the absence or presence of Fc-mutated blocking anti-CD27 mAb (1F5N297S) for 1 representative donor out of 4. Errors bars represent mean ± SD. Unpaired t test was used for statistical analysis.

(C) Top panel: Percentage of dividing VPD-stained CD4$^+$ or CD8$^+$ Tresp in the absence of Tregs (top) and in the presence of Tregs (bottom). Cells were treated with mAbs as described in (A) and as indicated in the figure. Bottom panel: Percentage suppression of proliferation of CD8$^+$ and CD4$^+$ Tresp for one representative donor out of 4 shown as mean ±SD (3 replicates per donor). Statistical significances were determined by one way-ANOVA with Bonferroni post-test.

(D) MLR assays were set up as described in (A). Percentage of suppression of proliferation of CD4$^+$ and CD8$^+$ Tresp by CD27$^-$CD70$^+$ Tregs for 4 independent donors. Each line shows a separate donor and each data point represents the mean of 3 replicate wells in the suppression test of each donor. Statistical significances were assessed using one way-ANOVA with Bonferroni post-test.

(E) Number of Tregs at the end of the MLR assay for 1 representative donor out of 4. Data were analysed by one way-ANOVA with Bonferroni post-test and are represented as mean ± SD.

C, D – Suppression graphs calculated based on division index

ns= non-significant, *P < 0.1, ***P < 0.001.

For a direct comparison between treatments, we then aimed to target CD27 and CD70 signalling within one single experiment. 4 weeks expanded total unsorted Tregs, expressing both CD27 and CD70, were pre-incubated with anti-CD27 mAbs in agonist and blocking conditions (varlilumab and anti-human IgG mAb or Fc-mutated mAb (1F5N297S)) or anti-CD70 blocking mAb before assessing their suppressive capacity in a MRL suppression test (Figure 4.7; left panel). Alternatively, anti-CD27 blocking mAb (1F5N297S) was added to the MLR assay (Figure 4.7A; right panel). As previously shown, while targeting CD27 signalling in Tregs did not affect Treg function, blocking the interaction between CD70$^+$ Tregs and CD27$^+$ responder T cells enhanced Treg suppressive potency (Figure 4.7B).

Therefore, these finding led us to a novel finding that CD70$^+$ Tregs provide co-stimulatory signals by ligating CD70 to CD27 on T cells. Importantly, this pro-inflammatory effect could be reverted using monoclonal antibodies against CD27 or CD70.

Figure 4.7

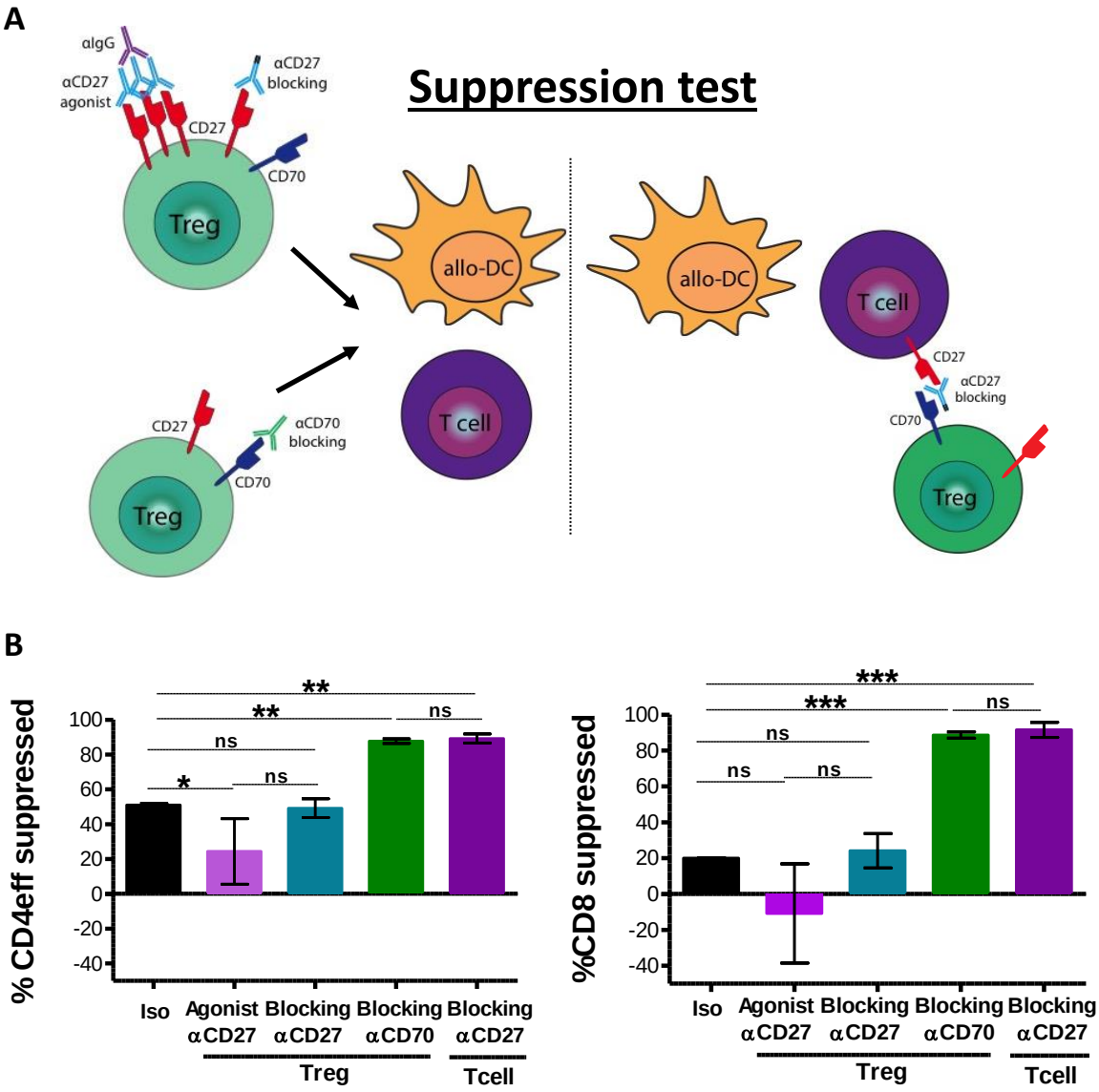

4.7. CD70, but not CD27, has an active role in Treg regulatory function.

(A) Cartoon depicting strategies targeting CD27/CD70 co-stimulation. Left panel: 4 weeks expanded total Tregs, expressing both CD27 and CD70, were pre-incubated with anti-CD27 mAbs in agonist and blocking conditions (varlilumab and anti-human IgG mAb or Fc-mutated 1F5N297S mAb) or anti-CD70 blocking mAb before assessing their suppressive capacity in a MRL suppression test. Right panel: alternatively, anti-CD27 blocking mAb (1F5N297S) was added to the co-culture of $CD3^{+}CD25^{-}$ responder T cells (Tresp), allogenic monocyte derived-DCs and expanded total Tregs.

(B) Percentage suppression of proliferation of $CD4^{+}$ and $CD8^{+}$ Tresp by Tregs when CD27/CD70 is targeted as labelled in the figure. Error bars represent mean ± SD for 3 replicate wells in 1 cell donor. Statistical significances were analysed using one way-ANOVA with Bonferroni post-test.

ns= non-significant, *P<0.05, **P<0.01, ***P < 0.001.

4.3.5. $CD70^+$ Tregs provide sufficient co-stimulatory signals to induce T cell proliferation in the absence of additional co-stimulation

After showing that $CD70^+$ Tregs enhance proliferation of T cells stimulated with allogenic DCs, we wondered whether CD70 expressed on Tregs might provide sufficient co-stimulatory signals to induce T cell proliferation in the absence of additional co-stimulation. Treg activity was therefore assessed in the absence of DC-driven stimulation. VPD-labelled Tresp were co-cultured with $CD27^+CD70^-$ Tregs or $CD27^-CD70^+$ Tregs in wells containing plate-bound anti-CD3 mAb (Figure 4.8A). In this setup, only $CD27^-CD70^+$ Tregs but not $CD27^+CD70^-$ Tregs induced T cell proliferation (Figure 4.8B,D). $CD8^+$ T cells consistently appeared more responsive to $CD27^-CD70^+$ Treg stimulation than $CD4^+$ T cells (Figure 4.8B-D). These results indicate that $CD70^+$ Tregs were capable to induce T cell proliferation upon TCR stimulation without the need for additional co-stimulation.

We explored the specificity of this response by pre-incubation of $CD27^-CD70^+$ Tregs with blocking anti-CD70 mAb prior to the subsequent culture with Tresp (Figure 4.8B-D), or by addition of anti-CD27 blocking antibody into the test (Figure 4.8D). Blocking the CD27-CD70 interaction tended to impair the pro-stimulatory effect given by $CD27^-CD70^+$ Tregs, without blocking it completely, suggesting the presence of additional pro-inflammatory mechanisms (Figure 4.8C,D).

Figure 4.8

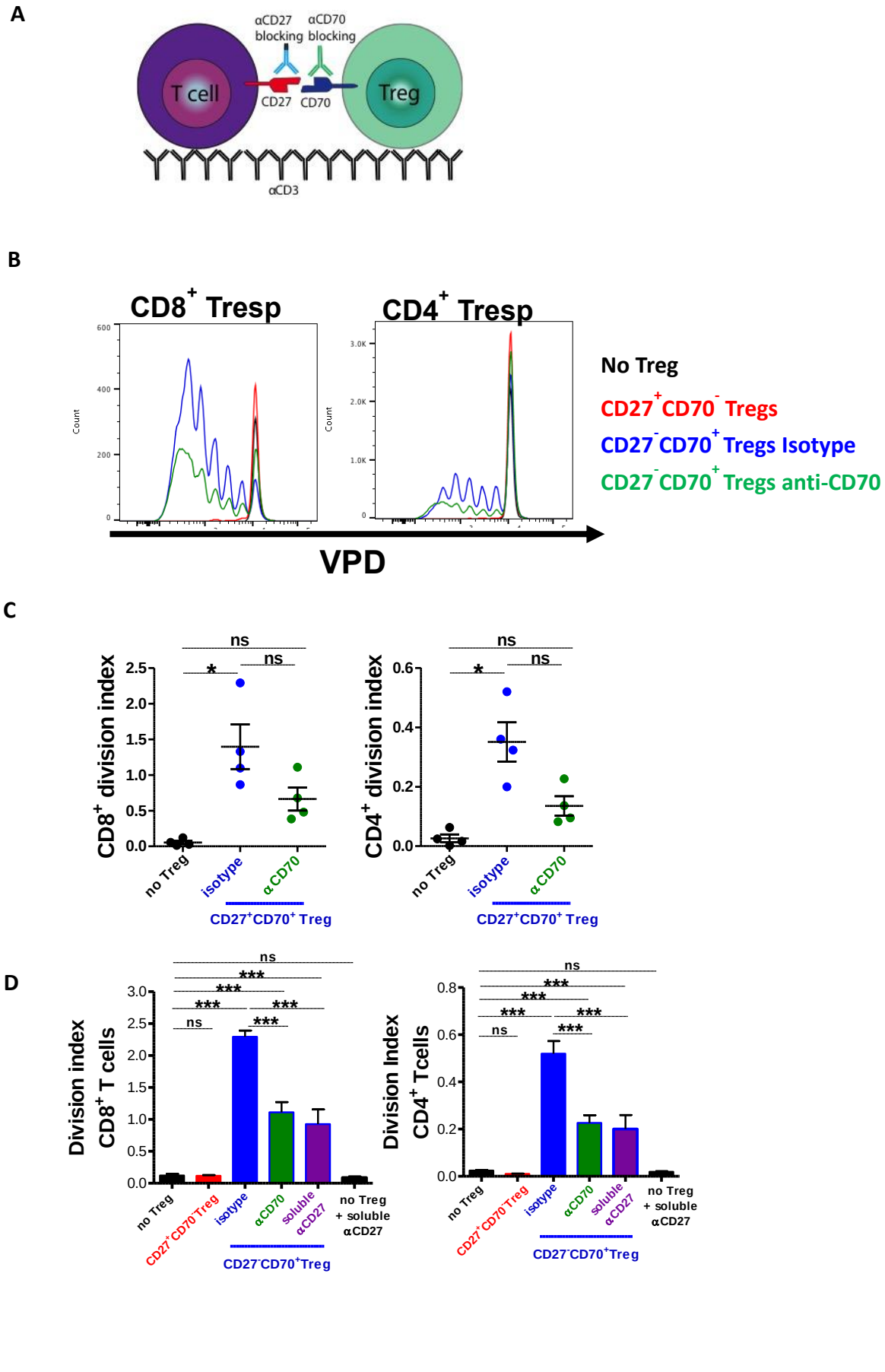
A
αCD27 blocking
αCD70 blocking
T cell
CD27
CD70
Treg
αCD3
B
CD8+ Tresp
CD4+ Tresp
Count
VPD
No Treg
CD27+CD70- Tregs
CD27-CD70+ Tregs Isotype
CD27-CD70+ Tregs anti-CD70
C
CD8+ division index
CD4+ division index
ns
*
no Treg
isotype
αCD70
CD27+CD70+ Treg
D
Division index CD8+ T cells
Division Index CD4+ Tcells
***
no Treg
CD27+CD70+Treg
isotype
αCD70
soluble αCD27
no Treg + soluble αCD27
CD27-CD70+Treg

4.8. CD70$^+$ Tregs provide sufficient co-stimulatory signals to induce T cell proliferation.

(A) Cartoon depicting strategies for blocking CD27/CD70 interaction between CD25$^-$CD3$^+$ responder T cells (Tresp) and Tregs. VPD-labelled Tresp were co-cultured with CD27$^+$CD70$^-$ Tregs or CD27$^-$CD70$^+$ Tregs in wells containing plate-bound anti-CD3 mAb (1µg/ml). CD27$^-$CD70$^+$ Tregs were pre-incubated with anti-CD70 blocking mAb or matched isotype antibody (20µg/ml) prior to subsequent culture with Tresp. Alternatively, soluble Fc-mutated blocking anti-CD27 mAb (1F5N297S) (20µg/ml) was added to the suppression assay to block CD27 on Tresp.

(B) FACS histograms show proliferation, by VPD dilution, of CD8$^+$ and CD4$^+$ Tresp in the absence of Tregs or when co-cultured with CD27/CD70 Treg subsets. One representative donor out of 3 is displayed.

(C) Proliferation of CD4$^+$ and CD8$^+$ Tresp is shown as division index when co-cultured with CD27$^-$CD70$^+$ Tregs pre-incubated with isotype mAb or blocking anti-CD70 mAb. Each data point represents the mean of 3 replicate wells in the suppression assay of each donor. n= 4 independent donors. Data were analysed using a Friedman test with Dunn's post-test for multiple comparisons.

(D) Proliferation of CD4$^+$ and CD8$^+$ Tresp, represented as division index, when co-cultured with CD27$^+$CD70$^-$ Tregs (red) or CD27$^-$CD70$^+$ Tregs pre-incubated with isotype (blue) or blocking anti-CD70 mAb (green) or in the presence of Fc-mutated blocking anti-CD27 mAb (purple) is shown. Error bars represent mean ± SD for 3 replicate wells in 1 cell donor. Statistical significances were assessed using one way-ANOVA with Bonferroni post-test.

ns= non-significant, *P<0.05, ***P < 0.001.

We next addressed the question whether CD4$^+$CD70$^+$ Tconv cells could also induce T cell proliferation. CD27$^-$CD70$^+$ Tconv cells were obtained by sorting CD27$^-$CD70$^+$ from 2 weeks expanded CD4$^+$ T cells and expanding them *in vitro* for 2 further weeks. Like CD27$^-$CD70$^+$ Tregs, CD4$^+$CD27$^-$CD70$^+$ Tconv cells were able to induce cell proliferation of autologous responder T cells when co-cultured in combination with TCR stimulation (Figure 4.9). We also studied the ability of CD70$^+$ regulatory or Tconv cells to induce cell proliferation of autologous responder T cells in the absence of anti-CD3 stimulation. CD70$^+$ Tregs and conventional T cells induced T cell proliferation only in the context of TCR simulation (Figure 4.9).

Figure 4.9

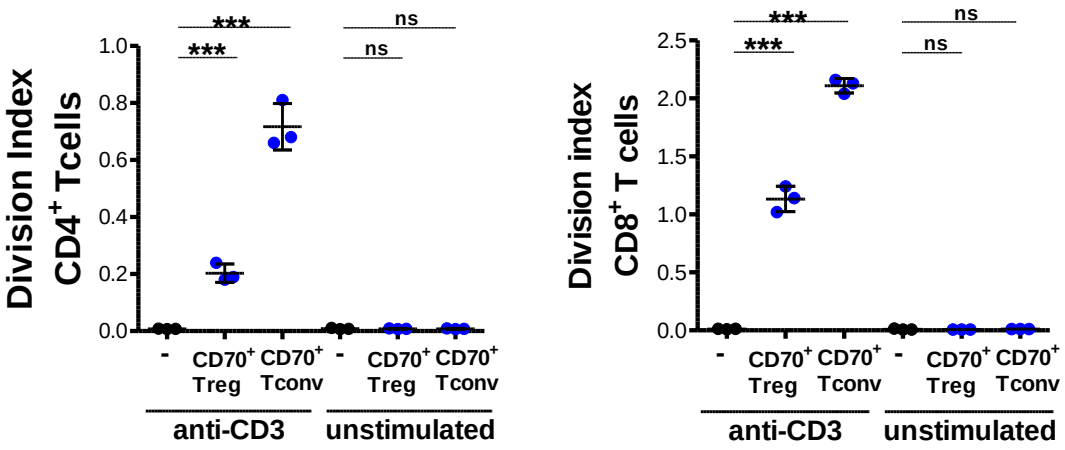

4.9. CD70$^+$ Tregs and CD70$^+$ Tconv induce T cell proliferation only with concurrent TCR stimulation.

VPD-stained CD25$^-$CD3$^+$ T cells (Tresp) were co-cultured with 4 weeks expanded CD27$^-$CD70$^+$ Tregs or CD4$^+$CD27$^-$CD70$^+$ conventional T cells (Tconv) in the presence or absence of TCR stimulation using 1µg/ml of plate bound anti-CD3 mAb. Proliferation of CD4$^+$ and CD8$^+$ Tresp is represented as division index. Error bars show mean ± SD for 3 replicate wells for 1 representative donor out of 2. Statistical significances were analysed using one way-ANOVA with Bonferroni post-test. ns= non-significant, ***P < 0.001.

4.3.6. The cytokine profile of CD27$^+$CD70$^-$ Tregs and CD27$^-$CD70$^+$ Tregs

Differential secretion of inhibitory and pro-inflammatory cytokines may also account for disparate effects of CD27/CD70 Treg subsets. RNA-seq analysis in 4 week-expanded CD27$^+$CD70$^-$ and CD27$^-$CD70$^+$ Tregs showed that IL-17A was the most differentially expressed gene between the two Treg subsets, being expressed 10 times more in the CD27$^-$CD70$^+$ Treg subset (Figure 4.10A). IL-17F, IL-26, IL-13, IL-5, LIF, IFN-γ, IL-22, IL-21, IL-12A, IL-6, IL-10 and IL-4 were also preferentially expressed in CD27$^-$CD70$^+$ Tregs over CD27$^+$CD70$^-$ Tregs (Figure 4.10A).

CD27$^-$CD70$^+$ Tregs also had higher mRNA expression levels of cytokine receptors IL-23R, IL-17RB, LIFR, IL-13RA1, IL-17RE and IL-7R compared to CD27$^+$CD70$^-$ Tregs. By contrast, the cytokines receptors IL1RL1 (also known as ST2), IL1RL2, IFN-γR2,

IL-36G, IL-11RA, IL1-R2 and CSF2RB (high affinity receptor for IL-3, IL-5 and GM-CSF) were preferentially expressed in the $CD27^{+}CD70^{-}$ Treg subset compared to $CD27^{-}CD70^{+}$ Tregs (Figure 4.10A).

Then, the cytokine profile of both Treg subsets was corroborated by measuring cytokine levels in the cell supernatant or by intracellular cytokine staining. Using a cytometry bead assay, the concentration of twelve T cell-derived cytokines was quantified in the supernatant of stimulated 4 weeks expanded $CD27^{+}CD70^{-}$ and $CD27^{-}CD70^{+}$ Treg cultures. Only IL-17A expression was significantly upregulated in $CD27^{-}CD70^{+}$ Tregs compared to $CD27^{+}CD70^{-}$ Tregs (Figure 4.10B). A trend towards higher production of IL5, IL-13 and IL-17F in $CD27^{-}CD70^{+}$ Tregs was also observed, while secretion levels of IFN-γ and anti-inflammatory IL-10 cytokines were similar between Treg subsets (Figure 4.10B). Intracellular cytokine stain for IL-10, IFN-γ and IL-17A also confirmed substantial overexpression of IL-17A in $CD27^{-}CD70^{+}$Tregs compared to $CD27^{+}CD70^{-}$ Tregs (Figure 4.10C).

These results hint that the CD27/CD70 pathway may influence cytokine production by Tregs, specially IL-17A expression. Moreover, since differences in expression of cytokine receptors were also observed, $CD27^{+}CD70^{-}$ and $CD27^{-}CD70^{+}$ Tregs may differ in the way the sense signals from the microenvironment, which may well affect their stability and function.

Figure 4.10

A

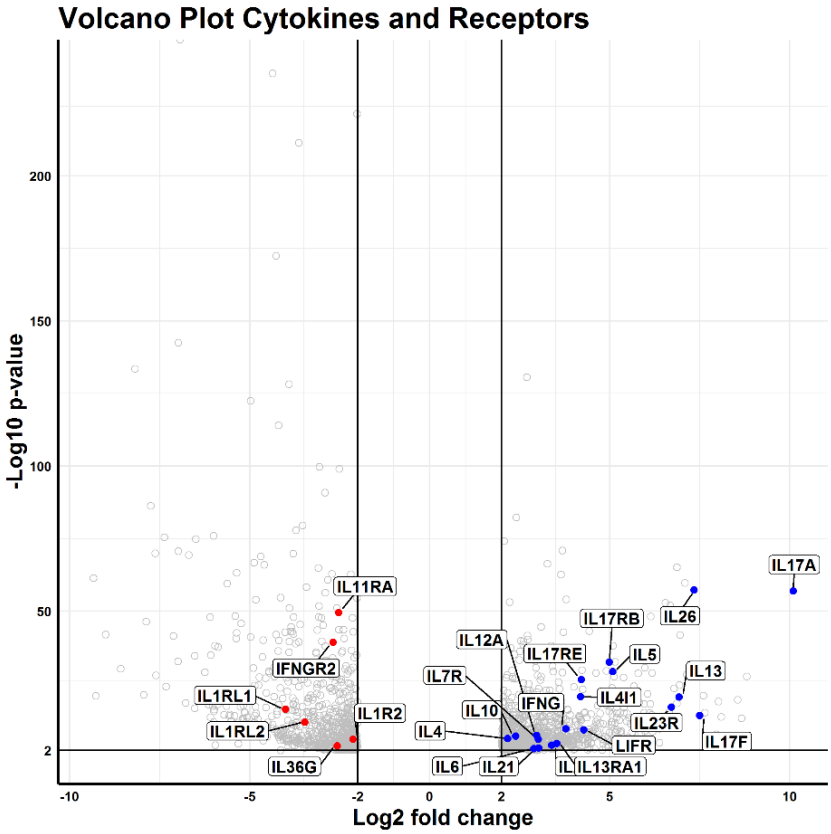
Volcano Plot Cytokines and Receptors
-Log10 p-value
Log2 fold change
200
150
100
50
2
-10
-5
-2
0
2
5
10
IL11RA
IFNGR2
IL1RL1
IL1RL2
IL1R2
IL36G
IL12A
IL7R
IL10
IL4
IL6
IL21
IFNG
IL17RE
IL17RB
IL5
IL4I1
IL26
IL13
IL23R
IL17F
IL17A
LIFR
IL13RA1

Figure 4.10

B

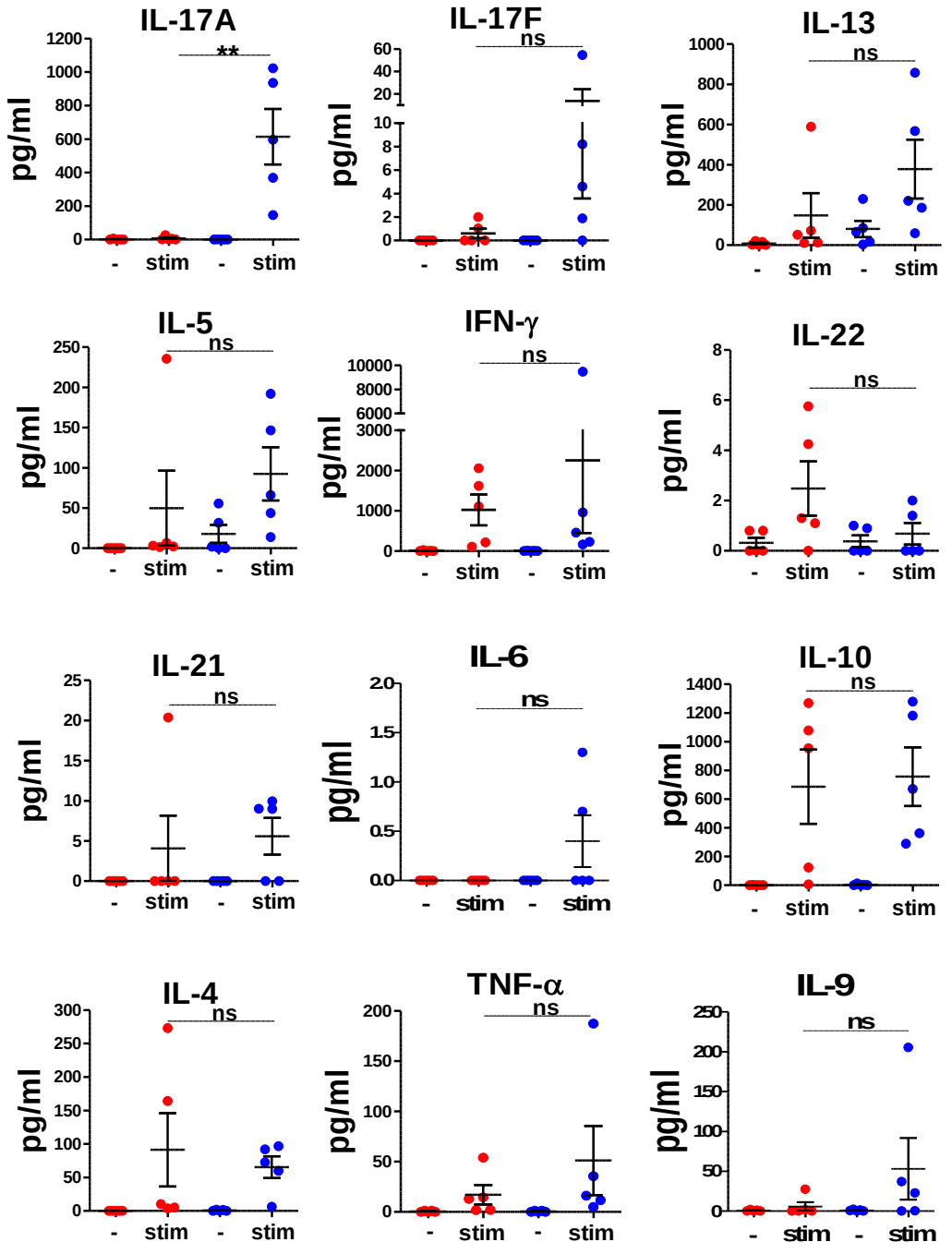
IL-17A
**
IL-17F
ns
IL-13
ns
IL-5
ns
IFN-γ
ns
IL-22
ns
IL-21
ns
IL-6
ns
IL-10
ns
IL-4
ns
TNF-α
ns
IL-9
ns
pg/ml
- stim - stim
CD27+CD70- Tregs
CD27-CD70+ Tregs

Figure 4.10

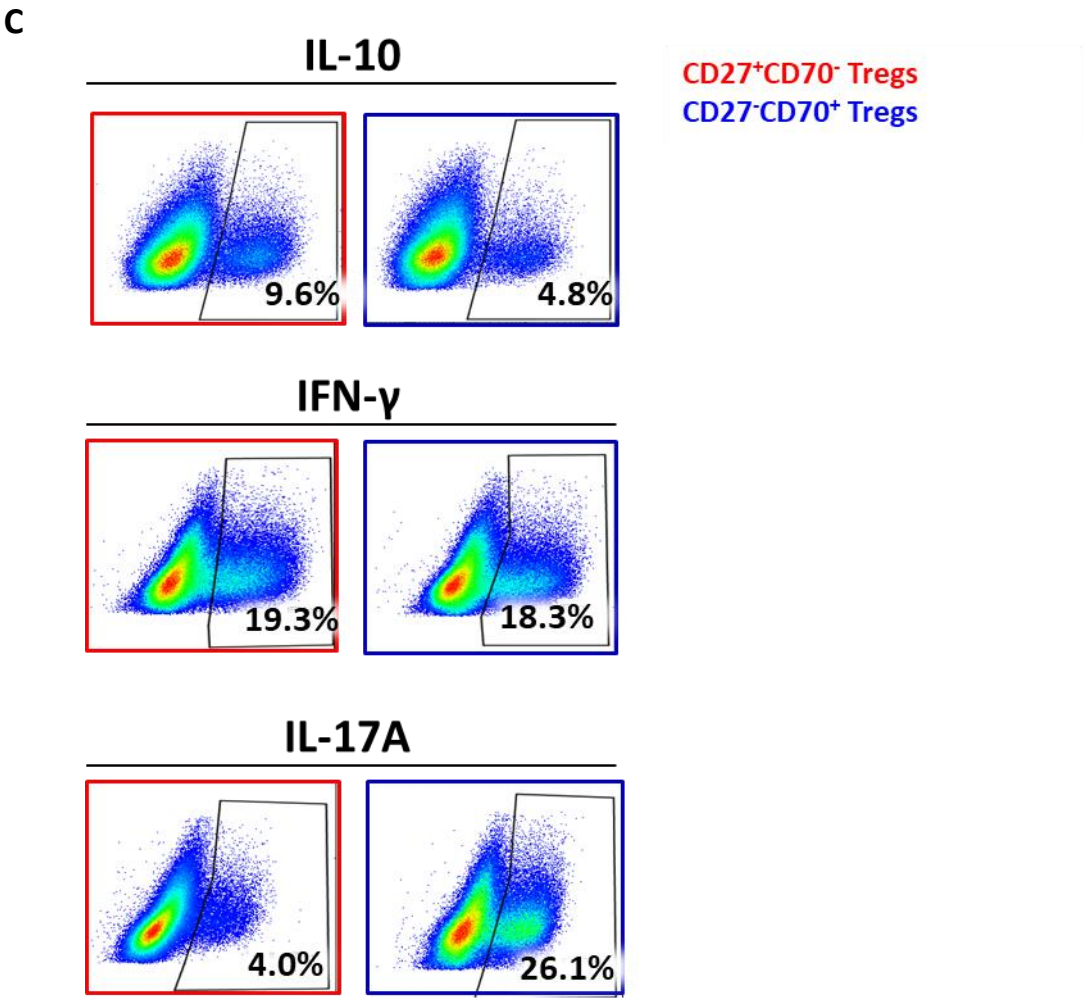

4.10. The cytokine profile of CD27$^+$CD70$^-$ Tregs and CD27$^-$CD70$^+$ Tregs

(A) Volcano plot of differentially expressed genes (each grey circle represents a gene) with p<0.01 (horizontal line) and log2FC>2 or <-2 (vertical lines). Genes encoding for cytokines and cytokine receptors are highlighted in red if overexpressed in CD27$^+$CD70$^-$ Tregs or blue if overexpressed in CD27$^-$CD70$^+$ Tregs.

(B) 4 weeks expanded CD27$^+$CD70$^-$ (red) or CD27$^-$CD70$^+$ (blue) Tregs were rested for 2 days prior a 72h-stimulation in the presence of rhIL-2 (250 U/ml) with or without anti-CD3/anti-CD28 coated beads (1 bead: 5 cells). A cytokine bead array assay was performed on these supernatants to measure expression of 12 different cytokines as labelled in the figure. (-) denotes unstimulated cells and (stim) represents Tregs that have been stimulated with anti-CD3/anti-CD28-coated beads. n=5 independent donors (each data point is the average of 3 replicate wells in the bead array assay of each donor). Statistical significance comparing stimulated CD27$^+$CD70$^-$ and CD27$^-$CD70$^+$ Tregs was assessed by Mann-Whitney test. Errors bars represent mean ± SEM.

(C) Percentage of IL-10$^+$, INF-γ$^+$ and IL-17A$^+$ cells analysed by intracellular cytokine staining in 4 weeks expanded CD27$^+$CD70$^-$ Tregs (red) and CD27$^-$CD70$^+$ Tregs (blue). Tregs were activated with phorbol myristate acetate (PMA) (100ng/ml) and ionomycin (1µg/ml) in the presence of Golgi protein inhibitor stop for 5 hours prior intracellular staining.

ns= non-significant, *P<0.05, **P<0.01, ***P < 0.001.

4.3.7. CD70 signalling does not regulate IL-17A cytokine production in expanded Tregs

Our previous results in section 4.3.6 suggest that CD27/CD70 expression may regulate the cytokine profile of Tregs. Using our well stablished protocol to block CD70 signalling, we explored the hypothesis that CD70 intracellular signalling may regulate cytokine expression in Tregs. 4 weeks expanded $CD27^{-}CD70^{+}$ Tregs were pre-incubated with isotype or anti-CD70 blocking mAb prior to 72 hours stimulation with anti-CD3/anti-CD28 coated beads and rhIL-2 (250 U/ml). Using a cytometric bead assay, the concentrations of twelve T cell-derived cytokines were quantified in the supernatants of stimulated Treg cultures. The concentration of none of the cytokines measured (IL-17A, IL-10, IFN-γ, TNF-α, IL-4, IL-5, IL-3, IL-17F, IL-6, IL-9, IL-22, IL-21) was affected by CD70 blockade (Figure 4.11A).

Still, we investigated further the role of CD70 in regulating IL-17A expression using a different strategy. 4 weeks expanded $CD27^{+}CD70^{-}$ and $CD27^{-}CD70^{+}$ Tregs were cultured for 72h with isotype or anti-CD70 blocking mAb in the presence of rhIL-2 (250 U/ml) with or without stimulation with anti-CD3 plate bound mAb or soluble anti-CD3 mAb and allo moDCs. After 3 days culture, levels of intracellular IL17A expression were measured by flow cytometry following activation with PMA and ionomycin in the presence of Golgi protein transport inhibitor. $CD27^{+}CD70^{-}$ Tregs did not express IL-17A in any stimulating condition. Different percentages of IL-17A-producing cells, ranging between 16% and 36%, were found within the $CD27^{-}CD70^{+}$ Treg population depending on the stimulus. Importantly, CD70 blockade did not affect the percentage of IL-17 producing cells in any of tested conditions (Figure 4.11B).

Together, these results indicate that CD70 expressed by Tregs does not regulate cytokine production.

Figure 4.11

A

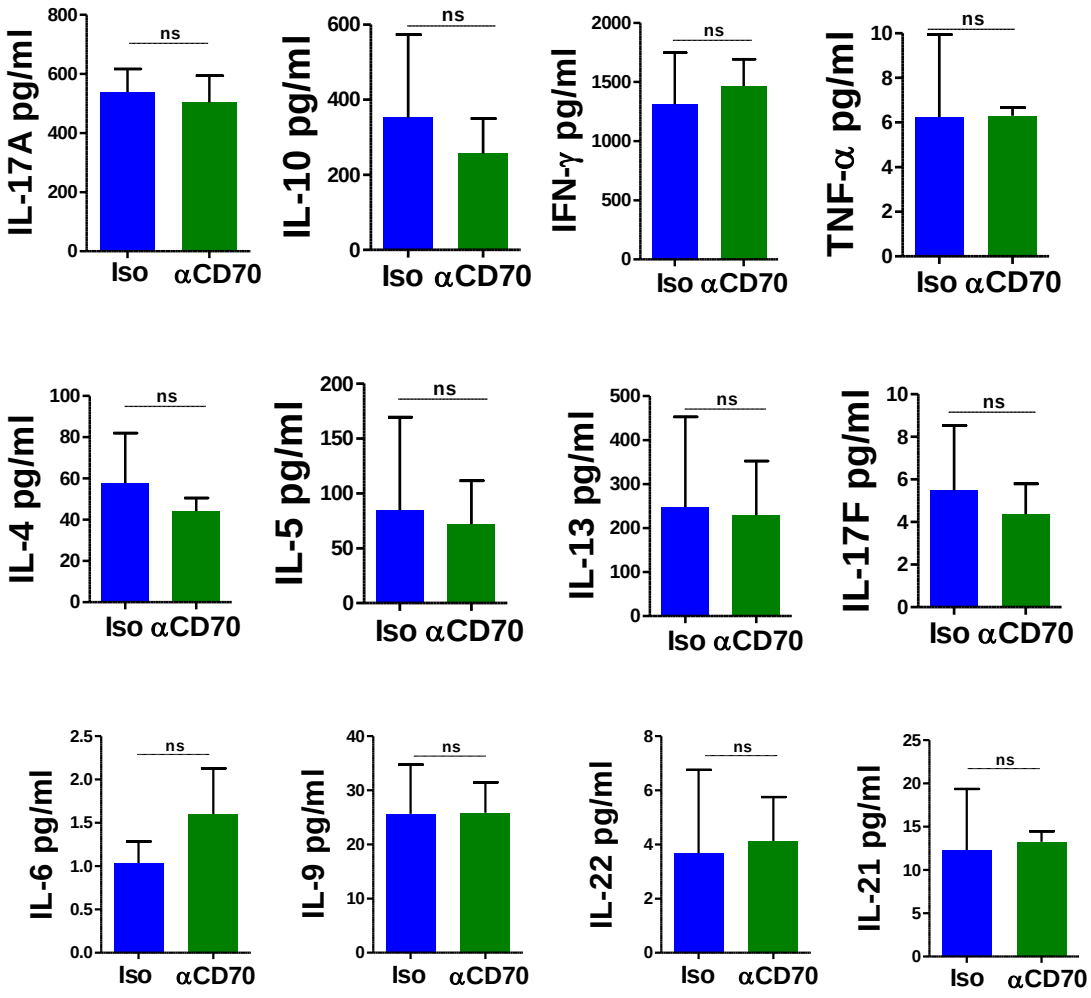
IL-17A pg/ml
IL-10 pg/ml
IFN-γ pg/ml
TNF-α pg/ml
IL-4 pg/ml
IL-5 pg/ml
IL-13 pg/ml
IL-17F pg/ml
IL-6 pg/ml
IL-9 pg/ml
IL-22 pg/ml
IL-21 pg/ml
ns
Iso
αCD70

Figure 4.11

B

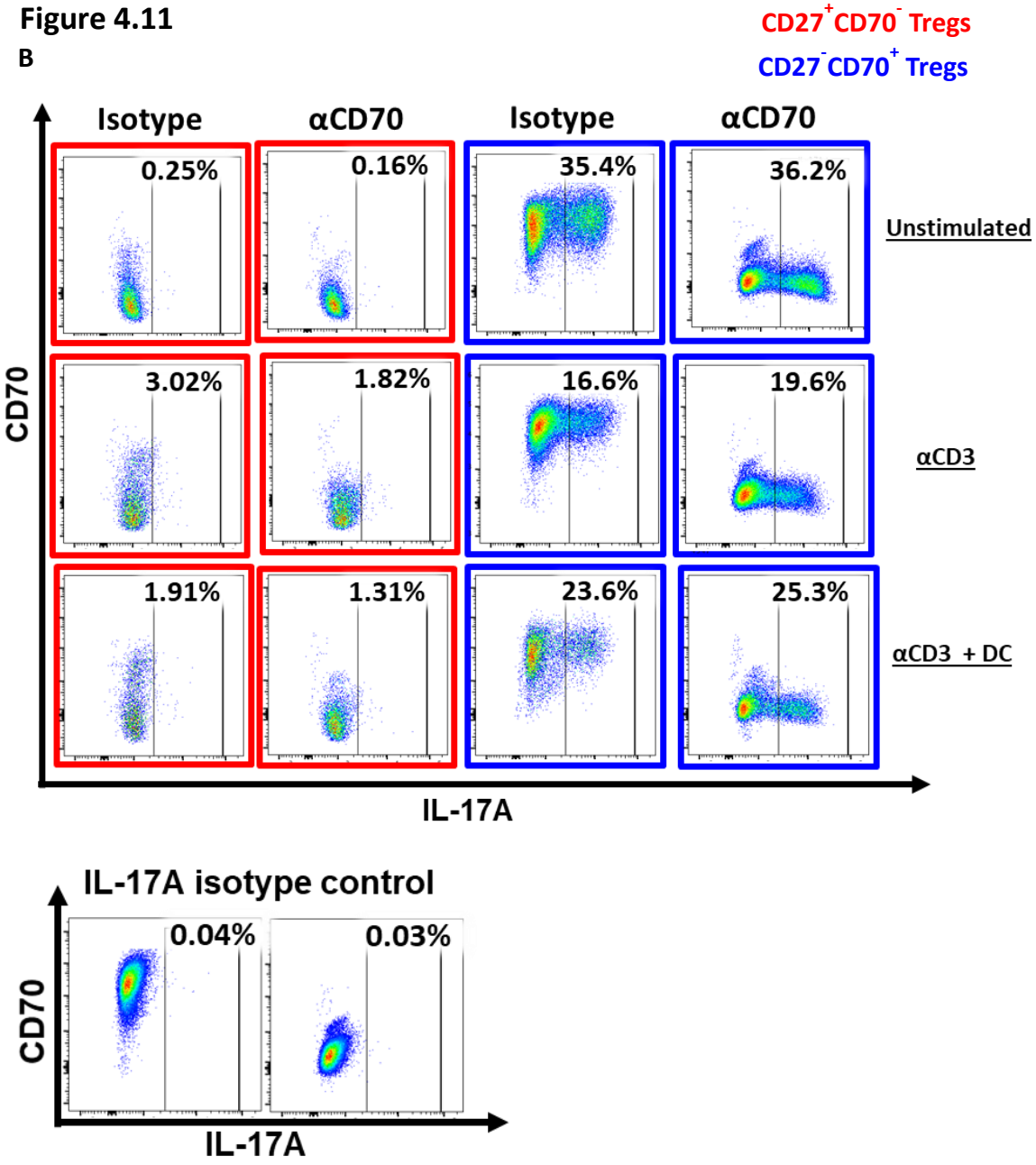

4.11. Cytokine production is not altered by CD70 signalling

(A) 4 weeks expanded, and 2 days rested $CD27^{-}CD70^{+}$ Tregs were pre-incubated for 1 hour with anti-CD70 blocking mAb or isotype control. After pre-incubation, Tregs were stimulated with anti-CD3/anti-CD28-coated beads (1 bead: 5 cells) and rhIL-2 (250 U/ml) for 72 hours. A cytokine bead array assay was performed on the supernatants of stimulated Tregs to measure expression of 12 different cytokines as labelled in the figure. 1 donor out of 2 is represented. Errors bars represent mean ± SD for 3 replicate wells. Statistical analysis was performed using unpaired t test and revealed no significant difference.

(B) 4 weeks expanded, and 2 days rested $CD27^{+}CD70^{-}$ and $CD27^{-}CD70^{+}$ Tregs were cultured for 72 hours with anti-CD70 blocking mAb or isotype control in the presence of rhIL-2 (250 U/ml) without further stimulation, or under stimulation with plate bound anti-CD3 mAb (1µg/ml) or allogenic monocyte derived-DCs (1:5 DC:Treg) and soluble anti-CD3 mAb (1µg/ml). IL-17A expression was analysed by flow cytometry following stimulation with phorbol myristate acetate (PMA) (100ng/ml) and ionomycin (1µg/ml) in the presence of Golgi protein inhibitor for 5 hours.

4.3.8. The increase in T cell proliferation mediated by $CD70^+$ Tregs is cell contact dependent rather than cytokine mediated

We then aimed to elucidate whether the restoration of Treg suppressive capacity achieved by blocking CD70 was due to changes in the ability of Tregs to release soluble factors or whether it relied solely on their capacity to physically establish cognate interactions with Tresp. Firstly, we measured cytokines levels in the supernatant of MLR suppression assays when $CD3^+CD25^-$ Tresp were stimulated with $CD27^+CD70^-$ Tregs or $CD27^-CD70^+$ Tregs pre-incubated with isotype or anti-CD70 blocking mAb.

When analysing supernatants of MLR assays of 4 independent donors using a cytometric bead assay, levels of IL-2, IL-4, IL-17F, IL-9, IL-21 and IL-22 were below the detection limit of the assay. With the exception of TNF-α, cytokine levels were higher when DC stimulated-Tresp were co-cultured with Tregs (mainly $CD27^-CD70^+$ Tregs), suggesting Treg-driven cytokine secretion. The concentration of IL-13 and IL-5 was significantly different between co-cultures with $CD27^+CD70^-$ Tregs and $CD27^-CD70^+$ Tregs, and a trend towards higher levels of other pro-inflammatory cytokines such as IL-17A, IL-6 and IFN-γ was also observed. Meanwhile, the concentration of anti-inflammatory IL-10 appeared at similar level for co-cultures with $CD27^+CD70^-$ or $CD27^-CD70^+$ Tregs (Figure 4.12).

Moreover, despite changes in suppressive capacity (Figures 4.4 and 4.5A), the concentration of neither of the measured cytokines (IL-17A, IL-10, IFN-γ, TNF-α, IL-5, IL-3 and IL-6) was found to be significantly altered when $CD27^-CD70^+$ Tregs have CD70 blocked (Figure 4.12). These results suggest that enhanced suppressive capacity by blocking CD70 on Tregs is not due to changes in cytokine levels.

Figure 4.12

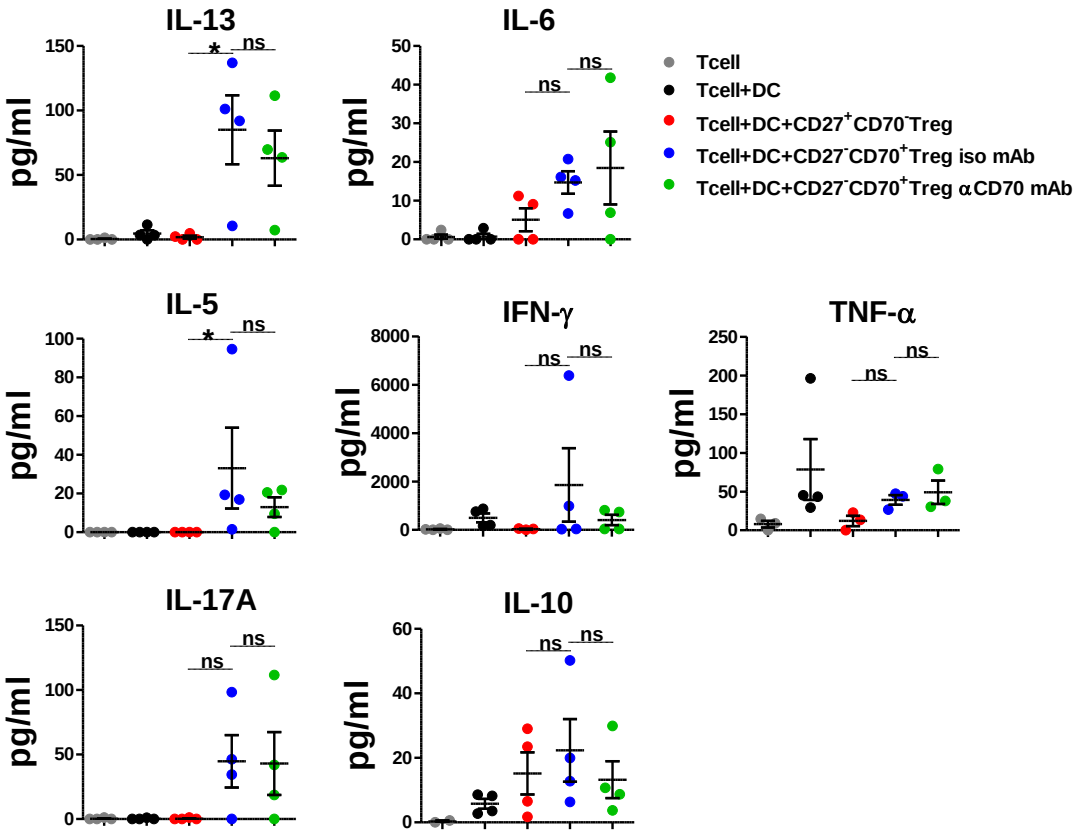

4.12. Cytokine secretion during MLR assay is not altered by blocking CD70 expressed on Tregs.

A 13-plex cytokine bead array assay was performed on the supernatants of MLR tests of 5 independent donors. $CD3^+CD25^-$ responder T cells (Tresp) unstimulated (grey) or stimulated with allogenic monocyte derived-DCs (black) were cultured for 5 days with expanded $CD27^+CD70^-$ Tregs (red), $CD27^-CD70^+$ Tregs pre-incubated with isotype mAb (blue) or $CD27^-CD70^+$ Tregs pre-incubated with anti-CD70 blocking mAb (green). Each data point is the average of 3 replicate wells in the suppression assay of each donor. Errors bars represent mean ± SEM. Statistical significance was assessed by Kruskal-Wallis test with Dunn's post-test, comparing cytokines levels between co-cultures containing $CD27^+CD70^-$ Tregs and $CD27^-CD70^+$ Tregs pre-incubated with isotype mAb and co-cultures of $CD27^-CD70^+$ Tregs pre-incubated with isotype mAb and $CD27^-CD70^+$ Tregs pre-incubated with anti-CD70 blocking mAb. Concentration of IL-4, IL-17F, IL-9, IL-21 and IL-22 cytokines were below the detection limit of the assay. ns= non-significant, *P<0.05.

Secondly, MLR suppression assays were designed within a transwell system. It consisted of a 96-well plate where Tresp and Tregs were physically separated within the receiver and the insert wells respectively by a membrane that prevents cell contact interactions, while allowing soluble factors to move between wells. Allo moDCs were added both to insert and receiver wells to stimulate Tregs and Tresp independently. Proliferation of Tresp was measured by VPD or CFSE dilution.

When DCs and $CD27^{-}CD70^{+}$ Tregs were placed in the insert and DCs and Tresp were placed in the receiver well (as depicted in Figure 4.13A), the pro-proliferative effect of $CD27^{-}CD70^{+}$ Tregs was completely abrogated (Figure 4.13B), demonstrating that a cognate interaction between $CD27^{-}CD70^{+}$ Tregs and Tresp was required for $CD70^{+}$ Treg-mediated proliferation.

As a control for the pro-proliferative effect of $CD27^{-}CD70^{+}$ Tregs, Tresp and allo moDCs alone or with the addition of $CD27^{-}CD70^{+}$ Tregs were cultured in the insert well so Tregs and Tresp can physically interact together (schematic view in Figure 4.13C). In this case, $CD27^{-}CD70^{+}$ Tregs substantially increased proliferation of $CD4^{+}$ and $CD8^{+}$ Tresp (Figure 4.13D).

It is possible that soluble factors are released subsequent to the Treg-Tcell cognate interaction and affect proliferation of Tresp, as it has been shown for IL-35 (*350*). To test this possibility, proliferation of Tresp in the receiver plate was studied when Tresp and allo moDCs with or without $CD27^{-}CD70^{+}$ Tregs were cultured in the insert plate. Still, this set up did not lead to the increased proliferation of Tresp in the receiver plate (Figure 4.13E).

Although $CD27^{-}CD70^{+}$ Tregs had the ability to secrete pro-inflammatory cytokines, our data demonstrate that the release of soluble factors by $CD27^{-}CD70^{+}$ Tregs did not play a major role in their pro-proliferative capacity *in vitro*. Instead, a cognate interaction between $CD27^{-}CD70^{+}$ Tregs with Tresp is required for Tregs to induce proliferation of T cells.

Figure 4.13

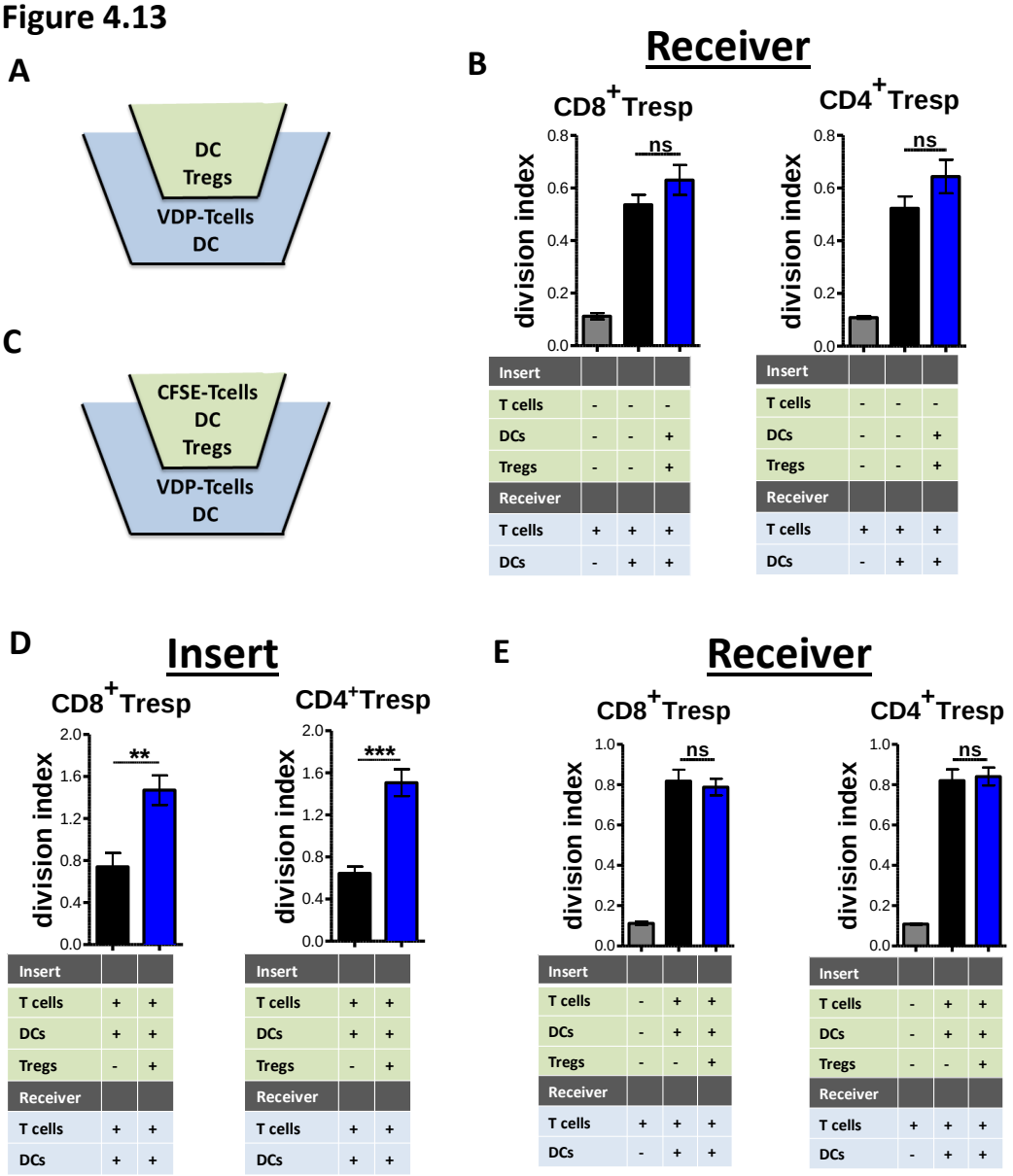

4.13. Increase in T cell proliferation by CD70$^+$ Tregs is cell contact dependent rather than cytokine mediated.

The requirement of cell interactions between Tregs and Tresp for the pro-inflammatory activity of 4 weeks expanded CD27$^-$CD70$^+$ Tregs was assessed using a transwell system.

(A-B) VPD-stained Tresp were cultured in the receiver plate with allogenic DCs. CD27$^-$CD70$^+$ Tregs were cultured in the insert plate with allogenic DCs. **(A)** Schematic representation of the experimental set up. **(B)** Proliferation of CD4$^+$ and CD8$^+$ Tresp studied by VDP dilution.

(C-E) VPD-labelled Tresp were cultured in the receiver plate with allogenic DCs. CD27$^-$CD70$^+$ Tregs were placed in the insert plate with allogenic DCs along with or without Tresp labelled with CFSE. **(C)** Schematic representation of the experimental set up. **(D)** Proliferation of CD4$^+$ and CD8$^+$ Tresp cultured in the insert plate was studied by measuring CFSE dilution. **(E)** Proliferation of CD4$^+$ and CD8$^+$ Tresp cultured in the receiver plate was studied by VPD dilution.

Proliferation of CD4$^+$ and CD8$^+$ Tresp was studied by flow cytometry measuring proliferation dye dilution and represented as division index. 1 blood donor out of 2 is shown. Error bars represent mean ± SD for 3 replicate wells. Statistical significance was assessed by unpaired t test. ns= non-significant, **P<0.01, ***P < 0.001.

4.3.9. Regulatory activity is not altered by blocking CD40L or PD-1 expressed on Tregs

In order to uncover additional mechanisms that may account for differential activity of CD27/CD70 Treg subsets, we analysed the expression of cell surface molecules associated to Treg activity by flow cytometry. Higher percentage of $CD27^{+}CD70^{-}$ Tregs expressed CD25 compared to $CD27^{-}CD70^{+}$ Tregs (Figure 4.14). Competition for IL-2 consumption has been described as a Treg-suppressive mechanism, depriving effector T cells of IL-2 (*192*). Moreover, CD25 expression is important for maintenance of the Treg signature (*351*). Expression of the ectoenzymes CD39 and CD73 has also been shown to be part of the diverse arsenal for Treg suppression (*176*). CD39 converts ATP to AMP, which is further metabolised to adenosine by CD73. Both, depletion of ATP and increased adenosine levels have and immune modulatory effect. ATP is usually secreted by damaged cells and acts as a pro-inflammatory molecule. On the other hand, adenosine inhibits T cell proliferation by upregulation of cytosolic cAMP and repression of IL-2 expression in Teffs (*176, 194*). No difference in CD39 or CD73 expression was observed between CD27/CD70 Treg subsets (Figure 4.14).

OX40, ICOS, 4-1BB and GITR are expressed by both activated Teff cells and Tregs. In Tconv cells, they act as co-stimulatory molecules promoting cell activation and proliferation, but their role in Tregs is less clear. Similar levels of 4-1BB, ICOS and GITR were observed between CD27/CD70 Treg subsets (Figure 4.14). 4-1BB also acts as a co-stimulatory molecule in Tregs promoting their proliferation (*67*). A tendency towards higher 4-1BB expression in $CD27^{-}CD70^{+}$ Tregs may relate with their increased survival capacity during resting (Figure 3.13D). ICOS expression differentiates 2 cell subsets of human thymic Tregs with differential suppressive machineries: $ICOS^{+}$ Tregs which express IL-10 and TGF-β and $ICOS^{-}$ Tregs which only secret TGF-β (*181*). Similar levels of ICOS expression correlates with no difference in IL-10 production between Treg

subsets (Figure 4.14 and Figure 4.10B). GITR is a marker of activated human Tregs and plays important roles in Treg differentiation and proliferation (*78*).

TIM-3, exhaustion marker for Tconv cells, identifies a specific cell subset of human Tregs with increased STAT3 function and an enhanced ability to suppress Th17 cell proliferation (*352*). Upregulation of TIM-3 in $CD27^{-}CD70^{+}$ Tregs (Figure 4.14), along with the acquisition of other Th17-like phenotypic characteristics such as overexpression of RORyt and IL-17, may indicate a specialisation of $CD27^{-}CD70^{+}$ Tregs towards Th17 regulation (not tested in our hands).

OX40 signalling prevents induction of murine Tregs from naive T cells in the periphery by inhibiting Foxp3 expression via BATF3/BATF and the AKT-mTOR pathway (*76, 77*), but if the same effect occurs in thymus-derived Tregs or in the human system is not known. We found an upregulation of OX40 expression in $CD27^{-}CD70^{+}$ Tregs compared to $CD27^{+}CD70^{-}$ Tregs (Figure 4.14), which could explain the downregulation of FOXP3 expression in the former subset (Figure 3.8B). However, our RNA-seq data did not point out differences in expression of BATF or BATF3.

PD-1/PD-L1 acts as a co-inhibitory receptor-ligand in Tconv, inducing exhaustion and cell dysfunction. The role of PD-1 in Treg activity is unclear. Some studies support a beneficial role for PD-1 in maintaining Treg stability and survival (*353, 354*), while others have shown that high PD-1 expression identifies a population of IFN-γ-producing Tregs with partial TSDR demethylation and impaired ability to suppress T cell proliferation (*355*).

In section 3.3.7 of Chapter 3, we described higher CD40L expression at mRNA and protein levels (Figure 3.14). It is well known that ligation of CD40 on APCs to CD40L on activated $CD4^{+}$ T cells increases antigen-presenting and co-stimulatory functions of APCs, which, subsequently induce proliferation of T cells (*63*). Importantly, a role for CD27/CD70 pathway has been established as a key signalling provided by activated DCs to transmit the help signal from $CD4^{+}$ T cells to $CD8^{+}$ T cells (*356, 357*). Given that $CD70^{+}$

Tregs also expressed higher levels of CD40L, it is plausible that CD40L may act along with CD70 in providing pro-inflammatory signals.

Figure 4.14

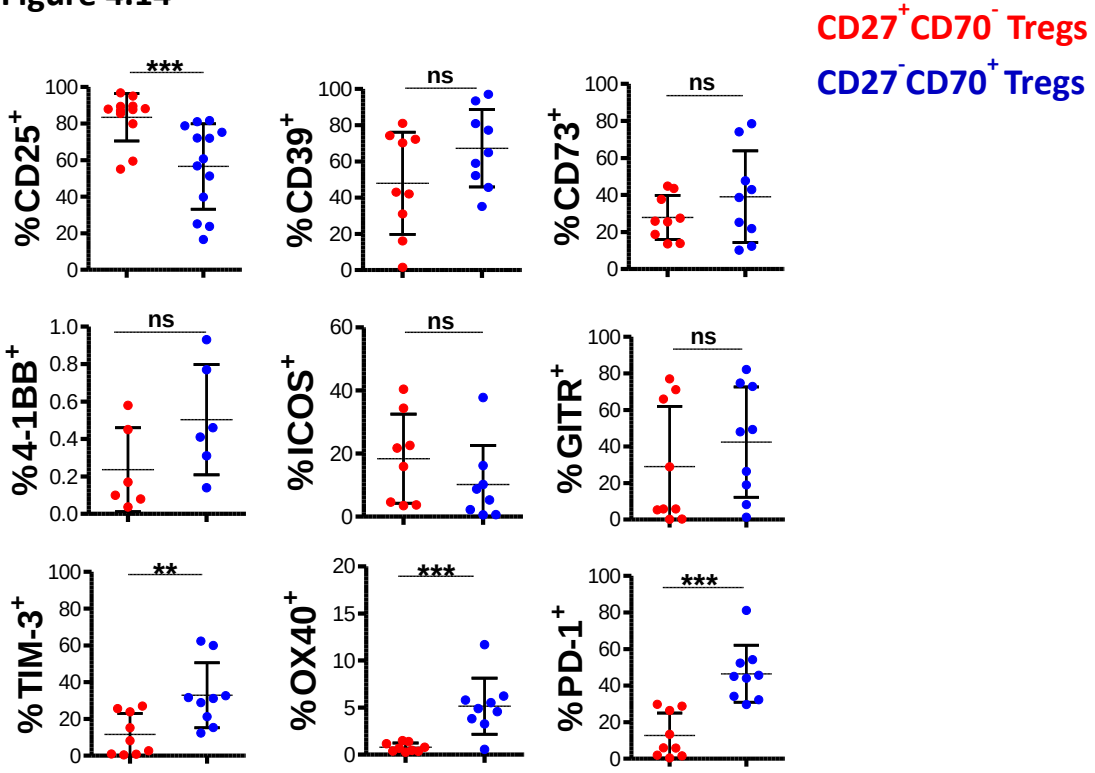

4.14. Expression of cell surface molecules in CD27$^+$CD70$^-$ Tregs and CD27$^-$CD70$^+$ Tregs.

Expression of different co-stimulatory, co-inhibitory and other Treg-associated functional markers were measured by flow cytometry in 4 weeks expanded CD27$^+$CD70$^-$ and CD27$^-$CD70$^+$ Tregs. N=6-13 independent donors. Statistical significance was assessed by Mann Whitney test. Errors bars represent mean ± SD. ns= non-significant, **P<0.01, ***P < 0.001.

We then studied whether PD-1 or CD40L expression on CD27$^-$CD70$^+$ Tregs might be relevant for their impaired suppressive activity and acquisition of pro-inflammatory functions. Higher CD40L and PD-1 expression in expanded CD27$^-$CD70$^+$ Tregs over CD27$^+$CD70$^-$Tregs was confirmed by flow cytometry (Figure 4.15A). Tregs were pre-incubated with anti-CD40L, anti-PD1 or anti-CD70 blocking mAbs before assessing Treg functionality within an *in vitro* MLR assay. While blocking CD70 on Tregs completely abrogated the pro-inflammatory effect of CD27$^-$CD70$^+$ Tregs, blockade of neither CD40L nor PD-1 affected Treg activity (Figure 4.15B). However, a positive control for the effect

of anti-PD-1 and anti-CD40L mAbs was not run in parallel and, therefore, their functional blocking activity cannot be ensured.

Figure 4.15

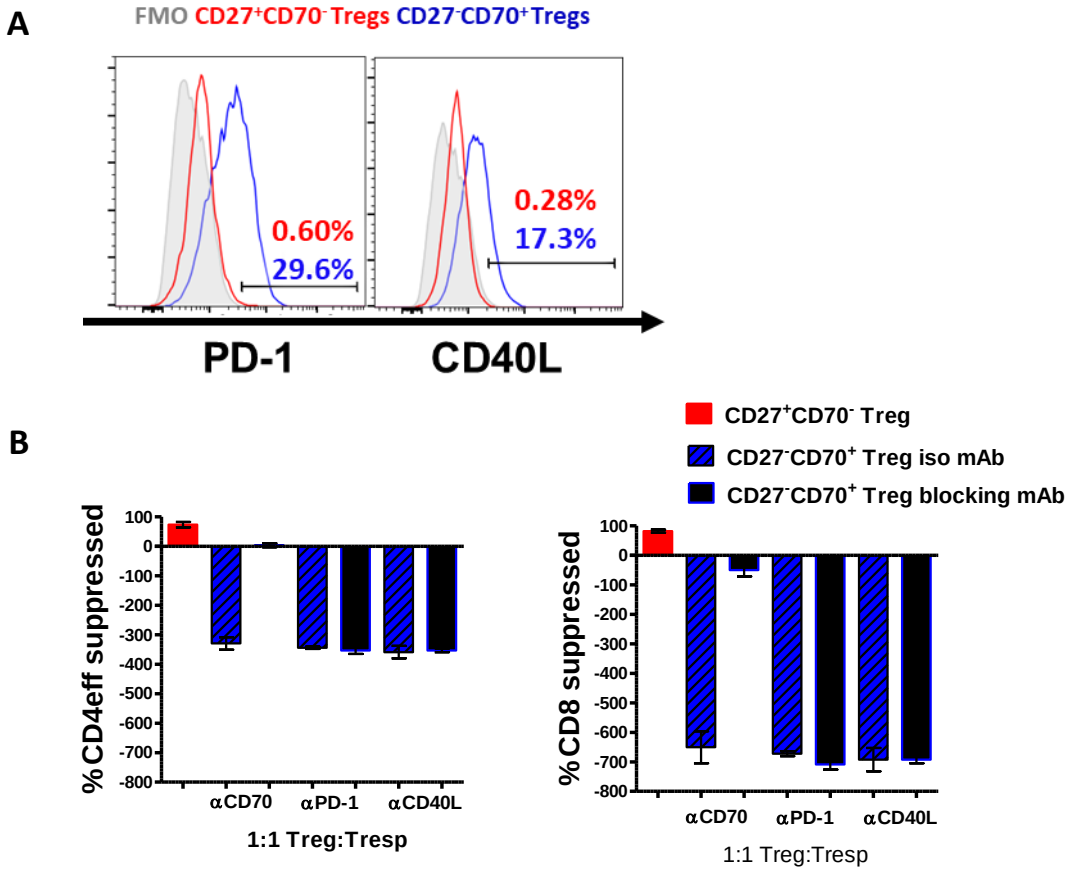

4.15. Treg regulatory activity is not altered by blocking CD40L or PD-1 expressed on Tregs.

(A) Percentage PD-1 and CD40L positive cells was measured within the 4 weeks expanded $CD27^+CD70^-$ (red) and $CD27^-CD70^+$ (blue) Treg cell product. Grey shadowed histogram represents fluorescence minus one control (FMO).

(B) 4 weeks expanded $CD27^-CD70^+$ Tregs were pre-incubated with anti-CD70, anti-PD1 or anti-CD40L blocking mAbs (or isotype matched antibodies) before assessing suppressive capacity in a MLR assay. VPD-stained $CD3^+CD25^-$ responder T cells (Tresp) were stimulated with allogenic monocyte derived- DCs in the presence or absence of Tregs. Tresp proliferation was studied by FACS analysing VDP dilution. Bar graphs represent percentage of suppression of $CD4^+$ and $CD8^+$ responder T cell proliferation by $CD27^+CD70^-$ Tregs (red) and antibody-incubated $CD27^-CD70^+$ Tregs (blue). One representative donor out of 2 (3 replicates wells in the suppression assay of each donor) is shown as mean ± SD.

4.4. Discussion

Having shown in Chapter 3 that $CD27^{+}CD70^{-}$ and $CD27^{-}CD70^{+}$ Treg phenotypes identify Treg subsets with differential functional stability upon long-term expansion, we hypothesised that targeting CD27/CD70 signalling might regulate Treg function. To test this hypothesis, we used previously validated blocking and stimulating monoclonal antibodies against human CD27 (*348, 349*).

Dhainaut *et al*. has recently proposed a potential mechanism to explain the superior potency of $CD27^{+}$ Tregs to suppress proliferation of Tconv cells; where $CD27^{+}$ Tregs ligate CD70 on DCs, resulting in endocytosis and degradation of the CD27/CD70 complex (*188*). Consequently, DCs are unable to provide CD70-mediated co-stimulation to Tresp (*188*). Similar regulation has been observed within the $CD27^{+}$ Tconv cell population, when CD27 is cleaved from $CD8^{+}$ T cells and binds to CD70 on APCs masking CD70 to provide co-stimulation to other T cells (*358*). Thus, competition of CD70 binding on APCs appears as a common mechanism to regulate CD27/CD70 co-stimulation. However, our experiments in which we blocked CD27 on Tregs and assessed their suppressive potency in a MLR test in the presence of DCs, showed no loss of Treg suppressive capacity (Figure 4.1). This indicates that CD27 does not play a non-redundant role in Treg mediated suppression. These findings are consistent with studies where Tregs from wild type and $CD27^{-/-}$ mice were shown to be equally able to suppress T cell proliferation *in vitro* (*70, 150*).

In the murine system, CD27 signalling rescues Treg from apoptosis during clonal deletion in the thymus and confer survival signals to mature Tregs by inhibiting the mitochondrial apoptosis pathway (*150*). Whether CD27 regulates survival in human mature Tregs is not clear. Enhanced potency of $CD27^{+}CD70^{-}$ Tregs could be explained if higher numbers of Tregs when CD27 signalling is stimulated, or lower Treg numbers when CD27 is blocked were observed after the suppression test. However, equal number of Tregs at the end of

the MLR suppression test was found in stimulating or blocking CD27 conditions, indicating that Treg survival or proliferation was not altered by CD27 signalling (Figure 4.1D).

Despite the apparent lack of function of CD27 in Treg activity, blocking CD27-CD70 interaction during a MLR suppression test by addition of anti-CD70 blocking mAb significantly increased Treg suppressive activity (Figure 4.2A,B). Since T cells and DCs can upregulate CD70 expression upon activation (*125*), in our MLR system anti-CD70 blocking mAb can potentially bind to $CD70^+$ Tregs and to activated Tresp and DCs. By staining with an anti-CD70 fluorophore-bound mAb competitive with anti-CD70 blocking mAb, we tracked which cells effectively bound anti-CD70 blocking mAb. We confirmed that $CD70^+$ Tregs had CD70 completely blocked, and anti-CD70 blocking mAb partially bound to activated $CD4^+$ and $CD8^+$ Tresp (Figure 4.2D).

Although not being statistically significant, CD70 blockade in co-cultures of Tresp and allogenic DCs tended to increase T cell proliferation (Figure 4.2A,B). Additional signals provided by DCs, either in the form of co-stimulation or soluble factors may explain these unexpected results. As for blocking CD70 in Tregs, addition of blocking anti-CD70 mAb to the suppression test did not affect Treg survival or proliferation (Figure 4.2C), suggesting a direct role for CD70 in the Treg suppressive mechanism. We, therefore, studied whether CD70 expressed on Tregs might be responsible for their impaired suppressive capacity. We found that blockade of CD70 on Tregs significantly impaired the pro-inflammatory activity of $CD27^-CD70^+$ Tregs (Figures 4.4A). Reinforcing our hypothesis for Treg instability, CD70 blockade completely restores suppressive capacity of 2 weeks expanded $CD27^-CD70^+$ Tregs (Figure 4.5B). However, after 4 weeks of expansion, the suppressive ability of $CD27^-CD70^+$ Tregs seemed to be hampered and, although their pro-inflammatory effect was abolished, restoration of suppressive capacity could not be assured in all donor tested (Figure 4.5A).

Interestingly, $CD70^+$ Tregs induced proliferation of $CD8^+$ T cells to a higher extend than $CD4^+$ T cells (Figure 4.6C,D). CD27 co-stimulation has been identified as the key pathway that delivers the help signal from $CD4^+$ Th cells to $CD8^+$ T cells (*356, 357, 359*). In this case, antigen presenting-DCs upregulate CD70 upon interaction with $CD4^+CD27^+$ T cells via CD40L-CD40 signalling, and transmit the help signal to trigger $CD8^+$ T cell response via the CD70-CD27 pathway (*356, 357*). Here, we show that Tregs induced $CD4^+$ and $CD8^+$ T cell proliferation via CD27-CD70 interaction also in the absence of DCs (Figure 4.8), demonstrating that $CD4^+CD70^+$ Tregs can provide direct co-stimulation to $CD4^+$ and $CD8^+$ T cells. Moreover, our data showing similar results of blocking CD70 on Tregs or CD27 on Tresp, in the presence or absence of DCs, demonstrate the specificity of the CD27/CD70 response (Figures 4.6 and 4.8D).

CD27 stimulation, either by ligation to an agonist anti-CD27 mAb or to CD70 expressed on APCs, is sufficient to induce T cell activation when combined with TCR stimulation (*71, 72, 349*). In agreement with these data, we show that $CD27^-CD70^+$ Tregs induce T cell proliferation only in the context of TCR stimulation, either by co-culture with allogenic DCs or by activation with anti-CD3 agonist mAb (Figure 4.9). Although previous studies have reported an inhibitory role for CD70 expression on T cells (*122, 123*), in our system *in vitro* expanded $CD4^+CD27^-CD70^+$ conventional T cells also induced T cell proliferation in TCR stimulated Tresp (Figure 4.9). However, further experiments are required to elucidate if increase in proliferation driven by CD70-expressing Tconv cells is due to CD27/CD70 signalling or due to other means such as production of pro-inflammatory cytokines (e.g. IL-2).

While having a substantial effect, blocking CD27-CD70 interaction did not completely impede the pro-inflammatory effect of $CD27^-CD70^+$ Tregs (Figure 4.8D), suggesting further pro-inflammatory mechanisms. In Chapter 3, we identified differential transcriptional expression of genes that regulate cytokine signalling pathways between CD27/CD70 Treg subsets (Figure 3.13A). In this Chapter, we have shown a pro-

inflammatory cytokine profile, both at mRNA and protein levels, specifically in the $CD27^-$ $CD70^+$ Treg population (Figure 4.10). Although CD27 signalling can influence polarisation of $CD4^+$ T cells and cytokine expression (*119, 312, 338-340*), whether CD27/CD70 signalling can regulate the cytokine profile of Tregs is not known.

Despite differences in transcription, we found similar levels of IFN-γ and IL-10 in CD27/CD70 Treg subsets (Figure 4.10). IL-17A, key effector cytokine for Th17 cell function, was specifically expressed by $CD27^-CD70^+$ Tregs (Figure 4.10). In this regard, Coquet *et al.* have shown that CD27 intracellular signalling hampers Th17 effector cell differentiation by epigenetically silencing *il17a* and *ccr6* gene expression via the c-Jun N-terminal kinase (JNK) pathway in mouse T cells (*312*). Although these results still remained to be validated in humans, it raises an interesting question whether CD27/CD70 signalling may influence the cytokine profile of human Tregs. Since CD70 expression on Tregs appears as a molecular switch activating pro-inflammatory functions, and providing that CD70 can transduce intracellular signalling itself in human T cells (*360*), we evaluated the role of CD70 in Treg polarisation. The concentration of none of the cytokines tested, including IL-17A and IL-10, was altered by blocking CD70 during Treg activation (Figure 4.11), indicating that CD70 does not influence their cytokine profile.

Tregs have multiple mechanisms to suppress T cell activation and proliferation either by cell-contact interactions or by the release of soluble factors (*183, 251*). The skewed cytokine profile towards a pro-inflammatory phenotype of $CD27^-CD70^+$ Tregs could plausibly contribute to a pro-inflammatory milieu that impedes immune regulation and promotes inflammation. However, although CD70 blockade in Tregs inhibited the pro-stimulatory effect of $CD27^-CD70^+$ Tregs, levels of cytokines during the MLR tests were not altered (Figure 4.12). These results, together with our co-culture assays in a transwell system (Figure 4.13) indicate that cytokines do not play a significant role in the pro-proliferative effect of $CD27^-CD70^+$ Tregs *in vitro*. Instead $CD27^-CD70^+$ Tregs require cell-contact interactions with Tresp to induce proliferation. Further experiments are needed to

clarify whether cytokine production may play a more important role in the function of Tregs *in vivo*.

Then we studied cell surface expression of other functional markers that may contribute to the pro-inflammatory effect of $CD27^{-}CD70^{+}$ Tregs (Figure 4.14), and selected CD40L and PD-1 proteins for further functional analysis. Despite that the literature provides the evidence for potential pro-inflammatory activity (*63*) or dysfunctional suppression (*355*), blockade of neither of these markers was able to impair the pro-inflammatory effect of $CD27^{-}CD70^{+}$ Tregs (Figure 4.15B). It is likely that differences in CD40L and PD-1 expression represent different activation stages of the cell subsets.

Given the data presented in this chapter, we propose that CD70, rather than CD27, has an active role in regulating Treg suppressive activity by providing co-stimulatory signals to Tresp. So far, the pro-inflammatory effect of the CD27-CD70 pathway has been identified when APCs deliver co-stimulation via CD70 to CD27-expressing T cells (*356, 357, 359*). Importantly, we have shown here, for first time to our knowledge, that $CD70^{+}$ Tregs can provide sufficient co-stimulatory signals to induce T cell activation even in the absence of APCs.

Chapter 5:
Generation of a potent and stable regulatory T cell product for clinical use based on lack of CD70 expression

5.1. Introduction

The therapeutic potential of *in vitro* expanded polyclonal Tregs to prevent rejection in humanised mouse models has been well documented (*303-306*). The challenge in translating this therapy into the clinic is to generate sufficient numbers of Tregs, while maintaining potent and stable suppressive properties. Suppressive function and stability of the expanded cell product is crucial for Treg therapy in solid organ transplantation, since infusion of non-suppressive or unstable cells has the potential to exacerbate the allogenic immune response and lead to organ damage. For adoptive transfer, Tregs are isolated from peripheral blood of patients and expanded *in vitro* to generate sufficient numbers before being re-infused into the patient. The efficacy of the therapy could be improved by enhancing specificity, stability and function of Tregs by gene editing or modifying *ex vivo* expansion conditions.

Diverse protocols for large-scale production of Tregs for clinical therapy have been developed and vary according to good manufacturing practice (GMP) requirements in different countries. The first obstacle when considering Tregs for clinical use is the isolation of an optimal Treg population using GMP-compatible methods. To date, clinical protocols predominantly use magnetic bead sorting for isolation of $CD4^+CD25^+$ cells. However, the purity of the isolated population is not as high as desirable and usually contains contaminating Teff cells expressing CD25. There is a wealth of data showing that the addition of chemical agents such as rapamycin during Treg expansion culture favours expansion of Tregs relative to Teff contaminants (*361-363*). Still, in order to

achieve maximal efficacy, billions of Tregs might need to be administered at multiple time points. Efforts are now focus on finding new strategies to isolate more potent Treg subsets or to enhance suppressive capacity of expanded Tregs so fewer Tregs will need to be infused.

Isolation by flow sorting (FACS) has the advantage of selecting Tregs based on several surface markers and differential expression intensities. However, since cell separation does not occur in a neither closed nor single use system, sterility is a major concern to agree with GMP regulations. Nonetheless, in the United States and Poland, Phase I trials are ongoing using non-GMP-compatible cell sorters (BD FACS Aria, California, USA) (*364*). Moreover, recent improvements in the biosafety of cell sorter devices such as the MACS-Quant Tyto (Miltenyi Biotec, Bisley, UK) and the BD Influx has facilitated their use in GMP environments and they are currently being tested for Treg therapies in the UK and Germany respectively. Selection of $CD4^+CD25^+CD127^-$ Tregs by FACS sorting ensures high Treg purity of the starting material (*167, 168*). Yet, plasticity within the $CD4^+CD25^+CD127^-$ Treg population still remains problematic (*307, 308*).

Genetic engineering of Tregs during *in vitro* expansion could be used to target molecules that regulate Treg functionality; disabling pathways that lead to instability or forcing the expression of molecules that enhance Treg function. In this regard, antigen specific Tregs have been shown to be more potent than polyclonal-expanded Tregs on a per-cell basis (*283, 299, 300*). Expression of transgenic TCRs or chimeric antigen receptor (CARs) to direct Treg antigen specificity has gained special interest in recent years, and CAR-Tregs are entering clinical trials (*298, 301, 302*). Moreover, overexpression of FOXP3 for enhancing suppressive capacity has also been addressed (*365*). CRISPR (clustered, regularly interspaced, short palindromic repeats)/Cas9 (CRISPR-associated protein 9) has emerged as a new genome editing tool that appears as more efficient, faster, safer and cheaper than previous techniques. Hence, CRISPR/Cas9 not only represents a relatively easy and inexpensive research tool to study gene function, but also can be used

for cell-based immunotherapies. In fact, pioneering clinical trials using CRISPR/Cas9 in T cells have just started and multiple strategies are currently ongoing to import this technique into Treg therapy.

Following our discovery that Tregs can provide co-stimulatory signals via expression of CD70, we were interested in determining whether a CD70-negative Treg cell product would show enhanced suppressive potency compared to the current Treg therapy. In this chapter, we explored 2 methods of generating a $CD70^-$ Treg cell product: depletion of $CD70^+$ cells by magnetic bead cell sorting in cell cultures expanded according to a GMP-like protocol or genetic engineering of Tregs using CRISPR/Cas9 technology to knockout CD70.

5.2. Objectives and hypotheses

Objective 1: To explore the feasibility of generating a human $CD70^-$ Treg cell product in compliance with current good manufacturing practices (GMP) in the UK.

Hypothesis 1: $CD70^-$ Treg cell product, obtained by magnetic cell isolation and culture in the presence of rapamycin, will exhibit more potent suppressive capacity than the total Treg product.

Objective 2: To optimise a protocol for generating a CRISPR/Cas9 mediated-$CD70^-$ Treg cell product.

Hypothesis 1: Human Tregs genetically engineered to do not express CD70 will exhibit more potent and stable suppressive capacity than wild-type Tregs upon prolonged *in vitro* expansion.

5.3. Results

5.3.1. Rapamycin preserves the CD27^{+}CD70^{-}FOXP3^{+} suppressive phenotype during a GMP-compatible Treg expansion protocol

In order to produce a Treg product in accordance with GMP requirements in the UK, we followed a protocol recently described by Fraser *et al*., with minor modifications to adapt it for our laboratory equipment (as depicted in Figure 5.1A) (*294*). Tregs were magnetically isolated from PBMCs by depletion of CD8^{+} cells and enrichment of CD25^{+} cells. Isolated CD8^{-}CD25^{+} cells were cultured with anti-CD3/anti-CD28 coated beads in the presence of rhIL-2 (500 U/ml) for 3 expansion cycles (36 days in total). Rapamycin (100nM) or control DMSO was added during cell expansion. In order to generate a CD70-depleted cell product, Tregs were separated into CD70^{+} and CD70^{-} cells after 2 cycles of expansion using anti-CD70 PE mAb and anti-PE magnetic beads. At the end of the 3rd expansion cycle, the phenotype and suppressive activity of unsorted, CD70^{-} and CD70^{+} cells were analysed (Figure 5.1A).

The addition of rapamycin had a drastic effect on the phenotype and expansion of Tregs. In comparison to the control culture in DMSO, the presence of rapamycin led to 8 times lower fold expansion over 36-days expansion culture (6974 ± 1928 and 878 ± 647 in DMSO and rapamycin respectively, mean ± SD) (Figure 5.1B). The major effect of rapamycin on cell proliferation was observed during the first 2 expansion cycles; 424.0 ± 1071 fold expansion in DMSO and 65.6 ± 40.5 in rapamycin (mean ± SD) (Figure 5.1C), while no significant difference was observed during the 3rd expansion cycle (Figure 5.1D). Although not statistically significant, CD70^{-} Tregs tended to proliferate more than CD70^{+} Tregs during the 3rd expansion cycle, and fold expansion was substantially diminished in the presence of rapamycin compared to DMSO in both populations (Figure 5.1E).

Figure 5.1

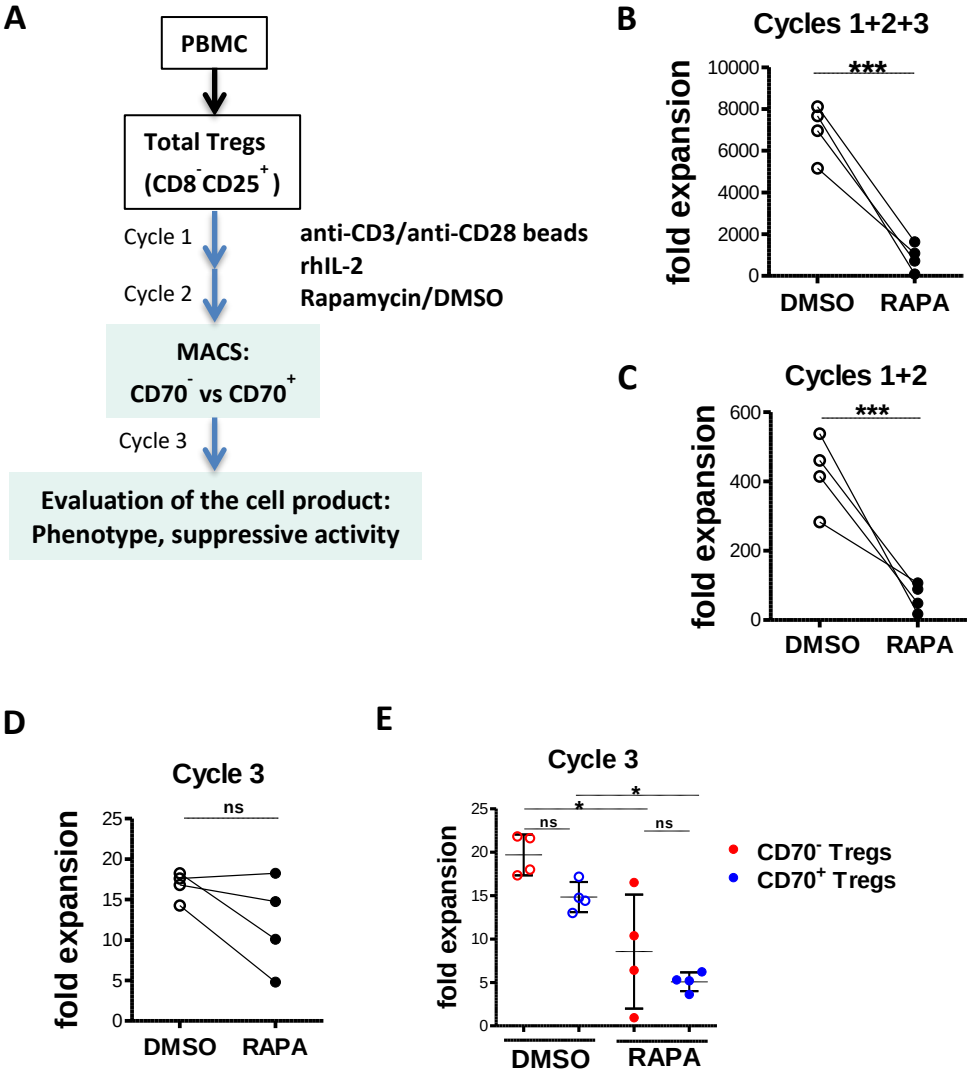

5.1. Rapamycin reduces proliferation capacity of CD4⁺CD25⁺ cells.

(A) Schematic representation of the GMP-like protocol for the isolation and expansion of Tregs. CD4⁺CD25⁺ Tregs were isolated by depletion of CD8⁺ cells and enrichment of CD25⁺ cells by magnetic beads sorting. Tregs were stimulated with anti-CD3/anti-CD28 coated beads in a 3:1 bead:cell ratio. Rapamycin (100nM) was added at the beginning of the culture, whereas rhIL-2 (500 U/m) was added after 3 days. Both rapamycin and rhIL-2 were replenished every 2-3 days. Cells were re-stimulated every 12 days adding new activation beads in a 1 bead :1 cell ratio. Prior to each re-stimulation, cells were rested for 2 days in the absence of rhIL-2. Tregs were separated into CD70⁺ and CD70⁻ cells after 2 cycles of expansion using anti-CD70 PE mAb and anti-PE magnetic beads. Phenotype and functional activity were assessed after 36 days of culture.

(B-D) Fold expansion of unsorted Tregs was calculated **(B)** over 36 days of expansion, **(C)** during cycles 1 and 2 or **(D)** during cycle 3 when cultured in the presence of DMSO or rapamycin. Statistical significance was calculated using an unpaired t test.

(E) Fold expansion during cycle 3 was calculated in CD70⁻ and CD70⁺ Tregs in the presence of DMSO or rapamycin. Statistical analysis was performed using one-way ANOVA with Bonferroni post-test. Error bars shown mean ± SD.

ns= non-significant, *P<0.05, ***P < 0.001.

In unsorted Tregs, the addition of rapamycin leads to a cell product with low CD70 and high CD27 and FOXP3 expression in comparison to DMSO cultures (Figure 5.2A; black columns). In CD70-depleted Tregs, CD70 expression was upregulated when cells were expanded in DMSO but not in rapamycin, whereas high CD70 expression was also maintained in $CD70^+$ Tregs cultured in rapamycin (Figure 5.2A). Rapamycin preserved CD27 expression in both $CD70^-$ and $CD70^+$ Treg products; however, CD27 levels were significantly higher in $CD70^-$ Tregs than $CD70^+$ Tregs (Figure 5.2A). It should be pointed out that kinetic changes of CD27/CD70 might be confuded by the greater outgrowth of effector T cells in DMSO control condition (>50% $FOXP3^-$ cells) compared with culture in the presence of rapamycin.

Rapamycin treatment altered Treg phenotype beyond CD27, CD70 and FOXP3. Rapamycin-expanded Tregs showed lower expression of CD40L and TIM-3 but higher CD62L levels compared to DMSO-expanded cells (Figure 5.2B). Similar CD25, CTLA-4, CD39 and PD-1 expression was observed between DMSO and rapamycin-treated cells (Figure 5.2B). No phenotypic difference in FOXP3, CD40L, TIM-3, CD62L, CD25, CTLA-4, CD39 or PD-1 was detected between unsorted, $CD70^-$ and $CD70^+$ Treg cell products (Figure 5.2A,B). Potential impurities within the expanded cell product may contain non-viable cells, neutrophils, B cells, NK cells, $CD8^+$ T cells, monocytes, red blood cells and platelets. For clinical therapy, contamination of erythrocytes and platelets is unlikely to pose any safety issues, so they are not routinely controlled. Previous analysis has shown that few non-T cells remain in the resulting cell product after expansion; consequently, the major non-Treg impurity is $CD8^+$ T cells. Percentages of $CD8^+$ cells were below 2% in all populations and conditions at the end of the 36-day expansion period (Figure 5.2C), well within the limit (10%) of release criteria for the ONE Study clinical trial.

Figure 5.2

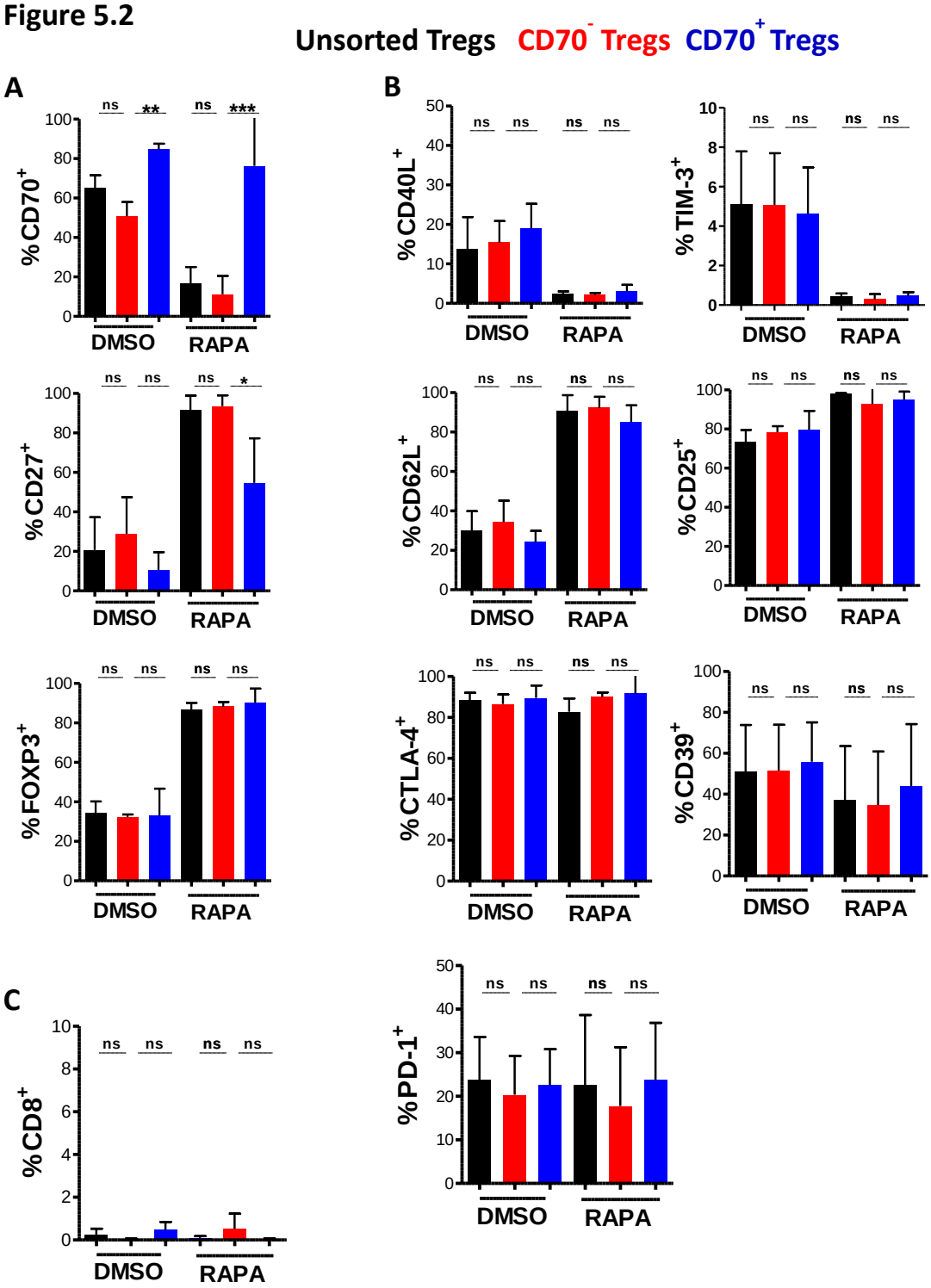

5.2. Rapamycin preserves the CD27$^+$CD70$^-$FOXP3$^+$ suppressive phenotype during a GMP-compatible Treg expansion protocol.

(A-C) CD70, CD27, FOXP3, CD40L, TIM-3, CD62L, CD25, CD39, CTLA-4, PD-1 and CD8 expression was analysed at the end of the expansion culture (day 36) described in Figure 5.1A in unsorted, CD70$^+$ and CD70$^-$ isolated Tregs. Data represent mean ± SD of 4 independent donors. Statistical significance was calculated by one-way ANOVA with Bonferroni post-test. ns= non-significant, *P<0.05, **P<0.01, ***P < 0.001.

We next wondered if the effect of rapamycin on Treg phenotype would be maintained if the treatment was discontinued. To investigate this question, after 3 cycles of expansion cells were cultured for 7 further days (cycle 4) switching between DMSO and rapamycin conditions (Figure 5.3A). Although not being statistically significant, a trend towards upregulation of CD70 and downregulation of CD27 and CD25 could be observed when rapamycin-expanded Tregs were cultured in the absence of the drug, which correlated with significant downregulation of FOXP3 expression (Figure 5.3B). Interestingly, when DMSO-expanded Tregs were treated with rapamycin, an opposite trend was observed; with CD70 being downregulated and CD27 and CD25 upregulated (Figure 5.3B). However, to confirm these observations, it would be necessary to study the effect of rapamycin withdrawal in more donors and at later time points.

Figure 5.3

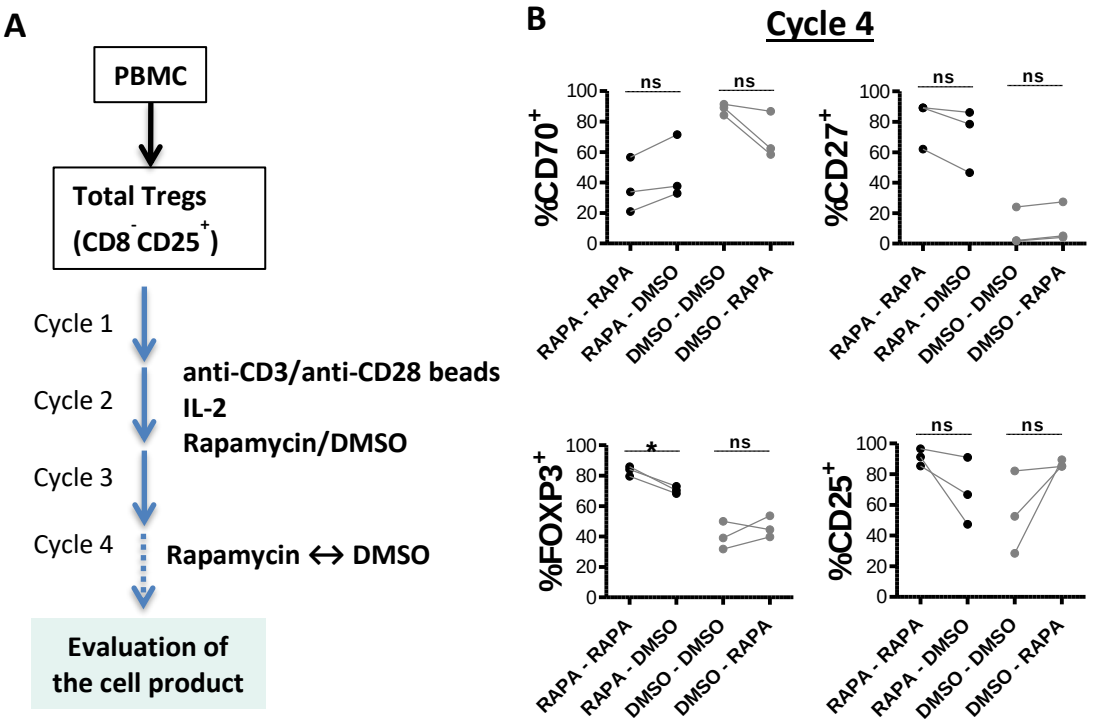

5.3. Treg phenotype after rapamycin withdrawal.

Analysis of phenotypic stability in Tregs after an additional 1-week culture switching rapamycin and DMO treatments. **(A)** Schematic representation of the expansion protocol. **(B)** Percentage of CD27, CD70, FOXP3 and CD25. One-way ANOVA with Bonferroni post-test for multiple comparisons was conducted. ns= non-significant, *P<0.05.

5.3.2. Depletion of $CD70^+$ cells enhances suppressive potency of the Treg product only in certain donors

In order to improve the current Treg cellular therapy, it is imperative to ensure that the CD70-depleted Treg product shows enhanced suppressive capacity compared to unsorted Tregs.

We studied unsorted, $CD70^-$ and $CD70^+$ Treg cell products generated in the presence of DMSO or rapamycin as depicted in Figure 5.1A for their capacity to suppress T cell proliferation in MLR suppression test. All Treg subpopulations generated in the presence of rapamycin showed superior suppressive potency than DMSO-treated Tregs (Figure 5.4A). In DMSO-expanded Tregs, $CD70^-$ Tregs were more suppressive than unsorted or $CD70^+$ Tregs. In rapamycin-expanded Tregs, $CD70^-$ Tregs appeared as suppressive as unsorted Tregs (Figure 5.4B). $CD70^-$ Tregs were more suppressive than $CD70^+$ Tregs only at low Treg:Tresp ratios (Figure 5.4B).

An alternative *in vitro* suppression test, similar to the assay used in the ONE Study clinical trial to evaluate suppressive potency of the clinical Treg product, was also performed. In this case, we compared the ability of unsorted and CD70-depleted Treg products to suppress the proliferation of co-cultured CFSE-labelled T responder cells stimulated with anti-CD3/anti-CD28 beads. There was no significant difference between the potency of the Treg subsets (Figure 5.4C).

Figure 5.4

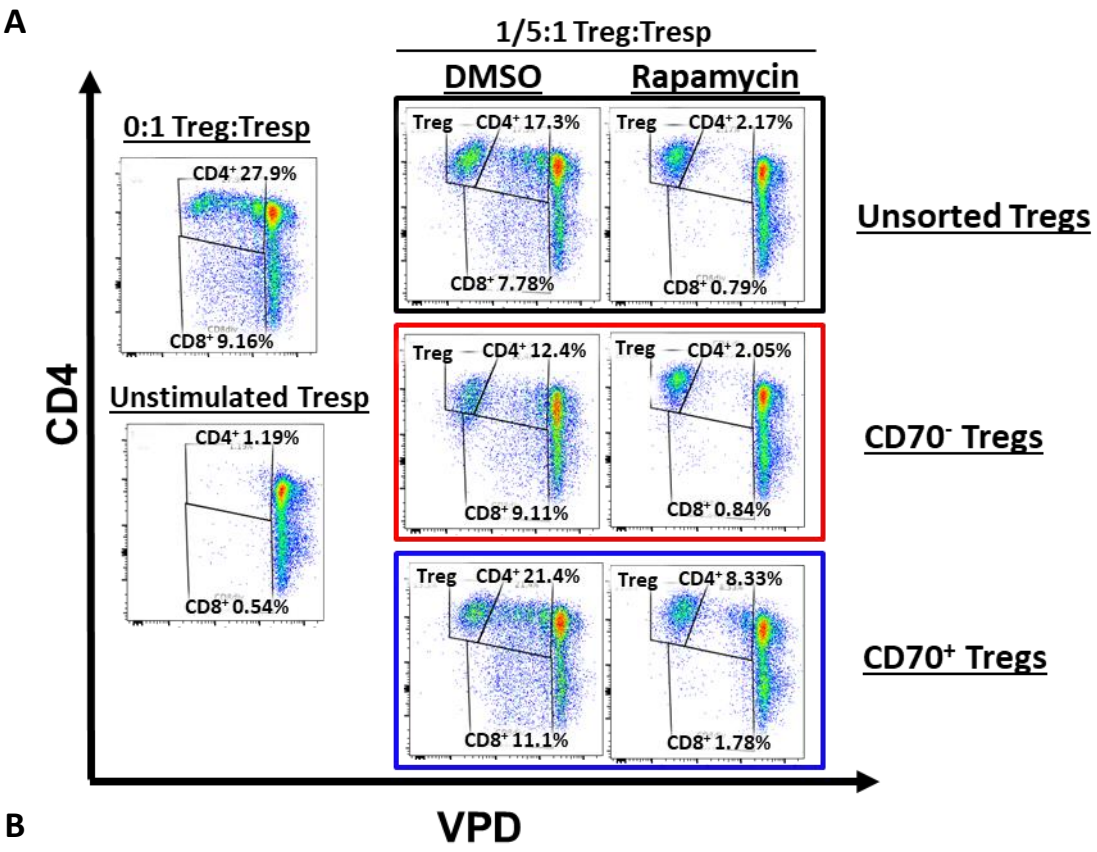
A
1/5:1 Treg:Tresp
DMSO
Rapamycin
0:1 Treg:Tresp
CD4+ 27.9%
CD8+ 9.16%
Unstimulated Tresp
CD4+ 1.19%
CD8+ 0.54%
Treg CD4+ 17.3%
CD8+ 7.78%
Treg CD4+ 2.17%
CD8+ 0.79%
Unsorted Tregs
Treg CD4+ 12.4%
CD8+ 9.11%
Treg CD4+ 2.05%
CD8+ 0.84%
CD70- Tregs
Treg CD4+ 21.4%
CD8+ 11.1%
Treg CD4+ 8.33%
CD8+ 1.78%
CD70+ Tregs
CD4
VPD

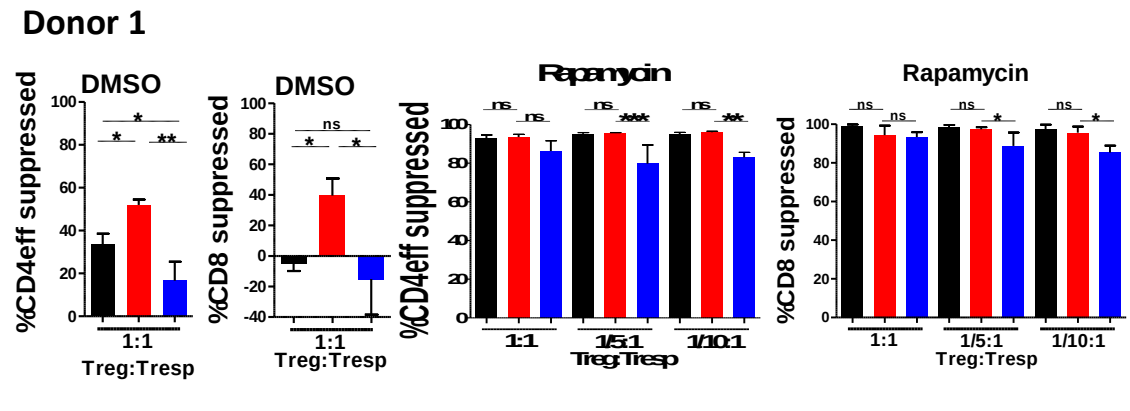
B
Donor 1
DMSO
%CD4eff suppressed
%CD8 suppressed
Rapamycin
1:1
1/5:1
1/10:1
Treg:Tresp

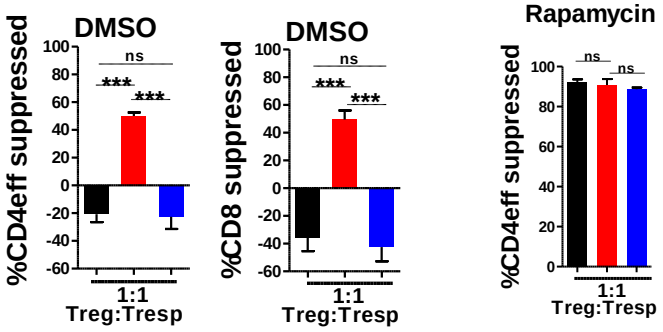
Donor 2
DMSO
Rapamycin
%CD4eff suppressed
%CD8 suppressed
1:1
Treg:Tresp

Figure 5.4

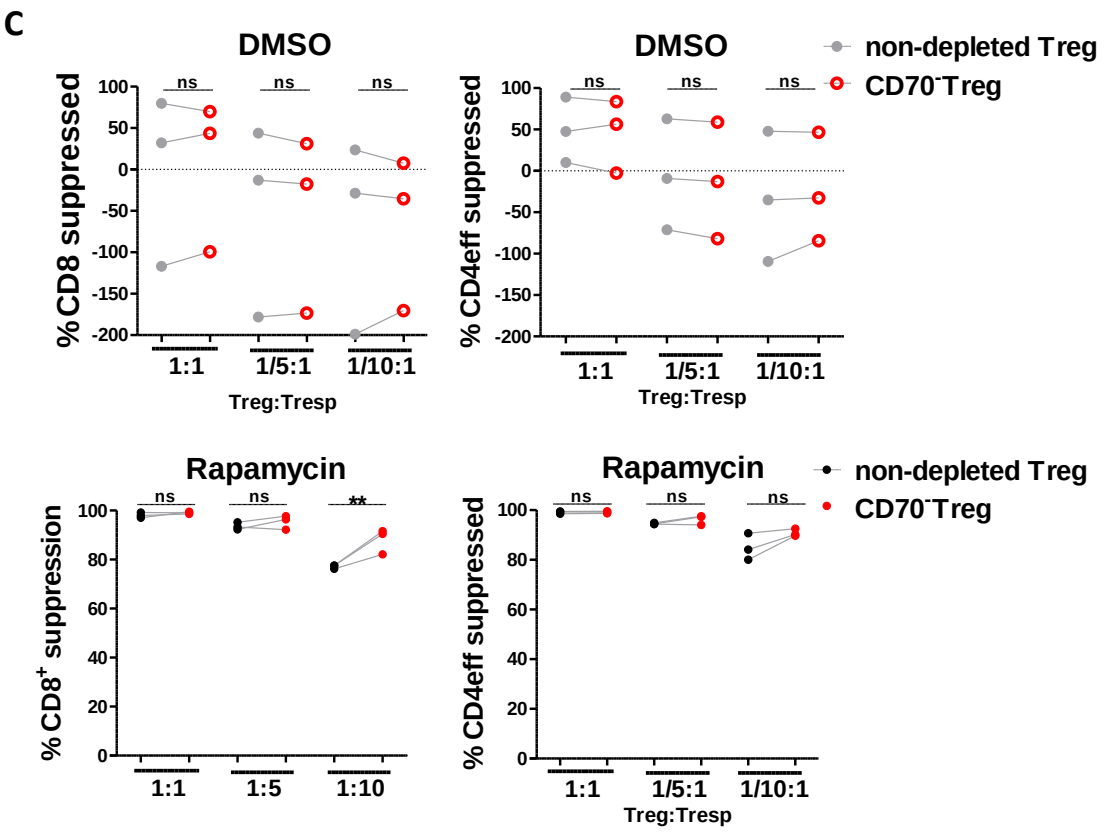

5.4. Depletion of CD70$^+$ cells after 2 cycles of expansion enhances suppressive potency of the DMSO-expanded Tregs but not of rapamycin-cultured Tregs.

(A-B) Suppressive capacity of unsorted, CD70$^-$ and CD70$^+$ isolated Tregs obtained in the presence of DMSO or rapamycin as described in Figure 5.1A was assessed in an *in vitro* MLR suppression test using CD3$^+$CD25$^-$ responder T cells (Tresp) labelled with VPD and stimulated with allogenic DCs (1 DC:5 Tresp). **(A)** Proliferation of CD4$^+$ and CD8$^+$ Tresp is shown by VPD dilution. **(B)** Percentage of suppression of CD8$^+$ and CD4$^+$ Tresp proliferation was calculated based on division index by VPD dilution. Error bars show mean ± SD for 3 replicates wells in the suppression test of 1 blood donor. 2 independent donors are shown.

(C) Suppressive capacity of unsorted and CD70 depleted Treg products obtained in the presence of (top panel) DMSO or (bottom panel) rapamycin as described in Figure 5.1A was assessed in an *in vitro* suppression test using CD3$^+$CD25$^-$ responder T cells (Tresp) labelled with CFSE and stimulated with anti-CD3/anti-CD28 coated beads (bead:cell ratio 1:42). CFSE dilution was studied by flow cytometry after 5 days of expansion and percentage of suppression of CD8$^+$ and CD4$^+$ Tresp proliferation was calculated based on division index. Each dot represents the average of 3 replicate wells in the suppression assay of 3 independent donors. Statistical significance was calculated by one way-ANOVA with Bonferroni post-test for multiple comparisons.

ns= non-significant, *P<0.05, **P<0.01, ***P < 0.001.

Next, we tested the effect of CD70 depletion at the end of the GMP-like expansion protocol (day 36) (Figure 5.5A). CD70 depletion resulted in a $CD27^{+}CD70^{-}$ cell product in rapamycin-expanded Tregs but in a mixed CD27/CD70 population in DMSO-expanded Tregs (Figure 5.5B).

Suppressive potency of unsorted and CD70-depleted Tregs was assessed in a MLR suppression test. DMSO-expanded Tregs showed impaired suppressive capacity. Interestingly, unsorted but not $CD70^{-}$ Tregs had pro-inflammatory activity and increased T cell proliferation (Figure 5.5C). When expanded in rapamycin, unsorted and $CD70^{-}$ Tregs showed potent suppressive capacity at high Treg:Tresp ratio (Figure 5.5D; left plots). However, at a lower Treg:Tresp ratio, unsorted Tregs from Donor 1 were not able to suppress T cell proliferation, whereas unsorted Tregs from Donor 2 were highly suppressive (Figure 5.5D; right plots). Treg suppressive potency correlated with proportion of $CD27^{-}CD70^{+}$ cells within the cell product of each donor: Donor 1 had 11.6% $CD27^{-}CD70^{+}$ cells, while Donor 2 had 4.01% $CD27^{-}CD70^{+}$ cells (Figure 5.5B). Importantly, depletion of $CD70^{+}$ cells in Donor 1 resulted in more potent cell product (Figure 5.5D; right plots).

These results reveal donor heterogeneity in CD27/CD70 expression upon expansion. Among those donors that downregulate CD27 and upregulate CD70, depletion of CD70 may improve the current protocol for Treg expansion.

Figure 5.5

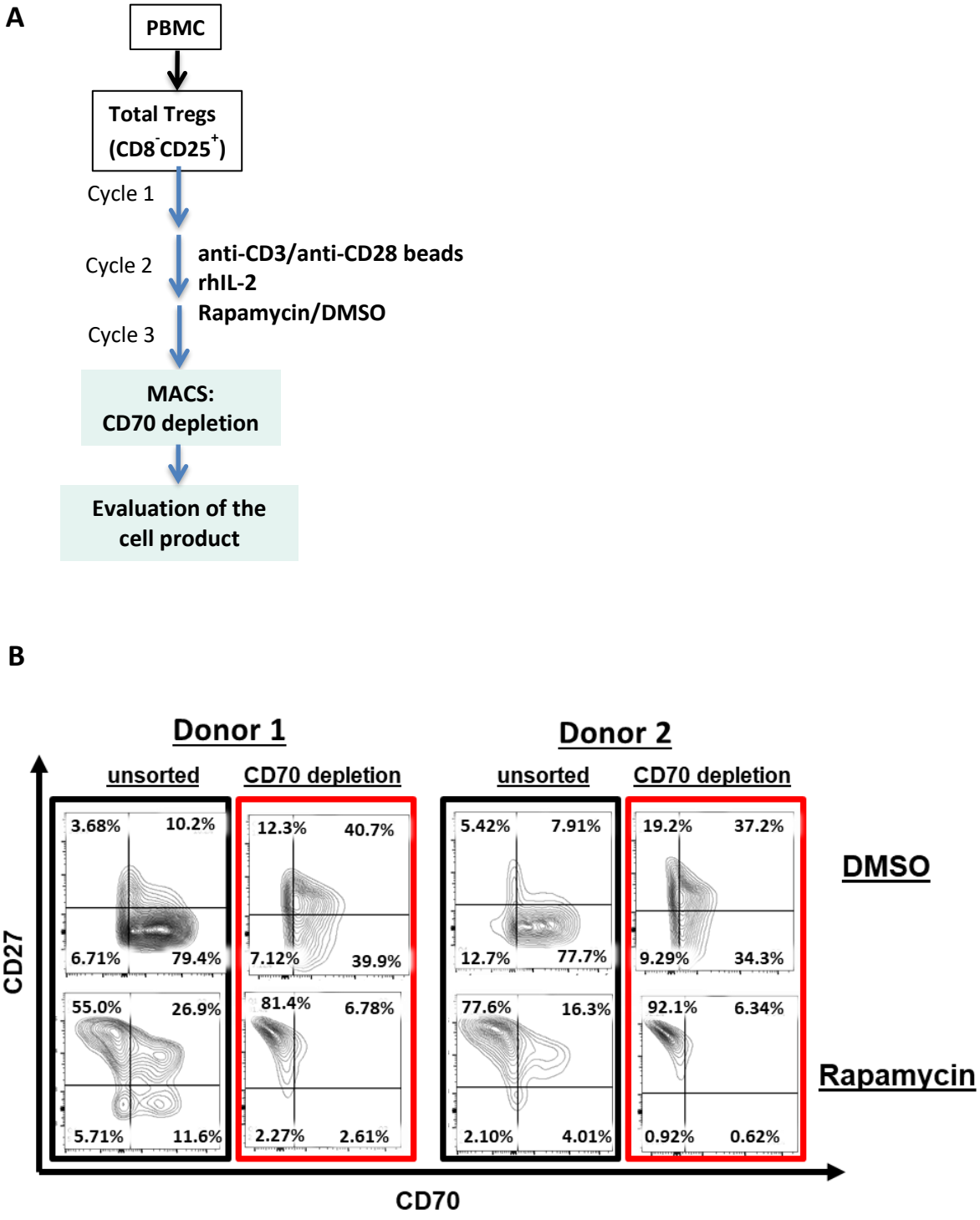
A
PBMC
Total Tregs
(CD8-CD25+)
Cycle 1
Cycle 2
anti-CD3/anti-CD28 beads
rhIL-2
Cycle 3
Rapamycin/DMSO
MACS:
CD70 depletion
Evaluation of the
cell product
B
Donor 1
Donor 2
unsorted
CD70 depletion
unsorted
CD70 depletion
3.68%
10.2%
6.71%
79.4%
12.3%
40.7%
7.12%
39.9%
5.42%
7.91%
12.7%
77.7%
19.2%
37.2%
9.29%
34.3%
DMSO
55.0%
26.9%
5.71%
11.6%
81.4%
6.78%
2.27%
2.61%
77.6%
16.3%
2.10%
4.01%
92.1%
6.34%
0.92%
0.62%
Rapamycin
CD27
CD70

Figure 5.5

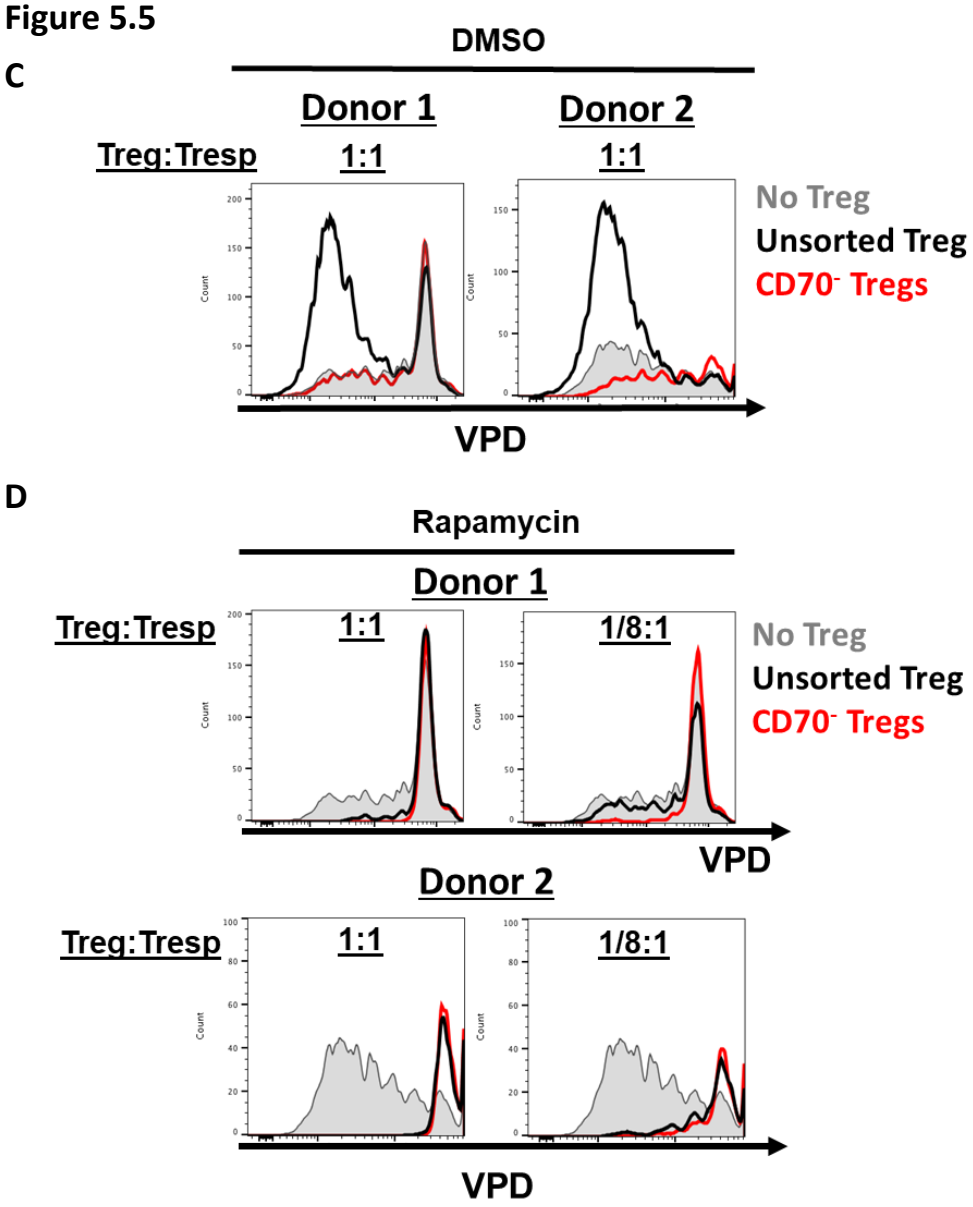

5.5. Depletion of CD70$^+$ cells at the end of the expansion enhances suppressive potency of the Treg product in donors that upregulate CD70.

(A) Schematic representation of an alternative GMP-like protocol for the generation of CD70$^-$ Tregs. CD4$^+$CD25$^+$ Tregs were isolated by depletion of CD8$^+$ cells and enrichment of CD25$^+$ cells by magnetic beads sorting. Tregs were stimulated with anti-CD3/anti-CD28 coated beads in a 3:1 bead:cell ratio. Rapamycin (100nM) or DMSO was added at the beginning of the culture, whereas IL-2 (500 U/m) was added after 3 days. Both rapamycin/DMSO and IL-2 were replenished every 2-3 days, and cells were rested for 2 days prior to re-stimulation. Cells were re-stimulated every 12 days adding new activation beads in a 1 bead : 1 cell ratio. At day 36 days of culture, CD70$^+$ cells were depleted by magnetic sorting. Phenotype and functional activity were assessed in unsorted and CD70-depleted Treg cell products.

(B) CD27 and CD70 phenotype was studied in unsorted and CD70-depleted Tregs expanded in DMSO or rapamycin. 2 donors are displayed.

(C-D) Suppressive capacity of unsorted and CD70-depleted Tregs was assessed *in vitro* as a decrease in proliferation of VPD-labelled CD3$^+$CD25$^-$ responder T cells stimulated with allogenic DCs (1 DC : 5 Tresp) in the presence of Tregs expanded in **(C)** DMSO or **(D)** rapamycin. Histograms represent CD8$^+$ Tresp proliferation in 2 independent donors.

5.3.3. CRISPR-Cas9 gene inactivation by coupling sgRNA lentiviral transduction and Cas9 mRNA electroporation

The $CD27^{+}CD70^{-}$ phenotype is not inheritably stable and Tregs convert to $CD27^{-}CD70^{+}$ cells upon expansion. Therefore, to generate a stable $CD70^{-}$ Treg population it is necessary to genetically silence CD70 expression. We generated CD70-deficient human Tregs by disrupting CD70 expression using CRISPR-Cas9 technology. CRISPR single guide RNA (sgRNA) sequence was transduced into Tregs using a third-generation self-inactivating 'terminal' lentiviral vector that expresses the reporter GFP protein coupled to CRISPR sgRNA embedded in the 3'LTR (*314*). Three different sgRNAs targeting exon 3 of *CD70* or one sgRNA targeting B_2M (hereinafter referred as 1_3, 2_3, 3_3 and B2M) were tested. *Streptococcus pyogenes* Cas9 (spCas9) was delivered as a mRNA (CleanCap™, polyadenylated, and optimized for mammalian systems) (*314*). A schematic representation of the genetic engineering process is illustrated in Figure 5.6.

Figure 5.6

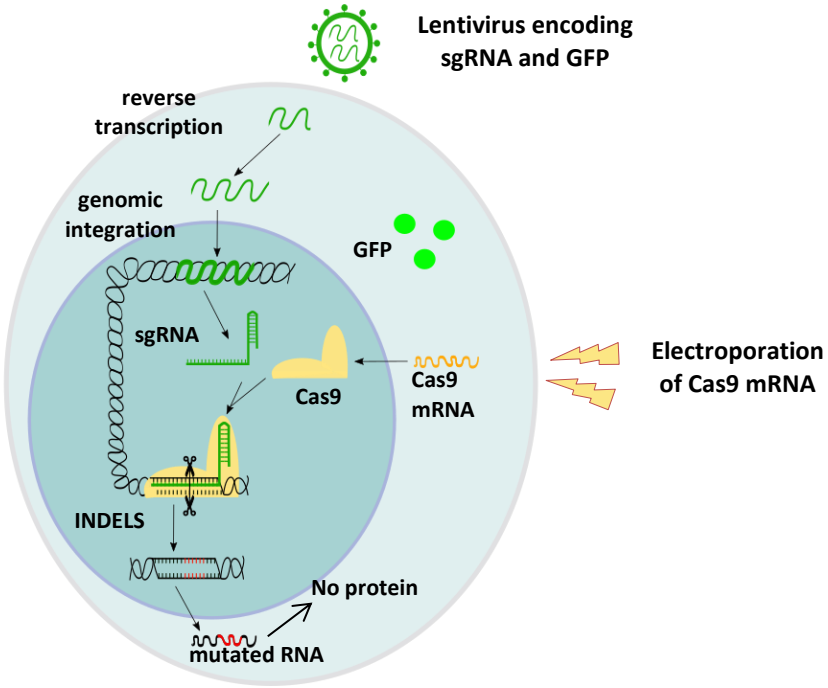

5.6. CRISPR-Cas9 gene inactivation by coupling sgRNA lentiviral transduction and Cas9 mRNA electroporation.

Schematic representation of the genetic editing process. Tregs were transduced with lentiviral particles that express the reporter GFP protein coupled to CRISPR single guide RNA (sgRNA) for CD70 or B_2M. Following reverse transcription, viral DNA is integrated into the host DNA, leading to expression of GFP and sgRNA. Tregs were electroporated with Cas9 mRNA, that translates into Cas9 protein inside the host Treg. sgRNA forms ribonucleoprotein complexes with Cas9, and this effect is restricted to transduced cells. sgRNA hybridises at its genomic target and guides the Cas9 nuclease to induce site-specific DNA cleavage. This DNA damage is repaired by cellular DNA repair mechanisms that are error-prone, and thus insertions and deletions (INDELs) may be introduced that can result in transcription of mutated mRNA and non-functional proteins.

We sought to design a protocol for optimal gene edition, while maximising the yield of stable modified Tregs. We coupled CRISPR-Cas9 gene editing with an existing protocol for high yield *in vitro* expansion of human Tregs (*304*) (Figure 5.7A). Tregs were *in vitro* expanded for one week using anti-CD3/anti-CD28 coated beads (1:1 cell:bead) in the presence of rhIL-2 (1000U/ml) and re-stimulated for 3 days prior lentiviral transduction (Figure 5.7A). It must be noted that positive transduction at MOI 5, measured by GFP expression 3 days post-transduction (day 13 of culture), ranged between 2.12% and

16.3% among different sgRNA constructs (Figure 5.7B). Of note, a comparison with additional experiments has shown that substantially higher transduction efficiency can be achieved if Tregs are transduced at the time of stimulation or 1 to 2 days after stimulation. 3 days post-transduction (as previously found to be optimal timing), stabilised spCas9 mRNA (*314*) was delivered by electroporation and cells were cultured overnight at 30^{o}C prior re-stimulation. Lentiviral transduced-Tregs that were not subjected to Cas9 mRNA electroporation were used as a control for genetic knockout (KO) effect. 3 days after electroporation (day 16 of culture), percentage of transduced Tregs within the expanded cell product was similar between electroporated (represented as +Cas9) and non-electroporated (-Cas9) Tregs (Figure 5.7C; left panel). KO efficiency, measured as loss of target protein expression and calculated as percentage of CD70^{+} or HLA-ABC^{+} cells in Cas9 electroporated Tregs compared to no-electroporated Tregs (100 - (%positive cells in Cas9Tregs * 100 / %positive cells in noCas9Tregs)), ranged between 47.83% and 65.07% (Figure 5.7C; right panel).

Cell viability, studied as percentage of 7AAD^{+} cells at day 16 of culture, or as fold expansion between day 13 and 20 of culture, was not significantly affected by electroporation (Figure 5.7D).

At day 20 of culture, KO efficiency increased to 70-85.4% within transduced cells (Figure 5.7E; left panel). Although KO efficiency was relatively high, the percentage of transduced Tregs was below 5% for the four sgRNAs studied (Figure 5.7E; middle panel) and sorting successfully transduced GFP^{+} Tregs was required. Given limited cell numbers, GFP purity within the isolated cell populations ranged between 21.8% and 99.1% among sgRNAs (Figure 5.7E; right panel). Importantly, similar GFP purities were obtained between Cas9 electroporated and non-electroporated paired of sgRNA-transduced Tregs (Figure 5.7E; right panel). Treg populations enriched in GFP^{+} cells were expanded for 7 further days prior to further analysis.

At day 27 of culture, KO efficiency within transduced GFP$^+$ Treg populations was over 80% for all sgRNAs tested (Figure 5.7F). Tregs transduced with sgRNAs 1_3 and 3_3 showed high transduction and KO efficiency within the total cell population (88.88% and 76.43% KO efficiency for sgRNAs 1_3 and 3_3 respectively) (Figure 5.7G). By contrast, low transduction efficiency for anti-CD70 sgRNA 2_3 and sgRNA targeting *B_2M* resulted in low KO efficacy within the total Treg product (Figure 5.7G).

Figure 5.7

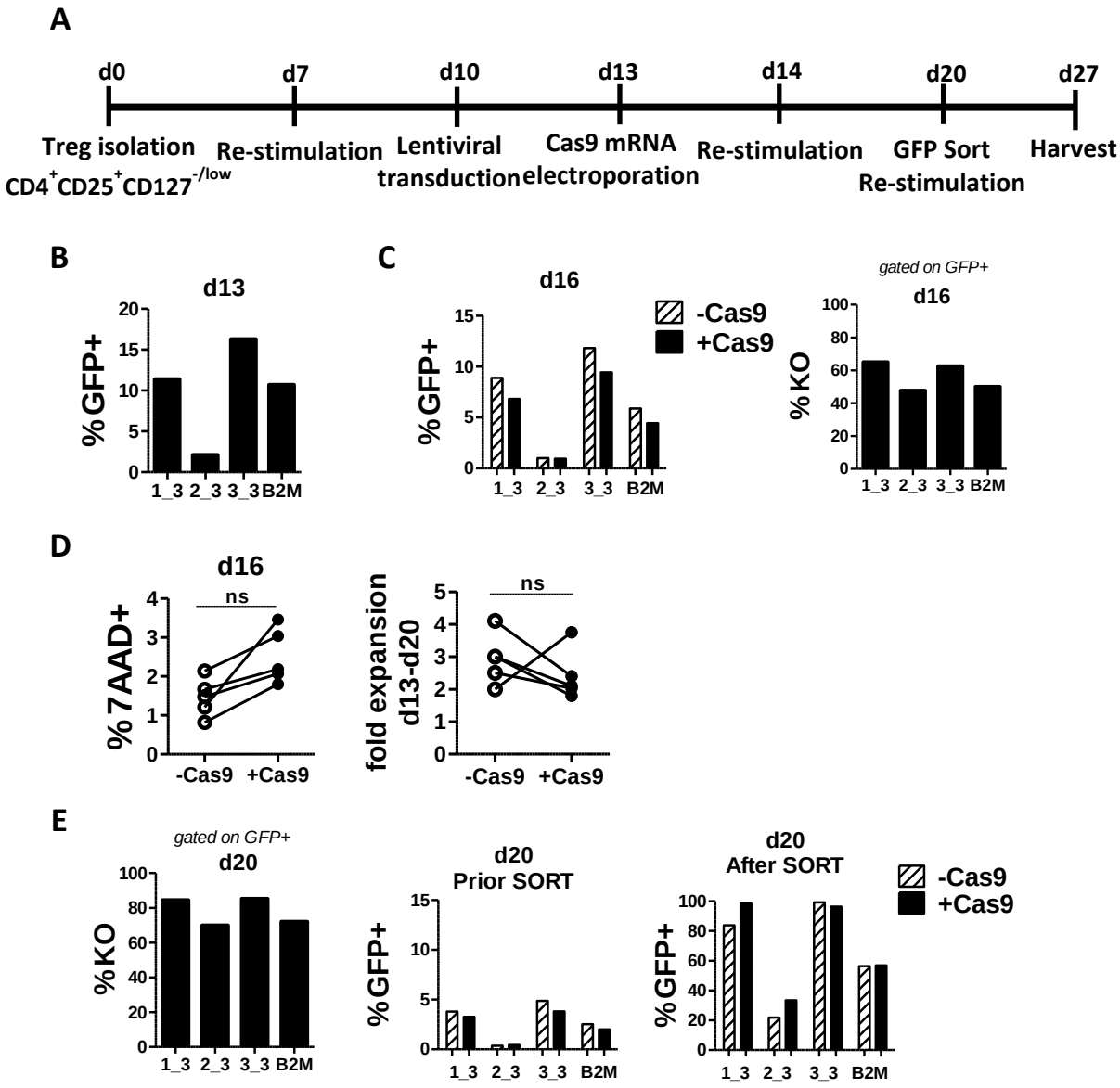

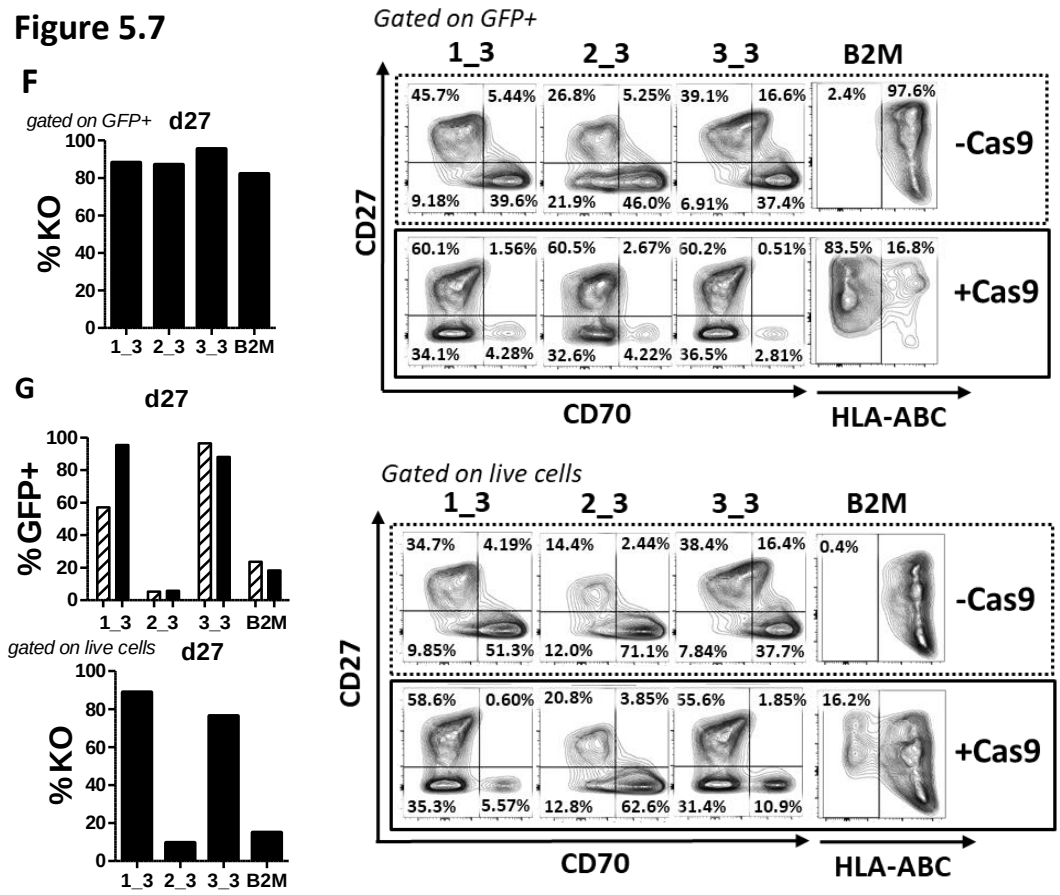

5.7. Stable CD70 knockout Treg cell product can be produced by CRISPR genome editing technology.

(A) Schematic overview of the procedure for CRISPR mediated-knockout on Tregs. $CD4^+CD25^+CD127^{-/low}$ Tregs expanded for 7 days were re-stimulated with anti-CD3/anti-CD28 coated beads and rhIL-2 prior lentiviral transduction (MOI 5). 4 lentiviral vectors containing different CRISPR sgRNA targeting *cd70* (1_2, 2_3 or 3_3 sgRNAs) or *b2m* (B2M) genes were studied. 3 days post transduction, Tregs were electroporated with spCas9 mRNA (100µg/ml), left at 30°C overnight and re-stimulated with anti-CD3/anti-CD28 coated beads and rhIL-2 the following day. 7 days after electroporation, positively transduced Tregs (identified by GFP expression) were flow sorted and then cultured for a further 7 days before analysis. Throughout the culture, cell cultures were divided and medium replenished as required.

(B) Transduction efficiency was assessed by flow cytometry as percentage of GFP^+ cells 3 days post transduction (day 13 of culture).

(C) 3 days post electroporation (day 16 of culture), (left panel) transduction efficiency and (right panel) knockout (KO) efficiency were studied by flow cytometry.

(D) Cell viability was assessed by measuring (left panel) 7-AAD 3 days post electroporation or (right panel) fold expansion between days 13 and 20 of culture. Statistical analysis, by Wilcoxon matched-pairs signed rank test, showed non-significant difference.

(E) (Left panel) KO efficiency and percentage of transduced cells (middle panel) before sorting and (right panel) after sorting at day 20 of culture are represented.

(F) Tregs were harvested and analysed at day 27 of culture. Left panel: Bar graph depicting KO efficiency for different sgRNAs. Right panel: Plots illustrating CD27, CD70 and HLA-ABC expression within GFP^+ transduced Tregs in Cas9-electroporated and non-electroporated Tregs.

(G) Left panel: Transduction and KO efficiencies within the bulk Treg cell product at day 27 of culture. Right panel: CD27, CD70 and HLA-ABC expression was analysed in bulk Treg cell cultures.

Moreover, molecular signatures of gene editing at the *CD70* locus were confirmed by PCR sequencing and ICE analysis in the total cell product (Figure 5.8). Most of the mutations involved were an insertion of 1bp (22.9%) or deletion of 23bp (21.46%), creating a KO-score of 75% when analysing the percentage of indels > 20bp or those resulting in frameshifts (Figure 5.8E).

Taken together, we have shown that CD70 genetic inactivation coupling lentiviral transduction for sgRNA delivery with Cas9 mRNA electroporation is feasible in human Tregs.

Figure 5.8

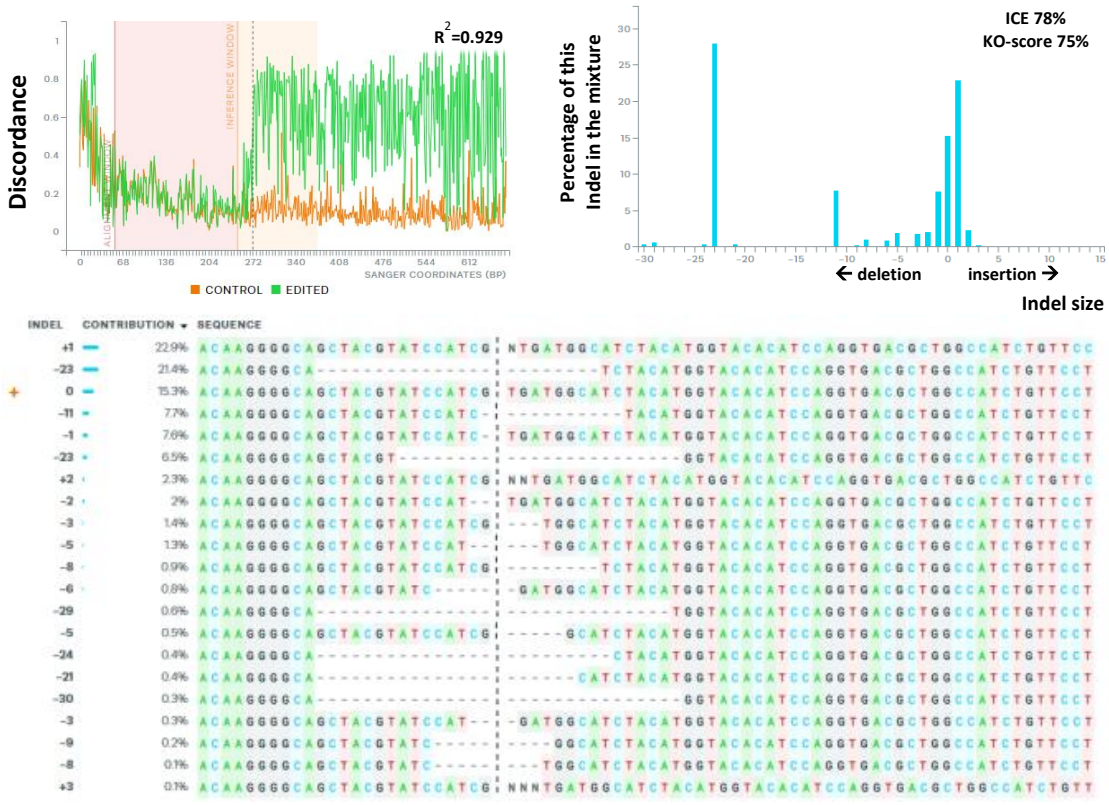

5.8. Molecular signature of CD70 knockout effect.

Genetic editing efficiency across the CD70 locus was confirmed by analysis using ICE algorithm. Top left panel: Level of discordance between control and edited samples matches before the PAM sequence (denoted by a dotted line) and is discordant after the cut site. Top right panel: Graph shows the distribution of the detected indels in the edited sample. X axis depicts the size of the indel and Y axis shows the frequency of each deletion in the cell product. Bottom panel: table showing all the sequences within the population. For each sequence, the number of nucleotides inserted or deleted and the relative abundance of each indel within the edited population is represented on the left. + indicates the wild type sequence, and its prevalence in the edited population. The vertical black dotted line shows the cut site. Base pair deletions are indicated by dashes, and insertions are indicated by "N" bases. sgRNA 1_3 is shown.

5.3.4. CD70-knockout Treg cell product has enhanced suppressive activity

CD70-KO Tregs were further characterised for differences in phenotype and functional activity. No consistent changes were observed in expression levels of CD27, CD25, FOXP3 or HELIOS due to CD70 deficiency (Figure 5.9A,B).

Similarly, no consistent difference in cytokine production (IL-10, IL-17A, IL-17F, TNF-α, IL-6, IL-13, IL-9 or IL-4) was detected between unmodified and CD70-KO Tregs (Figure 5.9C).

Figure 5.9

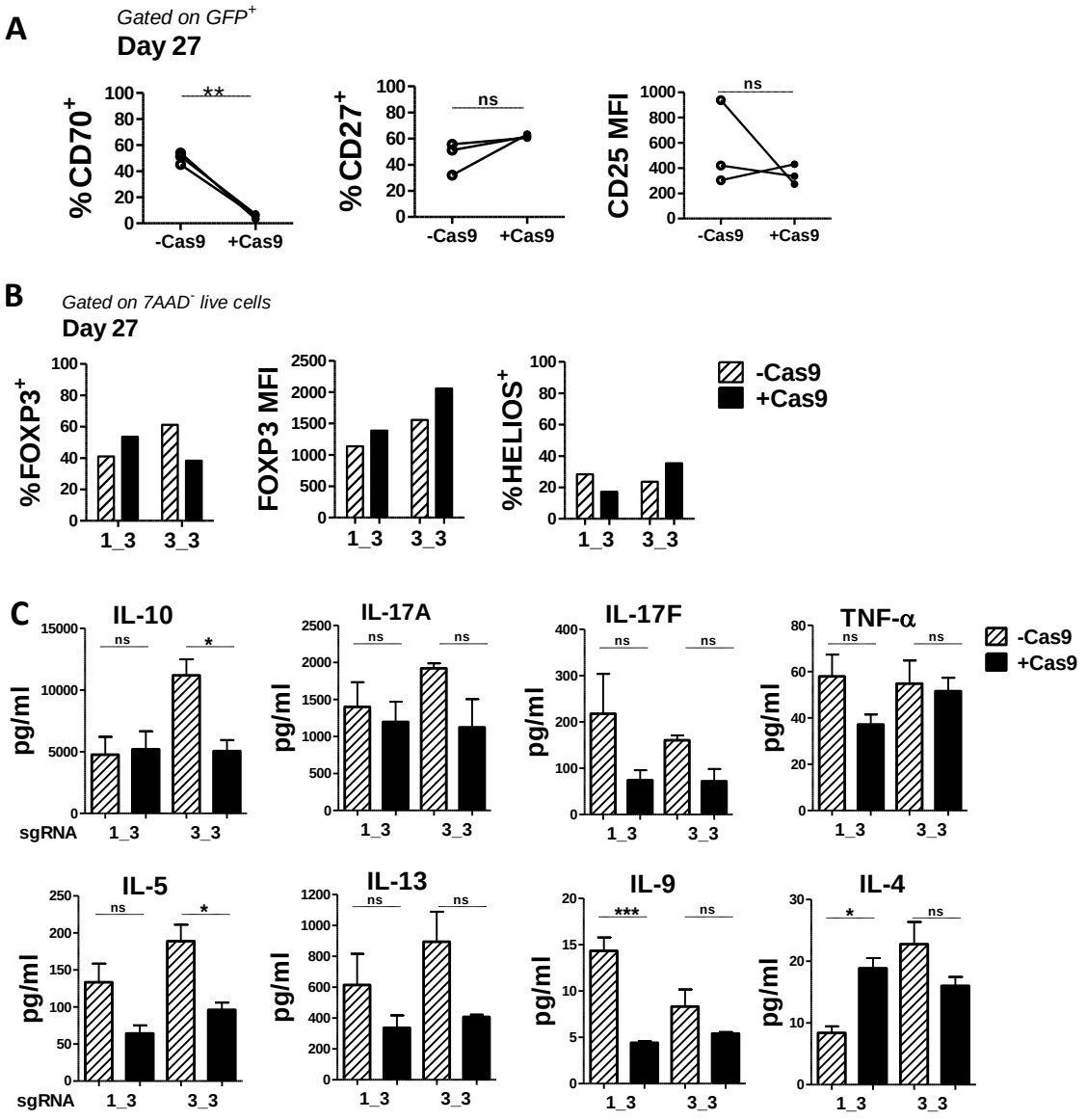

5.9. CD70-deficiency does not alter Treg phenotype beyond CD70 expression.

Tregs were transduced with a lentiviral vector containing CRISPR sgRNA for CD70 with (+Cas9) or without (-Cas9) subsequent Cas9 mRNA electroporation.

(A) CD70, CD27 and CD25 expression were analysed at day 27 by flow cytometry gating in GFP^+ Tregs transduced with sgRNAs 1_3, 2_3 and 3_3. Paired t test was conducted.

(B) FOXP3 and HELIOS expression levels within the bulk Treg product at day 27 are represented for Tregs transduced with sgRNAs 1_3 and 3_3.

(C) 27 days expanded CD70 KO and matched control Tregs were stimulated for 72h in the presence of rhIL-2 (250 U/ml) with anti-CD3/anti-CD28 coated beads (1 bead: 5 cells). A cytokine bead array assay was performed on these supernatants to measure expression of 12 different cytokines as labelled in the figure. Levels of IL-21, IL-22 and IL-6 were under the detection limit while IFN-γ expression was over the detection limit of the assay. Errors bars represent mean ± SD for 3 replicate wells. Statistical significance was studied by one-way ANOVA with Bonferroni post-test. Treg lines transduced with sgRNAs 1_3 and 3_3 are shown.

ns= non-significant, *P<0.05, **P<0.01, ***P < 0.001.

On functional assessment in a MLR suppression assay using VPD-labelled responder T cells stimulated with allo moDCs in the presence of Tregs, we found that CD70-KO Tregs (labelled as +Cas9) had enhanced suppressive potency compared to control Tregs (-Cas9) in both anti-CD70 sgRNAs tested (1_3 and 3_3) (Figure 5.10A). As a control, the suppressive ability of untransduced and anti-B_2M sgRNA transduced Tregs was also studied and demonstrated to be similar between Cas9 electroporated and non-electroporated Tregs (Figure 5.10B).

Figure 5.10

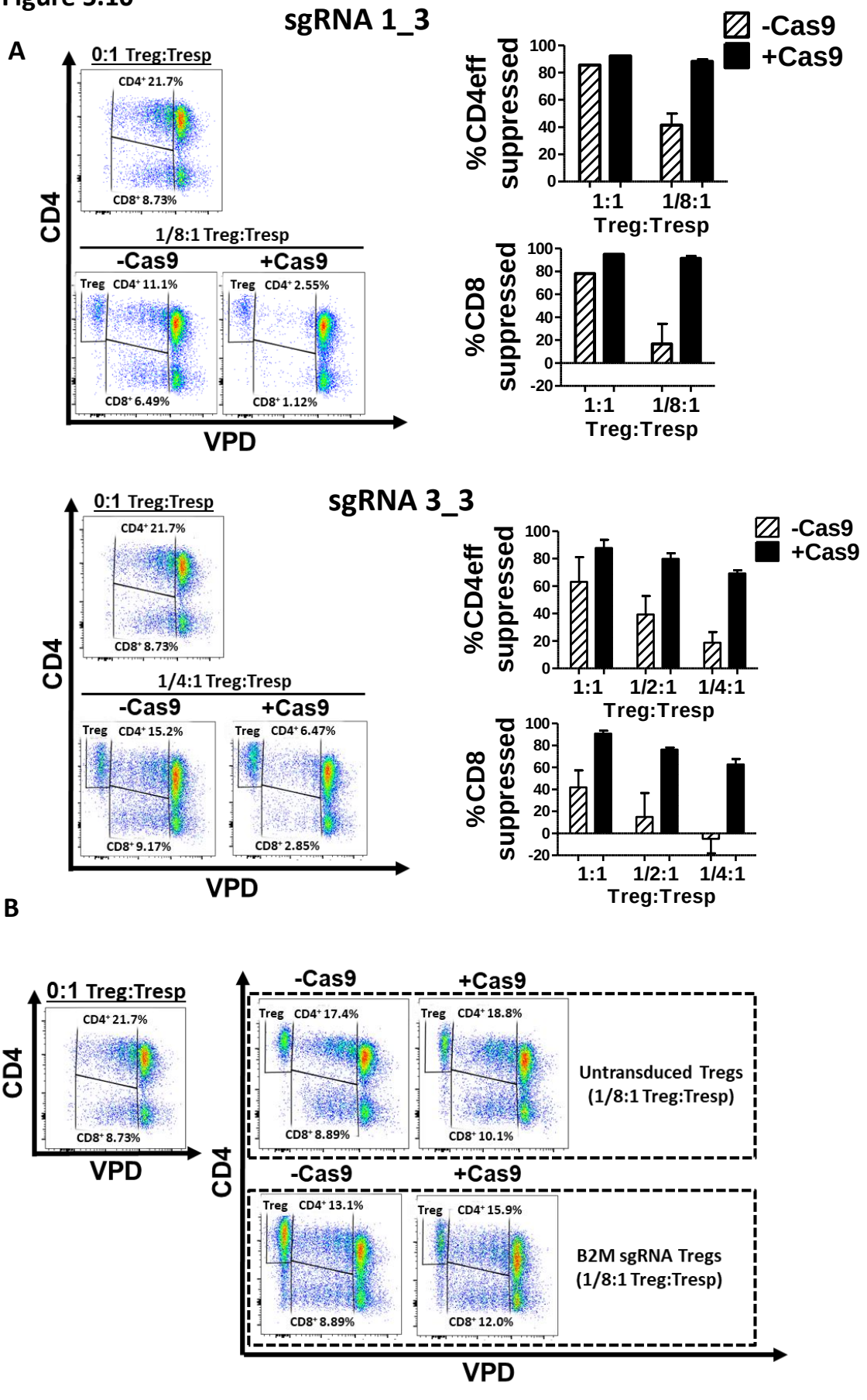
A
sgRNA 1_3
0:1 Treg:Tresp
CD4+ 21.7%
CD8+ 8.73%
CD4
1/8:1 Treg:Tresp
-Cas9
+Cas9
Treg CD4+ 11.1%
CD8+ 6.49%
Treg CD4+ 2.55%
CD8+ 1.12%
VPD
%CD4eff suppressed
%CD8 suppressed
-Cas9
+Cas9
1:1
1/8:1
Treg:Tresp
sgRNA 3_3
1/4:1 Treg:Tresp
Treg CD4+ 15.2%
CD8+ 9.17%
Treg CD4+ 6.47%
CD8+ 2.85%
1/2:1
1/4:1
B
0:1 Treg:Tresp
CD4+ 21.7%
CD8+ 8.73%
-Cas9
+Cas9
Treg CD4+ 17.4%
CD8+ 8.89%
Treg CD4+ 18.8%
CD8+ 10.1%
Untransduced Tregs
(1/8:1 Treg:Tresp)
Treg CD4+ 13.1%
CD8+ 8.89%
Treg CD4+ 15.9%
CD8+ 12.0%
B2M sgRNA Tregs
(1/8:1 Treg:Tresp)

5.10. CD70-knockout Tregs have enhanced suppressive activity.

Treg suppressive capacity was assessed *in vitro* by MLR suppression test, consisting of $CD3^+CD25^-$ responder T cells labelled with VPD and stimulated with allogenic monocyte derived-DCs in the presence or absence of Tregs.

(A) Left panel: Percentage of dividing VPD-stained $CD4^+$ or $CD8^+$ responder T cells (Tresp) in the absence of Tregs and in the presence of Tregs. Right panel: Percentage suppression of proliferation of $CD4^+$ Tresp and $CD8^+$ Tresp shown as mean ± SD (3 replicates wells in the suppression assays are plotted). Results for sgRNAs (top) 1_3 and (bottom) 3_3 targeting CD70 are shown.

(B) Suppressive capacity of Tregs that were untransduced or transduced with a lentiviral vector containing CRISPR sgRNA for B_2M with or without subsequent Cas9 mRNA electroporation is shown as an experimental control. FACS plots represent percentage of dividing VPD-stained $CD4^+$ or $CD8^+$ Tresp in the absence or presence of Tregs.

Three Treg subsets can be distinguished within the CD70-KO Treg population: $CD27^+CD70^-$ (red gate), $CD27^-CD70^+$ (blue gate) and $CD27^-CD70^-$ (green gate) cells (Figure 5.11 A; left plot). In order to further clarify the relevance of CD27 and CD70 expression in Treg function, we isolated these 3 Treg subpopulations by magnetic sorting and compared their suppressive activity. $CD27^+CD70^-$ and $CD27^-CD70^-$ cells were separated with high purity, however, due to technical issues, the $CD27^-CD70^+$ Treg subset contained some $CD27^+$ and $CD70^-$ cell contaminants (Figure 5.11A). When co-cultured with responder T cells activated with allo moDCs, the $CD27^-CD70^-$ Treg subset appeared as potent as $CD27^+CD70^-$ Tregs inhibiting T cell proliferation, while $CD27^-CD70^+$ Tregs had defective suppressive activity (Figure 5.11B). These data further corroborate our hypothesis that CD70 and not CD27 plays a role in the activity of Tregs. It is important to mention that these experiments were performed with only one donor and they need to be repeated before reaching a conclusion.

Figure 5.11

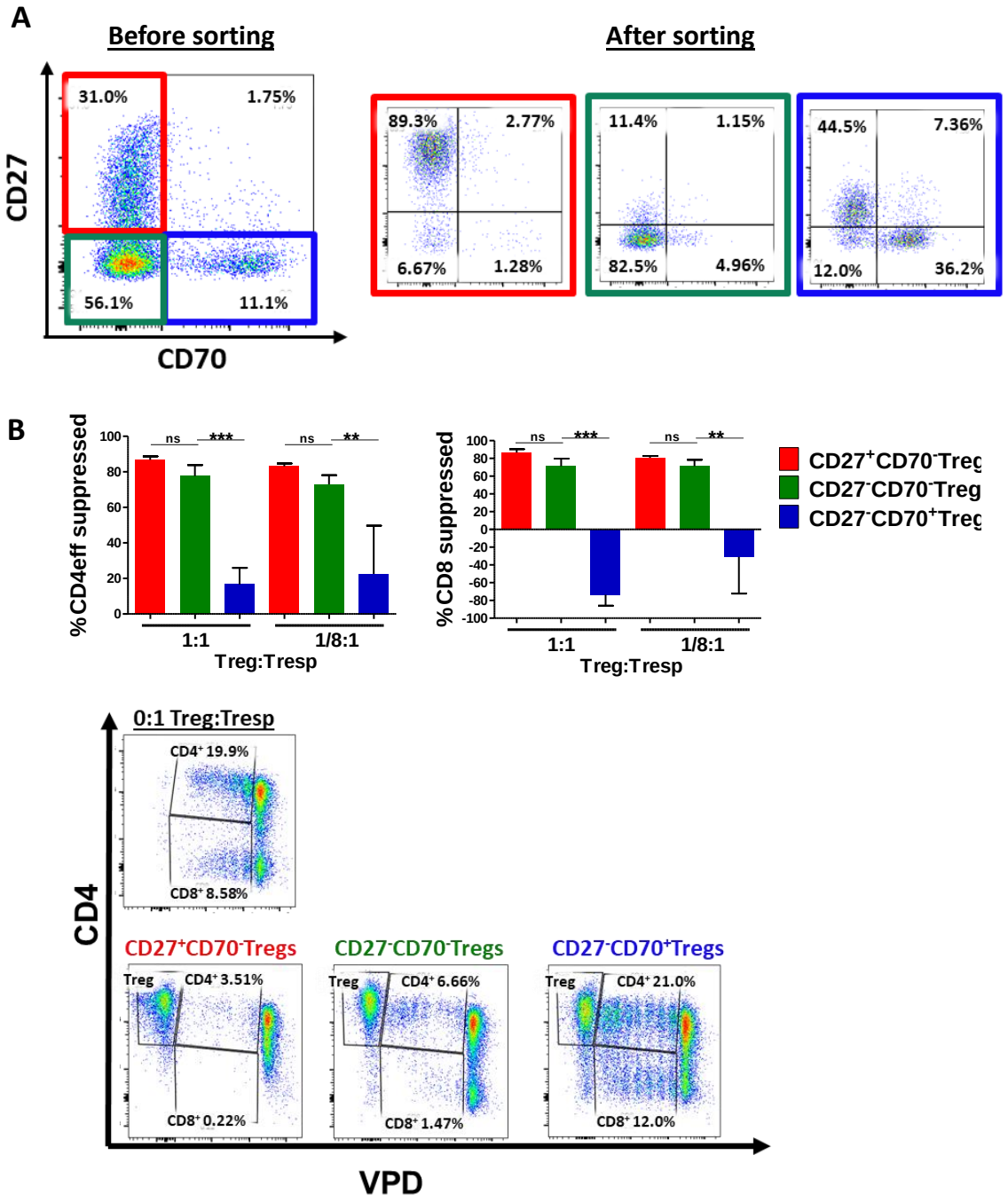

5.11. CD27$^-$CD70$^-$ Tregs (CD70-knockout) are as suppressive as CD27$^+$CD70$^-$ Tregs.

The CD70-knockout Treg population was sorted as: CD27$^+$CD70$^-$ (red), CD27$^-$CD70$^+$ (blue) and CD27$^-$CD70$^-$ (green) cells by magnetic separation after 33 days of *in vitro* expansion. **(A)** CD27 and CD70 expression was analysed prior and after sorting in each Treg subset. **(B)** Suppressive capacity of each Treg subset was assessed in a MLR suppression test. (Top panel) Percentage suppression of proliferation of CD4$^+$ Tresp and CD8$^+$ Tresp is shown as mean ± SD for 3 replicates wells. (Bottom panel) Percentage of dividing VPD-stained CD4$^+$ or CD8$^+$ responder T cells (Tresp) in the absence of Tregs and in the presence of different CD27/CD70 Treg subsets. Results from Tregs transduced with sgRNA 1_3 are shown. Statistical significance was calculated by one way-ANOVA with Bonferroni post-test for multiple comparisons. ns= non-significant, **P<0.01, ***P < 0.001.

5.3.5. Gene editing by CRISPR sgRNA/Cas9 ribonucleoproteins (RNPs)

Given the low efficiency rates in lentiviral transduction, we explored an alternative strategy to deliver CRISPR-Cas9 elements. Several studies have reported successful highly-efficient gene editing rates when transfecting Cas9 bound to sgRNA as ribonucleoproteins (RNPs) using target gene-specific CRISPR RNAs (crRNA) and tracer RNA (tracrRNAs), the latter mediates the interaction of crRNA with Cas9. The use of RNP transfection greatly facilitates the genetic engineering protocol, since it eliminates the need for cloning and lentiviral transduction.

We designed a protocol for CRISPR mediated-KO in human Tregs using RNP transfection (Figure 5.12A). 7 day-expanded Tregs were re-stimulated for 3 days prior electroporation of RNPs. Two different sgRNAs for *CD70* were assessed; targeting exon 1 (sgRNA 1_1) or exon 3 (sgRNA 3_3). Anti-B_2M sgRNA was used as a positive KO. Additionally, two Cas9 nuclease proteins were tested in parallel; one obtained from Integrated DNA Technologies as Sp HiFi Cas 9 nuclease (thereafter named as Cas9 IDT), and another produced at the Oxford Protein Facility (labelled as Cas9 OXF). Tregs electroporated with Cas9 without sgRNA were used as a control for KO effect. Cell viability, measured as fold expansion between days 10 and 24 of culture, was studied in non-electroporated Tregs, control Tregs electroporated with Cas9 protein without sgRNA and Tregs electroporated with sgRNA/Cas9 RNP. The electroporation process itself substantially reduced the proliferation capacity of Tregs, but, importantly, not major difference was observed between RNP and control Cas9 electroporation (+Cas9 OXF) (Figure 5.12B).

We achieved a KO efficiency for up to 82.8% for HLA-ABC and 93.8% for CD70, as measured by loss of protein expression 3, 7, and 14 days after electroporation (Figure 5.12C). sgRNA 1_1 resulted in higher KO efficiency than sgRNA 3_3, and KO efficiency

was greater using Cas9 protein from IDT than from Oxford Protein Facility for all conditions tested (Figure 5.12C). Consequently, percentage of $CD70^+$ Tregs was reduced in anti-CD70 RNP electroporated Tregs compared to control Cas9 electroporation, and the lowest level of CD70 expression was observed in Tregs electroporated with sgRNA 1_1 and Cas9 IDT (Figure 5.12D,E). Levels of CD27 expression did not differ between control and KO conditions (Figure 5.12D,E).

The particular cell donor studied here did not upregulate CD70 and downregulate CD27 expression to the extend usually observed during Treg prolonged expansion, consequently low proportion of $CD27^-CD70^+$ cells were present within the expanded Treg product and Tregs showed potent suppressive capacity even at low Treg:Tresp ratios, which could not be enhanced by CD70 inactivation (Figure 5.12F).

Figure 5.12

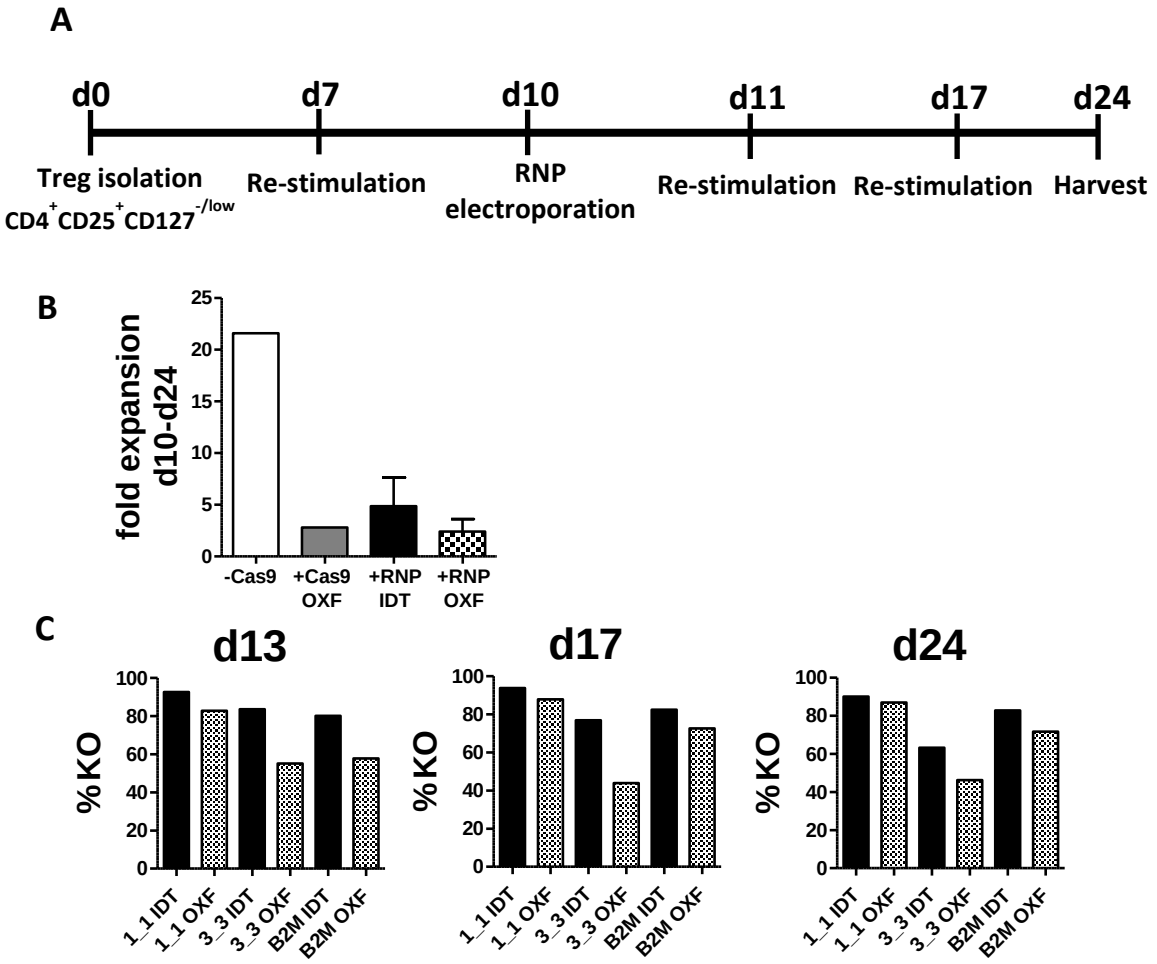

Figure 5.12

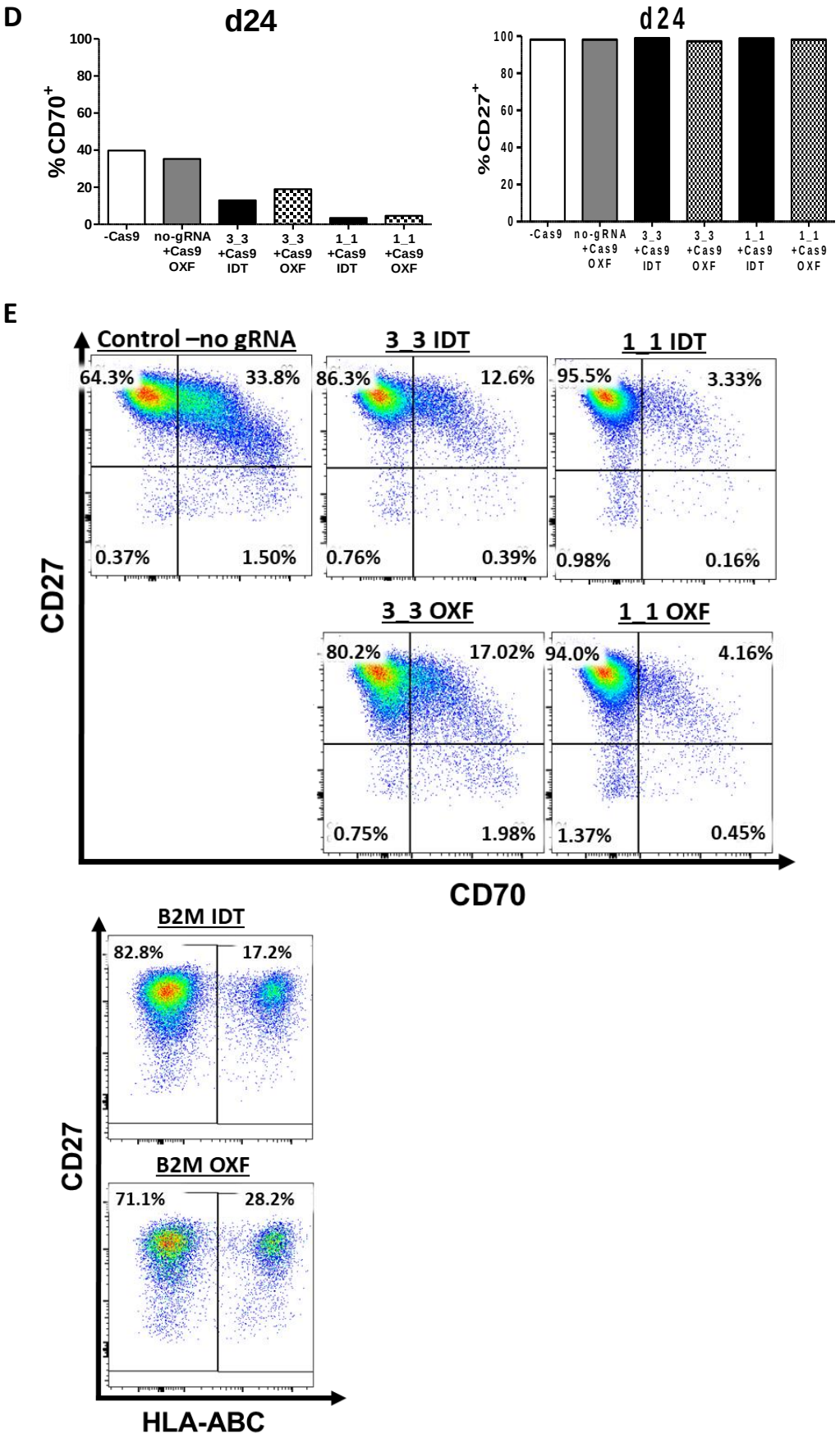
D
d24
% CD70+
100
80
60
40
20
0
-Cas9
no-gRNA +Cas9 OXF
3_3 +Cas9 IDT
3_3 +Cas9 OXF
1_1 +Cas9 IDT
1_1 +Cas9 OXF
d24
% CD27+
E
Control –no gRNA
64.3%
33.8%
0.37%
1.50%
3_3 IDT
86.3%
12.6%
0.76%
0.39%
1_1 IDT
95.5%
3.33%
0.98%
0.16%
3_3 OXF
80.2%
17.02%
0.75%
1.98%
1_1 OXF
94.0%
4.16%
1.37%
0.45%
CD27
CD70
B2M IDT
82.8%
17.2%
B2M OXF
71.1%
28.2%
CD27
HLA-ABC

Figure 5.12

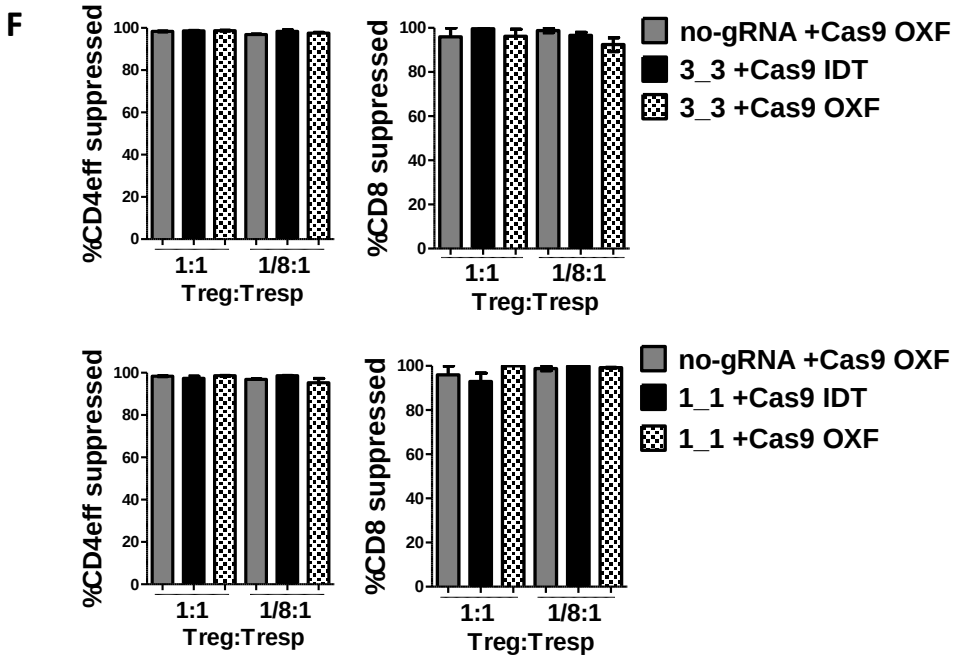

5.12. Gene editing by CRISPR sgRNA/Cas9 ribonucleoproteins (RNPs).

(A) Schematic overview of the protocol for CRISPR mediated-knockout in Tregs using sgRNA/Cas9 ribonucleoprotein (RNP). $CD4^+CD25^+CD127^{-/low}$ Tregs expanded for 7 days were re-stimulated with anti-CD3/anti-CD28 coated beads and rhIL-2 for 3 days prior RNP electroporation. Different CRISPR sgRNA targeting *cd70* (1_1, and 3_3 sgRNAs) or *b2m* (B2M) genes were studied. After electroporation, Tregs were left at 30ºC overnight and re-stimulated with anti-CD3/anti-CD28 coated beads and rhIL-2 the following day. 7 days after electroporation, Tregs were re-stimulated again before harvesting at day 24. Throughout culture, cell cultures were divided and medium replenished as required.

(B) Proliferation capacity was assessed by measuring fold expansion between days 10 and 24 of culture in non-electroporated Tregs, Tregs electroporated with Cas9 protein without sgRNA coupled (+Cas9 OXF) and Tregs electroporated with sgRNA/Cas9 RNP using Cas9 from IDT or from Oxford Protein Facility (OXF).

(C) Knockout (KO) efficiency was calculated by loss of protein expression by flow cytometry 3, 7 and 14 days post electroporation (day 13, 17 and 24 of culture) in Tregs electroporated with RNP comprising anti-CD70 sgRNAs 1_1 and 3_3 or anti-B_2M sgRNA and Cas9 protein from IDT or from Oxford Protein Facility (OXF).

(D) Tregs were harvested and analysed at day 24 of culture for CD70 and CD27 expression in different sgRNAs and Cas9 conditions.

(E) Plots illustrating CD27, CD70 and HLA-ABC expression in RNP-electroporated Tregs.

(F) The suppressive capacity of Tregs harvested at day 24 of culture was assessed *in vitro* by MLR suppression test, consisted of VPD-labelled $CD3^+CD25^-$ responder T cells (Tresp) stimulated with allogenic monocyte derived-DCs in the presence of Tregs (1 DC:5 Tresp). VDP dilution was studied by flow cytometry and percentage suppression of proliferation of $CD4^+$ Tresp and $CD8^+$ Tresp was calculated based on division index. Results for sgRNAs (top) 3_3 and (bottom) 1_1 targeting CD70 are shown. Error bars show mean ± SD.

5.4. Discussion

A rapamycin-based GMP-compatible protocol for the *ex vivo* expansion of clinical grade Tregs has been recently published (*294*). This protocol has been used for Treg therapy in the ONE Study, a multicenter phase I/IIa clinical trial in which Treg cellular therapy is investigated in renal transplantation. The ONE Study has confirmed the safety of adoptive transfer autologous Tregs, isolated from peripheral blood of patients as $CD8^{-}CD25^{+}$ cells by magnetic bead sorting and expanded *in vitro* in the presence of rapamycin.

It is known that the addition of rapamycin during *in vitro* Treg expansion prevents the development of IL-17-producing cells and preserves the expression of CD62L and CD27, which correlates with suppressive potency (*179, 294, 309, 366, 367*). Importantly, there is no information about CD70 expression in Tregs expanded following GMP-compliant protocols, cultured with or without rapamycin. We have adapted a GMP-compatible protocol presented by Fraser's *et al.* (*294*) to our laboratory equipment and showed that rapamycin prevents CD27 downregulation and CD70 upregulation (Figure 5.2A). It is known that, despite its preferential effect on Teff cells, culturing in the presence of rapamycin reduces the overall fold expansion of Tregs (*285, 363*), implying the need for repeated rounds of stimulation. Previously, Hippen *et al*. have reported downregulation of CD27 in Tregs cultured with rapamycin upon multiple re-stimulations, which correlated with loss of suppressive potency (*368*). In agreement with these results, we found that some donors developed a $CD27^{-}CD70^{+}$ cell subset after expansion (Figure 5.5B), and those donors showed reduced suppressive function (Figure 5.5D). We have demonstrated that depletion of $CD70^{+}$ cells by magnetic separation is possible and may increase the suppressive potency of the cell product, but only for certain donors (Figure 5.5D).

Rapamycin preferentially inhibits proliferation of Teff cells over Tregs, but it does not induce anergy of Teffs (*363*). Several mechanisms have been suggested to explain the

disparity impact of rapamycin on Tconv and Tregs, including different metabolic regulation and signalling pathways (*367, 369, 370*). Rapamycin binds to mammalian target of rapamycin (mTOR) and selectively inhibits PI3K-mediated signalling. It is possible that Tconv are more reliant on PI3K pathway, while Tregs may use Janus kinase/ signal transduced and activator of transcription 5 (JAK/STAT5) to transduce IL-2 signalling (*285, 371, 372*). Rapamycin also induces FOXP3 expression in Tconv and supports the proliferation of these iTregs (*373*). Therefore, when Tregs are isolated with low purity as bead-sorted $CD4^+CD25^+$ T cells, iTregs or Teffs could exert pro-inflammatory function after withdrawal of rapamycin. In support of this hypothesis, our results showed that the rapamycin-mediated suppressive phenotype tended to be reverted upon removal of the drug (Figure 5.3) although more donors need to be studied before reaching a conclusion.

Therefore, additional strategies to generate a cell product with stable suppressive function may augment the efficacy of the current therapy. More stringent strategies for Treg isolation, e.g. selection of $CD4^+CD25^+CD127^-$ Tregs by FACS sorting, and genetic engineering of key molecules that regulate Treg functionality might offer a solution to address this problem.

Clinical trials for adoptive transfer of T cells genetically modified using CRISPR gene editing tools have been recently started (*314, 374*). Given the pro-inflammatory effect of CD70, we sought to genetically silence CD70 in Tregs using CRISPR/Cas9 technology. We explored 2 strategies; viral delivery of sgRNA coupled with Cas9 mRNA electroporation or electroporation of sgRNA/Cas9 complex as a ribonucleoprotein (RNP). Georgiadis *et al*. have recently described an approach where sgRNA is delivered by lentiviral transduction and Cas9 is transfected as mRNA by electroporation. This method is considered to be highly safe compared to other strategies due to a transient effect of Cas9 and the design of a third-generation self-inactivating (SIN) lentivirus. Alternative approaches incorporate sgRNA and Cas9 expression in the lentiviral vector, leading to integration in the host genome. Constitutive expression of Cas9 is likely to cause a safety

risk in human trials for several reasons: development of an immune response due to its bacterial origin, and off targets effects as a result of continuing scission. For third-generation lentiviral system, the components for virus production are split across 4 plasmids. Moreover, sgRNA is embedded in the 3' LTR. Deletion of 3'LTR is transferred into 5'LTR after the first round of reverse transcription and abolishes the viral promoter activity, preventing transcription of the full-length virus and rendering the virus self-inactivating after integration (*375*).

We have adapted this approach for gene editing in Tregs using a SIN lentiviral vector containing GFP coupled to sgRNA expression. GFP was introduced in the system for ease of identification and isolation of successfully transduced Tregs. KO efficiencies were over 80% for CD70 and B_2M disruption, proving the validity of the sgRNAs (Figure 5.7F). Unfortunately, transduction efficiency was not optimal. When transduction and KO effects were coupled, we were able to generate high percentages of modified Tregs only in 2 out of 4 lines (Figure 5.7G). It is likely that a further optimisation will increase transduction efficiency in Tregs and subsequently improve the gene editing protocol.

As expected, genetic disruption of CD70 expression leads to Treg cell products with enhanced suppressive activity (Figure 5.10A). Expression of cytokines or other Treg associated molecules was not consistently altered in CD70-KO cell products compared to non-edited control cells (Figure 5.9), which supports our previous finding of CD70 providing direct co-stimulatory signalling.

Importantly, our CRISPR experiments demonstrate that CD27 does not have a crucial role in Treg stability or suppressive function and that inhibition of CD70 expression can restore Treg suppressive capacity to the same levels as observed in $CD27^+CD70^-$ Tregs (Figure 5.11).

Recent studies have reported successful gene editing with KO frequencies between 50% and 90% when transfecting pre-activated human T cells with Cas9 RNPs (*376-380*). This

strategy would eliminate the need for lentiviral transduction and for further selection, significantly simplifying the protocol. By targeting CD70 and B_2M, we have proven that human Tregs can be efficiently edited using Cas9 RNPs while preserving suppressive function. Although electroporation substantially impaired their proliferative capacity, CD70 KO Tregs could be expanded longer without acquiring CD70 and co-stimulatory effects (Figure 5.12).

Collectively, we found that CRISPR-mediated genetic engineering, using sgRNA-lentiviral transduction and Cas9 mRNA electroporation or Cas9 RNPs, lead to high knockout efficiency in activated human Tregs. As for the first approach, Georgiadis *et al*. have proven that the system is scalable and can be incorporated into a largely automated manufacturing process in conventional T cells (*314*). In fact, T cells manufactured according to this protocol are currently being used in a clinical trial in leukaemia paediatric patients at the Great Ormond Street Hospital in London. Furthermore, the use of a lentivirus that allows transgene expression opens the possibility to force expression of elements regulating stability and suppressive function in Tregs, such as Treg functional molecules (e.g. FOXP3 or IL-10), or chimeric antigen rectors (CARs) or TCRs for antigen specificity. On the downside, the use of lentivirus raises some safety concerns relating to potential oncogenesis or the generation of replication-competent lentivirus. Gene editing using Cas9 RNPs constitutes a safer option and more straightforward technique due to the lack of transduction step. However, optimisation of the protocol is needed to achieve relevant number of cells for clinical use.

Chapter 6: Conclusions and future directions

6.1. General discussion and limitations

As essential mediators of tolerance in autoimmune diseases and allogenic transplantation, Tregs are of prime interest in the field of cellular therapy. Due to their paucity in peripheral blood, Tregs need to be expanded *ex vivo* in order to obtain sufficient numbers for clinical application. A key breakthrough in the translational potential of Treg therapy has been the development of protocols for the successful isolation and *in vitro* expansion of human Tregs through successive rounds of polyclonal activation using anti-CD3 and anti-CD28 mAbs in the presence of high levels of IL-2 (*294, 297, 368*). Importantly, adoptive transfer of polyclonally expanded human Tregs has been proven to increase graft survival in several humanised mouse models of transplantation (*299, 303-306*). Yet challenges remain in their successful production to appropriate levels of purity. Previous studies on *ex vivo* expanded human Tregs have demonstrated that although $CD4^+CD25^+CD127^{-/low}$ Tregs display a regulatory phenotype and high suppressive potency after one or two cycles of expansion (*297*), there is an increase in methylation within the TSDR together with decreased levels of FOXP3 expression after extended TCR stimulation (*307*). In agreement with this, the data in this study show that *in vitro* stimulation and expansion of flow-sorted highly pure $CD4^+CD25^+CD127^-$ Tregs results in a final cell product that contains cells with unstable regulatory activity (Figure 3.6).

This thesis aimed to investigate the mechanisms by which some Tregs lose their suppressive properties after prolonged *in vitro* expansion in order to generate a more stable and potent Treg cell product for use in clinical therapy.

Several studies have previously reported that CD27 expression closely correlates with suppressive potency and allows the distinction between suppressive and non-suppressive cells in $CD4^+CD25^+$ expanded cell products (*179, 180, 311*). In Chapter 3, it

was shown that freshly isolated $CD4^+CD25^+CD127^-$ Tregs and $CD4^+$ Tconv cells have high CD27 and low CD70 expression and that both markers are upregulated following activation. However, upon repetitive stimulation through the TCR and CD28, some cells downregulate CD27 while expressing high levels of CD70 on the cell surface, resulting in distinct subpopulations with differential CD27 and CD70 expression levels (Figure 3.4). Regulation of CD27 and CD70 expression appears similar in Tregs and $CD4^+$ Tconv cells (although higher levels of $CD70^+$ cells are observed within the Treg population compared to $CD4^+$ Tconv) indicating that the CD27/CD70 phenotype does not distinguish between Treg and Tconv cells.

In Chapters 3 and 4, the $CD27^+CD70^-$ phenotype is shown to be associated with a Treg subset that shares important transcriptional elements with a previously identified Treg-signature (*174*). These cells retain potent suppressive activity and a hypomethylated TSDR after *in vitro* expansion. By contrast, $CD27^-CD70^+$ Tregs have significantly impaired suppressive capacity after prolonged expansion, promote T cell proliferation, and produce high levels of IL-17.

Despite extensive work exploring the function of CD27 in Tconv cells, the role of CD27 co-simulation in Tregs remains unclear. Contrasting studies have demonstrated that CD27 ligation results in either increased (*70, 150, 381*) or impaired (*349, 382*) Treg activation and survival. However, these studies were not performed in purified Tregs and may be confounded by the effect of activated non-Tregs stimulated via CD27. In Chapter 4, the role of CD27 and CD70 in the suppressive activity of Tregs is investigated.

Dhainaut *et al*. have shown that, in an *in vitro* co-culture of mouse T cells, Tregs and DCs, $CD27^+$ Tregs bind to CD70 expressed on activated DCs, resulting in endocytosis and degradation of the CD27/CD70 complex by DCs (*188*). Consequently, DCs lose CD70 expression on their cell surface and are unable to provide CD70-mediated co-stimulation to responder T cells. Using a similar set-up, we explored whether this mechanism may

explain the enhanced suppressive potency of $CD27^+CD70^-$ human Tregs. However, when responder T cells are co-cultured with allogenic monocyte-derived DCs in the presence of $CD27^+$ Tregs, blocking CD27 on Tregs does not result in impaired suppressive activity, indicating that CD27 does not play an essential role in their suppressive mechanism (Figure 4.1). These findings concur with studies where Tregs from wild type and $CD27^{-/-}$ mice display similar potency inhibiting $CD4^+$ and $CD8^+$ T cell proliferation *in vitro* (*70, 150*). It is assumed that DCs, in MLR assays, upregulate CD70 expression and provide co-stimulatory signals for T cell proliferation. However, using flow cytometry, we have not observed CD70 expression on the cell surface of DCs. CD70 cell surface expression has been described in certain subsets of DCs in the gut (*383*) or in DCs activated via CD40 co-stimulation and "danger" signals such as TLR stimulation (*73, 188, 384*). Moreover, CD70 is known to be tightly regulated and may cycle between intracellular and cell surface expression (*385*). Analysis of intracellular CD70 would show if human monocyte-derived DCs have the potential to express CD70 on their cell surface when activated in the presence of allogenic T cells. We therefore cannot be certain whether CD70 expressed on DCs is susceptible to regulation by $CD27^+$ Tregs in our MLR assays.

Here, we revealed the relevance of CD70 to the pro-inflammatory effect of expanded Tregs by a series of experiments using mAbs blocking CD70 expressed on Tregs or CD27 on responder T cells, with such blockade significantly reducing the pro-inflammatory activity of $CD70^+$ Tregs (Figure 4.6). These data indicate that $CD70^+$ Tregs can promote T cell proliferation by binding CD27 on responder T cells.

Interaction of CD70 with CD27 regulates their subsequent expression levels on the cell surface and, therefore, their consequent activity (*385*). Traditionally, it has been assumed that after binding to CD70, CD27 is cleaved from the cell surface and the extracellular part of the molecule is released as a soluble CD27 molecule (*386*). Indeed, levels of soluble CD27 in serum can be used as a marker of immune activation in several pathologies including cancer, autoimmune diseases and transplant rejection (*387-390*).

Recently, in elegant confocal scanning microscopy experiments, Dhainaut *et al*. have shown membrane exchange between DCs and Tregs at the immune synapse or via tunnelling nanotubes that allows DCs to uptake the CD27/CD70 complex and degrade it intracellularly (*188*). How CD27/CD70 is regulated during T cell-Treg interaction has not been shown yet. Utilising fluorescent microscopy or imaging flow cytometry technologies could confirm the direct interaction between $CD70^+$ Tregs and $CD27^+$ T cells, as well as providing further insight into how CD27 and CD70 are regulated in these cell subsets.

An additional interesting finding is that, when combined with TCR stimulation using anti-CD3 mAb, $CD70^+$ Tregs provide sufficient co-stimulatory signals to induce $CD4^+$ and $CD8^+$ T cell proliferation in the absence of allogenic DCs (Figure 4.8). It has been proposed that CD27 acts in concert with CD28 co-stimulation in activating T cells. CD28 co-stimulation amplifies TCR signalling and enhances cell cycle activity, while CD27 is not required for entry into the cell cycle but it promotes survival of activated T cells during successive rounds of stimulation and, in effect, increases the number of Teff cells (*71, 72*). Previous studies have investigated whether CD27 co-stimulation can lead to T cell activation and proliferation in the absence of CD28 signalling. Hendriks and colleagues, studying the role of CD27/CD70 signalling in $CD27^{-/-}$ and $CD28^{-/-}$ mice, have shown that CD27 is as important as CD28 for the generation of Teff cells in response to influenza infection, and the main determinant for accumulation of high numbers of Teff at the site of infection by promoting cell survival (*72*). Similar results were observed *in vitro*, where deliberate CD27 stimulation can rescue cell death upon TCR stimulation of CD28-deficient T cells (*72*).

In vitro, varlilumab (an agonistic anti-CD27 mAb) preferentially stimulates $CD8^+$ T cells relative to $CD4^+$ T cells (*349*). In mice with constitutive expression of CD70 on T cells, enhanced effector memory cell function is observed in $CD8^+$ T cells but not in $CD4^+$ T cells. The authors hypothesise that $CD8^+$ T cells can be activated via their TCRs by APCs and receive CD27 stimulation from $CD70^+$ T cells, whereas $CD4^+$ T cells may require TCR

stimulation and CD70 co-stimulation being provided by the same APC (*122*). In line with this theory, Keller and colleagues have shown that CD70 is co-delivered to the immunological synapse with MHC class II molecules in DCs (*391*). Interestingly, our data show that $CD27^{-}CD70^{+}$ Tregs express, at transcriptional and protein levels, MHC class II molecules (Figure 3.14B). Whether co-expression of both CD70 and MHC class II is necessary for $CD70^{+}$ Treg-mediated induction of $CD4^{+}$ T cell proliferation needs further clarification but could be important for the design of therapies to control CD27-mediated T cell activation.

Despite expression of MHC class II, $CD70^{+}$ Tregs do not induce T cell proliferation in the absence of TCR stimulation (Figure 4.9). Nevertheless, in the presence of an alloimmune response, infusion of $CD70^{+}$ Tregs could have a harmful effect and exacerbate alloreactive T cell responses. Our *in vivo* experiments show that $CD27^{-}CD70^{+}$ Tregs are not able to suppress homeostatic T cell proliferation, supporting a detrimental role for $CD27^{-}CD70^{+}$ Tregs relative to $CD27^{+}CD70^{-}$ Tregs (Figure 3.11). Further studies using *in vivo* models of allotransplantation could provide more information about the pattern of expression of CD27/CD70 and the role of $CD70^{+}$ Tregs during an alloimmune response.

A skewed phenotype towards a Th17-like phenotype is observed in the $CD27^{-}CD70^{+}$ Treg subset, with overexpression of RORγt and IL-17A and downregulation of FOXP3, compared to $CD27^{+}CD70^{-}$ Tregs. It is known that cytokines are decisive in influencing the progression of the alloimmune response and the ultimate outcome of the transplanted graft (*39*). In this regard, IL-17 expression has been found in rejecting grafts in human patients and Th17 cells have been shown to cause allograft rejection in murine models (*392-396*). Although acquisition of a Th17-like phenotype by *in vitro* expanded Tregs could indicate a more specialised regulatory function (*186*), Tregs with the potential to secrete IL-17 may propose a risk in transplant patients if infused as a cellular therapy.

FOXP3 physically interacts with RORγt, preventing its DNA-binding capacity and Th17 cell development (*330*). Of note, human Tregs express several splice variants of FOXP3 with distinct abilities to regulate RORγt function: full-length isoforms, isoforms that lack exon 2 or isoforms that lack exons 2 and 7 (*397*). Exon 2 contains sequences involved in the interaction with RORγt and isoforms lacking exon 2 do not interact with RORγt and do not prevent Th17 cell development (*330*). Additionally, isoforms lacking exons 2 and 7 facilitate Th17 differentiation (*398*). Our data is generated using anti-FOXP3 mAbs that does not distinguish between the 3 isoforms. It would be useful to investigate if Treg/Th17 conversion in CD27/CD70 Treg subsets is regulated by expression of different FOXP3 isoforms.

6.1.1. Selection of CD70$^-$ Tregs after *in vitro* expansion for enhanced immune therapy

Multiple reports studying freshly isolated and *in vitro* stimulated Tregs have demonstrated a high degree of heterogeneity at epigenetic, transcriptional, proteomics and functional levels. Differences in the Treg compartment may reflect Treg subsets with specialised functions or unstable Tregs that could promote rejection instead of tolerance. Importantly, phenotypic differences in cell surface markers allow selection of specific cell subsets within the *in vitro*-expanded Treg product before infusion.

Previous data have shown that Treg instability occurs primarily within the memory compartment (*178, 307, 345*). Interestingly, naive CD45RA$^+$ Tregs maintain a CD27$^+$CD70$^-$ phenotype for longer during *in vitro* expansion than memory CD45RA$^-$ Tregs (Figure 3.16E). By 4 weeks of expansion, memory Tregs show an almost complete CD27$^-$CD70$^+$ phenotype and functionally act to promote T cell proliferation. Furthermore, in long-term expanded naive Tregs, the CD27$^-$CD70$^+$ but not the CD27$^+$CD70$^-$ cell subset has a co-stimulatory effect on T cell proliferation (Figure 3.16G). Therefore, selection

based on CD27/CD70 expression after expansion may be a better strategy than expansion of CD45RA$^+$ naive Tregs for cellular therapy.

In Chapter 5 we explored several protocols to produce a Treg cell product depleted of CD70$^+$ Tregs. Treg expansion following current GMP-approved protocols already used for the ONE Study clinical trial (*294*) shows that addition of rapamycin during *ex vivo* culture leads to a cell product highly enriched in CD27$^+$CD70$^-$ cells (Figure 5.2). CD27$^-$CD70$^+$ cells were not identified within the expanded cell product of all donors analysed (Figure 5.5B) but, when present, CD27$^-$CD70$^+$ cells had slightly impaired suppressive activity (Figure 5.5D). Depletion of CD70$^+$ cells after expansion in the presence of rapamycin may therefore increase the efficacy of Treg therapy, but would represent a benefit for only certain patients: those whose cell products contain a significant proportion of cells expressing CD70.

6.1.2. Genetic modification for the permanent elimination of pro-inflammatory CD70$^+$ Tregs

The CD27$^+$CD70$^-$ phenotype is a transient phenotype and, upon re-stimulation, Tregs progressively convert to CD27$^-$CD70$^+$ cells. It is possible that, even if Tregs are isolated as CD27$^+$CD70$^-$ cells, they will convert to CD27$^-$CD70$^+$ cells once infused into the patient. Moreover, downregulation of CD27 and upregulation of CD70 in Tregs is enhanced in the presence of certain pro-inflammatory cytokines such as IL-1β and IL-6 (Figure 3.3), suggesting that pro-inflammatory cytokines released during the transplantation procedure may promote this conversion.

Treatment with anti-CD70 blocking mAb *in vivo* or genetic modification of Tregs to permanently inhibit CD70 expression are potential strategies to ensure blockade of CD70 function after Tregs are infused into patients. In Chapter 5, we described two clinically relevant protocols to silence CD70 expression in Tregs using CRISPR/Cas9 technology:

sgRNA delivered by a self-inactivating lentiviral vector coupled with Cas9 mRNA electroporation or electroporation of sgRNA/Cas9 complexes as ribonucleoproteins (RNPs). In both strategies, gene editing takes places during *in vitro* culture with transient Cas9 expression, and knockout efficiency can be assessed by flow cytometry before cells are infused into patients. Although we successfully knocked out CD70, further optimisation is needed to isolate and expand Tregs according to GMP requirements. We assessed the effect of disrupting CD70 expression in flow sorted $CD4^+CD25^+CD127^-$ Tregs, however, to fulfil current UK GMP requirements, Tregs would need to be isolated by magnetic selection, which results in a starting material with a lower Treg purity. It is therefore important to compare suppressive potency and long-term stability of the expanded cell product when magnetically-isolated Tregs are cultured in the presence of rapamycin and/or have CD70 knocked out. Nonetheless, flow cytometric sorting devices that fulfil GMP requirements are currently in use in the USA and are being tested in UK and Germany and would allow the isolation of Tregs by flow cytometry in the near future.

Optimisation is also required to improve the yield of edited Tregs to clinically-relevant doses. Transduction efficiency may be improved by either transducing cells earlier during expansion or by optimising viral concentration. Given the high knockout efficiency achieved (over 80%), once Tregs are transduced efficiently enough, it may be possible to isolate modified Tregs by depletion of $CD70^+$ cells without the need for sorting successfully transduced Tregs by GFP expression. As for the sgRNA/Cas9 RNP methodology, different ratios of sgRNA:Cas9 or electroporation conditions may also improve the efficiency of the protocol.

6.1.3. Treatment with anti-CD70 blocking antibodies

Another strategy to inhibit the pro-inflammatory effect of $CD70^+$ Tregs would be to treat patients with anti-CD70 blocking mAb after infusion of *in vitro* expanded Tregs. In this case, off target effects on other CD70-expressing cells need to be considered. CD70 is

transiently upregulated upon cell activation by DCs, B cells, NK cells and T cells (*73, 74, 188, 384, 399*). Moreover, constitutive CD70 expression has been reported in chronic viral infection, autoimmune diseases and cancer (*103-112*). It still remains to be determined whether CD70 is upregulated as part of the immune response to an allograft in humans and, if so, by which cell types. Murine data indicate that CD70 is expressed after allotransplantation and provides co-stimulation to enhance alloresponses. Experiments using anti-CD70 blocking mAb or $CD27^{-/-}$ mice in experimental models of allotransplantation have demonstrated a critical role for the CD27/CD70 pathway in $CD8^+$ T cell memory formation, allograft survival and the development of chronic allograft vasculopathy (*118, 126, 400*).

The *in vitro* assays in this thesis demonstrated that $CD70^+$ Tregs provide enough co-stimulation to induce T cell effector activity, suggesting that $CD70^+$ Tregs promote memory T cell alloimmunity *in vivo*. Alloreactive memory T cells are a major barrier for tolerance induction due to their capacity for accelerated rejection and their resistance to co-stimulation blockade and other immunosuppressive treatments (*47*). A key function of CD27 is to prevent death in activated T cells (*71*) and may be a relevant signalling pathway for effector and memory T cells that are resistant to CD28 or CD40L blockade (*273-275*). Several studies have indicated the potential for blocking the CD27-CD70 interaction to prevent $CD8^+$ memory T cell alloimmunity for the induction of durable transplantation tolerance (*118, 126, 400*). Therefore, anti-CD70 blocking mAb treatment, acting on $CD70^+$ Tregs or on other cell populations that express CD70 in the course of the immune response, might be beneficial for induction of tolerance to an allograft, particularly in sensitised transplant recipients.

6.1.4. Expanded $CD27^{-}CD70^{+}$ cells develop from unstable Tregs rather than from effector $CD4^{+}$ T cell contaminants

One of the main questions that arise from the data of this project is whether $CD27^{-}CD70^{+}$ Tregs are truly Tregs that lose their suppressive properties upon prolonged stimulation or whether these cells are a contaminant Teff population that expand after long-term *in vitro* culture. While it is possible that $CD70^{+}$ Tregs are actually Teff cells, $CD27^{-}CD70^{+}$ cells are present within highly pure freshly isolated $CD4^{+}CD25^{+}CD127^{-}$ Tregs, have similar levels of TSDR demethylation as $CD27^{+}CD70^{-}$ Tregs, and express high levels of FOXP3 (Figures 3.1 and 3.7C). Moreover, $CD27^{-}CD70^{+}$ Tregs suppress T cell proliferation after 2 weeks of expansion but lose this ability after 4 weeks (Figures 3.7A and 3.9). In addition, within $CD27^{+}CD70^{-}$ Tregs isolated to a high purity, some cells convert to $CD27^{-}CD70^{+}$ cells – when $CD27^{high}CD70^{-}$ Tregs are re-sorted from expanded $CD27^{+}CD70^{-}$ cells, they show increased suppressive ability (Figure 3.10). These data suggest that loss of suppressive potency upon prolonged stimulation is due to Treg instability which is restricted to $CD27^{-}CD70^{+}$ Tregs and driven by repetitive stimulation. The last piece of evidence that supports Treg instability comes from our genetic editing experiments disrupting CD70 expression. Within the same cell product, $CD27^{-}CD70^{+}$ Tregs are highly pro-inflammatory, whereas $CD27^{-}CD70^{-}$ Tregs are as suppressive as $CD27^{+}CD70^{-}$ Tregs (Figure 5.11), proving that pro-inflammatory $CD70^{+}$ Tregs can exert potent suppressive capacity when CD70 function is inhibited or completely lacking.

6.2. Future directions

6.2.1. Examining the physiological role and prevalence of $CD27^-CD70^+$ Tregs

It is important to understand whether $CD27^-CD70^+$ Tregs are an artefact resulting from *in vitro* stimulation or whether they also exist *in vivo* under certain pathological or physiological conditions. Although constitutive CD70 expression has been reported in B cells, DCs, NK cells, and T cells during chronic viral infections, autoimmune diseases and cancer (*103-112*), CD70 expression in the Treg population has not yet been examined. We show that repetitive *in vitro* cell stimulation leads to CD27 downregulation and CD70 upregulation, which is enhanced by certain pro-inflammatory cytokines (Figure 3.3). Pathogenic conversion of Tregs has been observed *in vitro* and *in vivo* and contributes to autoimmunity (*245, 328, 401*), allergy (*402*) and chronic viral infections (*403*). Hence, it is important to determine whether CD70 is upregulated by Tregs in autoimmunity or transplant rejection and whether this identifies non-functional Tregs. If so, analysis of the CD27/CD70 phenotype would be a potential approach for assessing Treg functionality *in vivo*.

6.2.2. Assessing CD70 function in Tregs *in vivo*

The transcriptomic data revealed significant discrepancies in the cytokine and chemokine profiles between $CD27^+CD70^-$ and $CD27^-CD70^+$ Treg subsets (Figures 3.13B and 4.10A), which may partially account for their disparate capacity to regulate T cell proliferation. Analysis of cytokines in supernatants of *in vitro* suppression tests along with data from MLR assays in a transwell system suggests that the pro-inflammatory effect of $CD70^+$ Tregs is not mediated by soluble factors, at least *in vitro* (Figures 4.12 and 4.13). However, it is likely that secretion of chemokines and cytokines plays a major role *in vivo*

allowing chemoattraction and regulation of other effector cells. Likewise, differential expression of chemokine and cytokine receptors would control migration and adaptability of Treg subsets to local environmental factors. Studying *in vivo* functionality of $CD27^-$ $CD70^+$ Tregs with or without functional CD70 (using anti-CD70 blocking mAb or CD70 knockout Tregs) may provide further information.

Previous studies investigating CD70 co-stimulation provided by Teff cells have reported different outcomes under transient or constitutive antigen exposure *in vivo*. For example, in the presence of chronic viral infection, CD70 co-stimulation provides survival signals to antigen-activated T cells for their maintenance that ultimately leads to T cell exhaustion and defective memory immune responses (*122, 404*). However, during transient infections, CD70-driven co-stimulation enhances T cell immune responses without resulting in T cell exhaustion (*122, 404*). In line with these data, O'Neill *et al*. have described a role for T cell-derived CD70 co-stimulation restraining inflammatory T cell responses by inducing T cell apoptosis in mouse models of autoimmune inflammatory bowel disease (IBD) and GvHD (*123*).

Likewise, despite the significant pro-inflammatory effect of CD70 co-stimulation provided by Tregs *in vitro*, $CD70^+$ Tregs could lead to different outcomes *in vivo* depending on the type of the immune response. In fact, our *in vitro* experiments show that $CD70^+CD4^+$ Tconv cells are capable of inducing T cell proliferation in a similar manner to $CD70^+$ Tregs (Figure 4.9), although additional experiments are needed to confirm if the pro-inflammatory effect of $CD70^+$ Tconv is provided by CD70 co-stimulation or through additional mechanisms. Due to the persistent presence of donor antigens in the transplantation setting, it is critical to study the ultimate effect of $CD70^+$ Tregs using *in vivo* models of allotransplantation.

6.2.3. Determining the epigenetic pattern of $CD27^{+}CD70^{-}$ and $CD27^{-}CD70^{+}$ Tregs

Increasing evidence shows that, although FOXP3 expression is crucial for Treg function, the development and maintenance of the Treg linage is controlled by epigenetic modifications at multiple genes, which regulate expression of Treg function-associated molecules such as FOXP3, CTLA-4 and CD25 among others. In Chapter 3, $CD27^{+}CD70^{-}$ and $CD27^{-}CD70^{+}$ Treg subsets were compared for their methylation status at the TSDR, the best characterised DNA region responsible for stable FOXP3 expression. Nonetheless, genome-wide methylation status studies have shown specific demethylation at other genes such as *ctla4*, *Il2ra* (CD25), *Tnfrsf18* (GITR), *Ikzf2* (Helios) and *Ikzf4* (Eos) in Tregs (thymic or peripheral) but not in *in vitro* induced iTregs or other Th cell subsets (*154*), indicating that tTregs have a characteristic DNA hypomethylated pattern that is broadly distributed genome-wide.

Although environmental factors can affect the stability of Tregs to a certain extent, the Treg-specific epigenome determines a heritable Treg-specific gene network and maintains stable Treg function (*154*). Therefore, the study of the Treg-epigenome would enable a better understanding of functional stability, plasticity and heterogeneity of the Treg population. It would be valuable to perform a genome-wide analysis of the methylation profile of CD27/CD70 Treg subsets to determine whether their differential stability is due to a distinct Treg-associated epigenome.

Furthermore, other epigenetic modifications (in addition to methylation), such as histone modifications, non-coding RNAs or nucleosome positioning, can control gene expression. Comparing chromatin accessibility genome-wide (by Assay for Transposase Accessible Chromatin sequencing (ATAC-seq)) could provide further information about DNA regions that are differentially regulated between CD27/CD70 Treg subsets.

6.2.4. Elucidating intracellular signalling downstream of CD27 and CD70 in Tregs

Members of the TNFRSF are subdivided into 3 categories: members with death domains, members that bind to TNF receptor-associated factor (TRAF) molecules and decoy receptors. CD27 and other TNFRSF members such as 4-1BB and OX40, binds to TRAF adaptor molecules and cascades intracellular signals. CD27 binds to TRAF2 and TRAF5 and signals to JNK and NF-κB pathways (*405, 406*). In addition, CD27 also interacts with the proapoptotic protein Siva-1, indicating a potential role in promoting apoptosis (*407*). As for other members of the TNFRSF such as CD40L or OX40L, reverse signalling has been reported for CD70 (*119*) in T cells (*360*), B cells (*408*) and NK cells (*399*). Identification of intracellular pathways activated by CD27 and CD70 in Tregs could provide more insight about their functions.

In T cells, CD27 ligation is known to induce upregulation of the antiapoptotic Bcl-XL molecule (*338, 409*). However, the transcriptomic data presented in this thesis did not reveal differences in the expression of antiapoptotic molecules between CD27/CD70 Treg subsets.

CD27 intracellular signalling represses IL-17 expression in murine Tconv cells by epigenetic silencing of the *il17a* gene (*312*). Since there is a skew towards a Th17-like phenotype in the $CD27^{-}CD70^{+}$ Treg subset compared with the $CD27^{+}CD70^{-}$ Treg subset (in terms of higher transcription of *RORC* and *IL-17A*), a role for CD27 in the stability of Tregs during *in vitro* expansion could be speculated. This could prevent conversion of Tregs to Th17-like cells and preserve the potent suppressive activity of $CD27^{+}CD70^{-}$ Tregs. It has not been possible to determine whether this epigenetic mechanism is active in human Tregs. However, if the CD27/CD70 pathway regulates the acquisition of a Th17-like phenotype by Tregs, it would be an interesting method to control Treg/Th17 plasticity. Our data show that activating CD27 signalling in expanded Tregs (by incubation with

agonist anti-CD27 mAb) prior to a 4-5 days suppression test does not result in enhanced Treg suppressive activity (Figure 4.1). Additional experiments culturing Tregs for longer periods with agonist or blocking anti-CD27 mAbs are therefore needed to assess whether CD27 signalling results in epigenetic modifications at the *il17a* locus in human Tregs, and in consequent changes in cytokine secretion upon long-term expansion. However, there was no consistent difference in IL-17A secretion in non-edited and CD70 knockout Treg cells (Figure 5.9C) and suppressive potency was similar in $CD27^{+}CD70^{-}$ and $CD27^{-}CD70^{-}$ Treg subsets (Figure 5.11), indicating that CD70, and not CD27, has a crucial role in the stability of Treg suppressive activity.

Moreover, RNA sequencing analysis in gene-edited Treg cell products, comparing $CD27^{+}CD70^{-}$, $CD27^{-}CD70^{+}$ and $CD27^{-}CD70^{-}$ Treg subsets, could provide further information about the pathways regulated by CD27 and CD70.

6.2.5. Optimising CRISPR/Cas9-mediated gene editing

Efficient genetic disruption using CRISPR/Cas9 technology of *cd70* and *b2m* is shown to result in loss of protein expression (Chapter 5). Treg function can therefore be altered by a relatively simple genetic engineering protocol that is compatible with the *in vitro* expansion procedure required for generation of Treg-based cellular therapies. CRISPR/Cas9 provides a valuable tool for assessing the biology of human Tregs and may allow for relatively easy knock-in and knockout effects with high specificity. We envisage this method being used to analyse the role of functional molecules and to confer a greater specificity or bespoke functionality on cells. For example, CRISPR/Cas9 tools have been used in adoptive T cell therapy to knock-in TCRs with specific reactivity and, simultaneously, to knockout endogenous TCR and CD52 to make T cells resistant to alemtuzumab (*314*). Similar approaches could be applied to Treg cellular therapy.

Although we provide the proof-of-concept that CRISPR/Cas9 editing tools can be used for improving Treg cellular therapy, crucial optimisation experiments are still required to standardise the protocol and increase the yield of gene-edited cells.

6.2.6. Determining stability of the CD27/CD70 phenotype in Tregs in the presence of immunosuppressive drugs

For cellular therapy, the combination of drugs with which patients are treated will affect the functionality of transferred Tregs. Rapamycin, but not cyclosporine A, has been shown to preserve CD27 expression during *in vitro* Treg expansion (*179*). Here we show that rapamycin also impedes CD70 upregulation, but the mechanism underlying this effect is not known. It would be valuable to study the effect of other common immunosuppressive drugs used by transplant patients on CD27/CD70 expression on Tregs in order to identify the most suitable tolerance-permissive therapies.

6.2.7. Exploring the role of the CD27/CD70 pathway in non-T cells

Although in this thesis the focus was on the role of the CD27/CD70 pathway in Treg stability and its ability to regulate other T cells, it is important to note that CD27 and CD70 are expressed by other immune cells. In human B cells, CD27 is upregulated after BCR stimulation and subsequently maintained at high levels, being a typical marker for memory B cells (*410*), whereas CD70 is expressed transiently upon activation (*73*). Both CD27 and CD70 intracellular signals affect the differentiation of B cells to plasma cells (*408*). DCs also upregulate CD70 upon diverse stimulating signals such as ligation of CD40 and TLR stimulation (*73, 188, 384*). A critical role for CD70 expressed on DCs to transfer help signals from $CD4^+$ T cells to $CD8^+$ T cells has been described (*356, 357, 359*). NK cells also express CD27, which distinguishes cell subsets with differential effector functions (*411*), as well as CD70, which enhances survival and effector activity (*399*). In γδT cells, CD27 expression discriminates between IFN-γ and IL-17-producing cells (*412*).

Interaction between different cell types expressing CD27/CD70 provides a layer of complexity for understanding the physiological relevance of the CD27/CD70 pathway. Given the crucial role of the immune cell populations that contribute to CD27-CD70 interaction in the immune response to an allograft, a deeper knowledge of the role of CD27/CD70 pathway would aid in the induction of transplantation tolerance.

6.3. Conclusion

This thesis explores new strategies to enhance the activity of Tregs, as a natural immune mechanism to induce tolerance to alloantigens, with the ultimate goal of reducing levels of immunosuppressive drugs and their toxic side effects in transplant patients. It is expected that induction of tolerance and avoidance of immunosuppressive drugs will allow a significant improvement in graft and patient survival and in the quality of life of hundreds of thousands of patients worldwide.

It is becoming increasingly appreciated that Tregs acquire specific programs to adapt their regulatory function to different immune settings (*186, 250, 251*). Moreover, conversion between the Treg and Tconv compartments has been observed (*243-248*), but the drivers of this functional plasticity are not completely defined.

We have identified IL-17 producing Tregs with impaired suppressive capacity within the *in vitro* expanded Treg product. These cells are confined to the $CD27^{-}CD70^{+}$ Treg phenotype and have the ability to provide co-stimulation and promote T cell proliferation. By the use of monoclonal antibodies or by genetically engineering Tregs, we have shown that CD70 blockade prevents pro-inflammatory activity of *in vitro* expanded human Tregs and may well enhance the efficacy and safety of Treg therapy.

References

1. N. B. a. Transplant, Organ Donation and Transplantation Activity Report 2017/18. (2018).
2. J. Bamoulid *et al.*, The need for minimization strategies: current problems of immunosuppression. *Transpl Int* **28**, 891-900 (2015).
3. J. Y. Niederkorn, Corneal transplantation and immune privilege. *Int Rev Immunol* **32**, 57-67 (2013).
4. J. P. Merrill, J. E. Murray, J. H. Harrison, W. R. Guild, Successful homotransplantation of the human kidney between identical twins. *J Am Med Assoc* **160**, 277-282 (1956).
5. J. P. Merrill *et al.*, Successful Homotransplantation of the Kidney between Nonidentical Twins. **262**, 1251-1260 (1960).
6. C. F. Barker, J. F. Markmann, Historical overview of transplantation. *Cold Spring Harb Perspect Med* **3**, a014977 (2013).
7. T. Gibson, P. B. Medawar, The fate of skin homografts in man. *J Anat* **77**, 299-310 294 (1943).
8. P. B. Medawar, The behaviour and fate of skin autografts and skin homografts in rabbits: A report to the War Wounds Committee of the Medical Research Council. *J Anat* **78**, 176-199 (1944).
9. P. B. Medawar, A second study of the behaviour and fate of skin homografts in rabbits: A Report to the War Wounds Committee of the Medical Research Council. *J Anat* **79**, 157-176 154 (1945).
10. R. E. Billingham, L. Brent, P. B. Medawar, Actively acquired tolerance of foreign cells. *Nature* **172**, 603-606 (1953).
11. A. M. Silverstein, The curious case of the 1960 Nobel Prize to Burnet and Medawar. *Immunology* **147**, 269-274 (2016).
12. J. M. Main, R. T. Prehn, Successful skin homografts after the administration of high dosage X radiation and homologous bone marrow. *J Natl Cancer Inst* **15**, 1023-1029 (1955).
13. R. Kuss, M. Legrain, G. Mathe, R. Nedey, M. Camey, Homologous human kidney transplantation. Experience with six patients. *Postgrad Med J* **38**, 528-531 (1962).
14. E. Thorsby, A short history of HLA. *Tissue Antigens* **74**, 101-116 (2009).
15. P. J. Morris, Transplantation--a medical miracle of the 20th century. *N Engl J Med* **351**, 2678-2680 (2004).
16. J. M. Grinyo, Why is organ transplantation clinically important? *Cold Spring Harb Perspect Med* **3**, (2013).
17. M. Coemans *et al.*, Analyses of the short- and long-term graft survival after kidney transplantation in Europe between 1986 and 2015. *Kidney Int* **94**, 964-973 (2018).
18. A. R. Levy *et al.*, Projecting long-term graft and patient survival after transplantation. *Value Health* **17**, 254-260 (2014).
19. D. Collett, P. J. Friend, C. J. Watson, Factors Associated With Short- and Long-term Liver Graft Survival in the United Kingdom: Development of a UK Donor Liver Index. *Transplantation* **101**, 786-792 (2017).
20. R. K. Gershon, K. Kondo, Infectious immunological tolerance. *Immunology* **21**, 903-914 (1971).
21. B. M. Hall, M. E. Jelbart, K. E. Gurley, S. E. Dorsch, Specific unresponsiveness in rats with prolonged cardiac allograft survival after treatment with cyclosporine. Mediation of specific suppression by T helper/inducer cells. *J Exp Med* **162**, 1683-1694 (1985).
22. S. Sakaguchi, N. Sakaguchi, M. Asano, M. Itoh, M. Toda, Immunologic self-tolerance maintained by activated T cells expressing IL-2 receptor alpha-chains (CD25).

Breakdown of a single mechanism of self-tolerance causes various autoimmune diseases. *J Immunol* **155**, 1151-1164 (1995).
23. J. D. Fontenot, M. A. Gavin, A. Y. Rudensky, Foxp3 programs the development and function of CD4+CD25+ regulatory T cells. *Nat Immunol* **4**, 330-336 (2003).
24. S. Hori, T. Nomura, S. Sakaguchi, Control of regulatory T cell development by the transcription factor Foxp3. *Science* **299**, 1057-1061 (2003).
25. R. Khattri, T. Cox, S. A. Yasayko, F. Ramsdell, An essential role for Scurfin in CD4+CD25+ T regulatory cells. *Nat Immunol* **4**, 337-342 (2003).
26. D. Zecher, N. van Rooijen, D. M. Rothstein, W. D. Shlomchik, F. G. Lakkis, An innate response to allogeneic nonself mediated by monocytes. *J Immunol* **183**, 7810-7816 (2009).
27. W. Liu, X. Xiao, G. Demirci, J. Madsen, X. C. Li, Innate NK cells and macrophages recognize and reject allogeneic nonself in vivo via different mechanisms. *J Immunol* **188**, 2703-2711 (2012).
28. M. H. Oberbarnscheidt *et al.*, Non-self recognition by monocytes initiates allograft rejection. *J Clin Invest* **124**, 3579-3589 (2014).
29. G. Opelz, T. Wujciak, B. Dohler, S. Scherer, J. Mytilineos, HLA compatibility and organ transplant survival. Collaborative Transplant Study. *Rev Immunogenet* **1**, 334-342 (1999).
30. M. Dierselhuis, E. Goulmy, The relevance of minor histocompatibility antigens in solid organ transplantation. *Curr Opin Organ Transplant* **14**, 419-425 (2009).
31. K. J. Wood, R. Goto, Mechanisms of rejection: current perspectives. *Transplantation* **93**, 1-10 (2012).
32. P. N. Rocha, T. J. Plumb, S. D. Crowley, T. M. Coffman, Effector mechanisms in transplant rejection. *Immunol Rev* **196**, 51-64 (2003).
33. W. Land *et al.*, The beneficial effect of human recombinant superoxide dismutase on acute and chronic rejection events in recipients of cadaveric renal transplants. *Transplantation* **57**, 211-217 (1994).
34. I. Muhlberger, P. Perco, R. Fechete, B. Mayer, R. Oberbauer, Biomarkers in renal transplantation ischemia reperfusion injury. *Transplantation* **88**, S14-19 (2009).
35. H. Kono, K. L. Rock, How dying cells alert the immune system to danger. *Nat Rev Immunol* **8**, 279-289 (2008).
36. D. A. Rao, J. S. Pober, Endothelial injury, alarmins, and allograft rejection. *Crit Rev Immunol* **28**, 229-248 (2008).
37. E. Asgari, W. Zhou, S. Sacks, Complement in organ transplantation. *Curr Opin Organ Transplant* **15**, 486-491 (2010).
38. E. Stites, M. Le Quintrec, J. M. Thurman, The Complement System and Antibody-Mediated Transplant Rejection. *J Immunol* **195**, 5525-5531 (2015).
39. P. T. Walsh, T. B. Strom, L. A. Turka, Routes to transplant tolerance versus rejection; the role of cytokines. *Immunity* **20**, 121-131 (2004).
40. K. R. Wyburn, M. D. Jose, H. Wu, R. C. Atkins, S. J. Chadban, The role of macrophages in allograft rejection. *Transplantation* **80**, 1641-1647 (2005).
41. D. F. LaRosa, A. H. Rahman, L. A. Turka, The innate immune system in allograft rejection and tolerance. *J Immunol* **178**, 7503-7509 (2007).
42. W. van der Touw, J. S. Bromberg, Natural killer cells and the immune response in solid organ transplantation. *Am J Transplant* **10**, 1354-1358 (2010).
43. C. P. Larsen, P. J. Morris, J. M. Austyn, Migration of dendritic leukocytes from cardiac allografts into host spleens. A novel pathway for initiation of rejection. *J Exp Med* **171**, 307-314 (1990).
44. B. Afzali, G. Lombardi, R. I. Lechler, Pathways of major histocompatibility complex allorecognition. *Curr Opin Organ Transplant* **13**, 438-444 (2008).

45. D. A. Boardman, J. Jacob, L. A. Smyth, G. Lombardi, R. I. Lechler, What Is Direct Allorecognition? *Curr Transplant Rep* **3**, 275-283 (2016).
46. R. M. Welsh, L. K. Selin, No one is naive: the significance of heterologous T-cell immunity. *Nat Rev Immunol* **2**, 417-426 (2002).
47. A. W. Bingaman, D. L. Farber, Memory T cells in transplantation: generation, function, and potential role in rejection. *Am J Transplant* **4**, 846-852 (2004).
48. O. B. Herrera *et al.*, A novel pathway of alloantigen presentation by dendritic cells. *J Immunol* **173**, 4828-4837 (2004).
49. P. I. Hornick *et al.*, Assessment of the contribution that direct allorecognition makes to the progression of chronic cardiac transplant rejection in humans. *Circulation* **97**, 1257-1263 (1998).
50. D. L. Mueller, M. K. Jenkins, R. H. Schwartz, Clonal expansion versus functional clonal inactivation: a costimulatory signalling pathway determines the outcome of T cell antigen receptor occupancy. *Annu Rev Immunol* **7**, 445-480 (1989).
51. R. H. Schwartz, D. L. Mueller, M. K. Jenkins, H. Quill, T-cell clonal anergy. *Cold Spring Harb Symp Quant Biol* **54 Pt 2**, 605-610 (1989).
52. M. K. Jenkins, C. A. Chen, G. Jung, D. L. Mueller, R. H. Schwartz, Inhibition of antigen-specific proliferation of type 1 murine T cell clones after stimulation with immobilized anti-CD3 monoclonal antibody. *J Immunol* **144**, 16-22 (1990).
53. Z. Liu, H. Fan, S. Jiang, CD4(+) T-cell subsets in transplantation. *Immunol Rev* **252**, 183-191 (2013).
54. M. C. Fantini *et al.*, Cutting edge: TGF-beta induces a regulatory phenotype in CD4+CD25- T cells through Foxp3 induction and down-regulation of Smad7. *J Immunol* **172**, 5149-5153 (2004).
55. N. Schmitt, H. Ueno, Regulation of human helper T cell subset differentiation by cytokines. *Curr Opin Immunol* **34**, 130-136 (2015).
56. E. J. Wherry, M. Kurachi, Molecular and cellular insights into T cell exhaustion. *Nat Rev Immunol* **15**, 486-499 (2015).
57. C. H. June, J. A. Ledbetter, M. M. Gillespie, T. Lindsten, C. B. Thompson, T-cell proliferation involving the CD28 pathway is associated with cyclosporine-resistant interleukin 2 gene expression. *Mol Cell Biol* **7**, 4472-4481 (1987).
58. C. E. Rudd, A. Taylor, H. Schneider, CD28 and CTLA-4 coreceptor expression and signal transduction. *Immunol Rev* **229**, 12-26 (2009).
59. P. S. Linsley, E. A. Clark, J. A. Ledbetter, T-cell antigen CD28 mediates adhesion with B cells by interacting with activation antigen B7/BB-1. *Proc Natl Acad Sci U S A* **87**, 5031-5035 (1990).
60. M. Azuma *et al.*, B70 antigen is a second ligand for CTLA-4 and CD28. *Nature* **366**, 76-79 (1993).
61. M. Collins, V. Ling, B. M. Carreno, The B7 family of immune-regulatory ligands. *Genome Biol* **6**, 223 (2005).
62. T. N. Golovina *et al.*, CD28 costimulation is essential for human T regulatory expansion and function. *J Immunol* **181**, 2855-2868 (2008).
63. I. S. Grewal, R. A. Flavell, The role of CD40 ligand in costimulation and T-cell activation. *Immunol Rev* **153**, 85-106 (1996).
64. Y. Burmeister *et al.*, ICOS controls the pool size of effector-memory and regulatory T cells. *J Immunol* **180**, 774-782 (2008).
65. R. I. Nurieva *et al.*, Generation of T follicular helper cells is mediated by interleukin-21 but independent of T helper 1, 2, or 17 cell lineages. *Immunity* **29**, 138-149 (2008).
66. C. Wang, G. H. Lin, A. J. McPherson, T. H. Watts, Immune regulation by 4-1BB and 4-1BBL: complexities and challenges. *Immunol Rev* **229**, 192-215 (2009).

67. P. Zhang *et al.*, Agonistic anti-4-1BB antibody promotes the expansion of natural regulatory T cells while maintaining Foxp3 expression. *Scand J Immunol* **66**, 435-440 (2007).
68. K. Sugita *et al.*, Participation of the CD27 antigen in the regulation of IL-2-activated human natural killer cells. *J Immunol* **149**, 1199-1203 (1992).
69. D. Maurer, W. Holter, O. Majdic, G. F. Fischer, W. Knapp, CD27 expression by a distinct subpopulation of human B lymphocytes. *Eur J Immunol* **20**, 2679-2684 (1990).
70. C. Claus *et al.*, CD27 signaling increases the frequency of regulatory T cells and promotes tumor growth. *Cancer Res* **72**, 3664-3676 (2012).
71. J. Hendriks *et al.*, CD27 is required for generation and long-term maintenance of T cell immunity. *Nat Immunol* **1**, 433-440 (2000).
72. J. Hendriks, Y. Xiao, J. Borst, CD27 promotes survival of activated T cells and complements CD28 in generation and establishment of the effector T cell pool. *J Exp Med* **198**, 1369-1380 (2003).
73. K. Tesselaar *et al.*, Expression of the murine CD27 ligand CD70 in vitro and in vivo. *J Immunol* **170**, 33-40 (2003).
74. J. Borst, J. Hendriks, Y. Xiao, CD27 and CD70 in T cell and B cell activation. *Curr Opin Immunol* **17**, 275-281 (2005).
75. L. Chen, D. B. Flies, Molecular mechanisms of T cell co-stimulation and co-inhibition. *Nat Rev Immunol* **13**, 227-242 (2013).
76. M. D. Vu *et al.*, OX40 costimulation turns off Foxp3+ Tregs. *Blood* **110**, 2501-2510 (2007).
77. X. Zhang *et al.*, OX40 Costimulation Inhibits Foxp3 Expression and Treg Induction via BATF3-Dependent and Independent Mechanisms. *Cell Rep* **24**, 607-618 (2018).
78. S. Ronchetti *et al.*, Glucocorticoid-induced tumour necrosis factor receptor-related protein: a key marker of functional regulatory T cells. *J Immunol Res* **2015**, 171520 (2015).
79. M. L. del Rio, C. L. Lucas, L. Buhler, G. Rayat, J. I. Rodriguez-Barbosa, HVEM/LIGHT/BTLA/CD160 cosignaling pathways as targets for immune regulation. *J Leukoc Biol* **87**, 223-235 (2010).
80. R. Zeiser *et al.*, Early CD30 signaling is critical for adoptively transferred CD4+CD25+ regulatory T cells in prevention of acute graft-versus-host disease. *Blood* **109**, 2225-2233 (2007).
81. P. S. Linsley *et al.*, CTLA-4 is a second receptor for the B cell activation antigen B7. *J Exp Med* **174**, 561-569 (1991).
82. K. Wing *et al.*, CTLA-4 control over Foxp3+ regulatory T cell function. *Science* **322**, 271-275 (2008).
83. N. Joller *et al.*, Cutting edge: TIGIT has T cell-intrinsic inhibitory functions. *J Immunol* **186**, 1338-1342 (2011).
84. X. Yu *et al.*, The surface protein TIGIT suppresses T cell activation by promoting the generation of mature immunoregulatory dendritic cells. *Nat Immunol* **10**, 48-57 (2009).
85. S. C. Wei, C. R. Duffy, J. P. Allison, Fundamental Mechanisms of Immune Checkpoint Blockade Therapy. *Cancer Discov* **8**, 1069-1086 (2018).
86. J. R. Sedy *et al.*, B and T lymphocyte attenuator regulates T cell activation through interaction with herpesvirus entry mediator. *Nat Immunol* **6**, 90-98 (2005).
87. A. H. Sharpe, G. J. Freeman, The B7-CD28 superfamily. *Nat Rev Immunol* **2**, 116-126 (2002).
88. S. Read, V. Malmstrom, F. Powrie, Cytotoxic T lymphocyte-associated antigen 4 plays an essential role in the function of CD25(+)CD4(+) regulatory cells that control intestinal inflammation. *J Exp Med* **192**, 295-302 (2000).

89. S. Paust, L. Lu, N. McCarty, H. Cantor, Engagement of B7 on effector T cells by regulatory T cells prevents autoimmune disease. *Proc Natl Acad Sci U S A* **101**, 10398-10403 (2004).
90. O. S. Qureshi *et al.*, Trans-endocytosis of CD80 and CD86: a molecular basis for the cell-extrinsic function of CTLA-4. *Science* **332**, 600-603 (2011).
91. A. Shahinian *et al.*, Differential T cell costimulatory requirements in CD28-deficient mice. *Science* **261**, 609-612 (1993).
92. M. C. Genovese *et al.*, Abatacept for rheumatoid arthritis refractory to tumor necrosis factor alpha inhibition. *N Engl J Med* **353**, 1114-1123 (2005).
93. B. D. Curti *et al.*, OX40 is a potent immune-stimulating target in late-stage cancer patients. *Cancer Res* **73**, 7189-7198 (2013).
94. R. H. Vonderheide, M. J. Glennie, Agonistic CD40 antibodies and cancer therapy. *Clin Cancer Res* **19**, 1035-1043 (2013).
95. A. Yonezawa, S. Dutt, C. Chester, J. Kim, H. E. Kohrt, Boosting Cancer Immunotherapy with Anti-CD137 Antibody Therapy. *Clin Cancer Res* **21**, 3113-3120 (2015).
96. H. A. Burris *et al.*, Safety and Activity of Varlilumab, a Novel and First-in-Class Agonist Anti-CD27 Antibody, in Patients With Advanced Solid Tumors. *J Clin Oncol* **35**, 2028-2036 (2017).
97. F. Vincenti *et al.*, A phase III study of belatacept-based immunosuppression regimens versus cyclosporine in renal transplant recipients (BENEFIT study). *Am J Transplant* **10**, 535-546 (2010).
98. T. Ahrends, J. Borst, The opposing roles of CD4(+) T cells in anti-tumour immunity. *Immunology*, (2018).
99. T. H. Watts, TNF/TNFR family members in costimulation of T cell responses. *Annu Rev Immunol* **23**, 23-68 (2005).
100. R. A. van Lier *et al.*, Tissue distribution and biochemical and functional properties of Tp55 (CD27), a novel T cell differentiation antigen. *J Immunol* **139**, 1589-1596 (1987).
101. R. Q. Hintzen *et al.*, Regulation of CD27 expression on subsets of mature T-lymphocytes. *J Immunol* **151**, 2426-2435 (1993).
102. R. G. Goodwin *et al.*, Molecular and biological characterization of a ligand for CD27 defines a new family of cytokines with homology to tumor necrosis factor. *Cell* **73**, 447-456 (1993).
103. A. De Milito *et al.*, Mechanisms of hypergammaglobulinemia and impaired antigen-specific humoral immunity in HIV-1 infection. *Blood* **103**, 2180-2186 (2004).
104. T. Hishima *et al.*, CD70 expression in thymic carcinoma. *Am J Surg Pathol* **24**, 742-746 (2000).
105. J. Diegmann *et al.*, Identification of CD70 as a diagnostic biomarker for clear cell renal cell carcinoma by gene expression profiling, real-time RT-PCR and immunohistochemistry. *Eur J Cancer* **41**, 1794-1801 (2005).
106. B. K. Han *et al.*, Increased prevalence of activated CD70+CD4+ T cells in the periphery of patients with systemic lupus erythematosus. *Lupus* **14**, 598-606 (2005).
107. J. Held-Feindt, R. Mentlein, CD70/CD27 ligand, a member of the TNF family, is expressed in human brain tumors. *Int J Cancer* **98**, 352-356 (2002).
108. H. Yin *et al.*, Hypomethylation and overexpression of CD70 (TNFSF7) in CD4+ T cells of patients with primary Sjogren's syndrome. *J Dermatol Sci* **59**, 198-203 (2010).
109. J. K. Park *et al.*, CD70-expressing CD4 T cells produce IFN-gamma and IL-17 in rheumatoid arthritis. *Rheumatology (Oxford)* **53**, 1896-1900 (2014).
110. M. Manocha *et al.*, Blocking CD27-CD70 costimulatory pathway suppresses experimental colitis. *J Immunol* **183**, 270-276 (2009).

111. W. W. Lee, Z. Z. Yang, G. Li, C. M. Weyand, J. J. Goronzy, Unchecked CD70 expression on T cells lowers threshold for T cell activation in rheumatoid arthritis. *J Immunol* **179**, 2609-2615 (2007).
112. K. Oelke *et al.*, Overexpression of CD70 and overstimulation of IgG synthesis by lupus T cells and T cells treated with DNA methylation inhibitors. *Arthritis Rheum* **50**, 1850-1860 (2004).
113. J. M. van Montfrans *et al.*, CD27 deficiency is associated with combined immunodeficiency and persistent symptomatic EBV viremia. *J Allergy Clin Immunol* **129**, 787-793 e786 (2012).
114. E. Salzer *et al.*, Combined immunodeficiency with life-threatening EBV-associated lymphoproliferative disorder in patients lacking functional CD27. *Haematologica* **98**, 473-478 (2013).
115. O. K. Alkhairy *et al.*, Novel mutations in TNFRSF7/CD27: Clinical, immunologic, and genetic characterization of human CD27 deficiency. *J Allergy Clin Immunol* **136**, 703-712 e710 (2015).
116. H. Abolhassani *et al.*, Combined immunodeficiency and Epstein-Barr virus-induced B cell malignancy in humans with inherited CD70 deficiency. *J Exp Med* **214**, 91-106 (2017).
117. S. Latour, S. Winter, Inherited Immunodeficiencies With High Predisposition to Epstein-Barr Virus-Driven Lymphoproliferative Diseases. *Front Immunol* **9**, 1103 (2018).
118. K. Yamaura *et al.*, Differential requirement of CD27 costimulatory signaling for naive versus alloantigen-primed effector/memory CD8+ T cells. *Am J Transplant* **10**, 1210-1220 (2010).
119. R. Arens *et al.*, Constitutive CD27/CD70 interaction induces expansion of effector-type T cells and results in IFNgamma-mediated B cell depletion. *Immunity* **15**, 801-812 (2001).
120. A. M. Keller, A. Schildknecht, Y. Xiao, M. van den Broek, J. Borst, Expression of costimulatory ligand CD70 on steady-state dendritic cells breaks CD8+ T cell tolerance and permits effective immunity. *Immunity* **29**, 934-946 (2008).
121. R. Arens *et al.*, Tumor rejection induced by CD70-mediated quantitative and qualitative effects on effector CD8+ T cell formation. *J Exp Med* **199**, 1595-1605 (2004).
122. K. P. van Gisbergen *et al.*, Protective CD8 T cell memory is impaired during chronic CD70-driven costimulation. *J Immunol* **182**, 5352-5362 (2009).
123. R. E. O'Neill *et al.*, T Cell-Derived CD70 Delivers an Immune Checkpoint Function in Inflammatory T Cell Responses. *J Immunol* **199**, 3700-3710 (2017).
124. K. Tesselaar *et al.*, Lethal T cell immunodeficiency induced by chronic costimulation via CD27-CD70 interactions. *Nat Immunol* **4**, 49-54 (2003).
125. M. A. Nolte, R. W. van Olffen, K. P. van Gisbergen, R. A. van Lier, Timing and tuning of CD27-CD70 interactions: the impact of signal strength in setting the balance between adaptive responses and immunopathology. *Immunol Rev* **229**, 216-231 (2009).
126. A. Yamada *et al.*, CD70 signaling is critical for CD28-independent CD8+ T cell-mediated alloimmune responses in vivo. *J Immunol* **174**, 1357-1364 (2005).
127. T. F. Rowley, A. Al-Shamkhani, Stimulation by soluble CD70 promotes strong primary and secondary CD8+ cytotoxic T cell responses in vivo. *J Immunol* **172**, 6039-6046 (2004).
128. A. Wasiuk *et al.*, CD27-Mediated Regulatory T Cell Depletion and Effector T Cell Costimulation Both Contribute to Antitumor Efficacy. *J Immunol* **199**, 4110-4123 (2017).
129. S. Crotty, A brief history of T cell help to B cells. *Nat Rev Immunol* **15**, 185-189 (2015).
130. G. E. Karahan, F. H. Claas, S. Heidt, B Cell Immunity in Solid Organ Transplantation. *Front Immunol* **7**, 686 (2016).
131. R. B. Colvin, R. N. Smith, Antibody-mediated organ-allograft rejection. *Nat Rev Immunol* **5**, 807-817 (2005).

132. S. Saadi, T. Takahashi, R. A. Holzknecht, J. L. Platt, Pathways to acute humoral rejection. *Am J Pathol* **164**, 1073-1080 (2004).
133. C. Wiebe *et al.*, Evolution and clinical pathologic correlations of de novo donor-specific HLA antibody post kidney transplant. *Am J Transplant* **12**, 1157-1167 (2012).
134. A. Loupy, S. C. Jordan, Transplantation: Donor-specific HLA antibodies and renal allograft failure. *Nat Rev Nephrol* **9**, 130-131 (2013).
135. H. Noorchashm *et al.*, B cell-mediated antigen presentation is required for the pathogenesis of acute cardiac allograft rejection. *J Immunol* **177**, 7715-7722 (2006).
136. Y. H. Ng, M. H. Oberbarnscheidt, H. C. Chandramoorthy, R. Hoffman, G. Chalasani, B cells help alloreactive T cells differentiate into memory T cells. *Am J Transplant* **10**, 1970-1980 (2010).
137. Q. Zeng *et al.*, B cells mediate chronic allograft rejection independently of antibody production. *J Clin Invest* **124**, 1052-1056 (2014).
138. B. Peng, Y. Ming, C. Yang, Regulatory B cells: the cutting edge of immune tolerance in kidney transplantation. *Cell Death Dis* **9**, 109 (2018).
139. Y. Xing, K. A. Hogquist, T-cell tolerance: central and peripheral. *Cold Spring Harb Perspect Biol* **4**, (2012).
140. A. Liston, S. Lesage, J. Wilson, L. Peltonen, C. C. Goodnow, Aire regulates negative selection of organ-specific T cells. *Nat Immunol* **4**, 350-354 (2003).
141. R. Pelanda, R. M. Torres, Central B-cell tolerance: where selection begins. *Cold Spring Harb Perspect Biol* **4**, a007146 (2012).
142. J. Stein-Streilein, R. R. Caspi, Immune privilege and the philosophy of immunology. *Front Immunol* **5**, 110 (2014).
143. P. Matzinger, Tolerance, danger, and the extended family. *Annu Rev Immunol* **12**, 991-1045 (1994).
144. S. Sakaguchi, Naturally arising Foxp3-expressing CD25+CD4+ regulatory T cells in immunological tolerance to self and non-self. *Nat Immunol* **6**, 345-352 (2005).
145. J. D. Fontenot *et al.*, Regulatory T cell lineage specification by the forkhead transcription factor foxp3. *Immunity* **22**, 329-341 (2005).
146. X. Tai, M. Cowan, L. Feigenbaum, A. Singer, CD28 costimulation of developing thymocytes induces Foxp3 expression and regulatory T cell differentiation independently of interleukin 2. *Nat Immunol* **6**, 152-162 (2005).
147. C. W. Lio, C. S. Hsieh, A two-step process for thymic regulatory T cell development. *Immunity* **28**, 100-111 (2008).
148. A. E. Moran *et al.*, T cell receptor signal strength in Treg and iNKT cell development demonstrated by a novel fluorescent reporter mouse. *J Exp Med* **208**, 1279-1289 (2011).
149. S. Malchow *et al.*, Aire Enforces Immune Tolerance by Directing Autoreactive T Cells into the Regulatory T Cell Lineage. *Immunity* **44**, 1102-1113 (2016).
150. J. M. Coquet *et al.*, Epithelial and dendritic cells in the thymic medulla promote CD4+Foxp3+ regulatory T cell development via the CD27-CD70 pathway. *J Exp Med* **210**, 715-728 (2013).
151. N. Arpaia *et al.*, Metabolites produced by commensal bacteria promote peripheral regulatory T-cell generation. *Nature* **504**, 451-455 (2013).
152. C. M. Sun *et al.*, Small intestine lamina propria dendritic cells promote de novo generation of Foxp3 T reg cells via retinoic acid. *J Exp Med* **204**, 1775-1785 (2007).
153. M. Yadav, S. Stephan, J. A. Bluestone, Peripherally induced tregs - role in immune homeostasis and autoimmunity. *Front Immunol* **4**, 232 (2013).
154. H. Morikawa, S. Sakaguchi, Genetic and epigenetic basis of Treg cell development and function: from a FoxP3-centered view to an epigenome-defined view of natural Treg cells. *Immunol Rev* **259**, 192-205 (2014).

155. Y. Zheng *et al.*, Role of conserved non-coding DNA elements in the Foxp3 gene in regulatory T-cell fate. *Nature* **463**, 808-812 (2010).
156. W. Lee, G. R. Lee, Transcriptional regulation and development of regulatory T cells. *Exp Mol Med* **50**, e456 (2018).
157. A. M. Thornton *et al.*, Expression of Helios, an Ikaros transcription factor family member, differentiates thymic-derived from peripherally induced Foxp3+ T regulatory cells. *J Immunol* **184**, 3433-3441 (2010).
158. K. Singh, M. Hjort, L. Thorvaldson, S. Sandler, Concomitant analysis of Helios and Neuropilin-1 as a marker to detect thymic derived regulatory T cells in naive mice. *Sci Rep* **5**, 7767 (2015).
159. M. Yadav *et al.*, Neuropilin-1 distinguishes natural and inducible regulatory T cells among regulatory T cell subsets in vivo. *J Exp Med* **209**, 1713-1722, S1711-1719 (2012).
160. A. M. Thornton *et al.*, Helios(+) and Helios(-) Treg subpopulations are phenotypically and functionally distinct and express dissimilar TCR repertoires. *Eur J Immunol*, (2019).
161. T. Akimova, U. H. Beier, L. Wang, M. H. Levine, W. W. Hancock, Helios expression is a marker of T cell activation and proliferation. *PLoS One* **6**, e24226 (2011).
162. R. A. Gottschalk, E. Corse, J. P. Allison, Expression of Helios in peripherally induced Foxp3+ regulatory T cells. *J Immunol* **188**, 976-980 (2012).
163. M. E. Himmel, K. G. MacDonald, R. V. Garcia, T. S. Steiner, M. K. Levings, Helios+ and Helios- cells coexist within the natural FOXP3+ T regulatory cell subset in humans. *J Immunol* **190**, 2001-2008 (2013).
164. E. Szurek *et al.*, Differences in Expression Level of Helios and Neuropilin-1 Do Not Distinguish Thymus-Derived from Extrathymically-Induced CD4+Foxp3+ Regulatory T Cells. *PLoS One* **10**, e0141161 (2015).
165. X. Li *et al.*, Helios expression in regulatory T cells promotes immunosuppression, angiogenesis and the growth of leukemia cells in pediatric acute lymphoblastic leukemia. *Leuk Res* **67**, 60-66 (2018).
166. B. M. Hall, M. E. Jelbart, S. E. Dorsch, Suppressor T cells in rats with prolonged cardiac allograft survival after treatment with cyclosporine. *Transplantation* **37**, 595-600 (1984).
167. W. Liu *et al.*, CD127 expression inversely correlates with FoxP3 and suppressive function of human CD4+ T reg cells. *J Exp Med* **203**, 1701-1711 (2006).
168. N. Seddiki *et al.*, Expression of interleukin (IL)-2 and IL-7 receptors discriminates between human regulatory and activated T cells. *J Exp Med* **203**, 1693-1700 (2006).
169. M. E. Brunkow *et al.*, Disruption of a new forkhead/winged-helix protein, scurfin, results in the fatal lymphoproliferative disorder of the scurfy mouse. *Nat Genet* **27**, 68-73 (2001).
170. C. L. Bennett *et al.*, The immune dysregulation, polyendocrinopathy, enteropathy, X-linked syndrome (IPEX) is caused by mutations of FOXP3. *Nat Genet* **27**, 20-21 (2001).
171. R. S. Wildin *et al.*, X-linked neonatal diabetes mellitus, enteropathy and endocrinopathy syndrome is the human equivalent of mouse scurfy. *Nat Genet* **27**, 18-20 (2001).
172. R. Khattri *et al.*, The amount of scurfin protein determines peripheral T cell number and responsiveness. *J Immunol* **167**, 6312-6320 (2001).
173. U. Baron *et al.*, DNA demethylation in the human FOXP3 locus discriminates regulatory T cells from activated FOXP3(+) conventional T cells. *Eur J Immunol* **37**, 2378-2389 (2007).
174. A. Ferraro *et al.*, Interindividual variation in human T regulatory cells. *Proc Natl Acad Sci U S A* **111**, E1111-1120 (2014).
175. R. Bhairavabhotla *et al.*, Transcriptome profiling of human FoxP3+ regulatory T cells. *Hum Immunol* **77**, 201-213 (2016).
176. G. Borsellino *et al.*, Expression of ectonucleotidase CD39 by Foxp3+ Treg cells: hydrolysis of extracellular ATP and immune suppression. *Blood* **110**, 1225-1232 (2007).

177. J. Ermann *et al.*, Only the CD62L+ subpopulation of CD4+CD25+ regulatory T cells protects from lethal acute GVHD. *Blood* **105**, 2220-2226 (2005).
178. P. Hoffmann *et al.*, Only the CD45RA+ subpopulation of CD4+CD25high T cells gives rise to homogeneous regulatory T-cell lines upon in vitro expansion. *Blood* **108**, 4260-4267 (2006).
179. J. J. Coenen, H. J. Koenen, E. van Rijssen, L. B. Hilbrands, I. Joosten, Rapamycin, and not cyclosporin A, preserves the highly suppressive CD27+ subset of human CD4+CD25+ regulatory T cells. *Blood* **107**, 1018-1023 (2006).
180. R. C. Duggleby, T. N. Shaw, L. B. Jarvis, G. Kaur, J. S. Gaston, CD27 expression discriminates between regulatory and non-regulatory cells after expansion of human peripheral blood CD4+ CD25+ cells. *Immunology* **121**, 129-139 (2007).
181. T. Ito *et al.*, Two functional subsets of FOXP3+ regulatory T cells in human thymus and periphery. *Immunity* **28**, 870-880 (2008).
182. C. Baecher-Allan, E. Wolf, D. A. Hafler, MHC class II expression identifies functionally distinct human regulatory T cells. *J Immunol* **176**, 4622-4631 (2006).
183. D. A. Vignali, L. W. Collison, C. J. Workman, How regulatory T cells work. *Nat Rev Immunol* **8**, 523-532 (2008).
184. M. Miyara *et al.*, Sialyl Lewis x (CD15s) identifies highly differentiated and most suppressive FOXP3high regulatory T cells in humans. *Proc Natl Acad Sci U S A* **112**, 7225-7230 (2015).
185. G. M. Mason *et al.*, Phenotypic Complexity of the Human Regulatory T Cell Compartment Revealed by Mass Cytometry. *J Immunol* **195**, 2030-2037 (2015).
186. T. Duhen, R. Duhen, A. Lanzavecchia, F. Sallusto, D. J. Campbell, Functionally distinct subsets of human FOXP3+ Treg cells that phenotypically mirror effector Th cells. *Blood* **119**, 4430-4440 (2012).
187. F. Fallarino *et al.*, Modulation of tryptophan catabolism by regulatory T cells. *Nat Immunol* **4**, 1206-1212 (2003).
188. M. Dhainaut *et al.*, Thymus-derived regulatory T cells restrain pro-inflammatory Th1 responses by downregulating CD70 on dendritic cells. *EMBO J* **34**, 1336-1348 (2015).
189. C. Asseman, S. Mauze, M. W. Leach, R. L. Coffman, F. Powrie, An essential role for interleukin 10 in the function of regulatory T cells that inhibit intestinal inflammation. *J Exp Med* **190**, 995-1004 (1999).
190. J. Banchereau, V. Pascual, A. O'Garra, From IL-2 to IL-37: the expanding spectrum of anti-inflammatory cytokines. *Nat Immunol* **13**, 925-931 (2012).
191. S. J. Patterson *et al.*, T regulatory cell chemokine production mediates pathogenic T cell attraction and suppression. *J Clin Invest* **126**, 1039-1051 (2016).
192. T. Barthlott *et al.*, CD25+ CD4+ T cells compete with naive CD4+ T cells for IL-2 and exploit it for the induction of IL-10 production. *Int Immunol* **17**, 279-288 (2005).
193. W. J. Grossman *et al.*, Human T regulatory cells can use the perforin pathway to cause autologous target cell death. *Immunity* **21**, 589-601 (2004).
194. J. Bodor *et al.*, Cyclic AMP underpins suppression by regulatory T cells. *Eur J Immunol* **42**, 1375-1384 (2012).
195. E. M. Shevach, Mechanisms of foxp3+ T regulatory cell-mediated suppression. *Immunity* **30**, 636-645 (2009).
196. C. I. Kingsley, M. Karim, A. R. Bushell, K. J. Wood, CD25+CD4+ regulatory T cells prevent graft rejection: CTLA-4- and IL-10-dependent immunoregulation of alloresponses. *J Immunol* **168**, 1080-1086 (2002).
197. C. F. Anderson, M. Oukka, V. J. Kuchroo, D. Sacks, CD4(+)CD25(-)Foxp3(-) Th1 cells are the source of IL-10-mediated immune suppression in chronic cutaneous leishmaniasis. *J Exp Med* **204**, 285-297 (2007).

198. M. J. Barnes *et al.*, CTLA-4 promotes Foxp3 induction and regulatory T cell accumulation in the intestinal lamina propria. *Mucosal Immunol* **6**, 324-334 (2013).
199. S. Cobbold, H. Waldmann, Infectious tolerance. *Curr Opin Immunol* **10**, 518-524 (1998).
200. N. Gagliani *et al.*, Coexpression of CD49b and LAG-3 identifies human and mouse T regulatory type 1 cells. *Nat Med* **19**, 739-746 (2013).
201. M. G. Roncarolo, S. Gregori, R. Bacchetta, M. Battaglia, Tr1 cells and the counter-regulation of immunity: natural mechanisms and therapeutic applications. *Curr Top Microbiol Immunol* **380**, 39-68 (2014).
202. S. Gregori, L. Passerini, M. G. Roncarolo, Clinical Outlook for Type-1 and FOXP3(+) T Regulatory Cell-Based Therapy. *Front Immunol* **6**, 593 (2015).
203. M. G. Roncarolo, S. Gregori, R. Bacchetta, M. Battaglia, N. Gagliani, The Biology of T Regulatory Type 1 Cells and Their Therapeutic Application in Immune-Mediated Diseases. *Immunity* **49**, 1004-1019 (2018).
204. H. L. Weiner, Induction and mechanism of action of transforming growth factor-beta-secreting Th3 regulatory cells. *Immunol Rev* **182**, 207-214 (2001).
205. L. W. Collison *et al.*, IL-35-mediated induction of a potent regulatory T cell population. *Nat Immunol* **11**, 1093-1101 (2010).
206. L. Cosmi *et al.*, Human CD8+CD25+ thymocytes share phenotypic and functional features with CD4+CD25+ regulatory thymocytes. *Blood* **102**, 4107-4114 (2003).
207. S. Bezie, I. Anegon, C. Guillonneau, Advances on CD8+ Treg Cells and Their Potential in Transplantation. *Transplantation* **102**, 1467-1478 (2018).
208. D. Kabelitz, C. Peters, D. Wesch, H. H. Oberg, Regulatory functions of gammadelta T cells. *Int Immunopharmacol* **16**, 382-387 (2013).
209. C. Peters, H. H. Oberg, D. Kabelitz, D. Wesch, Phenotype and regulation of immunosuppressive Vdelta2-expressing gammadelta T cells. *Cell Mol Life Sci* **71**, 1943-1960 (2014).
210. X. Jiang *et al.*, Mechanism of NKT cell-mediated transplant tolerance. *Am J Transplant* **7**, 1482-1490 (2007).
211. J. P. Jukes, K. J. Wood, N. D. Jones, Natural killer T cells: a bridge to tolerance or a pathway to rejection? *Transplantation* **84**, 679-681 (2007).
212. D. Sag, P. Krause, C. C. Hedrick, M. Kronenberg, G. Wingender, IL-10-producing NKT10 cells are a distinct regulatory invariant NKT cell subset. *J Clin Invest* **124**, 3725-3740 (2014).
213. L. Lynch *et al.*, Regulatory iNKT cells lack expression of the transcription factor PLZF and control the homeostasis of T(reg) cells and macrophages in adipose tissue. *Nat Immunol* **16**, 85-95 (2015).
214. S. C. Juvet, L. Zhang, Double negative regulatory T cells in transplantation and autoimmunity: recent progress and future directions. *J Mol Cell Biol* **4**, 48-58 (2012).
215. K. J. Wood, A. Bushell, J. Hester, Regulatory immune cells in transplantation. *Nat Rev Immunol* **12**, 417-430 (2012).
216. M. Ezzelarab, A. W. Thomson, Tolerogenic dendritic cells and their role in transplantation. *Semin Immunol* **23**, 252-263 (2011).
217. P. Trzonkowski *et al.*, First-in-man clinical results of the treatment of patients with graft versus host disease with human ex vivo expanded CD4+CD25+CD127- T regulatory cells. *Clin Immunol* **133**, 22-26 (2009).
218. M. F. Martelli *et al.*, HLA-haploidentical transplantation with regulatory and conventional T-cell adoptive immunotherapy prevents acute leukemia relapse. *Blood* **124**, 638-644 (2014).
219. C. G. Brunstein *et al.*, Infusion of ex vivo expanded T regulatory cells in adults transplanted with umbilical cord blood: safety profile and detection kinetics. *Blood* **117**, 1061-1070 (2011).

220. M. Di Ianni *et al.*, Tregs prevent GVHD and promote immune reconstitution in HLA-haploidentical transplantation. *Blood* **117**, 3921-3928 (2011).
221. R. Bacchetta *et al.*, Immunological Outcome in Haploidentical-HSC Transplanted Patients Treated with IL-10-Anergized Donor T Cells. *Front Immunol* **5**, 16 (2014).
222. M. Edinger, P. Hoffmann, Regulatory T cells in stem cell transplantation: strategies and first clinical experiences. *Curr Opin Immunol* **23**, 679-684 (2011).
223. A. Theil *et al.*, Adoptive transfer of allogeneic regulatory T cells into patients with chronic graft-versus-host disease. *Cytotherapy* **17**, 473-486 (2015).
224. E. K. Geissler, The ONE Study compares cell therapy products in organ transplantation: introduction to a review series on suppressive monocyte-derived cells. *Transplant Res* **1**, 11 (2012).
225. N. Marek-Trzonkowska *et al.*, Administration of CD4+CD25highCD127- regulatory T cells preserves beta-cell function in type 1 diabetes in children. *Diabetes Care* **35**, 1817-1820 (2012).
226. J. A. Bluestone *et al.*, Type 1 diabetes immunotherapy using polyclonal regulatory T cells. *Sci Transl Med* **7**, 315ra189 (2015).
227. N. Marek-Trzonkowska *et al.*, Therapy of type 1 diabetes with CD4(+)CD25(high)CD127-regulatory T cells prolongs survival of pancreatic islets - results of one year follow-up. *Clin Immunol* **153**, 23-30 (2014).
228. P. Desreumaux *et al.*, Safety and efficacy of antigen-specific regulatory T-cell therapy for patients with refractory Crohn's disease. *Gastroenterology* **143**, 1207-1217 e1202 (2012).
229. M. V. Dhodapkar, R. M. Steinman, Antigen-bearing immature dendritic cells induce peptide-specific CD8(+) regulatory T cells in vivo in humans. *Blood* **100**, 174-177 (2002).
230. N. Giannoukakis, B. Phillips, D. Finegold, J. Harnaha, M. Trucco, Phase I (safety) study of autologous tolerogenic dendritic cells in type 1 diabetic patients. *Diabetes Care* **34**, 2026-2032 (2011).
231. H. Benham *et al.*, Citrullinated peptide dendritic cell immunotherapy in HLA risk genotype-positive rheumatoid arthritis patients. *Sci Transl Med* **7**, 290ra287 (2015).
232. G. M. Bell *et al.*, Autologous tolerogenic dendritic cells for rheumatoid and inflammatory arthritis. *Ann Rheum Dis* **76**, 227-234 (2017).
233. A. Jauregui-Amezaga *et al.*, Intraperitoneal Administration of Autologous Tolerogenic Dendritic Cells for Refractory Crohn's Disease: A Phase I Study. *J Crohns Colitis* **9**, 1071-1078 (2015).
234. A. W. Thomson *et al.*, Prospective Clinical Testing of Regulatory Dendritic Cells in Organ Transplantation. *Front Immunol* **7**, 15 (2016).
235. B. D. Fleming, D. M. Mosser, Regulatory macrophages: setting the threshold for therapy. *Eur J Immunol* **41**, 2498-2502 (2011).
236. J. A. Hutchinson *et al.*, Cutting Edge: Immunological consequences and trafficking of human regulatory macrophages administered to renal transplant recipients. *J Immunol* **187**, 2072-2078 (2011).
237. J. M. Alvaro-Gracia *et al.*, Intravenous administration of expanded allogeneic adipose-derived mesenchymal stem cells in refractory rheumatoid arthritis (Cx611): results of a multicentre, dose escalation, randomised, single-blind, placebo-controlled phase Ib/IIa clinical trial. *Ann Rheum Dis* **76**, 196-202 (2017).
238. J. Tan *et al.*, Induction therapy with autologous mesenchymal stem cells in living-related kidney transplants: a randomized controlled trial. *JAMA* **307**, 1169-1177 (2012).
239. M. E. Reinders *et al.*, Autologous bone marrow-derived mesenchymal stromal cells for the treatment of allograft rejection after renal transplantation: results of a phase I study. *Stem Cells Transl Med* **2**, 107-111 (2013).

240. A. Y. Chhabra, S. T. Ildstad, Facilitating cells: role in inducing transplantation tolerance. *Curr Opin Organ Transplant* **23**, 546-551 (2018).
241. J. R. Leventhal, S. T. Ildstad, Tolerance induction in HLA disparate living donor kidney transplantation by facilitating cell-enriched donor stem cell Infusion: The importance of durable chimerism. *Hum Immunol* **79**, 272-276 (2018).
242. T. Kawai *et al.*, Long-term results in recipients of combined HLA-mismatched kidney and bone marrow transplantation without maintenance immunosuppression. *Am J Transplant* **14**, 1599-1611 (2014).
243. G. Oldenhove *et al.*, Decrease of Foxp3+ Treg cell number and acquisition of effector cell phenotype during lethal infection. *Immunity* **31**, 772-786 (2009).
244. M. Tsuji *et al.*, Preferential generation of follicular B helper T cells from Foxp3+ T cells in gut Peyer's patches. *Science* **323**, 1488-1492 (2009).
245. X. Zhou *et al.*, Instability of the transcription factor Foxp3 leads to the generation of pathogenic memory T cells in vivo. *Nat Immunol* **10**, 1000-1007 (2009).
246. H. J. Kim *et al.*, Stable inhibitory activity of regulatory T cells requires the transcription factor Helios. *Science* **350**, 334-339 (2015).
247. F. Polesso, M. Sarker, A. Anderson, D. C. Parker, S. E. Murray, Constitutive expression of NF-kappaB inducing kinase in regulatory T cells impairs suppressive function and promotes instability and pro-inflammatory cytokine production. *Sci Rep* **7**, 14779 (2017).
248. X. O. Yang *et al.*, Molecular antagonism and plasticity of regulatory and inflammatory T cell programs. *Immunity* **29**, 44-56 (2008).
249. Y. P. Rubtsov *et al.*, Stability of the regulatory T cell lineage in vivo. *Science* **329**, 1667-1671 (2010).
250. S. Sakaguchi, K. Wing, Y. Onishi, P. Prieto-Martin, T. Yamaguchi, Regulatory T cells: how do they suppress immune responses? *Int Immunol* **21**, 1105-1111 (2009).
251. Q. Tang, J. A. Bluestone, The Foxp3+ regulatory T cell: a jack of all trades, master of regulation. *Nat Immunol* **9**, 239-244 (2008).
252. S. A. McClymont *et al.*, Plasticity of human regulatory T cells in healthy subjects and patients with type 1 diabetes. *J Immunol* **186**, 3918-3926 (2011).
253. M. Dominguez-Villar, C. M. Baecher-Allan, D. A. Hafler, Identification of T helper type 1-like, Foxp3+ regulatory T cells in human autoimmune disease. *Nat Med* **17**, 673-675 (2011).
254. Z. Hovhannisyan, J. Treatman, D. R. Littman, L. Mayer, Characterization of interleukin-17-producing regulatory T cells in inflamed intestinal mucosa from patients with inflammatory bowel diseases. *Gastroenterology* **140**, 957-965 (2011).
255. K. S. Voo *et al.*, Identification of IL-17-producing FOXP3+ regulatory T cells in humans. *Proc Natl Acad Sci U S A* **106**, 4793-4798 (2009).
256. A. M. Pesenacker *et al.*, CD161 defines the subset of FoxP3+ T cells capable of producing proinflammatory cytokines. *Blood* **121**, 2647-2658 (2013).
257. G. Orlando *et al.*, Clinical operational tolerance after renal transplantation: current status and future challenges. *Ann Surg* **252**, 915-928 (2010).
258. J. Lerut, A. Sanchez-Fueyo, An appraisal of tolerance in liver transplantation. *Am J Transplant* **6**, 1774-1780 (2006).
259. C. I. Kingsley, S. N. Nadig, K. J. Wood, Transplantation tolerance: lessons from experimental rodent models. *Transpl Int* **20**, 828-841 (2007).
260. W. Chen, M. H. Sayegh, S. J. Khoury, Mechanisms of acquired thymic tolerance in vivo: intrathymic injection of antigen induces apoptosis of thymocytes and peripheral T cell anergy. *J Immunol* **160**, 1504-1508 (1998).
261. M. Sykes, Mixed chimerism and transplant tolerance. *Immunity* **14**, 417-424 (2001).

262. M. Sykes, D. H. Sachs, Mixed allogeneic chimerism as an approach to transplantation tolerance. *Immunol Today* **9**, 23-27 (1988).
263. J. D. Scandling *et al.*, Tolerance and withdrawal of immunosuppressive drugs in patients given kidney and hematopoietic cell transplants. *Am J Transplant* **12**, 1133-1145 (2012).
264. T. Fehr, M. Sykes, Clinical experience with mixed chimerism to induce transplantation tolerance. *Transpl Int* **21**, 1118-1135 (2008).
265. T. R. Spitzer *et al.*, Combined histocompatibility leukocyte antigen-matched donor bone marrow and renal transplantation for multiple myeloma with end stage renal disease: the induction of allograft tolerance through mixed lymphohematopoietic chimerism. *Transplantation* **68**, 480-484 (1999).
266. T. Kawai *et al.*, HLA-mismatched renal transplantation without maintenance immunosuppression. *N Engl J Med* **358**, 353-361 (2008).
267. S. X. Qin *et al.*, Induction of tolerance in peripheral T cells with monoclonal antibodies. *Eur J Immunol* **20**, 2737-2745 (1990).
268. C. P. Larsen *et al.*, Long-term acceptance of skin and cardiac allografts after blocking CD40 and CD28 pathways. *Nature* **381**, 434-438 (1996).
269. A. D. Kirk *et al.*, Treatment with humanized monoclonal antibody against CD154 prevents acute renal allograft rejection in nonhuman primates. *Nat Med* **5**, 686-693 (1999).
270. I. R. Ferrer *et al.*, Antigen-specific induced Foxp3+ regulatory T cells are generated following CD40/CD154 blockade. *Proc Natl Acad Sci U S A* **108**, 20701-20706 (2011).
271. T. Kawai, D. Andrews, R. B. Colvin, D. H. Sachs, A. B. Cosimi, Thromboembolic complications after treatment with monoclonal antibody against CD40 ligand. *Nat Med* **6**, 114 (2000).
272. T. Zhang, R. N. Pierson, 3rd, A. M. Azimzadeh, Update on CD40 and CD154 blockade in transplant models. *Immunotherapy* **7**, 899-911 (2015).
273. C. A. London, M. P. Lodge, A. K. Abbas, Functional responses and costimulator dependence of memory CD4+ T cells. *J Immunol* **164**, 265-272 (2000).
274. A. Valujskikh, B. Pantenburg, P. S. Heeger, Primed allospecific T cells prevent the effects of costimulatory blockade on prolonged cardiac allograft survival in mice. *Am J Transplant* **2**, 501-509 (2002).
275. S. M. Ensminger *et al.*, CD8+ T cells contribute to the development of transplant arteriosclerosis despite CD154 blockade. *Transplantation* **69**, 2609-2612 (2000).
276. S. K. Yoshinaga *et al.*, T-cell co-stimulation through B7RP-1 and ICOS. *Nature* **402**, 827-832 (1999).
277. C. Dong *et al.*, ICOS co-stimulatory receptor is essential for T-cell activation and function. *Nature* **409**, 97-101 (2001).
278. E. Ozkaynak *et al.*, Importance of ICOS-B7RP-1 costimulation in acute and chronic allograft rejection. *Nat Immunol* **2**, 591-596 (2001).
279. A. D. Schenk, V. Gorbacheva, M. Rabant, R. L. Fairchild, A. Valujskikh, Effector functions of donor-reactive CD8 memory T cells are dependent on ICOS induced during division in cardiac grafts. *Am J Transplant* **9**, 64-73 (2009).
280. K. J. Wood, S. Sakaguchi, Regulatory T cells in transplantation tolerance. *Nat Rev Immunol* **3**, 199-210 (2003).
281. V. H. Nguyen *et al.*, The impact of regulatory T cells on T-cell immunity following hematopoietic cell transplantation. *Blood* **111**, 945-953 (2008).
282. A. Bushell, E. Jones, A. Gallimore, K. Wood, The generation of CD25+ CD4+ regulatory T cells that prevent allograft rejection does not compromise immunity to a viral pathogen. *J Immunol* **174**, 3290-3297 (2005).
283. Q. Tang, J. A. Bluestone, Regulatory T-cell therapy in transplantation: moving to the clinic. *Cold Spring Harb Perspect Med* **3**, (2013).

284. M. Zaitsu, F. Issa, J. Hester, B. Vanhove, K. J. Wood, Selective blockade of CD28 on human T cells facilitates regulation of alloimmune responses. *JCI Insight* **2**, (2017).
285. M. Battaglia *et al.*, Rapamycin promotes expansion of functional CD4+CD25+FOXP3+ regulatory T cells of both healthy subjects and type 1 diabetic patients. *J Immunol* **177**, 8338-8347 (2006).
286. J. Hester, A. Schiopu, S. N. Nadig, K. J. Wood, Low-dose rapamycin treatment increases the ability of human regulatory T cells to inhibit transplant arteriosclerosis in vivo. *Am J Transplant* **12**, 2008-2016 (2012).
287. G. Whitehouse *et al.*, IL-2 therapy restores regulatory T-cell dysfunction induced by calcineurin inhibitors. *Proc Natl Acad Sci U S A* **114**, 7083-7088 (2017).
288. O. Boyman, M. Kovar, M. P. Rubinstein, C. D. Surh, J. Sprent, Selective stimulation of T cell subsets with antibody-cytokine immune complexes. *Science* **311**, 1924-1927 (2006).
289. S. Letourneau *et al.*, IL-2/anti-IL-2 antibody complexes show strong biological activity by avoiding interaction with IL-2 receptor alpha subunit CD25. *Proc Natl Acad Sci U S A* **107**, 2171-2176 (2010).
290. J. T. Sockolosky *et al.*, Selective targeting of engineered T cells using orthogonal IL-2 cytokine-receptor complexes. *Science* **359**, 1037-1042 (2018).
291. P. Hoffmann *et al.*, Isolation of CD4+CD25+ regulatory T cells for clinical trials. *Biol Blood Marrow Transplant* **12**, 267-274 (2006).
292. D. G. Wichlan, P. L. Roddam, P. Eldridge, R. Handgretinger, J. M. Riberdy, Efficient and reproducible large-scale isolation of human CD4+ CD25+ regulatory T cells with potent suppressor activity. *J Immunol Methods* **315**, 27-36 (2006).
293. J. H. Peters *et al.*, Clinical grade Treg: GMP isolation, improvement of purity by CD127 Depletion, Treg expansion, and Treg cryopreservation. *PLoS One* **3**, e3161 (2008).
294. H. Fraser *et al.*, A Rapamycin-Based GMP-Compatible Process for the Isolation and Expansion of Regulatory T Cells for Clinical Trials. *Mol Ther Methods Clin Dev* **8**, 198-209 (2018).
295. B. I. Moon, T. H. Kim, J. Y. Seoh, Functional Modulation of Regulatory T Cells by IL-2. *PLoS One* **10**, e0141864 (2015).
296. D. Sarkar *et al.*, Ex Vivo Expanded Autologous Polyclonal Regulatory T Cells Suppress Inhibitor Formation in Hemophilia. *Mol Ther Methods Clin Dev* **1**, (2014).
297. P. Hoffmann, R. Eder, L. A. Kunz-Schughart, R. Andreesen, M. Edinger, Large-scale in vitro expansion of polyclonal human CD4(+)CD25high regulatory T cells. *Blood* **104**, 895-903 (2004).
298. N. Safinia, C. Scotta, T. Vaikunthanathan, R. I. Lechler, G. Lombardi, Regulatory T Cells: Serious Contenders in the Promise for Immunological Tolerance in Transplantation. *Front Immunol* **6**, 438 (2015).
299. P. Sagoo *et al.*, Human regulatory T cells with alloantigen specificity are more potent inhibitors of alloimmune skin graft damage than polyclonal regulatory T cells. *Sci Transl Med* **3**, 83ra42 (2011).
300. S. Landwehr-Kenzel *et al.*, Novel GMP-compatible protocol employing an allogeneic B cell bank for clonal expansion of allospecific natural regulatory T cells. *Am J Transplant* **14**, 594-606 (2014).
301. K. G. MacDonald *et al.*, Alloantigen-specific regulatory T cells generated with a chimeric antigen receptor. *J Clin Invest* **126**, 1413-1424 (2016).
302. D. A. Boardman *et al.*, Expression of a Chimeric Antigen Receptor Specific for Donor HLA Class I Enhances the Potency of Human Regulatory T Cells in Preventing Human Skin Transplant Rejection. *Am J Transplant* **17**, 931-943 (2017).
303. O. Joffre *et al.*, Prevention of acute and chronic allograft rejection with CD4+CD25+Foxp3+ regulatory T lymphocytes. *Nat Med* **14**, 88-92 (2008).

304. S. N. Nadig *et al.*, In vivo prevention of transplant arteriosclerosis by ex vivo-expanded human regulatory T cells. *Nat Med* **16**, 809-813 (2010).
305. F. Issa *et al.*, Ex vivo-expanded human regulatory T cells prevent the rejection of skin allografts in a humanized mouse model. *Transplantation* **90**, 1321-1327 (2010).
306. D. C. Wu *et al.*, Ex vivo expanded human regulatory T cells can prolong survival of a human islet allograft in a humanized mouse model. *Transplantation* **96**, 707-716 (2013).
307. P. Hoffmann *et al.*, Loss of FOXP3 expression in natural human CD4+CD25+ regulatory T cells upon repetitive in vitro stimulation. *Eur J Immunol* **39**, 1088-1097 (2009).
308. A. L. Putnam *et al.*, Expansion of human regulatory T-cells from patients with type 1 diabetes. *Diabetes* **58**, 652-662 (2009).
309. C. Scotta *et al.*, Differential effects of rapamycin and retinoic acid on expansion, stability and suppressive qualities of human CD4(+)CD25(+)FOXP3(+) T regulatory cell subpopulations. *Haematologica* **98**, 1291-1299 (2013).
310. R. Arroyo Hornero *et al.*, CD45RA Distinguishes CD4+CD25+CD127-/low TSDR Demethylated Regulatory T Cell Subpopulations With Differential Stability and Susceptibility to Tacrolimus-Mediated Inhibition of Suppression. *Transplantation* **101**, 302-309 (2017).
311. C. R. Ruprecht *et al.*, Coexpression of CD25 and CD27 identifies FoxP3+ regulatory T cells in inflamed synovia. *J Exp Med* **201**, 1793-1803 (2005).
312. J. M. Coquet *et al.*, The CD27 and CD70 costimulatory pathway inhibits effector function of T helper 17 cells and attenuates associated autoimmunity. *Immunity* **38**, 53-65 (2013).
313. C. Boiers *et al.*, Lymphomyeloid contribution of an immune-restricted progenitor emerging prior to definitive hematopoietic stem cells. *Cell Stem Cell* **13**, 535-548 (2013).
314. C. Georgiadis *et al.*, Long Terminal Repeat CRISPR-CAR-Coupled "Universal" T Cells Mediate Potent Anti-leukemic Effects. *Mol Ther* **26**, 1215-1227 (2018).
315. K. Izawa *et al.*, Inherited CD70 deficiency in humans reveals a critical role for the CD70-CD27 pathway in immunity to Epstein-Barr virus infection. *J Exp Med* **214**, 73-89 (2017).
316. S. Sakaguchi, Naturally arising CD4+ regulatory t cells for immunologic self-tolerance and negative control of immune responses. *Annu Rev Immunol* **22**, 531-562 (2004).
317. I. R. Ferrer, J. Hester, A. Bushell, K. J. Wood, Induction of transplantation tolerance through regulatory cells: from mice to men. *Immunol Rev* **258**, 102-116 (2014).
318. S. Chandran *et al.*, Polyclonal Regulatory T Cell Therapy for Control of Inflammation in Kidney Transplants. *Am J Transplant* **17**, 2945-2954 (2017).
319. C. G. Brunstein *et al.*, Umbilical cord blood-derived T regulatory cells to prevent GVHD: kinetics, toxicity profile, and clinical effect. *Blood* **127**, 1044-1051 (2016).
320. N. Marek-Trzonkowska *et al.*, Factors affecting long-term efficacy of T regulatory cell-based therapy in type 1 diabetes. *J Transl Med* **14**, 332 (2016).
321. A. L. Putnam *et al.*, Clinical grade manufacturing of human alloantigen-reactive regulatory T cells for use in transplantation. *Am J Transplant* **13**, 3010-3020 (2013).
322. J. Wang, A. Ioan-Facsinay, E. I. van der Voort, T. W. Huizinga, R. E. Toes, Transient expression of FOXP3 in human activated nonregulatory CD4+ T cells. *Eur J Immunol* **37**, 129-138 (2007).
323. S. Floess *et al.*, Epigenetic control of the foxp3 locus in regulatory T cells. *PLoS Biol* **5**, e38 (2007).
324. J. K. Polansky *et al.*, DNA methylation controls Foxp3 gene expression. *Eur J Immunol* **38**, 1654-1663 (2008).
325. S. Kordasti *et al.*, Deep phenotyping of Tregs identifies an immune signature for idiopathic aplastic anemia and predicts response to treatment. *Blood* **128**, 1193-1205 (2016).

326. G. Liu, Y. Zhao, Toll-like receptors and immune regulation: their direct and indirect modulation on regulatory CD4+ CD25+ T cells. *Immunology* **122**, 149-156 (2007).
327. R. E. Hoeppli, D. Wu, L. Cook, M. K. Levings, The environment of regulatory T cell biology: cytokines, metabolites, and the microbiome. *Front Immunol* **6**, 61 (2015).
328. N. Komatsu *et al.*, Pathogenic conversion of Foxp3+ T cells into TH17 cells in autoimmune arthritis. *Nat Med* **20**, 62-68 (2014).
329. H. J. Koenen *et al.*, Human CD25highFoxp3pos regulatory T cells differentiate into IL-17-producing cells. *Blood* **112**, 2340-2352 (2008).
330. L. Zhou *et al.*, TGF-beta-induced Foxp3 inhibits T(H)17 cell differentiation by antagonizing RORgammat function. *Nature* **453**, 236-240 (2008).
331. J. C. Ochando *et al.*, Lymph node occupancy is required for the peripheral development of alloantigen-specific Foxp3+ regulatory T cells. *J Immunol* **174**, 6993-7005 (2005).
332. Y. Ding, J. Xu, J. S. Bromberg, Regulatory T cell migration during an immune response. *Trends Immunol* **33**, 174-180 (2012).
333. S. Fu *et al.*, CD4+ CD25+ CD62+ T-regulatory cell subset has optimal suppressive and proliferative potential. *Am J Transplant* **4**, 65-78 (2004).
334. I. Baine, S. Basu, R. Ames, R. S. Sellers, F. Macian, Helios induces epigenetic silencing of IL2 gene expression in regulatory T cells. *J Immunol* **190**, 1008-1016 (2013).
335. M. Sebastian *et al.*, Helios Controls a Limited Subset of Regulatory T Cell Functions. *J Immunol* **196**, 144-155 (2016).
336. M. Miyara *et al.*, Functional delineation and differentiation dynamics of human CD4+ T cells expressing the FoxP3 transcription factor. *Immunity* **30**, 899-911 (2009).
337. C. Schmidl *et al.*, Epigenetic reprogramming of the RORC locus during in vitro expansion is a distinctive feature of human memory but not naive Treg. *Eur J Immunol* **41**, 1491-1498 (2011).
338. M. F. van Oosterwijk *et al.*, CD27-CD70 interactions sensitise naive CD4+ T cells for IL-12-induced Th1 cell development. *Int Immunol* **19**, 713-718 (2007).
339. H. Soares *et al.*, A subset of dendritic cells induces CD4+ T cells to produce IFN-gamma by an IL-12-independent but CD70-dependent mechanism in vivo. *J Exp Med* **204**, 1095-1106 (2007).
340. Y. Xiao, V. Peperzak, A. M. Keller, J. Borst, CD27 instructs CD4+ T cells to provide help for the memory CD8+ T cell response after protein immunization. *J Immunol* **181**, 1071-1082 (2008).
341. S. Chellappa *et al.*, Regulatory T cells that co-express RORgammat and FOXP3 are pro-inflammatory and immunosuppressive and expand in human pancreatic cancer. *Oncoimmunology* **5**, e1102828 (2016).
342. M. A. Koch *et al.*, The transcription factor T-bet controls regulatory T cell homeostasis and function during type 1 inflammation. *Nat Immunol* **10**, 595-602 (2009).
343. Y. Wang, M. A. Su, Y. Y. Wan, An essential role of the transcription factor GATA-3 for the function of regulatory T cells. *Immunity* **35**, 337-348 (2011).
344. B. H. Yang *et al.*, Foxp3(+) T cells expressing RORgammat represent a stable regulatory T-cell effector lineage with enhanced suppressive capacity during intestinal inflammation. *Mucosal Immunol* **9**, 444-457 (2016).
345. J. B. Canavan *et al.*, Developing in vitro expanded CD45RA+ regulatory T cells as an adoptive cell therapy for Crohn's disease. *Gut* **65**, 584-594 (2016).
346. M. Ayyoub *et al.*, Human memory FOXP3+ Tregs secrete IL-17 ex vivo and constitutively express the T(H)17 lineage-specific transcription factor RORgamma t. *Proc Natl Acad Sci U S A* **106**, 8635-8640 (2009).
347. S. Z. Josefowicz, L. F. Lu, A. Y. Rudensky, Regulatory T cells: mechanisms of differentiation and function. *Annu Rev Immunol* **30**, 531-564 (2012).

348. L. Z. He *et al.*, Agonist anti-human CD27 monoclonal antibody induces T cell activation and tumor immunity in human CD27-transgenic mice. *J Immunol* **191**, 4174-4183 (2013).
349. V. Ramakrishna *et al.*, Characterization of the human T cell response to in vitro CD27 costimulation with varlilumab. *J Immunother Cancer* **3**, 37 (2015).
350. L. W. Collison, M. R. Pillai, V. Chaturvedi, D. A. Vignali, Regulatory T cell suppression is potentiated by target T cells in a cell contact, IL-35- and IL-10-dependent manner. *J Immunol* **182**, 6121-6128 (2009).
351. C. J. Workman, A. L. Szymczak-Workman, L. W. Collison, M. R. Pillai, D. A. Vignali, The development and function of regulatory T cells. *Cell Mol Life Sci* **66**, 2603-2622 (2009).
352. A. S. Gautron, M. Dominguez-Villar, M. de Marcken, D. A. Hafler, Enhanced suppressor function of TIM-3+ FoxP3+ regulatory T cells. *Eur J Immunol* **44**, 2703-2711 (2014).
353. B. Zhang, S. Chikuma, S. Hori, S. Fagarasan, T. Honjo, Nonoverlapping roles of PD-1 and FoxP3 in maintaining immune tolerance in a novel autoimmune pancreatitis mouse model. *Proc Natl Acad Sci U S A* **113**, 8490-8495 (2016).
354. T. Asano *et al.*, PD-1 modulates regulatory T-cell homeostasis during low-dose interleukin-2 therapy. *Blood* **129**, 2186-2197 (2017).
355. D. E. Lowther *et al.*, PD-1 marks dysfunctional regulatory T cells in malignant gliomas. *JCI Insight* **1**, (2016).
356. S. Feau *et al.*, The CD4(+) T-cell help signal is transmitted from APC to CD8(+) T-cells via CD27-CD70 interactions. *Nat Commun* **3**, 948 (2012).
357. T. Ahrends *et al.*, CD4(+) T Cell Help Confers a Cytotoxic T Cell Effector Program Including Coinhibitory Receptor Downregulation and Increased Tissue Invasiveness. *Immunity* **47**, 848-861 e845 (2017).
358. M. A. Burchill, B. A. Tamburini, R. M. Kedl, T cells compete by cleaving cell surface CD27 and blocking access to CD70-bearing APCs. *Eur J Immunol* **45**, 3140-3149 (2015).
359. M. S. Matter, C. Claus, A. F. Ochsenbein, CD4+ T cell help improves CD8+ T cell memory by retained CD27 expression. *Eur J Immunol* **38**, 1847-1856 (2008).
360. P. Garcia *et al.*, Signalling via CD70, a member of the TNF family, regulates T cell functions. *J Leukoc Biol* **76**, 263-270 (2004).
361. C. Peter, H. Waldmann, S. P. Cobbold, mTOR signalling and metabolic regulation of T cell differentiation. *Curr Opin Immunol* **22**, 655-661 (2010).
362. L. Strauss *et al.*, Selective survival of naturally occurring human CD4+CD25+Foxp3+ regulatory T cells cultured with rapamycin. *J Immunol* **178**, 320-329 (2007).
363. M. Battaglia, A. Stabilini, M. G. Roncarolo, Rapamycin selectively expands CD4+CD25+FoxP3+ regulatory T cells. *Blood* **105**, 4743-4748 (2005).
364. P. Trzonkowski *et al.*, Hurdles in therapy with regulatory T cells. *Sci Transl Med* **7**, 304ps318 (2015).
365. S. E. Allan *et al.*, Generation of potent and stable human CD4+ T regulatory cells by activation-independent expression of FOXP3. *Mol Ther* **16**, 194-202 (2008).
366. N. Safinia *et al.*, Successful expansion of functional and stable regulatory T cells for immunotherapy in liver transplantation. *Oncotarget* **7**, 7563-7577 (2016).
367. C. Liu, N. M. Chapman, P. W. Karmaus, H. Zeng, H. Chi, mTOR and metabolic regulation of conventional and regulatory T cells. *J Leukoc Biol* **97**, 837-847 (2015).
368. K. L. Hippen *et al.*, Massive ex vivo expansion of human natural regulatory T cells (T(regs)) with minimal loss of in vivo functional activity. *Sci Transl Med* **3**, 83ra41 (2011).
369. G. M. Delgoffe, T. P. Kole, R. J. Cotter, J. D. Powell, Enhanced interaction between Hsp90 and raptor regulates mTOR signaling upon T cell activation. *Mol Immunol* **46**, 2694-2698 (2009).
370. D. Valmori *et al.*, Rapamycin-mediated enrichment of T cells with regulatory activity in stimulated CD4+ T cell cultures is not due to the selective expansion of naturally

occurring regulatory T cells but to the induction of regulatory functions in conventional CD4+ T cells. *J Immunol* **177**, 944-949 (2006).
371. R. Zeiser *et al.*, Differential impact of mammalian target of rapamycin inhibition on CD4+CD25+Foxp3+ regulatory T cells compared with conventional CD4+ T cells. *Blood* **111**, 453-462 (2008).
372. S. J. Bensinger *et al.*, Distinct IL-2 receptor signaling pattern in CD4+CD25+ regulatory T cells. *J Immunol* **172**, 5287-5296 (2004).
373. S. A. Long, J. H. Buckner, Combination of rapamycin and IL-2 increases de novo induction of human CD4(+)CD25(+)FOXP3(+) T cells. *J Autoimmun* **30**, 293-302 (2008).
374. F. Baylis, M. McLeod, First-in-human Phase 1 CRISPR Gene Editing Cancer Trials: Are We Ready? *Curr Gene Ther* **17**, 309-319 (2017).
375. R. Zufferey *et al.*, Self-inactivating lentivirus vector for safe and efficient in vivo gene delivery. *J Virol* **72**, 9873-9880 (1998).
376. A. Hendel *et al.*, Chemically modified guide RNAs enhance CRISPR-Cas genome editing in human primary cells. *Nat Biotechnol* **33**, 985-989 (2015).
377. K. Schumann *et al.*, Generation of knock-in primary human T cells using Cas9 ribonucleoproteins. *Proc Natl Acad Sci U S A* **112**, 10437-10442 (2015).
378. D. Gomes-Silva *et al.*, CD7-edited T cells expressing a CD7-specific CAR for the therapy of T-cell malignancies. *Blood* **130**, 285-296 (2017).
379. J. Ren, Y. Zhao, Advancing chimeric antigen receptor T cell therapy with CRISPR/Cas9. *Protein Cell* **8**, 634-643 (2017).
380. L. J. Rupp *et al.*, CRISPR/Cas9-mediated PD-1 disruption enhances anti-tumor efficacy of human chimeric antigen receptor T cells. *Sci Rep* **7**, 737 (2017).
381. C. Riether, C. Schurch, A. F. Ochsenbein, Modulating CD27 signaling to treat cancer. *Oncoimmunology* **1**, 1604-1606 (2012).
382. L. A. Vitale *et al.*, Development of a human monoclonal antibody for potential therapy of CD27-expressing lymphoma and leukemia. *Clin Cancer Res* **18**, 3812-3821 (2012).
383. A. Laouar *et al.*, CD70+ antigen-presenting cells control the proliferation and differentiation of T cells in the intestinal mucosa. *Nat Immunol* **6**, 698-706 (2005).
384. P. J. Sanchez, J. A. McWilliams, C. Haluszczak, H. Yagita, R. M. Kedl, Combined TLR/CD40 stimulation mediates potent cellular immunity by regulating dendritic cell expression of CD70 in vivo. *J Immunol* **178**, 1564-1572 (2007).
385. M. Kuka, I. Munitic, M. L. Giardino Torchia, J. D. Ashwell, CD70 is downregulated by interaction with CD27. *J Immunol* **191**, 2282-2289 (2013).
386. W. A. Loenen *et al.*, The CD27 membrane receptor, a lymphocyte-specific member of the nerve growth factor receptor family, gives rise to a soluble form by protein processing that does not involve receptor endocytosis. *Eur J Immunol* **22**, 447-455 (1992).
387. S. M. Lens, K. Tesselaar, M. H. van Oers, R. A. van Lier, Control of lymphocyte function through CD27-CD70 interactions. *Semin Immunol* **10**, 491-499 (1998).
388. M. A. de Rie, F. Hamerlinck, R. Q. Hintzen, J. D. Bos, R. A. van Lier, Quantitation of soluble CD27, a T-cell activation antigen, and soluble interleukin-2 receptor in serum from patients with psoriasis. *Arch Dermatol Res* **283**, 533-534 (1991).
389. R. Q. Hintzen *et al.*, Elevated levels of a soluble form of the T cell activation antigen CD27 in cerebrospinal fluid of multiple sclerosis patients. *J Neuroimmunol* **35**, 211-217 (1991).
390. M. E. Chamuleau *et al.*, Serum levels of soluble CD27 in renal transplant recipients. *Transplantation* **54**, 932-936 (1992).
391. A. M. Keller *et al.*, Costimulatory ligand CD70 is delivered to the immunological synapse by shared intracellular trafficking with MHC class II molecules. *Proc Natl Acad Sci U S A* **104**, 5989-5994 (2007).

392. C. Van Kooten *et al.*, Interleukin-17 activates human renal epithelial cells in vitro and is expressed during renal allograft rejection. *J Am Soc Nephrol* **9**, 1526-1534 (1998).
393. E. Fabrega, M. Lopez-Hoyos, D. San Segundo, F. Casafont, F. Pons-Romero, Changes in the serum levels of interleukin-17/interleukin-23 during acute rejection in liver transplantation. *Liver Transpl* **15**, 629-633 (2009).
394. B. M. Vanaudenaerde *et al.*, The role of interleukin-17 during acute rejection after lung transplantation. *Eur Respir J* **27**, 779-787 (2006).
395. S. Heidt, D. S. Segundo, R. Chadha, K. J. Wood, The impact of Th17 cells on transplant rejection and the induction of tolerance. *Curr Opin Organ Transplant* **15**, 456-461 (2010).
396. F. Malard *et al.*, Increased Th17/Treg ratio in chronic liver GVHD. *Bone Marrow Transplant* **49**, 539-544 (2014).
397. S. E. Allan *et al.*, The role of 2 FOXP3 isoforms in the generation of human CD4+ Tregs. *J Clin Invest* **115**, 3276-3284 (2005).
398. R. K. Mailer *et al.*, IL-1beta promotes Th17 differentiation by inducing alternative splicing of FOXP3. *Sci Rep* **5**, 14674 (2015).
399. M. F. Al Sayed *et al.*, CD70 reverse signaling enhances NK cell function and immunosurveillance in CD27-expressing B-cell malignancies. *Blood* **130**, 297-309 (2017).
400. H. Dai *et al.*, Blockade of CD27/CD70 pathway to reduce the generation of memory T cells and markedly prolong the survival of heart allografts in presensitized mice. *Transpl Immunol* **24**, 195-202 (2011).
401. S. L. Bailey-Bucktrout *et al.*, Self-antigen-driven activation induces instability of regulatory T cells during an inflammatory autoimmune response. *Immunity* **39**, 949-962 (2013).
402. M. Noval Rivas *et al.*, Regulatory T cell reprogramming toward a Th2-cell-like lineage impairs oral tolerance and promotes food allergy. *Immunity* **42**, 512-523 (2015).
403. S. Bhela *et al.*, The Plasticity and Stability of Regulatory T Cells during Viral-Induced Inflammatory Lesions. *J Immunol* **199**, 1342-1352 (2017).
404. M. Matter, B. Odermatt, H. Yagita, J. M. Nuoffer, A. F. Ochsenbein, Elimination of chronic viral infection by blocking CD27 signaling. *J Exp Med* **203**, 2145-2155 (2006).
405. H. Akiba *et al.*, CD27, a member of the tumor necrosis factor receptor superfamily, activates NF-kappaB and stress-activated protein kinase/c-Jun N-terminal kinase via TRAF2, TRAF5, and NF-kappaB-inducing kinase. *J Biol Chem* **273**, 13353-13358 (1998).
406. L. A. Gravestein *et al.*, The TNF receptor family member CD27 signals to Jun N-terminal kinase via Traf-2. *Eur J Immunol* **28**, 2208-2216 (1998).
407. K. V. Prasad *et al.*, CD27, a member of the tumor necrosis factor receptor family, induces apoptosis and binds to Siva, a proapoptotic protein. *Proc Natl Acad Sci U S A* **94**, 6346-6351 (1997).
408. R. Arens *et al.*, Signaling through CD70 regulates B cell activation and IgG production. *J Immunol* **173**, 3901-3908 (2004).
409. D. G. Song *et al.*, CD27 costimulation augments the survival and antitumor activity of redirected human T cells in vivo. *Blood* **119**, 696-706 (2012).
410. U. Klein, K. Rajewsky, R. Kuppers, Human immunoglobulin (Ig)M+IgD+ peripheral blood B cells expressing the CD27 cell surface antigen carry somatically mutated variable region genes: CD27 as a general marker for somatically mutated (memory) B cells. *J Exp Med* **188**, 1679-1689 (1998).
411. A. Silva, D. M. Andrews, A. G. Brooks, M. J. Smyth, Y. Hayakawa, Application of CD27 as a marker for distinguishing human NK cell subsets. *Int Immunol* **20**, 625-630 (2008).
412. J. C. Ribot *et al.*, CD27 is a thymic determinant of the balance between interferon-gamma- and interleukin 17-producing gammadelta T cell subsets. *Nat Immunol* **10**, 427-436 (2009).

Publications

Peer-reviewed manuscripts

- “Expression patterns of critical co-stimulatory molecules direct the long-term stability and function of regulatory T cells”. Arroyo Hornero, R. *et al*. Under review in *Science Immunology*. Submitted in December 2018.

- “CD45RA distinguishes $CD4^{+}CD25^{+}CD127^{-/low}$ TSDR demethylated regulatory T cell subpopulations with differential stability and susceptibility to tacrolimus-mediated inhibition of suppression”. Arroyo Hornero R. *et al*. Transplantation. 2017 Feb; 101(2): 302–309.

Conference abstracts

- “Co-stimulatory modulation of human regulatory T cells for enhanced immunotherapy”. Arroyo Hornero, R. *et al.* Transplantation. 2018 July; 102(S1): S208.

- “Modulation of CD27/CD70 co-stimulatory pathway may allow for the generation of a more potent human regulatory T cell product for cell therapy”. Arroyo Hornero, R. *et al.* Transplantation. 2017 May; 101(5S-3): S34–S35.

- “CD45RA identifies TSDR demethylated regulatory T cells with a stable phenotype and suppressive cytokine profile”. Arroyo Hornero, R. *et al.* Transplantation. 2016 July; 100(7-S1): S280.